



# Green thoughts from Slovakia

## In Stara Lerna

I am writing this while staying in the beautiful resort of Stara Lerna in the mountains of Slovakia in Central Europe. My excuse for being here is the XXVIth Conference of Czech and Slovak organic chemists. Apart from my own lecture it is very pleasing to see how many of the lectures strongly link to green chemistry. While the emphasis of the green chemistry-related papers is mostly on synthetic methodology, catalysis and alternative reaction media we are also hearing about plant-based chemicals and innovative technology being applied to organic synthesis.

## Chemicals from crops

I was particularly conscious of the literally growing importance of chemicals from crops on the long drive here from Bratislava which, apart from the spectacular mountainous region, took us through large agricultural regions. In Europe the integration of eastern European countries will result in an enormous increase in the number of farms, typically smaller than those in countries such as the USA, but still adding up to an enormous resource for chemicals and materials as well as for food and energy. Crop-based chemicals are on the increase with, for example, about 5% of the commercial lubricants in several European countries being derived from crops. More research on extraction, separation and purification as well as the properties of the more unusual plant metabolites is required if we are to be in a position to properly exploit this sustainable resource.

## Materials based on biomass

Similarly we continue to see reports on new materials based on biomass and in this issue we can read about one 'fun' application for starch. I was also interested to see the use of starch-based trays for packaging vegetables in a supermarket in York. Such applications are an illustration of what can be achieved and should also be encouraged through more research and development.

## Being positive with green chemistry

These are examples of where green chemistry comes into direct contact with the consumer and, along with larger scale new processes such as the manufacture of polylactic acid, can be used to help show the general public easy-to-understand and refreshingly positive aspects of chemistry. The media is very quick to publicise negative news about chemicals and we need to restore the balance. I am sure that all of our readers will have been following the developments at the World Summit on Sustainable Development in Johannesburg and will have noticed that the one agreement that was quite quickly reached concerned the control of chemicals. The users as well as the manufacturers of chemicals are very concerned over these issues and we as practising chemists must help to show the way forward through innovative and imaginative research on new 'greener' products as well as synthetic routes and methodology.

James Clark, York, September 2002

## RSC JOURNALS GRANTS FOR INTERNATIONAL AUTHORS

Applications are invited from RSC journal authors wishing to receive funding from the RSC Journals Grants for International Authors scheme to visit laboratories outside their normal country of residence for one or both of the following objectives: to collaborate in research; to give or receive special expertise or training.

There are no restrictions on the countries between which visits may be made, but a significant proportion of these grants will be for visits to the UK and other European Union countries. Applicants should have a recent record of publishing in RSC journals. A grant will not exceed £2000.

Applications will be assessed by a panel chaired by the President of the RSC.

For the full criteria for applications and an application form, please see <http://www.rsc.org/jgrant> or contact: Dr Adrian P Kybett, Journals Grants for International Authors, Royal Society of Chemistry, Thomas Graham House, Science Park, Milton Road, Cambridge, UK CB4 0WF; e-mail [jga@rsc.org](mailto:jga@rsc.org)

RSC Members may also apply for Jones Travelling Fellowships to make overseas laboratory study visits. For further information and an application form, contact: Mr S Langer, Royal Society of Chemistry, Burlington House, Piccadilly, London W1V 0BN; e-mail [langer@rsc.org](mailto:langer@rsc.org); <http://www.rsc.org/lap/funding/fundpostdoc.htm>

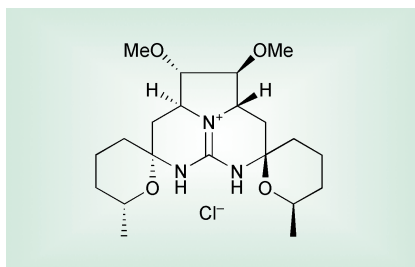


# Highlights

## Duncan Macquarrie reviews highlights from the recent literature

### Chiral phase transfer catalysts

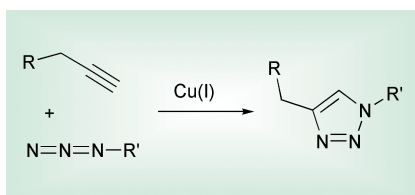
A new chiral phase transfer catalyst has been studied by a group in Japan. Kazuo Nagasawa and colleagues from the University of Tokyo have published details of a novel guanidinium-based



PTC, related structurally to some marine natural products (*Angew. Chem. Int. Ed.*, 2002, **41**, 2832). This metal-free catalyst can be used to effect highly enantioselective alkylation of glycine derivatives (up to 90% at conversions of >80%). The catalyst is reported to be recoverable.

### [1,3]-Dipolar cycloadditions

[1,3]-Dipolar cycloadditions are simple and efficient methods to build up complex molecules quickly. Valery Fokin, Barry Sharpless and co-workers at the Scripps Research Institute, USA, have now shown that it is possible to couple azides and alkynes under very mild

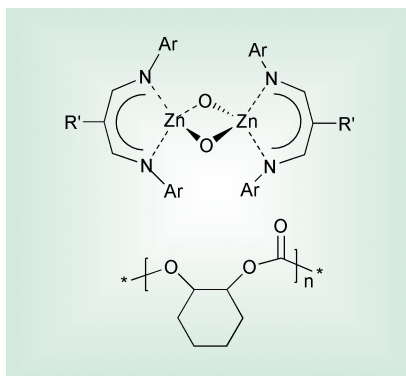


conditions using only a simple copper salt as catalyst. Their process involves the use of copper sulfate in water, which contains sodium ascorbate as reductant, producing the required Cu(I). This catalyst promotes the coupling, at room temperature, of azides and alkynes, crucially giving a single regioisomer, rather than the mixture obtained by purely thermal routes. The system seems to be tolerant of several functional groups (*Angew. Chem. Int. Ed.*, 2002, **41**, 2596).

### CO<sub>2</sub> and epoxides

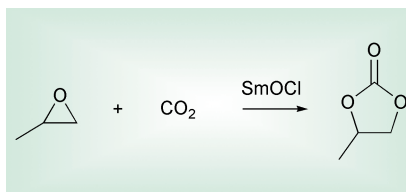
Epoxide-CO<sub>2</sub> polymers are a very interesting class of biodegradable

materials, which use directly carbon dioxide as a monomer. Geoffrey Coates and his group from Cornell University, USA, have now published results on an improved catalyst which can increase



activity and help to control molecular weight distribution in the polymers, a parameter with crucial impact on the materials properties of the resultant products (*Angew. Chem., Int. Ed.*, 2002, **41**, 2599). Their catalyst is based on an electrophilic binuclear zinc complex which activates the epoxide and kicks off the reaction sequence. Good molecular weights and narrow molecular weight distributions can be achieved using this system, making it a very promising route to novel polymeric materials.

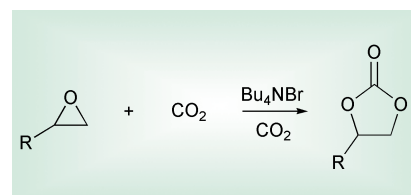
A variation on the above reaction of CO<sub>2</sub> and epoxides has been published by Toshiyasu Sakakura and colleagues from the National Institute of Advanced Science and Technology in Tsukuba, Japan (*J. Catal.*, 2002, **209**, 547). They have found that lanthanide oxychlorides are excellent catalysts for the formation of cyclic carbonates from epoxides and carbon dioxide. These useful products are



simply formed by mixing the components and heating in an autoclave for a few hours. Yields vary significantly depending on the lanthanide, but Sm gives the best results with propylene oxide (57.5% and 97.4% selectivity). The

addition of some DMF increased both these figures to 99%. The authors also propose that the development of higher surface area catalysts would dramatically aid the reaction.

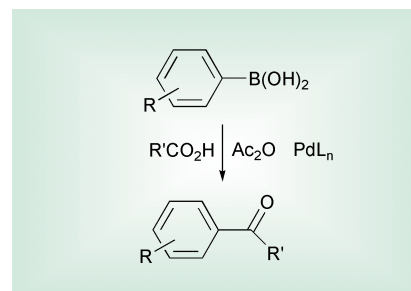
A second paper on the same reaction has been published by Vincenzo Caló and his group at the University of Bari, Italy



(*Org. Lett.*, 2002, **4**, 2561). They have found that simply dissolving an epoxide in molten tetra-butyl ammonium bromide or iodide and exposing the solution to 1 atm carbon dioxide was sufficient to provide the cyclic carbonate in yields of >80% in a few hours. A wide range of carbonates were synthesised using this method.

### C-C bond formation

Heck and Suzuki reactions are well-established C-C bond forming systems. Nonetheless, new variations of this rich chemistry are still appearing, and the latest involves the synthesis of ketones directly from acids. Akio Yamamoto's group at Waseda University,

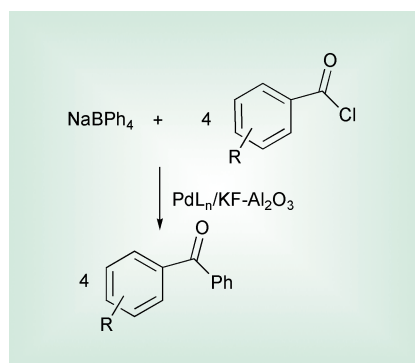


Japan, have demonstrated that carboxylic acids will couple with aryl boronic acids to give the corresponding ketones in excellent yield (*Bull. Soc. Chem. Jpn.*, 2002, **75**, 1333). Using phosphine-Pd complexes, acetic anhydride as activator, and mild conditions (dioxane, ca. 80 °C) they have demonstrated that a wide range of acids (aromatic and aliphatic) can be coupled in excellent yield in a short time.



Mechanistic details are given and a thorough series of reaction conditions have been studied.

An alternative route to unsymmetrical diaryl ketones has also been published by Jin-Xian Weng and colleagues from the Northwest Normal University in Lanzhou, China (*Bull. Chem. Soc. Jpn.*, 2002, **75**, 1381). Here a Pd catalyst catalyses the transfer of all four Ph

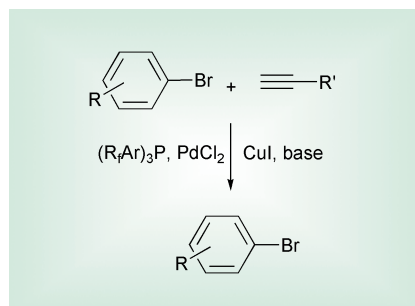


groups from sodium tetraphenyl borate to acyl chlorides, using a Pd complex supported on  $\text{KF-Al}_2\text{O}_3$ . Microwave irradiation was used, and excellent yields (64–98% yields) were obtained in 5 minutes in acetone as solvent. Other basic supports were less effective.

A short review on C–C bond formation in water has been published by Chao-Jun Li of Tulane University, New Orleans, USA (*Acc. Chem. Res.*, 2002, **35**, 533) in which the authors work on Cu, Pd and Ru catalysed C–C bond coupling reactions are described, along with Rh-catalysed olefin isomerisations.

### Fluorous biphasic conditions

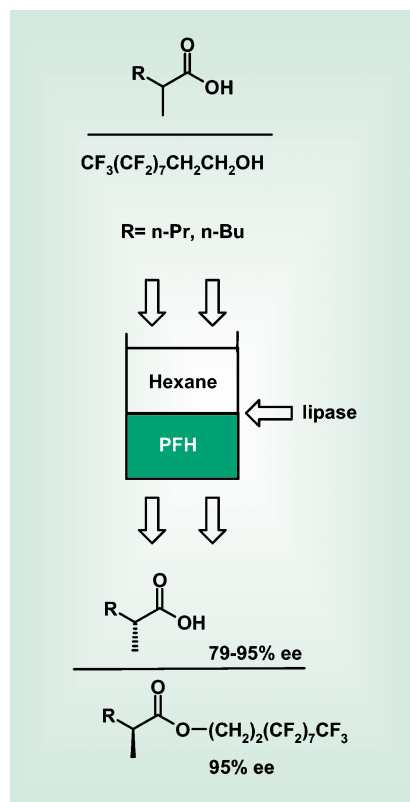
Fluorous biphasic conditions have been developed by Christian Markert and Willi Bannwarth of the University of Freiburg,



Germany, which allow the Sonogashira coupling to proceed efficiently and allow simple isolation of product and catalyst (*Helv. Chim. Acta*, 2002, **85**, 1877). Highly fluorinated phosphines are used as ligands for Pd and perfluorodimethyl-

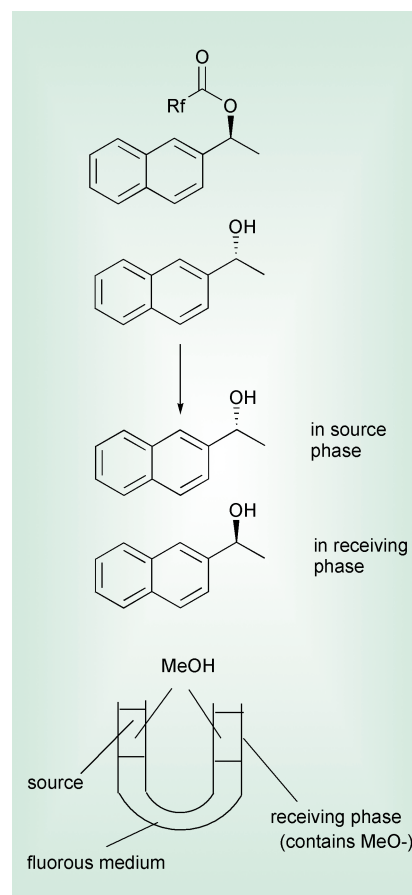
cyclohexane–DMF solvent system was used. CuI and base are also present as in the standard Sonogashira protocol. A range of systems were studied and good yields were generally found. The most active set of substrates were electron-deficient bromoalkenes, where near-quantitative yields were obtained.

Fluorous biphasic conditions have also been used by Petr Beier and David O'Hagan of the University of St Andrews, UK (*Chem. Commun.* 2002, 1680). They have used a lipase-catalysed transformation of a racemic ester with a highly fluorinated alcohol to effect



fluorous-phase enantiomeric partitioning. Here, the lipase allows only the transesterification of one enantiomer, rendering it fluorous-phase soluble, while leaving the other in the organic phase. Thus, the isolation of each enantiomer is reduced to simply cooling the homogeneous reaction mixture, allowing phase separation of the fluorous and organic phases, each of which contains one enantiomer.

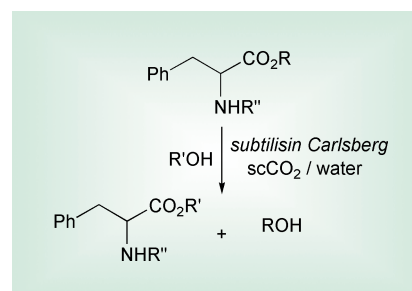
A similar concept has been applied by Dennis Curran and colleagues at the University of Pittsburgh, Fluorous Technologies Inc, and ASCA GmbH (*Org. Lett.*, 2002, **4**, 2585). In this variation a preliminary enzymatic deacylation of a racemic ester, in which



the fluorous part of the ester is the acid component, takes place. This mixture was then added to the reaction set-up shown, where partitioning of the two species followed by liberation of the alcohol from the ester leads to both enantiomers being isolated at separate parts of the reactor, both in excellent yields and selectivities.

### Supercritical fluids

There is considerable interest in such enzyme-catalysed transformations in supercritical fluids. A recent contribution to this area has been made by Andrew Smallridge and co-workers at Victoria University of Technology in Melbourne, Australia (*Aust. J. Chem.*, 2002, **55**, 259). They have found that transesterifications of phenylalanine esters proceeds

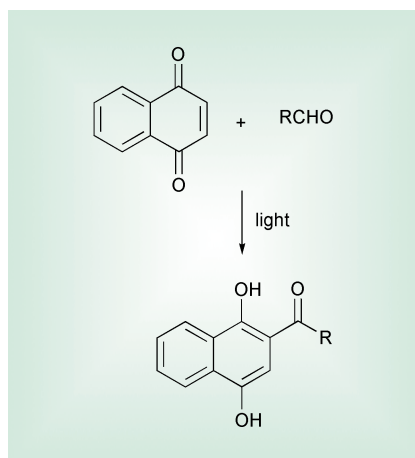




smoothly in  $\text{scCO}_2$  if the correct water concentration was used. The water is required for enzyme activity, and the concentrations required varied depending on the ester involved. There was a lesser sensitivity on the alcohol concentration. The reaction was completely stereospecific, with only L products being formed.

### “Photo-Friedel–Crafts” reaction

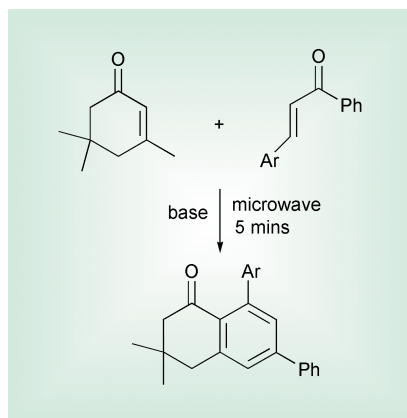
The so-called “photo-Friedel–Crafts” reaction is a potentially clean route to acylated quinones, avoiding the use of strong acid catalysts. The group led by Jochen Mattay at the University of Bielefeld, Germany, has utilised this route to acylate naphthoquinones (*Eur. J. Org. Chem.*, 2002, 2465). They found that, by irradiation of naphthoquinone



and an aldehyde, in the presence or absence of benzophenone, good yields (typically > 60%) of the acyl-naphthoquinone could be obtained. In contrast to the simple quinones, no esterification of the hydroxyl groups was noted.

### Microwave irradiation

Microwave irradiation has been used in a collaborative project between Andre Loupy and colleagues at the University Paris-Sud and the group led by Souâd Fkih Tétouani of the University of Rabat

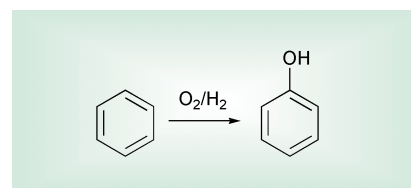


in Morocco (*Eur. J. Org. Chem.*, 2002, 2518). They studied the condensation of isophorone with chalcones to give diaryl  $\alpha$ -tetralones. They found that either NaOEt / Aliquat or  $\text{KF-Al}_2\text{O}_3$  gave excellent yields of the desired product

after a few minutes of microwave irradiation. Conventional heating gave good yields, but after much longer times.

### Hydroxylation of benzene

Direct and selective oxidation of hydrocarbons is a major challenge, especially when using oxygen as oxidant. Wilhelm Laufer and Wolfgang Hölderich of the RWTH Aachen have shown that such a challenge can be successfully met using salts of the highly acidic Nafion–silica composite materials (*Chem. Commun.*, 2002, 1684). They investigated the hydroxylation of benzene to phenol



using oxygen as oxidant. Their best results were obtained with Pd salts of nafion–silica composites (a perfluorinated sulfonic acid dispersed in a silica matrix). The presence of hydrogen was found to be important for the reaction. It was found that benzene could be hydroxylated to phenol with excellent selectivity, but with increasing levels of conversion, hydroquinone was formed by over-oxidation. A well-controlled continuous process was particularly effective at minimising this problem.



# Environmentally friendly products that are also fun

**Tim Colonnese, Bruce Bodio and Jeff Hardy describe how green chemistry is working its way into the nursery**

There are numerous projects by companies and organisations aimed at using renewable resources to make a myriad of materials and products. The complexity of such materials varies from very low technology, for instance the use of apple pomace<sup>1</sup> to absorb textile dyes from effluent, through to high-tech plastics to replace alternatives based on fossil fuels, polylactic acid (Cargill-Dow,<sup>2</sup> Natureworks<sup>TM</sup>) and polyhydroxyalkanoates (Metabolix<sup>3</sup>) being examples of these. KTM Industries<sup>4</sup> (in collaboration with National Starch and Chemical Company<sup>5</sup>) is one such company looking into novel uses of renewable materials, in particular starch.

KTM initially entered the market at the low-technology end, aiming at a novel market for renewable materials, namely children's toys. Using simple extrusion technology (licensed by National Starch and Chemical Company) KTM have developed biodegradable building blocks named Magic Nuudles (Magic Wet'n'Set in the UK, Pegadones in Spain and Portugal) which are essentially composed of cornstarch, water and food colouring. The blocks are stuck together simply by lightly wetting one side of a block and sticking it in the desired orientation to another block. The potential for building a wide variety of structures and shapes with minimal effort is huge (Fig. 1). But not only are these materials fun, they are also sustainable and biodegradable; in fact they are readily broken down simply by exposure to water. Magic Nuudles do not carry a choking hazard warning label, simply because they break down so quickly and have a tendency to stick to the inside of the mouth if accidentally ingested. Magic Nuudles have progressed from an initial turnover of \$216 at their first unveiling at Michigan State University Ag Exhibition to being

† Tim Colonnese is the CEO of KTM Industries (USA), Bruce Bodio is Managing Director of Bodio Limited (UK Company licensed to sell KTM products in the UK and Europe) and Jeff Hardy works at the Clean Technology Centre, University of York, UK (email: jjeh102@york.ac.uk).



*Fig. 4 Magic Wet'N'Set made to form a dragon and a castle*

available in over 10,000 stores in 12 countries (including the UK<sup>6</sup>) and having an annual turnover of greater than \$1 million.

Based on the success of Magic Nuudles, KTM have expanded their children's product range into several new products based on starch. Cornstruction Paper is sheets of starch based paper which can be cut and stuck together in a similar way to Magic Nuudles. The paper

is once again made completely from cornstarch, water and food colouring and is completely biodegradable. A new type of confetti has been introduced made from the Cornstruction paper. It has gained favour in the US because it is cost-effective and easy for churches and party halls to clean up with just water. Another product is GroovyKids Gloop, which is the world's first 100% biodegradable glue. The glue comes in

## KTM HISTORY

Founded in 1997 by four Michigan State University Professors, they are an emerging small company involved in the development and manufacture of environmentally friendly bio-based plastics for diverse industrial, and consumer markets. KTM stands for the three subsidiary companies:

**KidTech Tools, Inc.**—the subsidiary that makes the children's products including Magic Nuudles, Cornstruction Paper, Confetti and GroovyKids Gloop.

**TeleMorph, Inc.**—A concept to develop devices that provide three-dimensional output from computer-based data. The 3-D pieces would be made from biodegradable materials.

**Melting Media, Inc.**—The research arm of KTM, currently developing new and different types of biodegradable material.



six different colours and fragrances including Loco Coco, Gracie Grape, Polly Punch, Ollie Orange, Banzai Banana and Leon Lime which dry to a shiny finish and are easy to clean using water.

The most recent product that KTM have launched in co-operation with National Starch and Chemical Corporation is Green Cell biodegradable packaging material. Currently 3.4 billion kg of petroleum-based foams are used for this application, 95% of which is put straight into landfill at the end of life. Green Cell, which has similar protection and insulation properties compared to

polystyrene and polyethylene, is completely biodegradable and will not build up in landfill. The product was recently featured on the BBC television programme 'Tomorrows World' where it was used to successfully protect an expensive bottle of whisky when it was dropped off a bridge. Green Cell has already won a prestigious award from the Society of Plastic Engineers Inc. President and CEO Tim Colonnese said of this award, "Winning an award like this does two wonderful things for us. It helps gain exposure for Green Cell as this news will go into a lot of packaging and plastics-based periodicals, magazines and

newspapers; but also the award provides validation to this new material and helps establish important credibility with customers."

## References

- 1 T. Robinson, B. Chandran and P. Nigam, *Water Res.*, 2002, **36**, 2824–2830.
- 2 <http://www.cargilldow.com/natureworks.asp>.
- 3 <http://www.metabolix.com/>.
- 4 <http://www.ktmindustries.com>. Contact: Tim Colonnese Tel +1 517 7039140.
- 5 <http://www.nationalstarch.com>.
- 6 UK sales company Bodio Ltd, contact Bruce Bodio (<http://www.bodiold.com>). Tel. +44 (0)1380 728822.

# The disposal of environmentally harmful laboratory chemicals

**Iria Rodriguez a graduate student in the Green Chemistry Group at the University of York† describes a real problem encountered in a research laboratory. How can we dispose of laboratory-scale quantities of environmentally damaging chemicals?**

Legislation concerning dangerous and environmentally damaging chemicals has been dramatically increasing over recent years. Industry and universities across Europe have found that chemicals they have in stock from previous years are now banned or controlled. It can be expensive or very difficult to dispose of such chemicals. In this report we describe a real example we encountered in the Green Chemistry laboratory at York: the disposal/ destruction of dibromodifluoromethane‡.

Chlorofluorocarbons (CFCs) were invented in 1928 to replace sulfur dioxide as a coolant gas. They exhibited advantageous properties on numerous applications. Polyhalogenated methanes such as CFCs and halons (bromine-containing compounds) are chemically stable and have desirable thermophysical properties. They have been used as aerosols, propellants, electronic cleaning solvents, coolants for refrigeration units, blowing agents and in fire extinguishers. It was thought that this

class of compounds with such excellent properties had a great potential and in the 1950s they went into large-scale production. However, it was soon realised that the amount of chlorine in the stratosphere dramatically increased as a result of the release of these compounds.

CFCs are chemically very unreactive. For many compounds this inert nature would be an advantage, however because most of CFCs are gases they do not react in the atmosphere in the normal ways which remove pollutants. This means that after many years they drift up to the stratosphere where short-wave UV light dissociates them to produce chlorine and bromine. These act as catalysts in the decomposition of ozone, which plays a vital role in controlling the radiation reaching the earth surface. This problem wasn't taken very seriously until ozone depletion was recognised in the mid-1980s. This led to an international agreement restricting the manufacture of most CFCs.

Replacements for the CFCs have had to be discovered. Halon 1202 (CF<sub>2</sub>Br<sub>2</sub>) is one of the new substances that is not controlled by the Montreal protocol, which lists ozone-depleting substances that are to be phased out. It was thought

that Halon 1202 was destroyed before it reached the stratosphere. However, new research is changing this view. Recent studies indicate that these substances may also have the potential to damage the ozone layer. There is evidence that under the right conditions such substances and their breakdown products can travel far enough to reach the Earth's protective ozone shield. The compound is also likely to be a massive greenhouse gas.

We used Halon 1202 as a reagent in our research laboratories for several years. In particular, we studied the Burton route to trifluoromethylated aromatic compounds using CF<sub>2</sub>Br<sub>2</sub> as a source of the CF<sub>2</sub> carbene.

As part of the York Chemistry Department refurbishment we were asked to dispose of several hundreds grams of the compound which had been stored in the old cold room. A waste disposal company was contacted and they offered to take the Halon off our hands for a fee. Their method of disposal was to be to seal it in concrete blocks for landfill. The only alternative offered to us was to vent the compound to the atmosphere! We were unhappy with both of these 'solutions' and we decided to look for a different way to destroy the reagent.

† Green Chemistry Group, Department of Chemistry, University of York, York UK YO10 5DD.

‡ Alternative names: Freon 12-B2, Halon-1202, R12B2 and UN1941.



There are several methods reported in the literature, detailing the destruction of such compounds. Some of the technologies include:

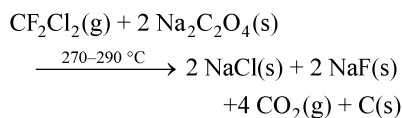
- Catalytic methods: catalytic hydrolysis,<sup>1–6</sup> electrocatalytic decomposition<sup>7</sup>
- Physical methods: combustion,<sup>8</sup> irradiation: laser-induced decomposition,<sup>9</sup> microwave discharge,<sup>10</sup> decomposition by solar energy,<sup>11</sup> plasma destruction<sup>12–13</sup>
- Biological methods<sup>14–16</sup>
- Chemical reduction: by use of sodium naphthalenide<sup>17–18</sup> or hydrogen<sup>19</sup>

The main drawbacks of these methods are the further consumption of resources and the harsh conditions required for the reaction. The high temperature, and in some cases high pressure, required are energy intensive and large amounts of waste are produced. In consequence these methods are generally expensive, resource depleting and shift the environmental burden to another part of the full life cycle.

In Australia, for example, Halons are destroyed at Australia's National Halon Bank using a plasma conversion process called PLASCOM™. Plascom uses superheated plasma at temperatures of more than 10,000 °C to completely breakdown the harmful substances. The gases, once destroyed, form harmless sodium halide salts that are diluted with water, before disposal. Such methods are not suitable on a small scale for example, in a University laboratory.

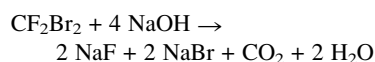
Methods for the destruction of such substances under mild conditions until need to be developed and in a way that

doesn't create new major environmental problems. One interesting method in the literature due to Crabtree and co-workers is the use of sodium oxalate to yield NaCl and NaF, carbon and CO<sub>2</sub> as outlined below.<sup>20</sup>



CFCs are passed through a packed bed of powdered sodium oxalate at 270 °C, with the utilisation of multipass apparatus for liquids. An inexpensive and non-corrosive agent is used and the products obtained are easily handled solids and gaseous CO<sub>2</sub>. However, this method is still quite energy intensive and consumes large quantity of another chemical.

On paper, the reaction of CF<sub>2</sub>Br<sub>2</sub> with sodium hydroxide is about as 'attractive' as any:



However, we have not been able to find any report which describes this as an effective method under reasonable conditions and our preliminary attempt to carry out the reaction in the laboratory have been inconclusive. We are also considering using the compound to make a useful laboratory reagent such as benzotrifluoride.

At the time of writing our problem remains unresolved but we hope it helps to highlight problems that can emerge with chemicals disposal even on a laboratory scale. We would welcome any suggestions or comments that you leave

as well as any other examples of problems encountered in disposing of hazardous chemicals on a relatively small scale.

## References

- 1 S. D. Witt, E. C. Wu, K. L. Loh and Y. N. Tang, *J. Catal.*, 1981, **71**, 270.
- 2 S. Imamura, T. Shiomi and S. Ishida, *Ind. Eng. Chem. Res.*, 1990, **29**, 1758.
- 3 S. Imamura, K. Imakubo and S. Furuyoshi, *Ind. Eng. Chem. Res.*, 1991, **30**, 2355.
- 4 S. Imamura, H. Shimizu, T. Haaga and S. Tsuji, *Ind. Eng. Chem. Res.*, 1993, **32**, 3146.
- 5 T. Aida and R. Higuchi, *Chem. Lett.*, 1990, 1147.
- 6 S. Okazaki and A. Kurosaki, *Chem. Lett.*, 1989, 1901.
- 7 Y. Kashiwagi and C. Kikuchi, *J. Electroanal. Chem.*, 2002, **518**, 51–55.
- 8 J. L. Graham and D. L. Hall, *Environ. Sci. Technol.*, 1986, **20**, 703.
- 9 R. Zitter, D. F. Koster, T. K. Chounhury and A. Cantoni, *J. Phys. Chem.*, 1990, **94**, 2374.
- 10 Th. Behiderhase and W. Hack, *Z. Phys. Chem.*, 2000, **1**, 95–99.
- 11 D. M. Blake, *Int. J. Refrig.*, 1988, **11**, 239–242.
- 12 A. B. Murphy and A. J. D. Farmer, *Plasma Chem. Plasma*, 2002, **22**, 371–385.
- 13 A. B. Murphy, *Ann. New York Acad. Sci.*, 1999, 106–123.
- 14 O. Aaron, *J. Biochem.*, 2002, **41**, 4847–4855.
- 15 A. Jesenska, *Appl. Environ. Microbiol.*, 2000, 219–222.
- 16 B. A. Denovan and S. E. Strand, *Chemosphere*, 1992, **24**, 935.
- 17 A. Oku, K. Kimura and M. Sato, *Chem. Lett.*, 1998, 1789.
- 18 A. Oku, K. Kimura and M. Sato, *Ind. Eng. Chem. Res.*, 1989, **28**, 1055.
- 19 S. D. Witt and E. C. Wu, *J. Catal.*, 1981, **71**, 270–277.
- 20 J. Burdeniuc and R. H. Crabtree, *Science*, 1996, **271**, 340.



# Efficient, halide free synthesis of new, low cost ionic liquids: 1,3-dialkylimidazolium salts containing methyl- and ethyl-sulfate anions

John D. Holbrey,<sup>\*a</sup> W. Matthew Reichert,<sup>a</sup> Richard P. Swatloski,<sup>a</sup> Grant A. Broker,<sup>a</sup> William R. Pitner,<sup>b</sup> Kenneth R. Seddon<sup>b</sup> and Robin D. Rogers<sup>a</sup>

<sup>a</sup> Center for Green Manufacturing and Department of Chemistry, The University of Alabama, Tuscaloosa, AL 35487, USA. E-mail: JHolbrey@bama.ua.edu

<sup>b</sup> The QUILL Research Centre, Queen's University of Belfast, Belfast BT9 5AG, Northern Ireland, UK

Received 9th May 2002

First published as an Advance Article on the web 5th September 2002

New low-cost ionic liquids containing methyl- and ethyl-sulfate anions can be easily and efficiently prepared under ambient conditions by the reaction of 1-alkylimidazoles with dimethyl sulfate and diethyl sulfate. The preparation and characterization of a series of 1,3-dialkylimidazolium alkyl sulfate and 1,2,3-trialkylimidazolium alkyl sulfate salts are reported. 1,3-Dialkylimidazolium salts containing at least one non-methyl *N*-alkyl substituent are liquids at, or below room, temperature. Three salts were crystalline at room temperature, the single crystal X-ray structure of 1,3-dimethylimidazolium methyl sulfate was determined and shows the formation of discrete ribbons comprising of two anion–cation hydrogen-bonded chains linked *via* intra-chain hydrogen-bonding, but little, or no inter-ribbon hydrogen-bonding. The salts are stable, water soluble, inherently 'chloride-free', display an electrochemical window of greater than 4 V, and can be used as alternatives to the corresponding halide salts in metathesis reactions to prepare other ionic liquids including 1-butyl-3-methylimidazolium hexafluorophosphate.

## Introduction

There is a widespread interest in room temperature ionic liquids (ILs) as new, non-volatile solvents in both academia and industry in research areas as diverse as electrochemistry, synthesis, catalysis, materials, separations, and biotechnology.<sup>1</sup> In our own research, we have exploited the different, and variable, properties of ILs for liquid–liquid separations for the partitioning of organic solutes<sup>2</sup> and metal ions,<sup>3</sup> in polymer synthesis,<sup>4,5</sup> and for the dissolution and processing of bio-materials such as cellulose.<sup>6</sup> However, despite the significant developments that have been made in both understanding the properties, and exploring the utility of ILs, they are still considered esoteric materials. In order to facilitate general acceptance and to promote the use of ILs when appropriate, cost and availability issues need to be addressed.

Alkylimidazolium ILs are, in most cases, prepared by alkylation of 1-methylimidazole with an alkyl halide (chloride or bromide).<sup>7,8</sup> The resulting organic salts can then be used directly as ILs,<sup>6,9</sup> as a component of a halometallate IL,<sup>10</sup> or for subsequent metathesis.<sup>11</sup> When halide salts are used for metathesis (for example, to hexafluorophosphate, tetrafluoroborate or bis(trifluoromethanesulfonyl)imide ILs), the presence of halide contamination in the resulting ILs can drastically change the physical properties,<sup>12</sup> and may result in catalyst poisoning and deactivation<sup>13</sup> if used as solvents for transition metal catalyzed reactions.<sup>14</sup> On this topic, it needs to be noted that precipitation of chloride as AgCl does not necessarily lead to entirely halide-free ILs; silver salts are soluble in ILs (for example in nitrate containing ILs) and the slow kinetics for precipitation of silver chloride from solutions in the presence of organic salts has been discussed by Reed and co-workers.<sup>15</sup> In addition, using alkyl halides as alkylating agents can lead to preparative issues on both a laboratory and industrial scale: for example, chloroethane is a volatile, low boiling liquid that

cannot be effectively handled in a laboratory without using pressure vessels.<sup>7</sup> On a larger scale, halide salts raise materials compatibility issues such as corrosion that have not yet been addressed thoroughly for ILs.

Alternative direct and indirect synthetic strategies have been used to prepare imidazolium ILs. Bonhôte *et al.*<sup>16a</sup> have described the synthesis of triflate- and trifluoroacetate-containing ILs by alkylation of 1-methylimidazole with ethyl triflate and ethyl trifluoroacetate respectively. These ILs have also been used as intermediates to prepare other ILs,<sup>16b</sup> with recycling of the valuable anion. Ue *et al.*<sup>17</sup> have prepared 1-ethyl-3-methylimidazolium methyl carbonate salts in solution, by the direct alkylation of 1-butylimidazole with dimethyl carbonate at 145 °C. ILs can be obtained from this route by neutralizing the solutions with acid, where methanol and CO<sub>2</sub> are the only byproducts. It is worth noting that dimethyl carbonate can be prepared directly from methanol and CO<sub>2</sub>.<sup>18,19</sup> Combining these two technologies may enable synthesis of imidazolium-derived ILs from 1-alkylimidazoles using methanol as the alkylation synthon, with H<sub>2</sub>O as the only side product. A wide range of 1,3-dialkylimidazolium ILs can also be prepared from the low-cost, widely available starting materials (glyoxal, formaldehyde, one or more alkylamines, and an acid) using a 'one-pot' synthesis.<sup>20</sup> The acid contributes the anion of the resulting ILs,

## Green Context

New ionic liquids are described, based on the alkylation of the imidazole nucleus with dialkyl sulfates. These new liquids exist as alkyl sulfate salts, are stable and show promise as alternative reaction media. The complete absence of halide ions from the synthesis is a major advantage of such a system. *DJM*



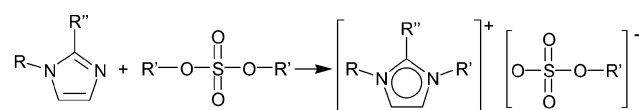
providing an extremely versatile direct synthesis of a wide variety of ILs. This procedure has also been used extensively for the synthesis of symmetrically dialkylated imidazolium salts<sup>21,22</sup> as precursors to imidazol-2-ylidene carbenes, of interest as ligands for the formation of transition metal coordination complexes. 1,3-Dialkylimidazolium salts have also been prepared by protonation of the corresponding imidazolylidene carbenes.<sup>23</sup>

In this paper, we describe the use of common industrial alkylating agents,<sup>24</sup> dimethyl sulfate and diethyl sulfate, for the preparation of ionic liquids based on the imidazolium cation. Two series of ILs, 1-alkyl-3-methylimidazolium methyl sulfate and 1-alkyl-3-ethylimidazolium ethyl sulfate, and related low melting salts containing C(2)-methylated imidazolium cations, have been prepared by alkylation of the appropriate imidazole with dimethyl sulfate or diethyl sulfate (Fig. 1). The salts synthesized are listed in Table 1. The use of **1** and **5** as solvents for enzymatic catalysis,<sup>25,26</sup> **4** in diesel desulfurization,<sup>27</sup> and the interactions of **1** with sc-CO<sub>2</sub><sup>28</sup> have been described in the literature, however the synthesis and properties of these ILs have not been reported.† In this report, the physical properties of these new ILs have been characterized; melting points or glass transition temperatures have been measured by differential scanning calorimetry, the thermal stability by thermogravimetric analysis, and the electrochemical window has been determined by cyclic voltammetry for one example, 1-ethyl-3-methylimidazolium ethyl sulfate (**5**). The single crystal X-ray structure of the solid salt, 1,3-dimethylimidazolium methyl sulfate (**1**), has also been determined.

## Results and discussion

### Synthesis

1,3-Dialkylimidazolium alkyl sulfate ILs were prepared by alkylation of 1-alkylimidazoles with dimethyl sulfate and diethyl sulfate in toluene as an inert solvent following the



**Fig. 1** General preparative route to alkylimidazolium-containing ILs.

† Note that two of the materials described here, **1** and **4**, are commercially available (from Fluka and Solvent Innovation). However, the 1,3-dimethylimidazolium methyl sulfate (98% purity) is described as a room temperature liquid.

**Table 1** Imidazolium alkyl sulfate salts prepared and their thermal properties. Glass transition ( $T_g$ ) and melting point (mp) from onset position were determined by DSC from the first heating cycle, after initially cooling samples to  $-100$  °C. Decomposition temperatures ( $T_{\text{decomp}}$ ) were determined by TGA, heating at  $10$  °C  $\text{min}^{-1}$  under nitrogen.

| Salt      | R                             | R'                            | R''             | Mp ( $\pm 1$ °C) | $T_g$ ( $\pm 1$ °C) | $T_{\text{decomp}}$ ( $\pm 1$ °C) | % mass loss (50–300 °C) |
|-----------|-------------------------------|-------------------------------|-----------------|------------------|---------------------|-----------------------------------|-------------------------|
| <b>1</b>  | CH <sub>3</sub>               | CH <sub>3</sub>               | H               | 43               | —                   | 396                               | 8.4                     |
| <b>2</b>  | C <sub>2</sub> H <sub>5</sub> |                               |                 |                  | –77                 | 390                               | 8.1                     |
| <b>3</b>  | C <sub>3</sub> H <sub>7</sub> |                               |                 |                  | –92                 | 389                               | 8.2                     |
| <b>4</b>  | C <sub>4</sub> H <sub>9</sub> |                               |                 | –5 <sup>a</sup>  | –92                 | 392                               | 9.0                     |
| <b>5</b>  | CH <sub>3</sub>               | C <sub>2</sub> H <sub>5</sub> | H               |                  | –65                 | 408                               | 15.4                    |
| <b>6</b>  | C <sub>2</sub> H <sub>5</sub> |                               |                 |                  | –82                 | 389                               | 14.3                    |
| <b>7</b>  | C <sub>3</sub> H <sub>7</sub> |                               |                 |                  | –97                 | 386                               | 13.0                    |
| <b>8</b>  | C <sub>4</sub> H <sub>9</sub> |                               |                 |                  | –84                 | 387                               | 15.7                    |
| <b>9</b>  | CH <sub>3</sub>               | CH <sub>3</sub>               | CH <sub>3</sub> | 116              | —                   | 372                               | 7.3                     |
| <b>10</b> | CH <sub>3</sub>               | C <sub>2</sub> H <sub>5</sub> |                 | 73               | —                   | 371                               | 14.3                    |

<sup>a</sup> Crystallized from the glassy phase on heating at  $-34$  °C.

scheme shown in Fig. 1. The alkylation can be run under solvent-free conditions, however, we found that using toluene as a solvent has a number of advantages over a solvent-free process. The alkylation reactions are very exothermic, and the solvent acts as a diluent and heat sink to moderate and control the reactivity. In addition, both reagents are soluble in toluene whereas the IL products form a biphasic, thus facilitating simple isolation of pure products. The alkyl sulfate salts prepared are listed in Table 1, and were isolated as colorless or pale yellow liquids, except for **1**, **9**, and **10** which precipitated from the reaction mixture as colorless crystalline solids. All the salts were dried at  $70$  °C under reduced pressure and finally under high vacuum to remove dissolved toluene, then characterized by IR, NMR and MS which showed that the isolated salts were pure, free from imidazole and dialkyl sulfate starting materials or toluene. Single crystals of **1** suitable for X-ray diffraction were obtained after allowing a sample of the molten salt to cool from  $50$  °C to room temperature, the structure was solved by direct methods.

The use of dialkyl sulfates as alkylating agents is preferred in industry over the use of alkyl halides; alkylation reactions are much faster (alkylation rates with dimethyl sulfate are 60 times faster than with methyl iodide), and require less costly processing equipment. The resultant salts can be considered as non-toxic, for example the LD<sub>50</sub>(rat) for sodium methyl sulfate is around  $5000$  mg  $\text{kg}^{-1}$ .<sup>24</sup> In addition, alkyl sulfate salts are less corrosive to the processing equipment than the corresponding halide salts, although degradation does liberate sulfuric acid.

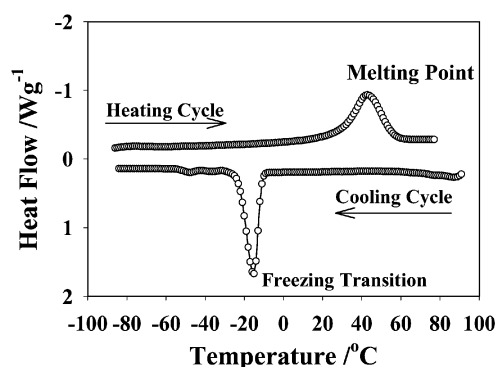
The stability of the alkyl sulfate anion, relative to the potential for the dialkyl sulfate to perform two alkylations, producing 1,3-dialkylimidazolium sulfate salts was tested by reacting methylimidazole and diethyl sulfate in a 2 : 1 mole ratio for 48 h at  $70$  °C. An equimolar mixture of 1-ethyl-3-methylimidazolium ethyl sulfate and unreacted 1-methylimidazole starting material were obtained, as shown by <sup>1</sup>H NMR spectroscopy. This indicates that the ethyl sulfate anion does not alkylate 1-alkylimidazole, which would lead to degradation of the IL *via* formation of sulfate salts.

### Thermal analysis

With the exception of **1**, **9** and **10**, all the materials prepared are liquids which did not crystallize on standing in a freezer ( $-15$  °C).

The thermal behavior of the salts was characterized by differential scanning calorimetry (DSC). The three crystalline salts all displayed a melting point on heating, and on cooling from the melt, crystallized. 1,3-Dimethylimidazolium methyl sulfate (**1**) was the lowest melting of the crystalline solids, with a melting point below  $50$  °C. In the DSC, **1** melts with a single

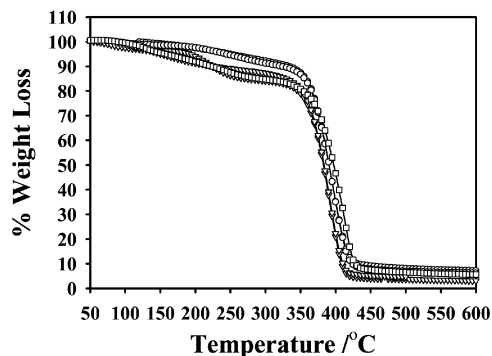
first order transition, no other solid–solid phase transitions were observed. The melting peak in the DSC is broad. This behavior has been noted previously for the low melting 1-ethyl-3-methylimidazolium tetrafluoroborate<sup>29</sup> and for ammonium and pyrrolidinium salts,<sup>30</sup> and may be an indication of solid–solid transitions coincident with the melting point. In contrast, the crystallization transition on cooling is sharp and well defined (Fig. 2). Super-cooling prior to crystallization at  $-18\text{ }^{\circ}\text{C}$  was observed in the DSC for **1**. This is a kinetic phenomenon and bulk molten samples crystallize on standing at room temperature. The two salts containing C(2)– $\text{CH}_3$  substituents on the imidazolium ring (**9** and **10**) were crystalline solids with higher melting points than the corresponding C(2)–H imidazolium salts. It is well known that the substitution of the C(2)–H with a methyl group on the imidazolium cation dramatically increases the melting points of the resulting salts in most cases.<sup>15,16</sup> Comparing the melting points of **1** and **9**, the increase in melting point with C(2)-methylation is  $73\text{ }^{\circ}\text{C}$ . Both salts crystallized from the melt on cooling, no solid–solid transitions below the melting point were observed.



**Fig. 2** DSC thermogram for 1,3-dimethylimidazolium methyl sulfate (**1**), showing the broad first order melting peak on heating, followed by supercooling in the DSC, and the sharp, well defined crystallization transition.

In the DSC experiments, all the room temperature liquids formed glasses at low temperature on cooling. In each case, the glass transition temperature ( $T_g$ ) was between  $-65\text{ }^{\circ}\text{C}$  to  $-97\text{ }^{\circ}\text{C}$ . The thermal behavior of the salts, determined from differential scanning calorimetry measurements are tabulated in Table 1. The  $T_g$  values are similar for all the materials and show only small variations as a function of cooling rate (between 2 and  $40\text{ }^{\circ}\text{C min}^{-1}$ ). The formation of glasses on cooling tends to be a general characteristic of the ambient temperature dialkylimidazolium derived ILs, in most cases, the glass transition temperatures are in the region  $-80$  to  $100\text{ }^{\circ}\text{C}$  for a wide range of anions and with alkyl chain lengths varying from butyl to decyl.<sup>29,31,32</sup> On heating **4** from the glassy low temperature state, an exothermic event associated with crystallization was observed at  $-34\text{ }^{\circ}\text{C}$ , followed by a melting transition at  $-5\text{ }^{\circ}\text{C}$ . This behavior could not be reproduced for the intermediate chain-length materials (**2** and **3**), although intermediate melting points (between  $-5$  and  $40\text{ }^{\circ}\text{C}$ ) would be predicted based on the general trends in melting points for ILs.<sup>33</sup>

Fig. 3 shows thermogravimetric analysis traces of the methyl sulfate and ethyl sulfate ILs. In all cases, the ILs show a gradual continuous 7–16% weight loss between 50 and  $350\text{ }^{\circ}\text{C}$ , followed by the main catastrophic weight loss event around  $350\text{--}400\text{ }^{\circ}\text{C}$  associated with decomposition of the IL cation. There appear to be no significant differences between the stability of the methyl sulfate- and ethyl sulfate-containing ILs. Both series of anions display a mass loss over the temperature range  $100\text{--}350\text{ }^{\circ}\text{C}$ , this is shown in Table 1, expressed as a percentage of the initial mass. The methyl sulfate-containing salts lose between 7–9 wt%, whereas the ethyl sulfate-containing ILs display mass losses between 13–16 wt%. These



**Fig. 3** Thermogravimetric trace for the ILs synthesized showing, in each case, the gradual continuous 7–16% weight loss between  $50\text{--}350\text{ }^{\circ}\text{C}$ , followed by decomposition between  $350\text{--}400\text{ }^{\circ}\text{C}$ .

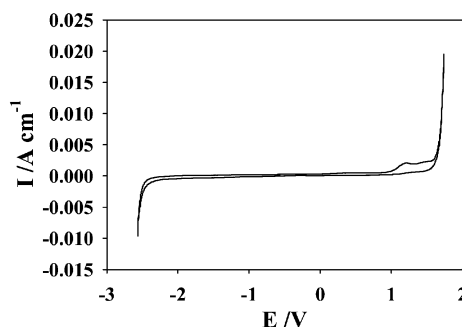
losses correspond to 16–22 and  $32\text{--}42\text{ g mol}^{-1}$ , respectively, for the methyl sulfate and ethyl sulfate ILs, and represent slow, thermal degradation of the anion to sulfate or hydrogensulfate.

### Solubility behavior

All of the salts prepared were miscible with water, and other polar solvents (for example, dichloromethane, acetonitrile and ethanol). This is similar to other hydrophilic ILs.<sup>34</sup> Interestingly, the ILs were readily miscible with acetone, whereas the solid salts (**1**, **9**, **10**) did not dissolve in acetone at room temperature. Again, this behavior closely resembles that of imidazolium chlorides;  $[\text{C}_2\text{mim}]\text{Cl}$  and  $[\text{C}_4\text{mim}]\text{Cl}$  can be crystallized from acetone solution, or precipitated by metathesis from the corresponding  $[\text{PF}_6]^-$  salts with lithium chloride in acetone.

### Electrochemistry

The electrochemical window of **5** was measured by cyclic voltammetry at room temperature. The cyclic voltammogram (Fig. 4) of the IL shows reductive and oxidative limits of  $-2.5$  and  $+1.75\text{ V}$ , respectively, relative to a  $\text{Ag}/\text{Ag}^+$  reference, which gives an electrochemical potential window of over 4 V. The reductive limit is consistent with reduction of the imidazolium cation, and occurs at the same potential seen in other ILs.<sup>10,16,35</sup> The oxidative limit, corresponds to decomposition of the ethyl sulfate anion.



**Fig. 4** Cyclic voltammogram of 1-ethyl-3-methylimidazolium ethyl sulfate (**5**), relative to  $\text{Ag}/\text{Ag}^+$  reference electrode, at  $22\text{ }^{\circ}\text{C}$  with glassy carbon working electrode and Pt counter electrode.

### Single crystal X-ray structure of 1,3-dimethylimidazolium methyl sulfate

Crystals of **1** suitable for X-ray diffraction were obtained by heating a 10 g sample of the salt to  $50\text{ }^{\circ}\text{C}$  under nitrogen and

then allowing the molten salt to cool to room temperature. There are surprisingly few published crystal structures of salts containing either 1,3-dialkylimidazolium cations or methyl sulfate anions. Single crystal structures of seven organic methyl sulfate salts were found in a search of the Cambridge Crystallographic Database, and the only 1,3-dimethylimidazolium salt structure reported is for the chloride salt,<sup>21</sup> in which each chloride ion displays extensive hydrogen-bonding to five imidazolium cations.

The crystal structure of **1** (Fig. 5) is comprised of two hydrogen-bonded cation–anion chains aligned in opposite directions, hydrogen bonded together to form ribbons. The only significant hydrogen bonds present are short contacts between the acidic ring-hydrogens C(2), C(4) and C(5), and the three terminal oxygen atoms of the sulfate anion. Each imidazolium cation participates in three hydrogen-bonds; two of which propagate the chain, while the third cross-links to the second chain, forming the discrete linear ribbon. The shortest donor...acceptor distances and donor–H...acceptor angles are shown in Table 2.

**Table 2** Hydrogen-bond distances (Å) and angles (°) from the crystal structure of **1**.

| Donor–<br>H...Ac<br>= ceptor | D–H/Å | H...A/Å | D...A/Å | D–H...A/° |
|------------------------------|-------|---------|---------|-----------|
| C(2)–H...O                   | 0.959 | 2.230   | 3.157   | 162       |
| C(4)–H...O                   | 0.888 | 2.253   | 3.139   | 175       |
| C(5)–H...O <sup>a</sup>      | 0.883 | 2.392   | 3.253   | 165       |

<sup>a</sup> Cross-chain hydrogen-bond in ribbon structure which connects the strands.

All the observed close-contacts are intra-ribbon hydrogen-bonds; no significant close contacts are observed at distances less than the sum of the van der Waals radii between atoms in adjacent ribbons. The absence of inter-ribbon hydrogen-bond stabilization may be significant in explaining the low melting points observed for **1**, compared to the corresponding chloride salt, since a melting mechanism could be envisaged in which the initial step involves breaking of weak van der Waals interactions between the ribbons, rather than the stronger combination of electrostatic and hydrogen-bonded interactions within the chains.

## Metathesis

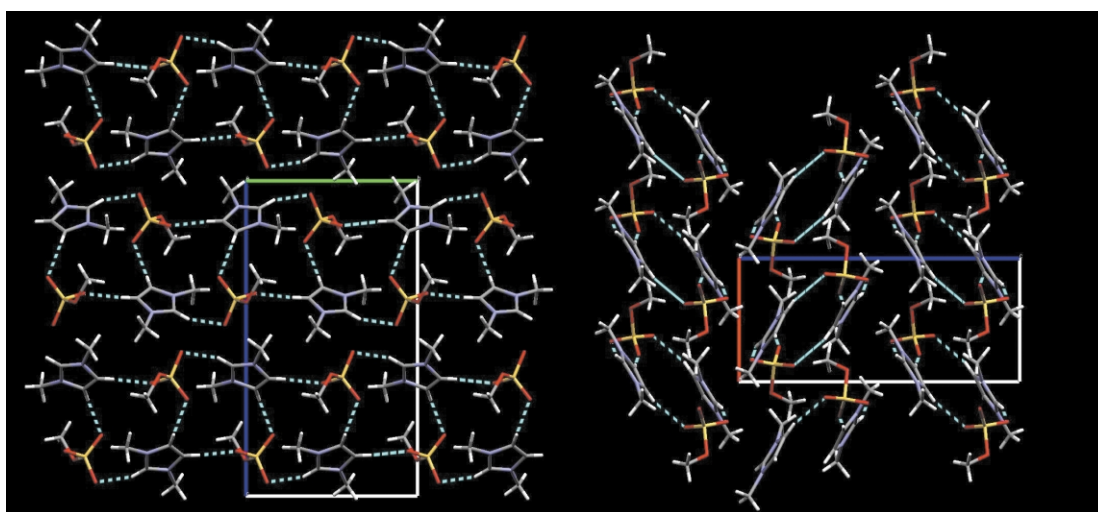
In addition to the simple, rapid synthesis, these alkyl sulfate ILs can be used as intermediates to prepare other ionic liquids by metathesis. The use of these new water soluble ILs as intermediates for the preparation of other ILs by metathesis was demonstrated by synthesizing the crystalline solid, [C<sub>1</sub>mim][PF<sub>6</sub>], and hydrophobic IL, [C<sub>4</sub>mim][PF<sub>6</sub>], from **1** and **4**, respectively, with hexafluorophosphoric acid.

In this metathesis, forming a hydrophobic IL, the alkyl sulfate salt can be used as an alternative to the corresponding chloride salt. The two steps, synthesis of alkyl sulfate ILs and metathesis can be segued into a semi-continuous batch process: imidazolium alkyl sulfate is prepared, the upper toluene later decanted, and the ionic liquid diluted with water. Hexafluorophosphoric acid is then added and the hexafluorophosphate IL is collected as the lower layer. In practice, using the procedure described, [C<sub>4</sub>mim][PF<sub>6</sub>] can be prepared in large quantities from commercially available starting materials (1-butylimidazole, dimethyl sulfate and hexafluorophosphoric acid) in less than 2 h, under ambient conditions with no heating.

These alkyl sulfate ILs can also be used in the preparation of other, hydrophilic ILs by metathesis in non-aqueous solvents. Results will be reported separately.

## Conclusions

Six new ambient temperature ILs are described which possess a number of desirable features, namely ease of preparation, low cost, wide electrochemical window, and air stability. In addition, and importantly, these ILs are intrinsically chloride-free, which offers a number of benefits for the development of new IL-based technologies. They can also be used in place of the respective halide salts when preparing other ILs by metathesis (for example, for synthesis of [C<sub>4</sub>mim][PF<sub>6</sub>]). The initial synthesis of these ILs is atom efficient and produces no waste, using the ILs for a subsequent metathesis step does produce a molar equivalent of salt (or acid) waste, but even in these non-optimized bench-top experiments, the overall process is quicker, less expensive and simpler than the corresponding synthesis *via* the conventional halide route, which can lead to cost and energy efficiencies through process intensification.



**Fig. 5** The crystal structure of **1** shows hydrogen-bonded chains along the *b* axis, comprising of two strands of hydrogen-bonded cations and anions in the view down the *a* axis (left) and the stacking of the ribbons along the *a* axis in the view down the *b* axis (right). No significant hydrogen-bonding contacts between adjacent chains are observed at distances less than the sum of the van der Waals radii.

## Experimental

Diethyl sulfate and dimethyl sulfate (Aldrich) were used as supplied, 1-methylimidazole (Aldrich) was vacuum distilled from CaH prior to use. Other 1-alkylimidazoles (ethyl, propyl, butyl) were prepared by condensation of formaldehyde, glyoxal, ammonium carbonate and the corresponding alkylamine using literature methods<sup>36</sup> and were isolated by distillation as colorless liquids in 40–60% yields. Infrared spectra were recorded as liquid films KBr plates on a Bio-Rad FTS-185 infrared spectrometer. <sup>1</sup>H and <sup>13</sup>C NMR spectra were recorded on Bruker WM500, AM500 and AM360 spectrometers in CDCl<sub>3</sub> relative to tetramethylsilane as an internal standard. Melting points and glass transition temperatures were determined by differential scanning calorimetry (TA 2620 DSC equipped with cryostat cooling, 5–20 mg samples, 5 °C min<sup>-1</sup> heating and cooling rates). Thermal decomposition profiles were collected by thermogravimetric analysis (TA 2950 TGA, 10 °C min<sup>-1</sup> heating rate under nitrogen). Cyclic voltammetry was carried out using an EG&G model 283 potentiostat/galvanostat at a glassy carbon disk electrode under nitrogen at ambient temperature (22 °C) with a platinum coil counter electrode and silver wire reference electrode (relative to 0.1 M AgNO<sub>3</sub> in [C<sub>4</sub>mim][NO<sub>3</sub>]).

Dialkylimidazolium alkyl sulfate ([1-R-3-R'-im][R'SO<sub>4</sub>]) ILs were prepared from 1-R-imidazole (R = methyl, ethyl, propyl, butyl) and R'SO<sub>4</sub> (R' = methyl and ethyl) by reaction of the dialkyl sulfate with the corresponding 1-alkylimidazole in toluene at room temperature. The reactions are spontaneous, and toluene was used as a diluent and heat-sink to moderate the highly exothermic reactions. A typical procedure, for the synthesis of 1-ethyl-3-methylimidazolium ethyl sulfate (**5**) from 1-methylimidazole and diethyl sulfate is described below.

### 1-Ethyl-3-methylimidazolium ethyl sulfate (**5**)

Diethyl sulfate (29 mL, 0.221 mol) was added dropwise to a solution of 1-methylimidazole (18.146 g, 0.221 mol) in toluene (100 mL) cooled in an ice-bath under dinitrogen at a rate to maintain the reaction temperature below 40 °C. **CAUTION! The reaction is highly exothermic.** Formation of the IL product was immediate and caused the initially clear solution to become opaque, followed by biphasic separation of the toluene solution and formation of a denser IL phase. After addition of the diethyl sulfate, the reaction mixture was stirred at room temperature for 1 h. The upper, organic phase was decanted and the lower, IL phase was washed with toluene (50 mL), dried with heating at 75 °C under reduced pressure to remove residual organic solvents, and finally *in vacuo* to yield the resulting 1-ethyl-3-methylimidazolium ethyl sulfate IL as a colorless hygroscopic liquid (48.2 g, 92%), free from starting materials. <sup>1</sup>H NMR, δ<sub>H</sub> (360 MHz, CDCl<sub>3</sub>) 1.279 (3H, t, NCH<sub>2</sub>CH<sub>3</sub>), 1.566 (3H, t, OCH<sub>2</sub>CH<sub>3</sub>), 4.028 (3H, s, NCH<sub>3</sub>), 4.067 (2H, q, OCH<sub>2</sub>), 4.333 (2H, q, NCH<sub>2</sub>), 7.617 (2H, s, C(4,5)H), 9.441 (1H, s, C(2)H). <sup>13</sup>C NMR, δ<sub>C</sub> (360 MHz, CDCl<sub>3</sub>) 13.7 (NCH<sub>2</sub>CH<sub>3</sub>), 14.0 (OCH<sub>2</sub>CH<sub>3</sub>), 34.6 (NCH<sub>3</sub>), 43.4 (NCH<sub>2</sub>CH<sub>3</sub>), 61.5 (OCH<sub>2</sub>CH<sub>3</sub>), 120.9, 122.4 (C(5)H, C(4)H), 135.0 (C(2)H). IR (liquid film) ν<sub>max</sub>/cm<sup>-1</sup>; 3149, 3106, 2933, 2861, 1678, 1574, 1467, 1380, 1339, 1227, 1170, 1060, 1019, 916, 852, 740.

### 1,3-Dimethylimidazolium methyl sulfate (**1**)

1-Methylimidazole (35.0 g, 0.423 mol) and dimethyl sulfate (41.0 mL, 0.433 mol) in toluene (150 mL) yielded **1** as colorless crystals (86.3 g, 98%). <sup>1</sup>H NMR, δ<sub>H</sub> (360 MHz, CDCl<sub>3</sub>) 3.685 (3H, s, OCH<sub>3</sub>), 3.991 (6H, s, NCH<sub>3</sub>), 7.610 (2H, d, *J* 1.62 Hz, C(4,5)H), 9.269 (1H, s, C(2)H).

### 1-Ethyl-3-methylimidazolium methyl sulfate (**2**)

1-Ethylimidazole (4.3 g, 0.0448 mol) and dimethyl sulfate (5 mL, 0.053 mol) in toluene (45 mL) yielded **2** as a colorless liquid (9.2 g, 93%). <sup>13</sup>C NMR, δ<sub>C</sub> (360 MHz, CDCl<sub>3</sub>) 13.6 (NCH<sub>2</sub>CH<sub>3</sub>), 35.2 (NCH<sub>3</sub>), 43.4 (NCH<sub>2</sub>CH<sub>3</sub>), 53.4 (OCH<sub>3</sub>), 121.3, 122.4 (C(5)H, C(4)H), 136.0 (C(2)H).

### 1-Propyl-3-methylimidazolium methyl sulfate (**3**)

1-Propylimidazole (11.41 g, 0.104 mol) and dimethyl sulfate (9.8 mL, 0.104) in toluene (70 mL) yielded **3** as a colorless liquid (21.4 g, 87%). <sup>13</sup>C NMR, δ<sub>C</sub> (500 MHz, CDCl<sub>3</sub>) 8.9 (NCH<sub>2</sub>CH<sub>2</sub>CH<sub>3</sub>), 21.8 (NCH<sub>2</sub>CH<sub>2</sub>CH<sub>3</sub>), 34.4 (NCH<sub>3</sub>), 49.3 (NCH<sub>2</sub>CH<sub>3</sub>), 52.4 (OCH<sub>3</sub>), 121.1, 122.2 (C(5)H, C(4)H), 135.2 (C(2)H).

### 1-Butyl-3-methylimidazolium methyl sulfate (**4**)

1-Butylimidazole (10.45 g, 0.0840 mol) and dimethyl sulfate (10.6 mL, 0.112 mol) in toluene (60 mL) yielded **4** as a colorless liquid (18.0 g, 86%). <sup>1</sup>H NMR, δ<sub>H</sub> (360 MHz, CDCl<sub>3</sub>) 0.935 (3H, t, *J* 7.2 Hz, CH<sub>2</sub>CH<sub>3</sub>), 1.352 (2H, m, CH<sub>2</sub>CH<sub>3</sub>), 1.881 (2H, m, CH<sub>2</sub>CH<sub>2</sub>), 3.370 (3H, s, NCH<sub>3</sub>), 3.710 (3H, s, OCH<sub>3</sub>), 4.260 (2H, t, *J* 7.33 Hz, NCH<sub>2</sub>), 7.580 (1H, t, *J* 1.73 Hz, C(4)H), 7.630 (1H, t, *J* 1.78 Hz, C(5)H), 9.418 (1H, s, C(2)H); <sup>13</sup>C NMR, δ<sub>C</sub> (500 MHz, CDCl<sub>3</sub>) 12.8 (NCH<sub>2</sub>CH<sub>2</sub>CH<sub>2</sub>CH<sub>3</sub>), 18.8 (NCH<sub>2</sub>CH<sub>2</sub>CH<sub>2</sub>CH<sub>3</sub>), 21.5 (NCH<sub>2</sub>CH<sub>2</sub>CH<sub>2</sub>CH<sub>3</sub>), 35.6 (NCH<sub>3</sub>), 49.0 (NCH<sub>2</sub>CH<sub>2</sub>CH<sub>2</sub>CH<sub>3</sub>), 53.6 (OCH<sub>3</sub>), 122.0, 123.4 (C(5)H, C(4)H), 136.4 (C(2)H).

### 1-Ethyl-3-ethylimidazolium ethyl sulfate (**6**)

1-Ethylimidazole (4.3 g, 0.0448 mol) and diethyl sulfate (6.5 mL, 0.050 mol) in toluene (35 mL) yielded **6** as a colorless liquid (11.0 g, 98%). <sup>13</sup>C NMR, δ<sub>C</sub> (500 MHz, CDCl<sub>3</sub>) 12.7 (NCH<sub>2</sub>CH<sub>3</sub>), 14.0 (OCH<sub>2</sub>CH<sub>3</sub>), 42.4 (NCH<sub>2</sub>CH<sub>3</sub>), 61.1 (OCH<sub>2</sub>CH<sub>3</sub>), 122.1 (C(5)H, C(4)H), 136.3 (C(2)H).

### 1-Propyl-3-ethylimidazolium ethyl sulfate (**7**)

1-Propylimidazole (9.5 g, 0.0863 mol) and diethyl sulfate (13.32 mL) in toluene (70 mL, 0.102 mol) yielded **7** as a colorless liquid (21.3 g, 93%). <sup>13</sup>C NMR, δ<sub>C</sub> (360 MHz, CDCl<sub>3</sub>) 9.6 (NCH<sub>2</sub>CH<sub>2</sub>CH<sub>3</sub>), 14.2 (NCH<sub>2</sub>CH<sub>3</sub>, OCH<sub>2</sub>CH<sub>3</sub>), 24.6 (NCH<sub>2</sub>CH<sub>2</sub>CH<sub>3</sub>), 32.6 (NCH<sub>2</sub>CH<sub>3</sub>), 44.0 (NCH<sub>2</sub>CH<sub>2</sub>CH<sub>3</sub>), 50.2 (NCH<sub>2</sub>CH<sub>3</sub>), 62.1 (OCH<sub>2</sub>CH<sub>3</sub>), 121.5, 121.8 (C(5)H, C(4)H), 135.2 (C(2)H).

### 1-Butyl-3-ethylimidazolium ethyl sulfate (**8**)

1-Butylimidazole (13 g, 0.1047 mol) and diethyl sulfate (16.15 mL, 0.123 mol) in toluene (70 mL) yielded **8** as a colorless liquid (27.2 g, 94%). <sup>1</sup>H NMR, δ<sub>H</sub> (500 MHz, CDCl<sub>3</sub>) 0.943 (3H, t, *J* 7.12 Hz, CH<sub>2</sub>CH<sub>3</sub>), 1.280 (3H, t, *J* 7.14 Hz, OCH<sub>2</sub>CH<sub>3</sub>), 1.370 (2H, m, CH<sub>2</sub>CH<sub>3</sub>), 1.573 (3H, t, *J* 7.14 Hz, NCH<sub>2</sub>CH<sub>3</sub>), 1.888 (2H, m, CH<sub>2</sub>CH<sub>2</sub>), 4.093 (2H, q, *J* 7.14 Hz, OCH<sub>2</sub>CH<sub>3</sub>), 4.285 (2H, t, *J* 7.7 Hz, NCH<sub>2</sub>CH<sub>2</sub>), 4.360 (2H, q, *J* 7.69 Hz, NCH<sub>2</sub>CH<sub>3</sub>), 7.561 (1H, d, 1.64 Hz, C(4)H), 7.652 (1H, d, 1.64 Hz, C(5)H), 9.562 (1H, s, C(2)H); <sup>13</sup>C NMR, δ<sub>C</sub> (500 MHz, CDCl<sub>3</sub>) 12.6 (NCH<sub>2</sub>CH<sub>2</sub>CH<sub>2</sub>CH<sub>3</sub>), 14.4, 14.8 (NCH<sub>2</sub>CH<sub>3</sub>, OCH<sub>2</sub>CH<sub>3</sub>), 18.6 (NCH<sub>2</sub>CH<sub>2</sub>CH<sub>2</sub>CH<sub>3</sub>), 31.3 (NCH<sub>2</sub>CH<sub>2</sub>CH<sub>2</sub>CH<sub>3</sub>), 44.2 (NCH<sub>2</sub>CH<sub>2</sub>CH<sub>2</sub>CH<sub>3</sub>), 48.8

(NCH<sub>2</sub>CH<sub>3</sub>), 62.2 (OCH<sub>2</sub>CH<sub>3</sub>), 121.7, 121.9 (C(5)H), C(4)H), 135.4 (C(2)H).

### 1,2,3-Trimethylimidazolium methyl sulfate (9)

1,2-Dimethylimidazole (10g, 0.1042 mol) and dimethyl sulfate (9.86 mL, 0.104 mol) yielded **9** as a colorless precipitate (22.4 g, 97%). <sup>13</sup>C NMR, δ<sub>C</sub> (500 MHz, CDCl<sub>3</sub>) 9.0 (C(2)CH<sub>3</sub>), 35.2 (NCH<sub>3</sub>), 54.0 (OCH<sub>3</sub>), 122.2 (C(4,5)H), a resonance from the tertiary C(2) nucleus was not observed.

### 1-Ethyl-2,3-dimethylimidazolium ethyl sulfate (10)

1,2-Dimethylimidazole (31.7 g, 0.330 mol) and dimethyl sulfate (43 mL, 0.328 mol) in toluene (70 mL) yielded **10** as a colorless solid (79.3 g, 96%). <sup>13</sup>C NMR (500 MHz, CDCl<sub>3</sub>) 9.5 (C(2)CH<sub>3</sub>), 14.9 (NCH<sub>2</sub>CH<sub>3</sub>), 15.1 (OCH<sub>2</sub>CH<sub>3</sub>), 35.1 (NCH<sub>3</sub>), 43.5 (NCH<sub>2</sub>CH<sub>3</sub>), 62.7 (OCH<sub>2</sub>CH<sub>3</sub>), 120.4, 122.8 (C(4)H, C(5)H), 143.5 (C(2)CH<sub>3</sub>).

### 1,3-Dimethylimidazolium hexafluorophosphate

To a solution of 1,2-dimethylimidazolium methyl sulfate (**1**, 23.6 g, 0.1135 mol) in water (100 mL) was added hexafluorophosphoric acid (16.5 mL, 64 wt% solution in water) with stirring, followed by a solution of sodium hydroxide (4.5 g, 0.1125 mol) in water (50 mL). Colorless crystals of 1,3-dimethylimidazolium hexafluorophosphate precipitated on cooling to 4 °C, and were collected by filtration. <sup>1</sup>H and <sup>13</sup>C NMR, and mp (87 °C, lit. 89 °C<sup>37</sup>) were consistent with formation of the hexafluorophosphate salt. A solid–solid transition at 61 °C was also observed prior to melting by DSC.

### 1-Butyl-3-methylimidazolium hexafluorophosphate

To a solution of **4** (5.0 g, 0.02 mol) in water (30 mL) was added dropwise with rapid stirring, hexafluorophosphoric acid (3.0 mL, 64 wt% solution in water), followed by sodium hydroxide (0.8 g, 0.02 mol) in water (50 mL). The IL separated from the reaction mixture as a colorless dense phase. The upper aqueous phase was decanted and the hydrophobic IL was washed with water (3 × 30 mL), then dried with heating *in vacuo* for 6–8 h at 60 °C. The IL produced was identical to that prepared by metathesis from [C<sub>4</sub>mim]Cl.<sup>2,31</sup>

### X-Ray structure of 1,3-dimethylimidazolium methyl sulfate (1)

A colorless single crystal (0.32 × 0.21 × 0.09 mm) was obtained by crystallization from the molten salt. Diffraction data was collected on a Siemens CCD area detector-equipped diffractometer with Mo-Kα (λ = 0.71073 Å) radiation at –100 °C using a stream of nitrogen gas. The crystal structure was solved by direct methods using the SHELXTL software package. All non-hydrogen atoms were anisotropically refined and all hydrogen atoms were located using difference Fourier maps and isotropically refined. *Crystal Data for 1*: formula C<sub>6</sub>H<sub>12</sub>N<sub>2</sub>O<sub>4</sub>S, *M* = 372.49, orthorhombic, space group *P*2<sub>1</sub>2<sub>1</sub>2<sub>1</sub> (no. 19), *a* = 6.2418(16), *b* = 9.747(2), *c* = 15.951(4) Å, *V* = 970.4(4) Å<sup>3</sup>, *T* = 173 K, *Z* = 4, μ(Mo-Kα) = 0.321 mm<sup>–1</sup>, *R*<sub>1</sub> = 0.0285, *wR*<sub>2</sub> = 0.0580 (*I* > 2σ(*I*)).

CCDC 190288. See <http://www.rsc.org/suppdata/gc/b2/b204469b/> for crystallographic data in CIF or other electronic format.

## Acknowledgments

This research has been supported by the U.S. Environmental Protection Agency's STAR program through grant number R-82825701-0. (Although the research described in this article has been funded in part by EPA, it has not been subjected to the Agency's required peer and policy review and therefore does not necessarily reflect the views of the Agency and no official endorsement should be inferred.) Additional support was provided to the Center for Green Manufacturing from the National Science Foundation Grant EPS-9977239.

## References

- See, for example: *Ionic Liquids: Industrial Applications for Green Chemistry*, ed. R. D. Rogers and K. R. Seddon, ACS Symposium Series 818, American Chemical Society, Washington DC, 2002.
- J. G. Huddleston, H. D. Willauer, R. P. Swatloski, A. E. Visser and R. D. Rogers, *Chem. Commun.*, 1998, 1765; A. E. Visser, R. P. Swatloski, W. M. Reichert, S. T. Griffin and R. D. Rogers, *Ind. Eng. Chem. Res.*, 2000, **39**, 3596.
- A. E. Visser, R. P. Swatloski, S. T. Griffin, D. H. Hartman and R. D. Rogers, *Sep. Sci. Technol.*, 2001, **36**, 785.
- K. Hong, H. Zhang, J. W. Mays, A. E. Visser, C. S. Brazel, J. D. Holbrey, W. M. Reichert and R. D. Rogers, *Chem. Commun.*, 2002, 1368.
- M. A. Klingshirn, G. A. Broker, J. D. Holbrey, K. H. Shaughnessy and R. D. Rogers, *Chem. Commun.*, 2002, 1394; C. Hardacre, J. D. Holbrey, S. P. Katdare and K. R. Seddon, *Green Chem.*, 2002, **4**, 143.
- R. P. Swatloski, S. K. Spear, J. D. Holbrey and R. D. Rogers, *J. Am. Chem. Soc.*, 2002, **124**, 4974.
- J. S. Wilkes, J. A. Levisky, R. A. Wilson and C. L. Hussey, *Inorg. Chem.*, 1982, **21**, 1263.
- B. K. M. Chan, N.-H. Chang and M. R. Grimmitt, *Aust. J. Chem.*, 1977, **30**, 2005.
- R. X. Ren and J. X. Wu, *Org. Lett.*, 2002, **3**, 3727.
- A. A. Fannin, D. A. Floreani, L. A. King, J. S. Landers, B. J. Piersma, D. J. Stech, R. L. Vaughn, J. S. Wilkes and J. L. Williams, *J. Phys. Chem.*, 1984, **88**, 2614.
- J. S. Wilkes and M. J. Zaworotko, *Chem. Commun.*, 1992, 965.
- K. R. Seddon, A. Stark and M.-J. Torres, *Pure Appl. Chem.*, 2001, **72**, 2275.
- Y. Chauvin and H. Olivier-Bourbigou, *CHEMTECH*, 1995, 30.
- T. Welton, *Chem. Rev.*, 1999, **99**, 2071; J. D. Holbrey and K. R. Seddon, *Clean Prod. Proc.*, 1999, **1**, 223; P. Wasserscheid and W. Keim, *Angew. Chem., Int. Ed.*, 2000, **39**, 3772; R. Sheldon, *Chem. Commun.*, 2001, 2399; C. M. Gordon, *Appl. Catal. A*, 2001, **222**, 101.
- A. S. Larsen, J. D. Holbrey, F. S. Tham and C. A. Reed, *J. Am. Chem. Soc.*, 2000, **122**, 7264.
- (a) P. Bonhôte, A. P. Dias, N. Papageorgiou, K. Kalyanasundaram and M. Grätzel, *Inorg. Chem.*, 1996, **35**, 1168; (b) K. R. Seddon, A. J. Carmichael and M. J. Earle, *World Pat.*, WO 01/40146, June 7 2001.
- M. Ue, M. Takeda, T. Takahashi and M. Takehara, *Electrochem. Solid-State Lett.*, 2002, **5**, A119.
- D. Delle Donne, F. Rivetti and U. Romano, *Appl. Catal. A*, 2001, **221**, 241.
- Z. Kricsfalussy, H. Waldmann and H.-J. Traenckner, *Ind. Eng. Chem. Res.*, 1998, **37**, 856.
- A. J. Ardeuengo III, *US Pat.*, 5,077,414, Dec 31, 1991.
- A. J. Ardeuengo III, H. V. R. Dias, R. L. Harlow and M. Kline, *J. Am. Chem. Soc.*, 1992, **114**, 5530.
- W. A. Herrmann, L. J. Goossen, G. R. J. Artus and C. Köcher, *Organometallics*, 1997, **16**, 2472.
- M. J. Earle and K. R. Seddon, *World Pat.*, WO 01/77081 October 18, 2001.
- W. B. McCormack and B. C. Lawes, *Sulfuric and Sulfurous Esters*, in *Kirk Othmer Encyclopedia of Chemical Technology*, Wiley, New York, 4th Edition, 1997, **vol. 23**, p. 409.
- S. H. Schöfer, N. Kaftzik, P. Wasserscheid and U. Kragl, *Chem. Commun.*, 2001, 425.
- R. A. Sheldon, R. M. Lau, M. J. Sorgedragler, F. van Rantwijk and K. R. Seddon, *Green Chem.*, 2002, **4**, 147.
- A. Bösmann, L. Datsevich, A. Jess, A. Lauter, C. Schmitz and P. Wasserscheid, *Chem. Commun.*, 2001, 2494.

- 28 L. A. Blanchard, Z. Gu and J. F. Brennecke, *J. Phys. Chem. B*, 2001, **105**, 2437.
- 29 J. D. Holbrey and K. R. Seddon, *J. Chem. Soc., Dalton Trans.*, 1999, 2133.
- 30 J. Golding, S. Forsyth, D. R. MacFarlane, M. Forsyth and G. B. Deacon, *Green Chem.*, 2002, **4**, 223.
- 31 J. G. Huddleston, A. E. Visser, W. R. Reichert, H. D. Willauer, G. A. Broker and R. D. Rogers, *Green Chem.*, 2001, **3**, 156.
- 32 C. M. Gordon, J. D. Holbrey, A. R. Kennedy and K. R. Seddon, *J. Mater. Chem.*, 1998, **8**, 2627.
- 33 J. D. Holbrey and R. D. Rogers, *Melting Points and Phase Diagrams*, in *Ionic Liquids in Synthesis*, ed. P. Wasserscheid and T. Welton, Wiley-VCH, Weinheim, 2002, pp. 41–55.
- 34 J. D. Holbrey, A. E. Visser and R. D. Rogers, *Solubility and Solvation in Ionic Liquids*, in *Ionic Liquids in Synthesis*, ed. P. Wasserscheid and T. Welton, Wiley-VCH, Weinheim, 2002, pp. 68–81.
- 35 J. Fuller, R. T. Carlin and R. A. Osteryoung, *J. Electrochem. Soc.*, 1987, **144**, 3881.
- 36 A. J. Arduengo III, *US Pat.*, 6,177,575, Jan 23, 2001.
- 37 S. V. Dzyuba and R. A. Bartsch, *Chem. Commun.*, 2001, 1466.



# Life cycle inventory analysis of hydrogen production by the steam-reforming process: comparison between vegetable oils and fossil fuels as feedstock

Maximiliano Marquovich, Guido W. Sonnemann, Francesc Castells and Daniel Montané\*

Rovira i Virgili University, Department of Chemical Engineering, Avinguda dels Països Catalans 26, 43007 – Tarragona (Catalunya), Spain. E-mail: dmontane@etseq.urv.es; Fax: (+34) 977 558 544; Tel: (+34) 977 559 652

Received 17th April 2002

First published as an Advance Article on the web 16th September 2002

A life cycle inventory analysis has been conducted to assess the environmental load, specifically CO<sub>2</sub> (fossil) emissions and global warming potential (GWP), associated to the production of hydrogen by the steam reforming of hydrocarbon feedstocks (methane and naphtha) and vegetable oils (rapeseed oil, soybean oil and palm oil). Results show that the GWPs associated with the production of hydrogen by steam reforming in a 100 years time frame are 9.71 and 9.46 kg CO<sub>2</sub>-equivalent/kg H<sub>2</sub> for natural gas and naphtha, respectively. For vegetable oils, the GWP decreases to 6.42 kg CO<sub>2</sub>-equivalent/kg H<sub>2</sub> for rapeseed oil, 4.32 for palm oil and 3.30 for soybean oil. A dominance analysis determined that the part of the process that has the largest effect on the GWP is the steam reforming reaction itself for the fossil fuel-based systems, which accounts for 56.7% and 74% of the total GWP for natural gas and naphtha, respectively. This contribution is zero for vegetable oil-based systems, for which harvesting and oil production are the main sources of CO<sub>2</sub>-eq emissions.

## Introduction

The potential of hydrogen as a clean fuel and energy carrier has made sustainable energy systems based on hydrogen a real possibility in the mid-term future, mainly if it is used with natural gas in conventional engines, and fuel cell systems are implemented at a latter stage.<sup>1</sup> Although the environmental advantages of hydrogen over fossil fuels are unquestionable when considered at a local level, the disadvantages may outweigh the benefits when considered on a global level, if hydrogen is produced by current methods. Hydrogen is produced on an industrial scale from natural gas, liquefied petroleum gas (LPG) and naphtha by catalytic steam reforming, and from heavy oil fractions by partial oxidation.<sup>2</sup> Both processes are well established, but the former is the most economical for large-scale hydrogen production.<sup>3</sup> Large amounts of carbon dioxide are generated when hydrogen is produced by steam reforming of hydrocarbons, both as a reaction byproduct and in the flue gas of the reformer furnace. The environmental benefits of a hydrogen-based energy system may therefore be questionable if the demand for hydrogen has to be covered by intensive use of fossil resources through steam reforming, which is clearly a net contributor to carbon dioxide emissions. Depending on the efficiencies of the production, distribution and use of hydrogen, the hydrogen-based scenario may even be less favorable environmentally than the direct use of fossil fuels.

We believe that the true potential of a hydrogen-based energy system may only be achieved if hydrogen is made available from renewable resources. A promising way to produce renewable hydrogen is to use liquid biofuels as feedstocks for the steam reforming process, especially for small-scale reforming for distributed energy generation systems based on fuel cells. Ethanol has been considered by several researchers for hydrogen production.<sup>4</sup> Ethanol steam reforming has been studied with different catalysts prepared from Cu, Ni, Zn and Rh

on alumina. One of the main applications is the use of ethanol as a fuel for molten carbonate<sup>5–7</sup> and polymer electrolyte<sup>8</sup> fuel cells. The production of hydrogen by steam-reforming of biomass fast-pyrolysis oil (bio-oil) has been shown to be feasible, and laboratory studies on the reforming of bio-oil fractions and model compounds have concluded that they can be effectively converted to hydrogen using commercial catalysts and technology for the steam reforming of naphtha.<sup>9–13</sup> Recently we focused on vegetable oils, which are a particular form of biomass that has already attracted considerable interest as renewable feedstock for the production of liquid fuels (bio-diesel)<sup>14–18</sup> and chemicals.<sup>19–21</sup> Due to their very low oxygen content and high hydrogen to carbon ratio, which is close to that of naphtha, vegetable oils have stoichiometric hydrogen yields that are significantly higher than those of bio-oil, which is formed by a mixture of highly oxygenated compounds. In a laboratory study using a commercial nickel-based catalyst, we have established that vegetable oils are effectively converted to hydrogen with technology that at present is used for the steam reforming of liquid hydrocarbons.<sup>22–24</sup>

## Green Context

The so-called hydrogen economy is becoming a dominant topic, with much impetus being behind a drive to move towards a hydrogen-based energy production. This paper describes the impact of this switch in terms of the impact of producing hydrogen from various sources, including petrochemical feedstocks and biomass. The biomass systems have considerably lower global warming potentials compared to the petrochemical based routes, for which the steam reforming process is a major burden. Within the biomass alternatives, considerable variations exist, the reasons for which are discussed.

DJM

In this paper we report a quantitative analysis of the environmental load, and of CO<sub>2</sub> emissions and the global warming potential (GWP), associated to the production of hydrogen by steam reforming several feedstocks. Two fossil fuels, methane and naphtha, are compared with three vegetable oils, rapeseed oil, soybean oil and palm oil. The case studied focuses on a steam-reforming plant with 50 000 Nm<sup>3</sup> h<sup>-1</sup> of hydrogen located on the Mediterranean coast of Spain, and includes feedstock production in several areas of the world and transportation to the reforming plant. We also conducted a dominance analysis to determine which parts of the process have the largest effects on the results.

## Results and discussion

The results of the LCI analysis are presented in Table 1. The table shows the figures for the most important resources consumed and emissions released by the system for the five feeds, three biomass feedstocks and two fossil fuels that are studied. Air and water emissions are expressed per kg of hydrogen produced, the resource consumption is in kg, and the total primary energy in MJ, also in terms of kg of hydrogen.

### Air emissions

Carbon dioxide is the main component of the total air emissions for both fossil and biomass feedstocks. The CO<sub>2</sub> generated when vegetable oils are steam reformed comes from biomass, and the CO<sub>2</sub> sequestered in the biomass is carried through the LCA as CO<sub>2</sub> (biomass) *versus* CO<sub>2</sub> (fossil), which results from combustion or decomposition of fossil sources. The net CO<sub>2</sub> emission from the biomass in the system is assumed to be zero: CO<sub>2</sub> generated by steam reforming vegetable oils is assumed to be offset by the uptake of CO<sub>2</sub> during biomass growth. Plants use solar energy to fix carbon from carbon dioxide during photosynthesis. It is assumed that the CO<sub>2</sub> taken up by the biomass will be released back to the environment through the decomposition of plant residue left in the field after harvesting, or in the H<sub>2</sub>-production process. Thus the net CO<sub>2</sub> balance for growing and disposal of biomass is zero. Therefore, the CO<sub>2</sub> (biomass) results are not included in the impact assessment phase for calculating greenhouse gas potential.

Systems based on fossil fuels emit 7.58 kg of CO<sub>2</sub> per kg of H<sub>2</sub>, when the feed is natural gas and 9.40 kg of CO<sub>2</sub> per kg of H<sub>2</sub> when the feed is naphtha. Biomass-based scenarios have significantly lower CO<sub>2</sub> emissions: 1.94 kg, 3.14 kg, and 2.61 kg, for rapeseed, soybean, and palm oil, respectively. This results in average savings of CO<sub>2</sub> emissions of 70% between both scenarios. For fossil fuels, approximately 72–74% of the carbon dioxide comes from the SR process, while plant operation (*i.e.*, natural gas combustion and water treatment) is the main source (60–90%) of CO<sub>2</sub> emissions for vegetable oil-based systems. Although very different models for feed transport were assumed for each system, this stage does not make an important contribution to the net CO<sub>2</sub> emissions. The lowest and highest limits for the contribution of transportation correspond to rapeseed oil and palm oil, which emit 97 g and 370 g of carbon dioxide when the amount of feed needed to produce 1 kg of H<sub>2</sub> is transported to the plant. This is 5% and 16% of the total CO<sub>2</sub> emissions for each system, respectively.

Besides CO<sub>2</sub>, other major air emissions from the systems include particulates, CO, CH<sub>4</sub>, SO<sub>x</sub>, NO<sub>x</sub>, N<sub>2</sub>O, non-methane hydrocarbons (NMHCs), and hydrogen chloride (HCl). Very few emissions, other than CO<sub>2</sub>, come from the SR process itself. For all five cases studied, most particulates (> 89%) come from the water-treatment process. Carbon monoxide emissions are primarily a result of raw material transport and are four times larger when H<sub>2</sub> is produced from palm oil or soybean oil rather than from the other feeds, since these substrates are assumed to be transported very long distances. Methane is emitted in considerable amounts by two of the five options. The natural gas-based reformer releases 86 g of methane per kg of hydrogen, with 93% of this amount originated from fugitive losses. The palm oil-based reformer releases 69 g of CH<sub>4</sub> per kg of hydrogen, 91% of which comes from the production of the palm oil. None of the other feeds surpasses 7 g of net CH<sub>4</sub> emissions per kg of hydrogen. Nitrous oxide emissions are strictly related to the production of vegetable oils. Only the rapeseed oil-based case shows significant N<sub>2</sub>O emissions (250 times the amount for soybean oil), which is caused by the extensive use of fertilizers during plant growing.

### Resource consumption and water emissions

Coal, natural gas, and oil (in ground) were chosen as the flows in the environmental inventory which indicate the depletion of

**Table 1** LCI results for H<sub>2</sub> production from fossil and biomass feedstock (for 1 kg of hydrogen produced)

| Environmental load                                    | Fossil-fuel feedstock |                       | Biomass feedstock: vegetable oils |                        |                        |                        |
|---|-----------------------|-----------------------|-----------------------------------|------------------------|------------------------|------------------------|
|   | Natural gas           | Naphtha               | Rapeseed oil                      | Soybean oil            | Palm oil               |                        |
| <b>Resources</b>                                      |                       |                       |                                   |                        |                        |                        |
| Coal (in ground)                                      | kg                    | $3.67 \times 10^{-2}$ | $1.84 \times 10^{-2}$             | $2.51 \times 10^{-1}$  | $7.24 \times 10^{-2}$  | $1.85 \times 10^{-2a}$ |
| Natural gas (in ground)                               | kg                    | 2.64                  | $6.90 \times 10^{-1}$             | $7.69 \times 10^{-1}$  | $7.04 \times 10^{-1}$  | $5.15 \times 10^{-1a}$ |
| Oil (in ground)                                       | kg                    | $1.75 \times 10^{-2}$ | 2.47                              | $-5.68 \times 10^{-3}$ | $2.18 \times 10^{-1}$  | $1.41 \times 10^{-1a}$ |
| Total primary energy                                  | MJ                    | 118.0                 | 136.4                             | 41.0                   | 42.4                   | 29.2 <sup>a</sup>      |
| <b>Air emissions</b>                                  |                       |                       |                                   |                        |                        |                        |
| Carbon dioxide (CO <sub>2</sub> , fossil)             | kg                    | 7.58                  | 9.40                              | 1.94                   | 3.14                   | 2.61                   |
| Carbon monoxide (CO)                                  | g                     | 1.71                  | 1.04                              | 1.07                   | 3.98                   | 4.09                   |
| Hydrocarbons (except methane)                         | g                     | 2.05                  | $1.96 \times 10^1$                | $6.04 \times 10^{-1}$  | $1.03 \times 10^1$     | 5.61                   |
| Hydrogen chloride (HCl)                               | g                     | $1.49 \times 10^{-2}$ | $1.60 \times 10^{-2}$             | $4.62 \times 10^{-2}$  | $4.77 \times 10^{-2}$  | $1.49 \times 10^{-2a}$ |
| Methane (CH <sub>4</sub> )                            | g                     | $8.64 \times 10^1$    | 2.04 <sup>a</sup>                 | 6.33                   | 5.85                   | $6.94 \times 10^1$     |
| Nitrogen oxides (NO <sub>x</sub> as NO <sub>2</sub> ) | g                     | 3.21                  | 8.15                              | -2.17                  | 9.05                   | $1.60 \times 10^1$     |
| Nitrous oxide (N <sub>2</sub> O)                      | g                     | $1.79 \times 10^{-2}$ | $1.38 \times 10^{-2a}$            | $1.35 \times 10^1$     | $4.65 \times 10^{-2}$  | $1.42 \times 10^{-2a}$ |
| Particulates (unspecified)                            | g                     | 63.9                  | 81.8                              | 86.5                   | 86.7                   | 91.9                   |
| Sulfur oxides (SO <sub>x</sub> as SO <sub>2</sub> )   | g                     | $8.14 \times 10^{-1}$ | 2.97                              | -5.25                  | $1.11 \times 10^1$     | $1.38 \times 10^1$     |
| <b>Water emissions</b>                                |                       |                       |                                   |                        |                        |                        |
| Acids (H <sup>+</sup> )                               | g                     | $7.50 \times 10^{-4}$ | $3.16 \times 10^{-3}$             | $9.40 \times 10^{-4a}$ | $9.40 \times 10^{-4a}$ | $4.46 \times 10^{-3}$  |
| COD (Chemical Oxygen Demand)                          | g                     | $5.99 \times 10^{-2}$ | $9.76 \times 10^{-2}$             | $1.16 \times 10^{-2a}$ | 1.25                   | 4.51                   |
| Oils (unspecified)                                    | g                     | $1.52 \times 10^{-1}$ | $2.14 \times 10^{-2a}$            | $2.42 \times 10^{-2a}$ | $2.65 \times 10^{-2a}$ | $1.65 \times 10^{-1}$  |

<sup>a</sup> Values with less reliability because feed contribution is not included.



natural resources. The total primary energy, calculated from the values of these flows and expressed in MJ (Table 1), shows that fossil fuel-based systems consume approximately three times more energy from natural resources than vegetable-oil based systems. This is due to the direct use of natural gas or naphtha as process feeds.

With regard to water emissions, the total number of water pollutants was smaller than other emissions. There was no significant difference in the amount of each pollutant between feeds, except for COD (chemical oxygen demand), which was two orders of magnitude higher for vegetable oils than for natural gas or naphtha. COD is associated with eutrophication potential impact, and more than 99% of water emissions are related to the production of vegetable oils. The largest value is for palm oil, which emits 4.5 g of COD per kg of hydrogen. If COD is transformed into CO<sub>2</sub> through subsequent water treatment processes, an extra of 6.2 g of CO<sub>2</sub> are released into the atmosphere. Although not significant in comparison to the main carbon dioxide emission sources in the process, it should be added to the total emissions of carbon dioxide.

### Greenhouse gases and global warming potential

The total amount of greenhouse gases has to be quantified if the GWP of each system is to be evaluated. Although CO<sub>2</sub> is the most important greenhouse gas and is the main emission for all the systems, the GWP is a combination of CO<sub>2</sub>, CH<sub>4</sub>, and N<sub>2</sub>O emissions, as mentioned above. The GWP, as well as the contribution of each greenhouse gas, is shown in Table 2, for a 20, 100, and 500-year time frame. If the capacity of each gas to contribute to the warming of the atmosphere is taken into account, the GWP of a system can be normalized to CO<sub>2</sub>-equivalence and its overall contribution to global climate change described. It is clear from this table that CO<sub>2</sub> is the main contributor in all the systems, except for rapeseed oil and palm oil, for which feed production generates large quantities of N<sub>2</sub>O and CH<sub>4</sub>, respectively. Although CH<sub>4</sub> and N<sub>2</sub>O emissions are considerably lower than CO<sub>2</sub> emissions on a mass basis (1.94 kg

of CO<sub>2</sub>/kg of H<sub>2</sub> versus 14 g of N<sub>2</sub>O/kg of H<sub>2</sub> for rapeseed oil, and 2.61 kg of CO<sub>2</sub>/kg of H<sub>2</sub> versus 69 g of CH<sub>4</sub>/kg of H<sub>2</sub> for palm oil) both gases contribute significantly to the global GWP due to their high individual GWPs. The general trend is that biomass-based systems have significantly lower GWP than systems based on fossil fuels. Data in Table 2 also show how GPW decreases as the time frame increases. This trend is more acute for those systems whose GPW depends mainly on N<sub>2</sub>O and/or CH<sub>4</sub>. For a 100-year period, a typical frame in LCA, both natural gas and naphtha-based systems have a GPW around 9.50–9.70 kg CO<sub>2</sub>-eq/kg H<sub>2</sub>. This is in good agreement with previous studies.<sup>25</sup> In the same time frame, biomass-based systems have GWPs of 6.40, 3.30, and 4.30 kg CO<sub>2</sub>-eq/kg H<sub>2</sub> for rapeseed oil, soybean oil, and palm oil, respectively. In terms of GWP, soybean oil is the best feedstock for producing hydrogen by steam reforming of vegetable oils, since it decreases the GWP by 65% in comparison to fossil fuels. Palm oil and rapeseed oil only allow GWP reductions of 55% and 33%, respectively.

Table 3 shows a deeper analysis of the parts of the process that emit more carbon dioxide equivalents for two of the systems studied, natural gas and soybean oil. The process was divided into its 5 main steps, each of which was then analyzed for a 100-year time frame. For natural gas, the SR process accounts for 56.7% of the greenhouse gas emissions, while these emissions are zero when the source is a biomass-derived substrate like vegetable oils. For soybean oil, most emissions come primarily from the operation of the reforming plant (fuel combustion and water treatment), and account for 55% of the overall GWP. For the natural gas-based system, however, plant operation (including natural gas losses) generates 3.59 kg of CO<sub>2</sub>-eq/kg of H<sub>2</sub>, that is 37.0% of the total CO<sub>2</sub>-eq emissions. The feed production stage in the natural gas-based case emits 0.31 kg of CO<sub>2</sub>-eq/kg of H<sub>2</sub> (3.1% of total GWP), while the CO<sub>2</sub>-eq emissions during the production of soybean oil are around four times greater, that is 1.16 kg of CO<sub>2</sub>-eq/kg of H<sub>2</sub> (35.1% of total GWP of this system). The contribution of feed transport to the total GWP is similar for natural gas and soybean oil. Transport of natural gas over a 2000 km of gas pipelines

**Table 2** Global Warming Potential results for H<sub>2</sub> production from fossil and biomass feedstock, for 20, 100, and 500 years (for 1 kg of hydrogen produced)

|                  | IPCC value | GWP (kg CO <sub>2</sub> -equivalence/kg H <sub>2</sub> )<br>Fossil-fuel feedstock |                         | Biomass feedstock: vegetable oils |                         |                         |
|------------------|------------|---|-------------------------|-----------------------------------|-------------------------|-------------------------|
|                  |            | Natural gas   | Naphtha                 | Rapeseed oil                      | Soybean oil             | Palm oil                |
| 20 years         |            |   |                         |                                   |                         |                         |
| <b>TOTAL</b>     |            | <b>12.95</b>  | <b>9.53</b>             | <b>6.26</b>                       | <b>3.52</b>             | <b>6.92</b>             |
| CO <sub>2</sub>  | 1          | 7.58  | 9.40                    | 1.94                              | 3.14                    | 2.61                    |
| CH <sub>4</sub>  | 62         | 5.36  | 0.13                    | 0.39                              | 0.36                    | 4.30                    |
| N <sub>2</sub> O | 290        | 5.2 × 10 <sup>-3</sup>  | 4.0 × 10 <sup>-3</sup>  | 3.93                              | 1.35 × 10 <sup>-2</sup> | 4.1 × 10 <sup>-3</sup>  |
| 100 years        |            |   |                         |                                   |                         |                         |
| <b>TOTAL</b>     |            | <b>9.71</b>   | <b>9.46</b>             | <b>6.42</b>                       | <b>3.30</b>             | <b>4.32</b>             |
| CO <sub>2</sub>  | 1          | 7.58  | 9.40                    | 1.94                              | 3.14                    | 2.61                    |
| CH <sub>4</sub>  | 24.5       | 2.12  | 5.0 × 10 <sup>-2</sup>  | 1.5 × 10 <sup>-1</sup>            | 1.4 × 10 <sup>-1</sup>  | 1.70                    |
| N <sub>2</sub> O | 320        | 5.7 × 10 <sup>-3</sup>  | 4.4 × 10 <sup>-3</sup>  | 4.33                              | 1.5 × 10 <sup>-2</sup>  | 4.5 × 10 <sup>-3</sup>  |
| 500 years        |            |   |                         |                                   |                         |                         |
| <b>TOTAL</b>     |            | <b>8.23</b>   | <b>9.42</b>             | <b>4.42</b>                       | <b>3.20</b>             | <b>3.14</b>             |
| CO <sub>2</sub>  | 1          | 7.58  | 9.40                    | 1.94                              | 3.14                    | 2.61                    |
| CH <sub>4</sub>  | 7.5        | 6.48 × 10 <sup>-1</sup>   | 1.53 × 10 <sup>-2</sup> | 4.75 × 10 <sup>-2</sup>           | 4.39 × 10 <sup>-2</sup> | 5.21 × 10 <sup>-2</sup> |
| N <sub>2</sub> O | 180        | 3.2 × 10 <sup>-3</sup>  | 2.5 × 10 <sup>-3</sup>  | 2.44                              | 8.4 × 10 <sup>-3</sup>  | 2.6 × 10 <sup>-3</sup>  |

**Table 3** Sources of system Global Warming Potential. Greenhouse gas emissions (CO<sub>2</sub>-eq) for a 100 year time frame

| System      | Total (kg/kg of H <sub>2</sub> ) | % from feed production | % from transport | % from SR process | % from plant operation | % from electricity |
|-------------|----------------------------------|------------------------|------------------|-------------------|------------------------|--------------------|
| Natural gas | 9.71                             | 3.1                    | 2.6              | 56.7              | 37.0                   | 0.6                |
| Soybean oil | 3.30                             | 35.1                   | 7.9              | 0.0               | 55.0                   | 2.0                |

emits 0.25 kg of CO<sub>2</sub>-eq/kg of H<sub>2</sub> (2.6% of total GWP), while the transport of soybean oil emits 0.19 kg of CO<sub>2</sub>-eq/kg of H<sub>2</sub> (7.9% of total GWP). In both systems the generation of electricity accounts for less than 2% of the GWP. Finally, other parts of the process like plant construction, and decommissioning and construction of pipelines, were neglected in the life cycle analysis because of the low emissions of greenhouse gases. Their contribution to overall GWP is as low as 0.3% of the total amount.<sup>25</sup>

### Improvement opportunities

In this section we aim to identify the opportunities for reducing the environmental impact of the system, and in particular the Global Warming Potential.

The results outlined in the sections above show that plant operation accounts for 55% of the total GWP in steam reforming soybean oil. Steam reforming is a very mature technology, and changes in plant design or catalysts are not expected to improve yields, although minor changes in the process and catalysts may be needed to operate satisfactorily with vegetable oils. However, the use of biomass-derived fuels to provide heat in the furnace, instead of burning natural gas, appears to be one way of reducing CO<sub>2</sub> emissions. Regarding the choice of the vegetable oil to be used as feed, it seems extremely important to select one which minimizes N<sub>2</sub>O and CH<sub>4</sub> emissions during the crop growing or the oil production steps. Legumes like soybeans fix nitrogen more easily than other crops, leading to less fertilizer demand and lower N<sub>2</sub>O emissions. Besides, crops that need considerable amounts of fertilizers may overbalance the environmental advantages.

### Limitations of the study

In addition to the many assumptions stated, the results presented in this study are based on secondary data, *i.e.* data obtained from published sources such as databases, industry or government publications, journals, or books. Consequently, the level of reliability depends on the information used, and although these circumstances are not enough to change the global tendency of the results, the absolute values may of course differ from real situations.

## Fundamentals

### Life cycle assessment (LCA) overview

According to the United Nations Environmental Program,<sup>26</sup> life cycle assessment is the process of evaluating the effects that a product, service or activity has on the environment throughout its life cycle, commonly referred to as 'cradle-to-grave'. In the case of a product, the life cycle starts when the raw material is extracted and then includes the manufacture of intermediate products, their transportation, distribution, and utilization and their final disposal, which often refer to multiple parallel paths such as recycling, incineration, or landfill. Life Cycle Assessment (LCA) has been developed as a systematic tool to determine the impact that a product has on the environment throughout its life cycle. LCA is used to comprehensively quantify and interpret the flows to and from the environment and it is based on a balance of the inputs (consumption of raw material and energy) and the outputs (emissions and wastes as well as co-products) of the system considered. The ISO standards 14040 to 14043 outline the different phases of an LCA. According to the ISO 14000 series, an LCA involves the following steps:

- (1) the definition of the goal and the scope of the study.
- (2) the inventory, in which the inputs and outputs from a life cycle are calculated and tabulated.
- (3) the life cycle impact assessment, in which the inventory data are associated with specific environmental impacts. These are evaluated and quantified.
- (4) the interpretation, which describes the implications to decision makers.

LCA can serve to identify and quantify those aspects of a process or product that generate significant environmental burdens. Moreover, as used in the present work, it is extremely useful for comparing two or more processes that produce a common material or utility, in terms of environmental impacts.

### Functional unit and system boundaries

The functional unit, also known as the production amount, is the basis of the analysis and was chosen to be one kilogram of hydrogen produced. The system to be analyzed here and its boundaries when the feed is rapeseed oil are presented in Fig. 1. The study accounts for the production of the feedstocks, their

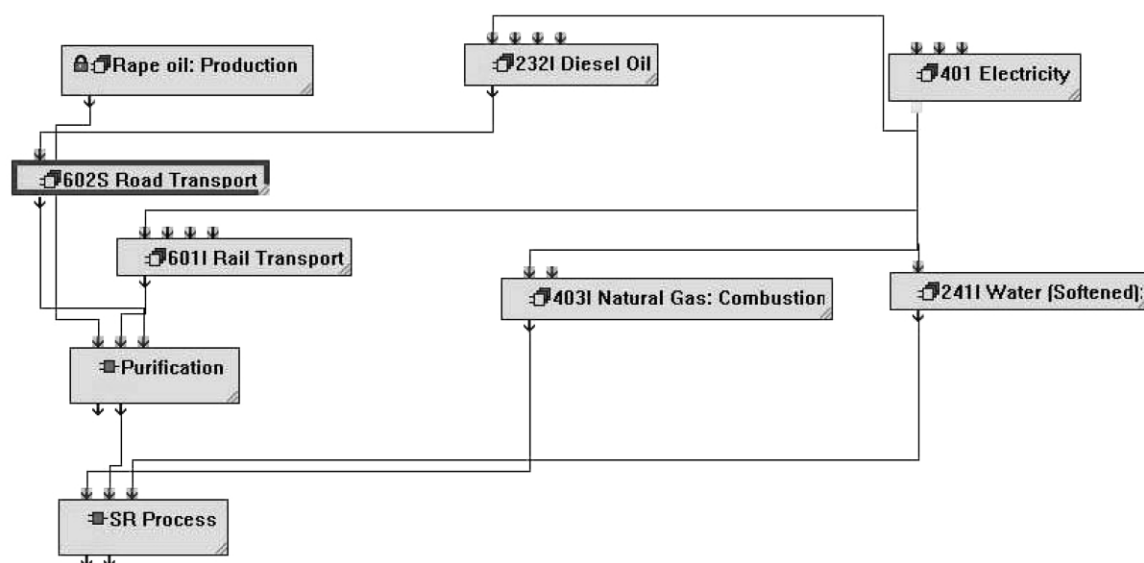


Fig. 1 System (steam reforming of rapeseed oil) and its boundaries.

transport to the plant and the steam-reforming process, including the life cycles of other main material and energy inflows. As the use and the end of life phases are not included, this is a so-called 'cradle-to-gate' study. This is justifiable because the use and end of life phases are identical for the product hydrogen. Only the feed options and their processing are different and that is why we compared them.

## Software and data

The LCA software package used to track the material, and the energy inputs and outputs between the process blocks within the system was Tools for Environmental Analysis and Management (TEAM), by Ecobilan, Inc. The life cycle inventory data for the following process blocks were available in the TEAM database, known as Data for Environmental Analysis and Management (DEAM):

- Combustion of natural gas
- Production of electricity (Europe)
- Production of softened water
- Sea transport (tanker)
- Rail transport (european average)
- Road transport (truck 16t)
- Production of heavy fuel oil
- Production of diesel oil

The data sources for DEAM were APME, ETH Zurich and BUWAL 250 and 232. The inventory data for processes within the system that were not available in DEAM or that we preferred to be taken from exactly known sources were entered manually into TEAM. Data for the following process blocks were obtained from the cited literature:

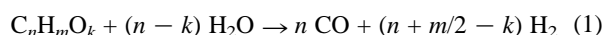
- Natural gas production, Algeria<sup>27</sup>
- Naphta production, South European situation<sup>28</sup>
- Rapeseed oil production<sup>29</sup>
- Palm oil production<sup>30</sup>
- Soybean oil production<sup>31</sup>
- Gas transport by pipeline from Algeria<sup>27</sup>

The analysis performed does not account for the catalysts or the monoethanolamine used in the CO<sub>2</sub> removal plant, since they have a minor incidence on the total balance.<sup>25</sup> Furthermore, these contributions are common for all the feedstocks studied here.

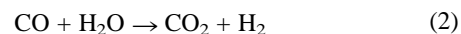
## Steam-reforming plant and utility balance

The feed used at present for the industrial steam reforming process is normally natural gas, but other hydrocarbons such as naphtha or LPG are also used. Hydrogen can also be obtained by steam reforming of vegetable oils.<sup>22</sup> Although the feasibility of using this substrate as feed for the process is still being studied, results from laboratory studies indicate that vegetable oils may be converted with existing catalysts and technology for naphtha reforming.

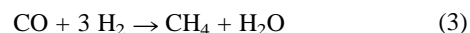
The basic steps in a conventional steam-reforming plant are the reformer, the shift converter and the purification unit. First, a synthesis gas is generated by steam reforming the organic feed, then supplementary hydrogen is generated by reacting the synthesis gas in one or more shift converters and, finally, the gas is purified by removing carbon dioxide, methanating the remaining carbon oxides, and cooling. The steam-reforming process presented here is based mainly on the data and descriptions contained in the literature.<sup>2,32,33</sup> Fig. 2 shows a flowsheet of a conventional steam-reforming process. The main stages in the process are as follows: (a) *Reforming*. After being desulfurized and purified, the feed is mixed with superheated steam over a nickel-based catalyst in the reformer. The strongly endothermic reaction occurs at temperatures above 550 °C and the process heat is supplied by radiant combustion of natural gas fuel. The steam-reforming reaction of an oxygenated feed (C<sub>n</sub>H<sub>m</sub>O<sub>k</sub>) is the following:



(b) *High and low-temperature shift*. After the reformer, the process gas mixture contains CO and H<sub>2</sub> and it passes through a heat recovery step and is fed into a water gas shift reactor to produce additional H<sub>2</sub>. Normally two stages of conversion (high temperature and low temperature) are used to reduce the CO content to a concentration of approximately 0.2–0.4 in volume percentage. This exothermic reaction occurs at temperatures ranging from 200 to 400 °C over copper–zinc and iron oxide catalysts.

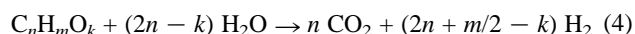


(c) *Carbon dioxide removal*. The major diluent, CO<sub>2</sub>, is removed in a scrubbing unit by means of the monoethanolamine process. The final CO<sub>2</sub> content of the product is approximately 0.1% in weight. Other processes for CO<sub>2</sub> removal such as pressure swing adsorption (PSA) are also available. (d) *Methanation*. The residual CO and CO<sub>2</sub> in the H<sub>2</sub> stream after the CO<sub>2</sub> is removed is further converted to CH<sub>4</sub> by a methanation reaction:



(e) *Cooling*. The hot product gas is cooled to 25 °C with cooling water. Water is separated and the product, containing 97–98% H<sub>2</sub> in weight, exits at 25 °C and 2.4 MPa. The main impurity of the product is methane.

The main overall chemical reaction for the steam reforming of an organic compound can be obtained by adding the reforming and shift reactions as follows.



Reaction (4) gives the utility balance for the process that is presented in Table 4. Five different feeds are listed with their respective input and output streams. Methane (CH<sub>4</sub>) and naphtha (C<sub>7</sub>H<sub>16</sub>) are the two hydrocarbons that are most widely used as feedstocks to produce hydrogen by steam reforming, while rapeseed oil (C<sub>24.4</sub>H<sub>37.6</sub>O<sub>2</sub>), soybean oil (C<sub>17.8</sub>H<sub>33</sub>O<sub>2</sub>), and palm oil (C<sub>16.9</sub>H<sub>35</sub>O<sub>2</sub>) are the alternative feeds which are

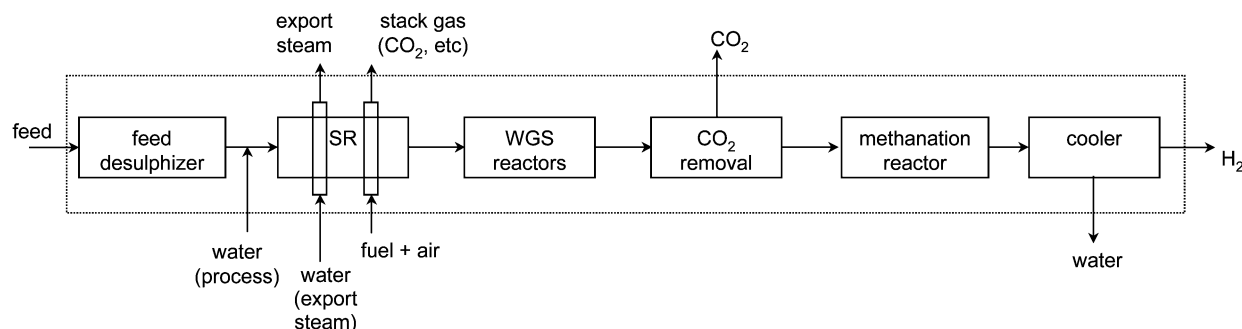


Fig. 2 Diagram of the steam-reforming process.

proposed to produce hydrogen *via* a sustainable path. For each feed, a global balance of the SR plant has been performed with the following assumptions:

- The steam-to-carbon ratio at the reformer entrance was set at the typical value of 6.
- The final product at the exit of the plant was pure hydrogen. A typical hydrogen concentration of 97% in weight is obtained.
- For simplicity in hydrogen-yield calculation, natural gas was considered as pure methane and the desulfuration unit required for natural gas and naphtha was not accounted for in the balances.
- The combustion of natural gas (fuel) to supply the energy requirements of the plant, took place in an excess of 40% air. The amount of fuel required to provide the heat duty to produce 1 kg of product was the same for all the feeds, and equivalent to 20% of the natural gas used as feed. This value, based on the literature,<sup>34,35</sup> was chosen with conservative criteria.
- No co-product credit was allocated for the export steam.

In addition to the steam reforming utility balance, gas losses through fugitive emissions have been taken into account. There is a natural gas loss of 4% in the total cradle-to-gate analysis for hydrogen,<sup>25</sup> *i.e.* about 40 g of methane is liberated per kg of natural gas. Naphtha losses were calculated in a similar manner. Around 12% of the total natural gas losses are due to fugitive

emissions from processing. Thus, assuming the same rate of losses for naphtha processing, we considered the naphtha emissions to be 5 g of unspecified hydrocarbons per kg of naphtha.

### Inventory data for feeds and transport processes

The inventory data used for the different fossil and biomass-derived feeds are presented in Table 5. Fig. 3 shows a general overview of the production steps for these feeds. The following section outlines the assumptions made in the literature for obtaining the inventory data of each feed. Particular attention is paid to the fabrication patterns since they are less familiar in LCA databases.

**Natural gas.** The life cycle inventory data of the Algerian natural gas have been used for natural gas production. These data include the exploration, extraction and processing of the natural gas. The drilling statistics on boring show that around 30% of the drill tests are successful, as the specific drill capacity  $3.2 \times 10^{-6} \text{ m m}^{-3}$  is taken into account. The main air emissions of the extraction are the emissions from the torches as well as

**Table 4** Steam-reforming process utility balance for life cycle inventory analysis. All quantities are expressed in kilograms

| Stream                             | Fossil-fuel feedstocks <sup>a</sup> |         | Vegetable oils <sup>b</sup> |             |          |
|------------------------------------|-------------------------------------|---------|-----------------------------|-------------|----------|
|                                    | Natural gas                         | Naphtha | Rapeseed oil                | Soybean oil | Palm oil |
| <b>Inputs (kg)</b>                 |                                     |         |                             |             |          |
| Feed                               | 2.00                                | 2.27    | 2.73                        | 2.78        | 2.74     |
| Water (process)                    | 13.50                               | 17.18   | 19.13                       | 19.19       | 18.51    |
| Water (export steam)               | 13.50                               | 9.82    | 7.88                        | 7.81        | 8.49     |
| Natural gas (fuel)                 | 0.40                                | 0.40    | 0.40                        | 0.40        | 0.40     |
| Air (40% excess)                   |                                     |         |                             |             |          |
| <b>Outputs (kg)</b>                |                                     |         |                             |             |          |
| Product (H <sub>2</sub> 97% wt)    | 1.00                                | 1.00    | 1.00                        | 1.00        | 1.00     |
| CO <sub>2</sub> fossil (process)   | 5.50                                | 7.00    | 0.00                        | 0.00        | 0.00     |
| Water                              | 9.00                                | 11.45   | 13.06                       | 13.15       | 12.71    |
| Export steam                       | 13.50                               | 9.82    | 7.88                        | 7.81        | 8.49     |
| CO <sub>2</sub> fossil (stack gas) | 1.07                                | 1.07    | 1.07                        | 1.07        | 1.07     |

<sup>a</sup> Natural gas is assumed to be methane (CH<sub>4</sub>) and naphtha has a chemical formula equal to C<sub>7</sub>H<sub>16</sub>. <sup>b</sup> The chemical formula of rapeseed oil, soybean oil, and palm oil are respectively (C<sub>24.4</sub>H<sub>37.6</sub>O<sub>2</sub>), (C<sub>17.8</sub>H<sub>33</sub>O<sub>2</sub>), (C<sub>16.9</sub>H<sub>35</sub>O<sub>2</sub>), which corresponds to a weighted average of the major fatty acids present in each vegetable oil.

**Table 5** Life-cycle inventory data for production of the feeds (for 1 kg of feed)

| Environmental load                                    |    | Fossil-fuel feedstock |                       | Biomass feedstock: vegetable oils |                       |                       |
|---|----|-----------------------|-----------------------|-----------------------------------|-----------------------|-----------------------|
|   |    | Natural gas           | Naphtha               | Rapeseed oil                      | Soybean oil           | Palm oil              |
| <b>Resources</b>                                      |    |                       |                       |                                   |                       |                       |
| Coal (in ground)                                      | kg | $7.60 \times 10^{-3}$ | $3.32 \times 10^{-4}$ | $8.50 \times 10^{-2}$             | $1.94 \times 10^{-2}$ | n.c. <sup>a</sup>     |
| Natural gas (in ground)                               | kg | 1.03                  | $7.82 \times 10^{-2}$ | $9.30 \times 10^{-2}$             | $6.76 \times 10^{-2}$ | n.c. <sup>a</sup>     |
| Oil (in ground)                                       | kg | $4.37 \times 10^{-3}$ | 1.05                  | $-1.75 \times 10^{-2}$            | $5.10 \times 10^{-2}$ | n.c. <sup>a</sup>     |
| Total primary energy                                  | MJ | 45.7                  | 49.8                  | 5.4                               | 10.9                  | n.c. <sup>a</sup>     |
| <b>Air emissions</b>                                  |    |                       |                       |                                   |                       |                       |
| Carbon dioxide (CO <sub>2</sub> , fossil)             | g  | $1.06 \times 10^2$    | $1.58 \times 10^2$    | $2.90 \times 10^{-1}$             | $3.99 \times 10^2$    | $1.48 \times 10^2$    |
| Carbon monoxide (CO)                                  | g  | $3.02 \times 10^{-1}$ | $8.00 \times 10^{-2}$ | $-5.51 \times 10^{-2}$            | $9.93 \times 10^{-1}$ | $9.30 \times 10^{-1}$ |
| Hydrocarbons (except methane)                         | g  | $4.24 \times 10^{-1}$ | 3.00                  | $-4.56 \times 10^{-1}$            | 3.00                  | 1.14                  |
| Hydrogen chloride (HCl)                               | g  | $8.06 \times 10^{-4}$ | $9.02 \times 10^{-4}$ | $1.15 \times 10^{-2}$             | $1.19 \times 10^{-2}$ | n.c. <sup>a</sup>     |
| Methane (CH <sub>4</sub> )                            | g  | 1.88                  | n.c. <sup>a</sup>     | 1.15                              | $5.62 \times 10^{-1}$ | $2.30 \times 10^1$    |
| Nitrogen oxides (NO <sub>x</sub> as NO <sub>2</sub> ) | g  | $5.80 \times 10^{-1}$ | 1.55                  | -1.74                             | 1.80                  | 3.40                  |
| Nitrous oxide (N <sub>2</sub> O)                      | g  | $1.33 \times 10^{-3}$ | n.c. <sup>a</sup>     | 4.95                              | $1.15 \times 10^{-2}$ | n.c. <sup>a</sup>     |
| Particulates (unspecified)                            | g  | $7.58 \times 10^{-2}$ | $2.12 \times 10^{-1}$ | $1.75 \times 10^{-1}$             | $3.65 \times 10^{-1}$ | 3.45                  |
| Sulfur oxides (SO <sub>x</sub> as SO <sub>2</sub> )   | g  | $6.73 \times 10^{-2}$ | 1.00                  | -2.24                             | 2.06                  | 1.46                  |
| <b>Water emissions</b>                                |    |                       |                       |                                   |                       |                       |
| Acids (H <sup>+</sup> )                               | g  | $2.02 \times 10^{-5}$ | $9.99 \times 10^{-4}$ | n.c. <sup>a</sup>                 | n.c. <sup>a</sup>     | $1.30 \times 10^{-3}$ |
| COD (Chemical Oxygen Demand)                          | g  | $2.53 \times 10^{-2}$ | $3.85 \times 10^{-2}$ | n.c. <sup>a</sup>                 | $4.45 \times 10^{-1}$ | 1.64                  |
| Oils (unspecified)                                    | g  | $6.27 \times 10^{-2}$ | n.c. <sup>a</sup>     | n.c. <sup>a</sup>                 | n.c. <sup>a</sup>     | $4.90 \times 10^{-2}$ |

<sup>a</sup> n.c.: not considered.

the gas emissions due to losses, ventilation and repairs. The emissions of the process to water and soil are mining waters, soil pollution by lubricating oils, fats or detergents (often dispersed through rain water) and emissions by the further treatment of the drilling sludge. The processing consists of drying and separating higher hydrocarbons. The most common drying process is the glycol-based adsorption process. The higher hydrocarbons are considered to be separated by a modern technology based on electricity.<sup>27</sup> The natural gas is assumed to be transported for an average of 2000 km through pipelines from Algeria to the South European Mediterranean coast. Natural gas is almost exclusively transported in pipelines that are powered by compressors with gas turbines. The average pipeline has been assumed to have a lifetime of 50 years.<sup>27</sup>

**Naphtha.** The main output from refineries is the naphtha fraction, which is used for petrochemical products. However, a number of cracker operators also take in a variety of other hydrocarbon products from refineries. Since the inputs and outputs of refineries are partitioned over all usable products, the

term 'refined products' has been used as the functional unit rather than naphtha, since they all have the same input and output characteristics. The inventory data that we chose correspond to the average gross inputs and outputs associated with the production of one kilogram of refinery products for the average south European case, in which all crude oil is derived from sources other than the North Sea.<sup>28</sup> Naphtha production depends on the transport of the crude oil from the extraction site to the refinery. As it has been considered that all crude oil is derived from sources other than the North Sea, an average transport of 15000 km in overseas tankers has been taken into account; 36% of the crude oil is imported from Africa to South Europe, 12% from Eastern Europe, 44% from the Middle East and only 8% from the Western hemisphere.<sup>28</sup>

**Rapeseed oil.** The inventory data for the production of rapeseed oil assumes that energy carriers are consumed as well as mineral sources, with the related airborne emissions. Co-products have been taken into account as benefits. For the farming of rapeseed, the standard German situation has been

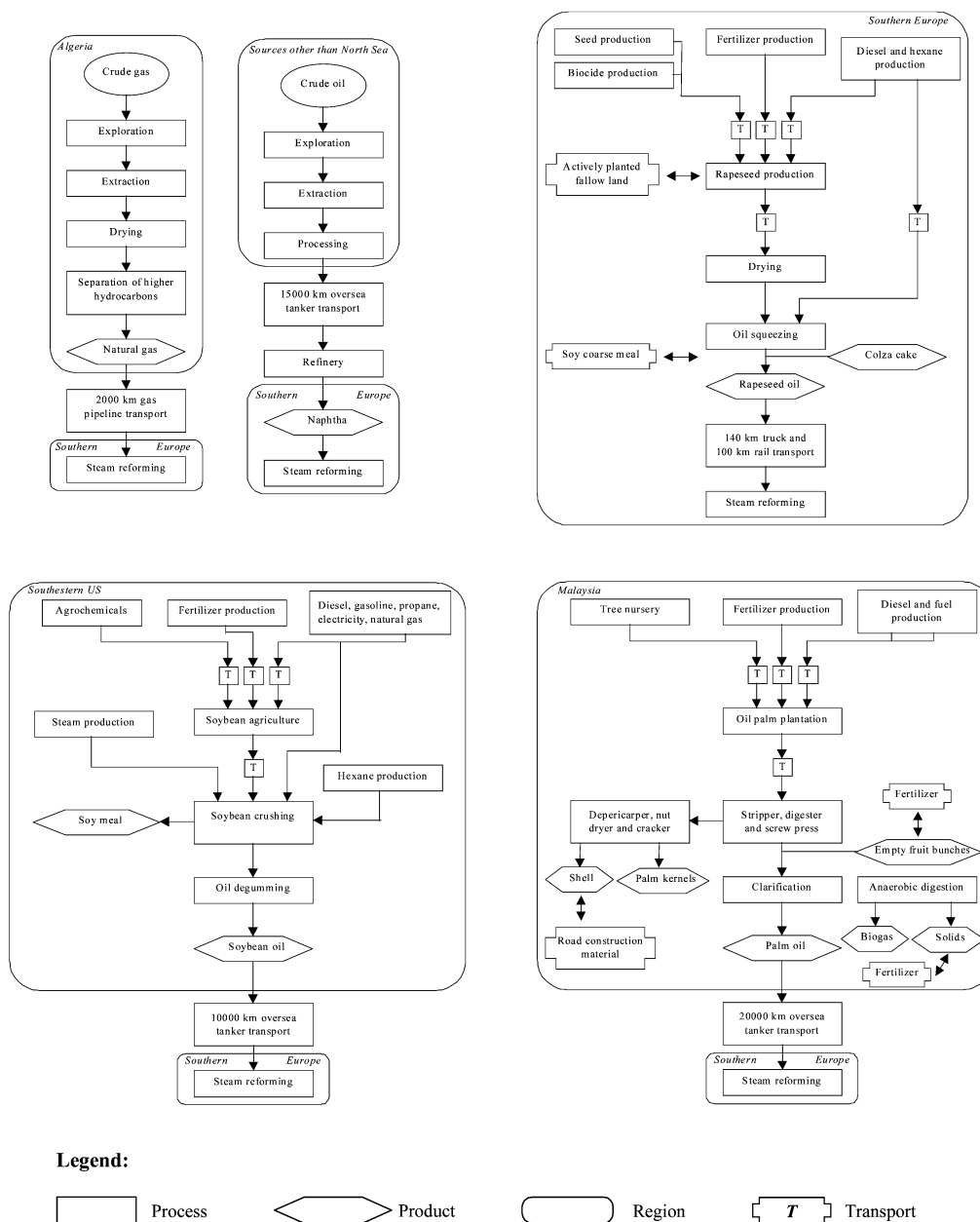


Fig. 3 Simplified flow sheet of the production steps for the considered feeds.

taken as the basis. In conventional agriculture, synthetic pesticides and a huge amount of mineral fertilizer are used. The analysis used has assumed an average yield of 3.1 tons of rapeseed per ha. The main operations assessed in the balance have been plowing, sowing, fertilizer and pesticide application, mowing and harrowing the rape stubbles. Except for the emissions from the production and application of the fertilizer, N<sub>2</sub>O and NH<sub>3</sub> emissions are generated by nitrification and denitrification processes. The type of agricultural land used as reference is actively planted fallow land, which requires such basic operations as cultivation engineering, sowing and moving. The emissions and consumption of resources in the production of the seed have also been taken into account. Rapeseed oil is assumed to be produced in decentralized, small enterprises. First the rapeseed is cleaned and dried, and then it is separated in a ratio of 1:2 from the colza cake which is used as fodder. It is refined by sedimentation and filtration, and sold. In the whole balance, two co-product credits have been allocated: (1) for the use of the land as actively planted fallow land and (2) for the substitution of soy coarse meal by the co-product colza cake. For the allocation, the average protein content has been taken as the basis. The production of soy includes the cultivation of the beans, the fabrication of coarse meal with soy oil as co-product and both transatlantic and continental transport by ship. The origin is assumed to be the U.S.<sup>29</sup> It has also been assumed that the rapeseed oil is produced in the agricultural regions themselves, and that it is transported in small trucks to logistic centers, which send parts to the steam reforming process plant by train. Hence, of a total transport distance of 240 km, we have taken into account the following assumptions for rapeseed oil transport: 140 km of road transport in a 16t truck and 100 km of average European rail transport.<sup>29</sup> The truck transport requires diesel oil as a particular life cycle data input.

**Soybean oil.** The inventory data for soybean oil have been extracted from a study on biodiesel production in the U.S. The analysis includes the agricultural part, transport to the crusher, and the crushing, and is based on data from soybean farms of the major producing states of the country. Potassium, phosphate and phosphorous fertilizers, and agrochemicals are used to replace minerals in the soil, but only small amounts of nitrogen fertilizer are required by the soybean plant. It is assumed that most of the soybeans that are moved 120 km from field to crusher are transported by heavy-duty trucks. The energy emissions resulting from loading and unloading the soybeans are also included. The model of the soybean crushing process is based, as a starting point, on a typical production unit located in the southeastern region of the United States. This corresponds to a production of almost 400 metric tons/day of crude, degummed soybean oil, obtained from 95000 kg h<sup>-1</sup> of soybeans (or 2273 metric tons/day). The facility uses solvent extraction to recover the oil. The beans are prepared by removing their hulls, grinding and flaking. The flaked beans are then subjected to an extraction step in which hexane is used to remove the soybean oil. The extracted beans are dried and ground to produce a marketable meal product. Oil-containing hexane is then processed to separate the volatile hexane phase from the oil. The hexane solvent is recovered and recycled as much as possible. Finally, the oil product is washed with water to remove gums before it is stored or shipped. The shipping of meal is not included in the LCI. An allocation technique based on the mass output of soybean crushing is used as the baseline for this study (soybean oil 18% and soybean meal 82%, by weight).<sup>31</sup> It is assumed that soybean oil going from US to Europe travels 10 000 km by sea.<sup>29</sup>

**Palm oil.** A palm tree bears its first fruits between the ages of 30 and 36 months, and may produce a harvest every 10 to 21

days throughout its productive life, which lasts 20 to 25 years. Our analysis used data from Malaysia, and it has been assumed that fresh fruit bunches are produced on plantations of approximately 135 trees per ha, yielding a production rate of 18 000 kg ha<sup>-1</sup>. The fresh fruit bunches are harvested manually and taken by wheelbarrows or diesel tractor to the plantation's access roads, where they are loaded in trucks or trailers for shipment to the palm mill. For this agriculture step, it has also been assumed that the replanted area represents 0.4% of the total planted area per year and that over-aged palm trees are burned. It has been also assumed that the total fertilizer requirements are purchased fertilizer, plus the additional fertilizer value of land-applied palm oil mill effluent, empty fruit bunches and other organic sources. Furthermore, the inventory data include diesel fuel for tractors, heavy equipment for infrastructure and fuel for irrigation and drainage pumps. In the palm oil mill, the fruit bunches are sent to a stripper where the fruitlets are separated from the rest. This results in empty fruit branches that have been assumed to be applied directly to the plantation soil as fertilizer substitute. The amount of fertilizer displaced by the application of empty fruit branches is used to allocate co-product credit. Nearly the same proportions of empty fruit branches and crude palm oil are produced. The crude palm oil is a mixture of oil, water and fruit solids, which is clarified in a continuous centrifugal settling tank operation. The anaerobic digestion of palm oil mill effluents produces biogas that can be collected and burned to produce energy, for which co-product credit has also been allocated. Nevertheless, this anaerobic process is responsible for methane emissions. The remaining solids are dried and applied also as a substitute for fertilizer in the palm plantations. Later on, the fiber is separated from the nut and the shell is split from the kernel. The fiber and the shells are used as fuel for the mill. Excess shells are used as a base or surface material on the numerous roads of the plantation. Co-product allocation has been applied for the shell material used in road construction.<sup>30</sup> The transport of the palm oil from Malaysia to Southern Europe has been taken into account assuming an overseas transport of 20 000 km. This transport process requires the special consumption of the life cycle inventory data of heavy fuel oil.

## Impact assessment with global warming potential

The environmental loads taken into account in this study are coal, natural gas, oil and total primary energy for the resources; the air emissions are carbon dioxide (fossil), carbon monoxide, hydrocarbons (except methane), hydrogen chloride, methane, nitrogen oxides, nitrous oxide, particulates (unspecified), and sulfur oxides; and the water emissions are acids, chemical oxygen demand and oils (unspecified). Specific organic compounds are not considered because they were not balanced in the literature which was the source of the environmental loads of the feeds.

The main focus of this study is to compare the CO<sub>2</sub> emissions of various feedstocks which use steam reforming technology to produce hydrogen. Nevertheless, other contributors to global warming, such as methane and nitrous oxide, must be taken into account when the impact of the process is analyzed. To account for these contributors, we used the method for quantitatively evaluating potential man-made contributions to global warming from emissions occurring during the life cycle of a product.<sup>36</sup> Potential contributors to global warming are defined as substances which (1) absorb infrared radiation and have an atmospheric lifetime which is sufficient to make a significant contribution to warming or (2) have a petrochemical origin and are degraded with release of CO<sub>2</sub>. For direct emissions of CO<sub>2</sub> which result in a net contribution to the atmospheric content, only fossil CO<sub>2</sub> has to be considered. To determine the potential contribution to global warming for a given substance other than

**Table 6** Lifetimes and GWP values (direct contribution for the most important greenhouse gases for 20, 100, and 500 years)

| Substance      | Formula          | Lifetime years        | GWP (kg CO <sub>2</sub> /kg substance) |            |           |
|----------------|------------------|-----------------------|--|------------|-----------|
|                |                  |                       | 20 years                               | 100 years  | 500 years |
| Carbon dioxide | CO <sub>2</sub>  | 150 ± 30 <sup>a</sup> | 1                                      | 1          | 1         |
| Methane        | CH <sub>4</sub>  | 14.5 ± 2.5            | 62 ± 20                                | 24.5 ± 7.5 | 7.5 ± 2.5 |
| Nitrous oxide  | N <sub>2</sub> O | 120                   | 290                                    | 320        | 180       |

<sup>a</sup> The lifetime of CO<sub>2</sub> is not well defined. The residual quantity rapidly decays to about 40% over the first 50 years, followed by a slow decline over the next several hundred years.

carbon dioxide, the Global Warming Potential (GWP) is defined. The emissions for the substance are expressed as emissions which are equivalent to the reference substance carbon dioxide (CO<sub>2</sub>). In practice, precise calculations of the cumulative contribution to warming require computer models that take into account the chemical composition of the atmosphere.<sup>37</sup> The GWP for a greenhouse gas (i) is thus calculated as the contribution to warming for a given quantity (weight) of gas (i) divided by the contribution to warming for a corresponding quantity of CO<sub>2</sub>. The formula for the equivalence factor of gas (i) is:

$$GWP_i = \frac{\int_0^T a_i \cdot c_i(t) dt}{\int_0^T a_{CO_2} \cdot c_{CO_2}(t) dt} \quad (5)$$

where:

- $a_i$  is the gas's specific IR absorption coefficient, its instantaneous radiative forcing, assuming that the composition of the atmosphere remains the same (unit  $Wm^{-2} ppm^{-1}$ ),
- $c_i(t)$  is the time-dependent residual concentration of gas (i) deriving from the pulse-emission in question in 1986 (unit ppm),
- $a_{CO_2}$  and  $c_{CO_2}(t)$  are the magnitudes of the corresponding emission of CO<sub>2</sub>.

Eqn. (5) expresses the contribution to warming over the time of integration for a defined emission scenario for gas (i). A frequently used scenario is a momentary emission of 1 Gt of the gas in question in 1986. Otherwise, the composition of the atmosphere is assumed to be constant. The contribution to warming is integrated over the chosen time  $T$  and divided by the contribution to warming from 1 Gt of CO<sub>2</sub> emitted in the same manner.<sup>38</sup> The length ' $T$ ' of the time interval over which the substance's warming effect is integrated is of significance for how the GWP weights the relative effects of the various greenhouse gases. A small  $T$  value (10–50 years) will weight the short-lived gases relatively more heavily, while a large  $T$  value (200–1000 years) will assign greater weight to the long-lived greenhouse gases. From the expression for GWP it follows that the choice of ' $T$ ' is of greatest significance for those substances whose atmospheric lifetimes deviate significantly from the lifetime of CO<sub>2</sub>, which is not well defined. The residual quantity rapidly decays to about 40% over the first 50 years, followed by a slow decline over the next several hundred years.<sup>36</sup> The choice of the time interval ' $T$ ' is determined by the climatic effects to be assessed. The temperature of the continents is thus expected to reach equilibrium with the atmospheric temperature relatively quickly. To solve the problem of choosing ' $T$ ', several decades have been proposed as a suitable period of time. By comparison, the warming of the world's oceans will require several centuries to reach equilibrium.<sup>39</sup> Using the best estimates of IR absorption half-lives for the individual greenhouse gases, the International Panel of Climate Change (IPCC) has calculated GWP values which express the direct contribution of a substance to man-made global warming for 20, 100 and 500 years. The values used in this study are given in Table 6 (the GWP value for methane represents the sum of direct and indirect contributions).

## Dominance analysis

A dominance analysis was conducted to determine the parameters that had the largest effects on the results. In this way, the effect that each part of the process had on the total emissions was determined and the most significant parts identified. The global process analyzed here was divided into five categories or sub-processes: (1) feed, the environmental loads of the raw material, (2) transport, the displacement of the feed from its starting point to the Mediterranean coast of Spain, (3) process, the steam reforming reaction itself, (4) plant operation, the combustion of natural gas, the gas losses due to fugitive emissions, and the treatment (softening) of the water consumed in the SR reaction, and finally, (5) electricity and others.

## Conclusions

The LCA analysis that we have carried out for the production of hydrogen by steam reforming shows that vegetable oils are a promising feed for the process from an environmental perspective. The overall Global Warming Potential (GWP) may be reduced by 60% if traditional fossil fuel feeds like natural gas or naphtha are replaced by vegetable oils, even though they may release into the atmosphere more than twice the CO<sub>2</sub>-eq than fossil fuels during the feed-production step. It should also be noted that the CO<sub>2</sub> emission is not the only parameter to be evaluated for this type of system; the GWP, which is a combination of CO<sub>2</sub>, CH<sub>4</sub> and N<sub>2</sub>O emissions, needs to be evaluated. Of the three vegetable oils studied, soybean oil provides the largest GWP reduction because the emissions of nitrous oxide are low during growing.

## Acknowledgements

The authors are indebted to the Catalan Regional Government and the Spanish Government for financial support (projects 2001SGR-00323 and PPQ2001-1215, respectively). M. Markevich and Guido Sonnemann are obliged to the Universitat Rovira i Virgili for economic support. P. Spath, from the National Renewable Energy Laboratory (NREL), is also acknowledged for her valuable comments and collaboration in obtaining some of the data used in this study.

## References

- 1 J. Quakernaat, *Int. J. Hydrogen Energy*, 1995, **20**, 485.
- 2 D. E. Ridler and M. U. Twigg, in *Catalyst Handbook*, 'Steam Reforming', ed. M. V. Twigg, Wolfe Publishing Ltd, Cleveland (UK), 1989.
- 3 M. Steinberg and H. C. Cheng, *Int. J. Hydrogen Energy*, 1989, **14**, 797.

- 4 T. A. Milne, C. C. Elam and R. J. Evans, *Hydrogen from Biomass. State of the Art and Research Challenges. International Energy Agency. Agreement on the Production and Utilization of Hydrogen, Task 16: Hydrogen from Carbon-Containing Materials, IEA/H2/TR-02/001*, 2001.
- 5 S. Cavallaro and S. Freni, *Int. J. Hydrogen Energy*, 1996, **21**, 465.
- 6 S. Cavallaro and S. Freni, *J. Power Sources*, 1998, **76**, 190.
- 7 S. Cavallaro, *Energy Fuels*, 2000, **14**, 1195.
- 8 T. Rampe, A. Heinzl and B. Vogel, (2000). Hydrogen Generation from Ethanol by Allothermal Reforming. *Progress in Thermochemical Biomass Conversion*, Tyrol, Austria, 17-22 September.
- 9 E. Chornet, D. Wang, D. Montané, S. Czernik, D. Johnson and M. Mann, in *Proceedings of the 1995 U.S. DOE Hydrogen Program Review, 'Biomass to Hydrogen Via Fast Pyrolysis and Catalytic Steam Reforming'*, NREL/CP-430-20036; National Renewable Energy Laboratory; Golden, CO, 1995, **vol. 2**, pp. 707–730.
- 10 D. Wang, D. Montané and E. Chornet, *Appl. Catal., A*, 1996, **143**, 245.
- 11 D. Wang, S. Czernik, D. Montané, M. Mann and E. Chornet, *Ind. Eng. Chem. Res.*, 1997, **36**, 1507.
- 12 D. Wang, S. Czernik and E. Chornet, *Energy Fuels*, 1998, **12**, 19.
- 13 M. Marquovich, S. Czernik, E. Chornet and D. Montané, *Energy Fuels*, 1999, **13**, 1160.
- 14 Y. Ali and M. A. Hanna, *Bioresource Technol.*, 1994, **50**, 153.
- 15 M. Stumbort, A. Wong and E. Hogan, *Bioresource Technol.*, 1996, **56**, 13.
- 16 F. Karaosmanoglu, K. B. Cigizoglu, M. Tüter and S. Ertekin, *Energy Fuels*, 1996, **10**, 890.
- 17 G. Wenzel and P. S. Lammers, *J. Agric. Food Chem.*, 1997, **45**, 4748.
- 18 A. W. Scwab, G. J. Dykstra, E. Selke, S. C. Sorenson and E. H. Pryde, *J. Am. Oil Chem. Soc.*, 1988, **65**, 1781.
- 19 F. Billaud, V. Dominguez, P. Broutin and C. Busson, *J. Am. Oil Chem. Soc.*, 1995, **72**, 1149.
- 20 R. O. Idem, S. P. R. Katikaneni and N. N. Bakhshi, *Energy Fuels*, 1996, **10**, 1150.
- 21 S. P. R. Katikaneni, J. D. Adjaye and N. N. Bakhshi, *Energy Fuels*, 1995, **9**, 599.
- 22 M. Marquovich, R. Coll and D. Montané, *Ind. Eng. Chem. Res.*, 2000, **39**, 2140.
- 23 M. Marquovich, X. Farriol, F. Medina and D. Montané, *Ind. Eng. Chem. Res.*, 2001, **40**, 4757.
- 24 M. Marquovich, F. Medina and D. Montané, *Cat. Comm.*, 2001, **2**, 119.
- 25 P. L. Spath and M. K. Mann, *Life Cycle Assessment of Hydrogen Production via Natural Gas Steam Reforming*, National Renewable Energy Laboratory (NREL), Golden, CO, TP-570-27637, 2000.
- 26 UNEP (United Nations Environmental Program). (1996). *Life Cycle Assessment: What it is and how to do it. UNEP Publication*, Paris, ISBN: 9280715461.
- 27 R. Frischnecht, P. Hofstetter, I. Knoepfel, M. Ménarda and P. Suter, *Ökoinventare für Energiesysteme, 3rd edn.*, Laboratorium für Energiesysteme, ETH, Zürich, 1996.
- 28 I. Boustead, *Eco-profiles of the European plastics industry, Report 2: Olefin feedstock sources, European Center for Plastics in the Environment (PWMI)*, Brussels, 1993.
- 29 J. Borken, A. Patyk and G. A. Reinhardt, *Basisdaten für ökologische Bilanzierungen, Einsatz von Nutzfahrzeugen in Transport, Landwirtschaft und Bergbau*, Vieweg Verlagsgesellschaft, Wiesbaden, 1999.
- 30 F. Hirsinger, K. P. Schick and M. Stalmans, *Tenside Surfactants Deterg.*, 1995, **32**, 420.
- 31 J. Sheehan, V. Camobreco, J. Duffield, M. Grabosky and H. Shapouri, *Life Cycle Inventory of Biodiesel and Petroleum Diesel for Use in an Urban Bus*, National Renewable Energy Laboratory (NREL), Golden, CO, SR-580-24089H, 1998.
- 32 M. A. Rosen, *Int. J. Hydrogen Energy*, 1991, **16**, 207.
- 33 J. Rostrup-Nielsen, *Chem. Eng. Prog.*, 1977, **73**, 87.
- 34 N. M. Patel, R. A. Davis and N. Eaton, *Oil Gas J.*, 1994, **3**, 54.
- 35 D. J. Fleshman, *Chem. Eng. Prog.*, 1993, Oct., 20.
- 36 D. L. Albritton, R. G. Derwent, I. S. A. Isaksen, M. Lal and D. J. Wuebbles, in *Climate change 1994, Radiative forcing of climate change and an evaluation of the IPCC Is92 emission scenarios, 'Trace gas radiative forcing indices'*, ed. J. T. Houghton, L. G. Meira Filho, J. Bruce, H. Lee, B. A. Callander, E. Haites, N. Harris and K. Maskell, Cambridge University Press, New York, 1995.
- 37 J. Rotmans, *IMAGE, An Integrated Model to Assess the Greenhouse Effect*, Kluwer Academic Publishers, Netherlands, 1990.
- 38 M. Hausschild and H. Wenzel, *Environmental Assessment of Products, Volume 2: Scientific background*, Chapman & Hall, Cambridge, 1998.
- 39 J. T. Houghton, G. J. Jenkins and J. J. Ephraums, *Climate Change, The IPCC scientific assessment*, Cambridge University Press, New York, 1990.





# Palladium-catalyzed Ullmann-type coupling with zinc in the presence of H<sub>2</sub>O in liquid carbon dioxide

Jinheng Li,<sup>\*a</sup> Yexiang Xie,<sup>a</sup> Huanfeng Jiang<sup>b</sup> and Mingcai Chen<sup>b</sup>

<sup>a</sup> Institute of Fine Catalysis and Synthesis, College of Chemistry and Chemical Engineering, Hunan Normal University, Changsha 410081, China

<sup>b</sup> Guangzhou Institute of Chemistry, Chinese Academy of Sciences, P.O. 1122, Guangzhou 510650, China

Received 19th July 2002

First published as an Advance Article on the web 2nd September 2002

Carbon dioxide was used not only as a reaction medium but also as a reagent to activate ArCl in the palladium-catalyzed Ullmann-type coupling. In liquid carbon dioxide not only various aromatic iodides and bromides but also aromatic chlorides, non-reactivated substrates in earlier reports, were coupled in moderate to good yields in the presence of Pd/C, zinc and H<sub>2</sub>O at room temperature overnight.

In the last 6 years, more and more attention has been focused on carbon dioxide (liquid and supercritical) replacing the conventional organic solvents.<sup>1,2</sup> For environmental reasons CO<sub>2</sub> is a preferred reaction medium. In addition, the advantages of the reactions in CO<sub>2</sub> include the high solubility of gaseous reactants, rapid diffusion of solutes, and possible weakening of the solvation around the reactants. All the properties can provide substantial selectivity and rate enhancement.

The Ullmann coupling, generally using copper as catalyst,<sup>3,4</sup> is one of the most important methods for the formation of carbon-carbon bonds in organic chemistry. Recently it has attracted more and more attention for the use of palladium and reductive reagents as catalytic systems instead of copper.<sup>5,6</sup> Li *et al.* reported that the coupling reaction of ArI and ArBr could be carried out smoothly in the presence of Pd/C and zinc in water. Although the addition of co-solvent (acetone)<sup>5a</sup> or phase-transfer catalyst (PTC: crown ether)<sup>5b</sup> to the reaction system could facilitate the coupling, the coupling of ArCl could not occur. Sasson *et al.*<sup>5c</sup> described that ArCl could be coupled in the presence of Pd/C, Zn, and PTC (PEG-400 or TBAB) in water, but base and high temperature (60–120 °C) were required. Thus, development of a green and generally applicable reaction system for the Ullmann coupling of ArX (Scheme 1 X = I, Br, and Cl) still seems highly desirable. It was the first example that the Ullmann coupling could be carried out smoothly in the presence Pd/C, Zn and H<sub>2</sub>O in liquid CO<sub>2</sub>.

We firstly chose coupling of iodobenzene as a model reaction system in the presence of Pd/C and zinc.† As shown in Table 1, the presence of both H<sub>2</sub>O and CO<sub>2</sub> affected the coupling of iodobenzene to some extent (entries 1, 2, and 5, in Table 1). In the absence of H<sub>2</sub>O, conversion of iodobenzene was only 14% and yield of biphenyl is 12% in liquid CO<sub>2</sub> (entry 1). In the absence of CO<sub>2</sub>, a previous study<sup>5a</sup> of Pd/C and zinc in Ullmann type coupling with iodobenzene reported a 21% yield of the desired coupling product using H<sub>2</sub>O as solvent. Indeed, under similar conditions, we found a low 27% yield of biphenyl (entry 2). Remarkably, the yield was increased to 58% when both H<sub>2</sub>O and liquid CO<sub>2</sub> were present (entry 5).<sup>7</sup> A trace of the product

was obtained in the absence of zinc (entry 3). The yield was somewhat decreased to 44% when the amount of 5% Pd/C was decreased to 200 mg (entry 4). Unfortunately, coupling of 4-nitroiodobenzene failed.

In liquid CO<sub>2</sub>, not only various aromatic iodides and bromides but also aromatic chlorides, non-reactivated substrates in the earlier reports, were coupled in moderate to good yields in the presence of Pd/C, zinc and H<sub>2</sub>O at room

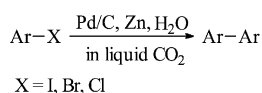
**Table 1** Palladium-catalyzed Ullmann coupling in liquid CO<sub>2</sub><sup>a</sup>

| Entry           | ArX   | Isolated yield (%) |
|-----------------|---|--------------------|
| 1 <sup>b</sup>  | C <sub>6</sub> H <sub>5</sub> I               | 12                 |
| 2 <sup>c</sup>  | C <sub>6</sub> H <sub>5</sub> I               | 27                 |
| 3 <sup>d</sup>  | C <sub>6</sub> H <sub>5</sub> I               | Trace              |
| 4 <sup>e</sup>  | C <sub>6</sub> H <sub>5</sub> I               | 44                 |
| 5               | C <sub>6</sub> H <sub>5</sub> I               | 58                 |
| 6               | C <sub>6</sub> H <sub>5</sub> Br              | 49                 |
| 7               | C <sub>6</sub> H <sub>5</sub> Cl              | 50                 |
| 8               | <i>p</i> -MeC <sub>6</sub> H <sub>4</sub> I   | 60                 |
| 9               | <i>o</i> -MeC <sub>6</sub> H <sub>4</sub> I   | 42                 |
| 10              | <i>p</i> -MeOC <sub>6</sub> H <sub>4</sub> I  | 54                 |
| 11              | <i>p</i> -MeOC <sub>6</sub> H <sub>4</sub> Br | 53                 |
| 12 <sup>f</sup> | α-Chloronaphthalene                           | 30                 |
| 13 <sup>g</sup> | α-Chloronaphthalene                           | 92                 |

<sup>a</sup> Reaction conditions: ArX (2 mmol), Pd/C (5%, 400 mg), Zn (260 mg), H<sub>2</sub>O (1 mL), CO<sub>2</sub> (6 MPa) at room temperature overnight. <sup>b</sup> In the absence of H<sub>2</sub>O, the conversion is 14% which was detected by GC analysis. <sup>c</sup> In the absence of CO<sub>2</sub>. <sup>d</sup> In the absence of zinc. <sup>e</sup> Pd/C (5%, 200 mg). <sup>f</sup> The conversion is 31% which was detected by GC analysis. <sup>g</sup> Pd/C (5%, 600 mg).

## Green Context

The use of carbon dioxide as an environmentally benign solvent has been one of the success stories of green chemistry. Here we see a new application where the role of the CO<sub>2</sub> goes beyond that of a solvent to include apparent substrate activation. The synthetically useful Ullmann coupling reaction can be effectively extended beyond the normal ArBr and ArI to the considerably less expensive ArCl which gives the additional advantage of a reduction in the weight of the by-product. **JHC**



**Scheme 1**

temperature overnight (entries 5–13), although coupling of  $\alpha$ -chloronaphthalene required addition of more Pd/C (600 mg, entries 12 and 13).

On the basis of the above results, several points are noteworthy: (a) the presence of CO<sub>2</sub> and H<sub>2</sub>O was critical under our conditions. In the absence of CO<sub>2</sub> selectivity toward the coupling was rather low and coupling of aromatic chlorides could not occur. In the absence of H<sub>2</sub>O the reaction was slow; (b) the yields of the coupling in liquid CO<sub>2</sub> is similar to the previous reports using Pd/C, Zn, promoter (co-solvent or PTC) and H<sub>2</sub>O as the catalytic system. But in liquid CO<sub>2</sub> not only various aromatic iodides and bromides but also aromatic chlorides, non-reactivated compounds under the earlier reports' reaction conditions, could be coupled in moderate to good yields without additional promoters; and (c) although the effect of CO<sub>2</sub> on the selectivity of the reaction is not clean, it is at least sure that its acidity is a factor in influencing the selectivity.

Although further investigation is needed to settle the mechanism, we provide a new green route to couple not only aromatic iodides and bromides but also aromatic chlorides in moderate to good yields in liquid CO<sub>2</sub>.

## Acknowledgement

We thank Hunan Normal University for financial support.

## Notes and references

† A typical procedure for the Ullmann coupling of ArX is as follows: ArX (2 mmol) was added to a mixture of Pd/C (5%, 400 mg, 0.18 mmol), zinc powder (260 mg, 4 mmol), and H<sub>2</sub>O (1 mL) in HF-25 autoclave. Liquid CO<sub>2</sub> was then transferred into the autoclave to 6 MPa. The reaction mixture was stirred at room temperature overnight. After the gas was vented, the residue was extracted (ether), dried (anhydrous Na<sub>2</sub>SO<sub>4</sub>) and purified by preparative

TLC on silica gel (light petroleum–ethyl ether). Under the above reaction conditions, all ArX were converted completely which were detected by GC analyses.

- (a) L. Jia, H. Jiang and J. Li, *Green Chem.*, 1999, **1**, 91; (b) L. Jia, H. Jiang and J. Li, *Chem. Commun.*, 1999, 985; (c) J. Li and H. Jiang, *Chem. Commun.*, 1999, 2369; (d) J. Li, H. Jiang and M. Chen, *Green Chem.*, 2001, **3**, 137 and references cited therein (e) G. Li, H. Jiang and J. Li, *Green Chem.*, 2001, **3**, 250; (f) R. A. Brown, P. Pollet, E. Mckoon, C. A. Eckert, C. L. Liotta and P. G. Jessop, *J. Am. Chem. Soc.*, 2001, **123**, 1254 and references cited therein (g) P. Munshi, A. D. Main, J. C. Linshan and P. G. Jessop, *J. Am. Chem. Soc.*, 2002, **124**, 7963.
- For representative reviews, see: (a) *Chemical Synthesis using Supercritical Fluids*, eds. P. G. Jessop and W. Leitner, Wiley-VCH, Weinheim, 1999; (b) P. G. Jessop, T. Ikariya and R. Noyori, *Chem. Rev.*, 1999, **99**, 475; (c) J. Li, L. Jia and H. Jiang, *Chinese J. Org. Chem.*, 2000, **20**, 293; (d) R. S. Oakes, A. A. Clifford and C. M. Rayner, *J. Chem. Soc., Perkin Trans. 1*, 2001, 917.
- (a) G. Bringmann, R. Walter and R. Weirich, *Angew. Chem., Int. Ed. Engl.*, 1990, **29**, 977; (b) S. Zhang, D. Zhang and L. S. Liebeskind, *J. Org. Chem.*, 1997, **62**, 2312 and references cited therein.
- For Ni catalyzed Ullmann-type couplings, see: (a) K. Takagi, N. Hayama and K. Sasaki, *Bull. Chem. Soc. Jpn.*, 1984, **57**, 1887; (b) G. Meyer, Y. Rollin and J. Perichon, *J. Organomet. Chem.*, 1987, **333**, 263.
- For Pd/C catalyzed Ullmann-type couplings using Zn and water as the reducing reagent, see: (a) S. Ventrakaman and C. J. Li, *Org. Lett.*, 1999, **1**, 1133; (b) S. Ventrakaman and C. J. Li, *Tetrahedron Lett.*, 2000, **41**, 4831 and references cited therein (c) S. Mukhopadhyay, G. Rothenberg, D. Gitis and Y. Sasson, *Org. Lett.*, 2000, **2**, 211.
- For Pd/C catalyzed Ullmann-type couplings using other reducing reagents, see: formate salts as the reducing reagents: (a) S. Mukhopadhyay, G. Rothenberg, D. Gitis, H. Wiener and Y. Sasson, *J. Chem. Soc., Perkin Trans. 2*, 1999, 2481; (b) Hydrogen gas as the reducing reagents (c) S. Mukhopadhyay, G. Rothenberg, H. Wiener and Y. Sasson, *Tetrahedron*, 1999, **55**, 14763 and references cited therein.
- To check the basic mass balance of the coupling, the dried extraction, which did not separate, was directly detected by GC-MS analysis. The analysis results showed that C<sub>6</sub>H<sub>5</sub>I was completely converted to 64% of diphenyl and 36% C<sub>6</sub>H<sub>6</sub>.



# Selective oxidation of cyclohexane in compressed CO<sub>2</sub> and in liquid solvents over MnAPO-5 molecular sieve

Zhenshan Hou, Buxing Han,\* Liang Gao, Zhimin Liu and Guanying Yang

The Center for Molecular Science, Institute of Chemistry, The Chinese Academy of Sciences, Beijing 100080, China. E-mail: Hanbx@pplas.icas.ac.cn

Received 11th January 2002

First published as an Advance Article on the web 23rd July 2002

The selective oxidation reaction of cyclohexane with MnAPO-5 molecular sieve catalyst to produce cyclohexanol and cyclohexanone was carried out in compressed CO<sub>2</sub> at 398.2 K using oxygen as an oxidant, and the reaction mixture was controlled to be in the two-phase region, very close to the critical point, and in the supercritical (sc) region of the reaction system. The effect of a small amount of butyric acid cosolvent on the reaction in scCO<sub>2</sub> was also studied. The reaction was also conducted in liquid butyric acid, benzene and CCl<sub>4</sub>, and in the absence of any solvent. It has been observed that the conversion and selectivity of the reaction in compressed CO<sub>2</sub> change considerably with the phase behavior or the apparent density of the reaction system. Addition of a small amount (0.2 mol%) of butyric acid cosolvent to scCO<sub>2</sub> enhances the conversion significantly, and the selectivity also changes considerably. The by-products of the reaction in compressed CO<sub>2</sub> with and without the cosolvent are much less than that of the reaction in liquid solvents or in the absence of solvents. It is advantageous to conduct the reaction in supercritical CO<sub>2</sub>.

## Introduction

The catalytic oxidation, especially partial oxidation of hydrocarbons constitutes one of the major challenges in present chemistry.<sup>1–3</sup> Different oxidants have been used in these reactions. Oxidation using molecular oxygen is very attractive because it is inexpensive, readily available, and environmentally benign. Transformation of cyclohexane into cyclohexanone and cyclohexanol is among the principal target reactions since these oxidation products are used as feedstock in some industrial processes.<sup>4,5</sup>

There are several advantages to conduct reactions in supercritical fluids (SCFs).<sup>6–8</sup> For instance, reaction rate, selectivity and reaction equilibrium can be tuned by pressure or a small amount of cosolvent. Environmentally benign SCFs, such as CO<sub>2</sub> and water, can be used to replace hazardous organic solvents. Several papers have been published for the oxidation of cyclohexane in the presence of compressed CO<sub>2</sub>. Wu *et al.* reported aerobic oxidation of cyclohexane to yield cyclohexanol and cyclohexanone in the presence of Fe-porphyrin catalyst and acetaldehyde in scCO<sub>2</sub>. They found that the reaction rate had maximum value in the vicinity of CO<sub>2</sub> critical pressure.<sup>9</sup> In the absence of any catalyst, Mukhopadhyay *et al.*<sup>10,11</sup> studied the mechanism and kinetic properties of the oxidation reaction of cyclohexane with oxygen in compressed CO<sub>2</sub> at relatively high reaction temperature (410–433 K), which followed a free-radical mechanism.

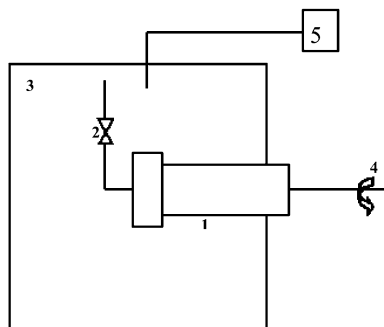
Metal-containing aluminophosphate molecular sieves offer tremendous potential as catalysts in the oxidation reactions to transform hydrocarbons into valuable products.<sup>12–14</sup> Metal-containing aluminophosphate molecular sieves can be used in cyclohexane oxidation with O<sub>2</sub> as an oxidant without any promoter, and some elegant researches have been performed for the oxidation in liquid solvents<sup>15</sup> or in the absence of solvent.<sup>16</sup> In the reaction processes, how to reduce the environmentally hazardous waste and by-products is a challenging topic because the desired products (cyclohexanone and cyclohexanol) are more easily oxidizable by O<sub>2</sub> than cyclohexane. Reaction in compressed CO<sub>2</sub> with metal-containing aluminophosphate

molecular sieves may be an effective way to reduce the by-products and wastes in the oxidation of cyclohexane, and the phase behavior of the reaction system may be an important factor to affect the conversion and selectivity of the reaction.

In this work, we study the phase behavior and critical parameters of the reaction system for the oxidation of cyclohexane in compressed CO<sub>2</sub> using oxygen as an oxidant to produce cyclohexanol and cyclohexanone. On the basis of the phase behavior study, the reaction is conducted in compressed CO<sub>2</sub> (with and without cosolvent) in both the two-phase region and in the supercritical region, and MnAPO-5 molecular sieve is used as a catalyst. The reaction is also carried out in some liquid organic solvents and in the absence of solvent. We focus on (1) how the phase behavior of the reaction system affects conversion and the selectivity; (2) how a small amount of cosolvent (butyric acid) in CO<sub>2</sub> influences the conversion and the selectivity; (3) the advantages to perform the reaction in compressed CO<sub>2</sub>. The apparatus for the high-pressure reactions is shown in Fig. 1.

## Green Context

Oxidation is one of the most important methods of adding functionalities to an organic molecule. This is particularly true for hydrocarbons where low molecular weight starting materials are converted into valuable acids, ketones and alcohols. There are numerous oxidation methods, many of which are environmentally unacceptable due, for example, to the use of toxic stoichiometric oxidants. Here, the most attractive of oxidants, oxygen itself, is used in combination with the environmentally benign solvent CO<sub>2</sub>, and an easy-to-handle and recoverable solid catalyst. This green chemistry method is used to oxidise cyclohexane. *JHC*

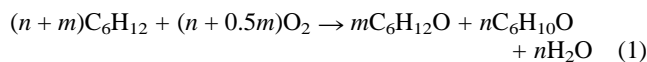


**Fig. 1** Experimental apparatus for the reaction at high-pressure. 1. Reactor 2. Valve 3. Air bath 4. Driving motor 5. Temperature controller.

## Results and discussion

### Phase behavior of the reaction system

The phase behavior of a reaction system usually changes with reaction time or conversion.<sup>8,17,18</sup> Therefore, the phase behavior and the critical parameters of the reaction system are crucial for selecting the reaction conditions. We can write the oxidation reaction in this work in terms of eqn. (1).



Only a small amount of by-products were observed under the reaction conditions of this work as  $\text{CO}_2$  was used as solvent, so they were neglected in the study of phase equilibrium. Initially, the reaction system contains three components,  $\text{CO}_2$  (solvent),  $\text{C}_6\text{H}_{12}$  and  $\text{O}_2$ , and there are six components during the reaction process,  $\text{CO}_2$ ,  $\text{C}_6\text{H}_{12}$ ,  $\text{O}_2$ ,  $\text{C}_6\text{H}_{12}\text{O}$ ,  $\text{C}_6\text{H}_{10}\text{O}$  and  $\text{H}_2\text{O}$ . The composition of the reaction system is a function of original molar ratio (before reaction) of  $\text{CO}_2:\text{C}_6\text{H}_{12}:\text{O}_2$ , the conversion of  $\text{C}_6\text{H}_{12}$  ( $\alpha$ ), and the selectivity for  $\text{C}_6\text{H}_{12}\text{O}$  and  $\text{C}_6\text{H}_{10}\text{O}$  ( $n/m$ ). In other words, the composition of the reaction system at a fixed original molar ratio can be calculated based on the conversion of  $\text{C}_6\text{H}_{12}$  and the selectivity. It can be known from the phase law that in single phase region, two phase region, and at the critical point the degrees of freedom are respectively 2, 1, and 0 at fixed conversion and selectivity. Thus, the phase behavior at fixed conversion can be expressed by two-dimensional phase diagrams, such as a pressure vs. temperature phase diagram and a density vs. temperature phase diagram.

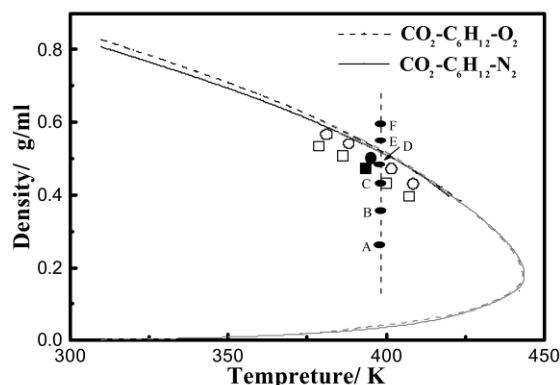
In this work we used  $\text{N}_2$  to replace  $\text{O}_2$  for the phase behavior study for two reasons. First, oxidation reaction may occur during the experiment if  $\text{O}_2$  is used, which affects the phase behavior measurement. Second, among the compounds, the physical properties of  $\text{N}_2$  are most similar to that of  $\text{O}_2$ . To verify this assumption is reasonable, we calculated the phase behavior of  $\text{CO}_2\text{-C}_6\text{H}_{12}\text{-N}_2$  and  $\text{CO}_2\text{-C}_6\text{H}_{12}\text{-O}_2$  systems using the Peng–Robinson equation of state (PR EOS),<sup>19</sup> which is a widely used method for phase behavior calculation. The critical parameters of the components used in the calculation are listed in Table 1.<sup>20</sup> In the calculation the binary interaction coefficients  $k_{ij}$  of  $\text{CO}_2\text{-C}_6\text{H}_{12}$  and  $\text{C}_6\text{H}_{12}\text{-N}_2$  pairs used were 0.101 and 0.037, respectively, which were obtained by regression of phase equilibrium data of the binary mixtures.<sup>21</sup> The  $k_{ij}$  of  $\text{C}_6\text{H}_{12}\text{-O}_2$  was assumed to be equal to that of  $\text{C}_6\text{H}_{12}\text{-N}_2$  pair,

**Table 1** Critical parameters of the components<sup>20</sup>

| Compounds     | $M_w$ | $T_c/\text{K}$ | $P_c/\text{bar}$ | $\omega$ |
|---------------|-------|----------------|------------------|----------|
| Cyclohexane   | 84.16 | 553.5          | 40.7             | 0.212    |
| $\text{O}_2$  | 31.99 | 154.6          | 50.4             | 0.025    |
| $\text{CO}_2$ | 44.01 | 304.1          | 73.8             | 0.239    |
| $\text{N}_2$  | 28.01 | 126.2          | 33.9             | 0.039    |

and those of  $\text{CO}_2\text{-O}_2$  and  $\text{CO}_2\text{-N}_2$  were set to zero. The calculated density ( $\rho$ ) vs. temperature phase diagrams of  $\text{CO}_2\text{-C}_6\text{H}_{12}\text{-N}_2$  ( $\text{CO}_2:\text{cyclohexane}:\text{N}_2 = 7:2:1$ ) and  $\text{CO}_2\text{-C}_6\text{H}_{12}\text{-O}_2$  ( $\text{CO}_2:\text{cyclohexane}:\text{N}_2 = 7:2:1$ ) systems are shown in Fig. 2. The system is single phase outside the envelopes, and separates into two phases within the envelopes. The results in Fig. 2 indicate that the differences of the  $\rho\text{-T}$  curves of the two systems is not considerable. The main reasons are that the physical properties of  $\text{N}_2$  and  $\text{O}_2$  are similar and their concentrations in the corresponding solutions are low (10 mol%). This suggests that  $\text{N}_2$  can be used to replace  $\text{O}_2$  for the phase behavior measurements.

It should be noted that the phase behavior calculation using an equation of state can not give accurate results for the complex mixtures, although we believe that the PR EOS can give much better information for the difference between the above  $\text{O}_2$ -containing systems and the  $\text{N}_2$ -containing systems. Thus, we determined the critical parameters and the phase equilibrium data of the reaction system with original molar ratio of  $\text{CO}_2:\text{cyclohexane}:\text{N}_2 = 7:2:1$ . The mixtures were prepared from the pure chemicals for the phase behavior measurements. Fig. 2 shows the results for the reaction system at  $n/m = 1$  (eqn. (1)), and  $\alpha = 0$  and 0.1. It is shown that the value of  $\alpha$  has little effect on the critical parameter of the system in the conversion range. The  $\rho\text{-T}$  phase diagram is shown because we used a batch reactor and the experiments were carried out at different densities. The figure illustrates that the calculated and the experimental phase separation densities show a similar trend with the variation of temperature for the  $\text{CO}_2\text{-C}_6\text{H}_{12}\text{-N}_2$  system. However, the calculated data are about 10% larger. We used the experimental data as reference for the selection of reaction conditions.



**Fig. 2** The experimental and calculated phase separation pressure. (—)  $\text{CO}_2:\text{C}_6\text{H}_{12}:\text{N}_2 = 7:2:1$  (calculated from PR EOS); (---)  $\text{CO}_2:\text{C}_6\text{H}_{12}:\text{O}_2 = 7:2:1$  (calculated from PR EOS); (□)  $\text{CO}_2:\text{C}_6\text{H}_{12}:\text{N}_2 = 7:2:1$  (experimental); (○)  $\text{CO}_2:\text{C}_6\text{H}_{12}:\text{N}_2:\text{C}_6\text{H}_{12}\text{O}:\text{C}_6\text{H}_{10}\text{O} = 7:1.8:0.9:0.1:0.1$  (experimental); (●) critical point ( $\text{CO}_2:\text{C}_6\text{H}_{12}:\text{N}_2:\text{C}_6\text{H}_{12}\text{O}:\text{C}_6\text{H}_{10}\text{O} = 7:1.8:0.9:0.1:0.1$ ); Points A, B, C, D, E, F correspond to the selected reaction conditions.

### Selection of reaction conditions

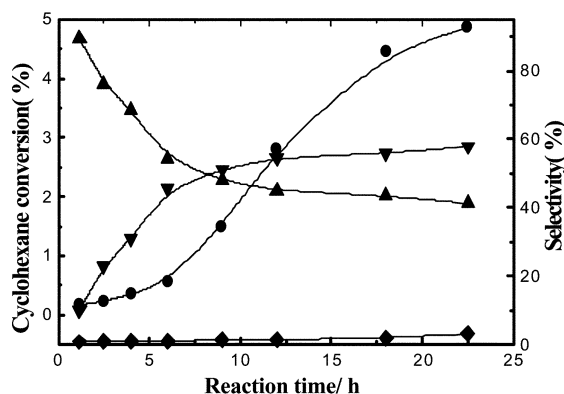
In this work we focus on the reaction in different phase regions at a temperature slightly higher than the critical temperature of the reaction system. If the temperature is too high or too low, the system can not exhibit fully the properties of SCFs. The critical temperature ( $T_c$ ) of the reaction system with  $\alpha = 0$  and 0.1 ( $n/m = 1$ ), are 392.8 and 395.3 K, respectively, at the original molar ratio of  $\text{CO}_2:\text{cyclohexane}:\text{O}_2 = 7:2:1$ , which can be known from the experimental data shown in Fig. 2. It can be expected that the  $T_c$  of the reaction system is in the range 392.8–395.3 K as  $\alpha < 0.1$ . Our pre-experiments showed that reaction rate at

398.2 K was suitable for our study. Therefore, in all the experiments, we chose the composition of the feedstock to be  $\text{CO}_2$ :cyclohexane: $\text{O}_2 = 7:2:1$ , and the reaction temperature was 398.2 K. The weight ratio of cyclohexane to MnAPO-5 was 45:1. This could meet our expectation that the reaction temperature was slightly higher than the  $T_c$  of the reaction system with desired reaction rate in the presence of the catalyst, and the reaction rate without the catalyst was very slow. (Our blank tests at this temperature indicated that the conversion was less than 0.3% in the absence of the catalyst in the reaction time range studied). Thus, the reactions were carried out in the two-phase region, near the critical point, and supercritical region of the reaction system.

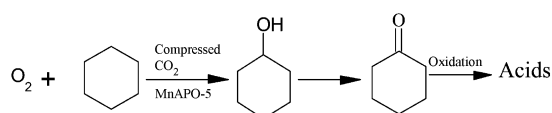
### Effect of reaction time on the selective oxidation

The results of the oxidation of cyclohexane at 398.2 K for different reaction times are presented in Fig. 3. The density of the reaction system is  $0.481 \text{ g ml}^{-1}$ . As expected, the conversion of cyclohexane increases with reaction time.

It can be seen from Fig. 3 that cyclohexanone and cyclohexanol are the major products and the amount of the by-products, which are mainly organic acid and hydroperoxide, is very small. This indicates that over MnAPO-5 molecular sieve, this reaction possesses very high selectivity for the desired products (cyclohexanone and cyclohexanol) under the experimental conditions using  $\text{CO}_2$  as solvent. In addition, an increase in the selectivity for cyclohexanone and decrease in the selectivity for cyclohexanol with increasing conversion or reaction time suggest that cyclohexanone may be formed by a consecutive oxidation of cyclohexanol. To get further evidence for this mechanism, we also performed the cyclohexanol oxidation reaction under the same conditions. After reaction of 8 h, the cyclohexanol conversion reached about 52%, corresponding approximately to the selectivity for cyclohexanone in the cyclohexane oxidation of 8 h in Fig. 3. This supports further the argument that cyclohexanone is formed by a consecutive oxidation of cyclohexanol. Therefore, the reaction sequence may be expressed by Scheme 1.



**Fig. 3** The dependence of conversion and selectivity on the reaction time at 398.2 K and apparent density  $\rho = 0.481 \text{ g ml}^{-1}$ . (—●—) Cyclohexane conversion, (—▼—), selectivity for cyclohexanone, (—▲—), selectivity for cyclohexanol, (—◆—), selectivity for others.



**Scheme 1**

### Reactions in different phase regions

In order to study the effect of phase behavior of the reaction system on the reaction, we conducted the reaction in the two-phase region, the supercritical region, and near the critical point by controlling the density of the reaction system, and the reaction time was 17 h. The selected conditions are shown in Fig. 2 by A, B, C, D, E and F. Points A, B and C are in two-phase region, point D is very close to the critical point of the reaction system and points E and F are in the supercritical region. Fig. 4 displays the conversion and selectivity as a function of the apparent density. The results show that the phase behavior has a considerable influence on the conversion, selectivity, and the amount of the by-products of the oxidation reaction.

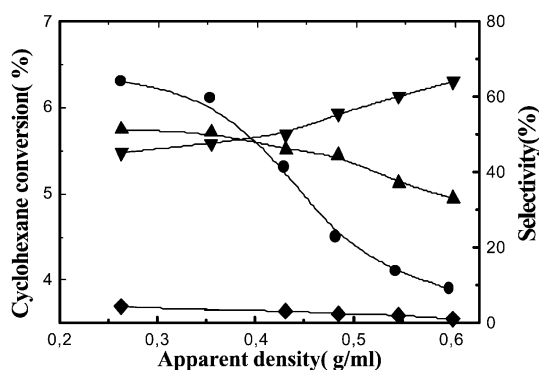
The conversion is higher when the reaction mixture is in the two-phase region. One of the main reasons is that the catalyst contacts with the liquid phase in the reactor. In other words, the reaction takes place mainly in the liquid phase. It is obvious that the concentration of  $\text{CO}_2$  in the liquid phase is lower. Thus less active sites of the catalyst may be occupied by  $\text{CO}_2$ , and more active sites are available for the reactants, which is favorable for the reaction of cyclohexane. The concentration of the  $\text{CO}_2$  in the liquid phase increases with the density in the two-phase region. In addition, as the density is increased, the solubility of organic molecules in the  $\text{CO}_2$  phase increases and more reactants are desorbed from the surface of the molecular sieve. Therefore the reaction rate is reduced.

The conversion in the single-phase region also decreases monotonously with increasing density. The main reason may be that the volume concentration of  $\text{CO}_2$  increases with increasing density of the reaction system because the original molar ratio of  $\text{CO}_2$ : $\text{C}_6\text{H}_{12}$ : $\text{O}_2$  is the same in all the experiments, and thus more active sites on the surface of the catalyst are occupied by  $\text{CO}_2$  at higher density. The assumption that  $\text{CO}_2$  occupies active sites is supported by the fact that the conversion and the amount of by-products are higher in the absence of  $\text{CO}_2$ , which will be discussed in the following sections (Table 2).

The amount of the by-products in the two-phase region is relatively high. The main reason may be that diffusion coefficient of the liquid reaction mixture is smaller. Therefore, the products exist in the molecular sieve for a longer time, and they can react further with oxygen.

It is very interesting that the selectivity for cyclohexanol is reduced and that for cyclohexanone is enhanced at higher density. The selectivity for cyclohexanol is higher than that for cyclohexanone at  $\rho < 0.4 \text{ g ml}^{-1}$ . This can be explained as follows:

cyclohexane,  $\text{O}_2$  and  $\text{CO}_2$  are nonpolar, while the primary product, cyclohexanol, has a strong polar group  $-\text{OH}$ . It can be expected that the interaction between cyclohexanol and the surface of the catalyst is stronger. Hence, the effect of  $\text{CO}_2$  on



**Fig. 4** The dependence of conversion and selectivity on apparent density after reaction for 17 h. (—●—) Cyclohexane conversion, (—▼—) selectivity for cyclohexanone, (—▲—), selectivity for cyclohexanol, (—◆—) selectivity for others.

**Table 2** Selective oxidation of cyclohexane with molecular oxygen over MnAPO-5 in different solvents

| Solvent  | Conversion (%) | Selectivity (%)                  |                                  |        |
|--|----------------|----------------------------------|----------------------------------|--------|
|  |                | C <sub>6</sub> H <sub>12</sub> O | C <sub>6</sub> H <sub>10</sub> O | Others |
| No solvent <sup>a</sup>                          | 9.6            | 40.4                             | 47.2                             | 12.4   |
| Butyric acid <sup>a</sup>                        | 18.2           | 24.3                             | 46.2                             | 29.5   |
| Benzene <sup>a</sup>                             | 4.2            | 40.1                             | 56.4                             | 3.5    |
| CCl <sub>4</sub> <sup>a</sup>                    | 3.8            | 50.6                             | 48.1                             | 2.3    |
| CO <sub>2</sub> <sup>a</sup>                     | 2.8            | 56.1                             | 43.4                             | 0.5    |
| CO <sub>2</sub> <sup>b</sup>                     | 4.4            | 42.8                             | 56.3                             | 0.9    |
| CO <sub>2</sub> + 0.2% butyric acid <sup>a</sup> | 7.8            | 40.1                             | 59.1                             | 0.8    |

The reactions were carried out at 398.2 K; the weight ratio of cyclohexane to catalyst is 45:1 in all experiments; the molar ratio of solvent:cyclohexane:oxygen is 7:2:1; the apparent density is 0.481 g ml<sup>-1</sup> for CO<sub>2</sub> as solvent;<sup>a</sup> Reaction time is 12 h; <sup>b</sup> Reaction time is 17 h

the adsorption of cyclohexane and O<sub>2</sub> should be more significant than that of cyclohexanol. Thus the reaction rate of the first step in Scheme 1 is reduced more significantly than the second step. This effect is larger at higher density, and thus the selectivity for cyclohexanone is relatively higher.

### Reaction at other conditions

In this work reaction experiments were also performed in liquid butyric acid, benzene and CCl<sub>4</sub>, and in the absence of any solvent. The reaction temperature, the molar ratio of the solvent:cyclohexane:O<sub>2</sub>, and mass ratio of cyclohexane:catalyst were the same as those of the reaction with CO<sub>2</sub> as solvent. The results are listed in Table 2.

The conversion of the reaction in butyric acid is larger than that in the nonpolar solvents or in the absence of solvent. One of the main reasons may be that butyric acid affects the catalyst surface more significantly because its strong polarity. For the same reaction time, the conversion of cyclohexane in the liquid solvents is higher than that in CO<sub>2</sub>, and the amount of by-products in the liquid solvents is also larger, as can be seen from Table 2. However, it is interesting that at similar conversions (reaction time in CO<sub>2</sub> is longer), the amount of by-products is lower for the reaction carried out in CO<sub>2</sub>. One of the reasons is that the diffusion coefficients of cyclohexanol and cyclohexanone in CO<sub>2</sub> are larger than those in the liquid solvents, and thus they can diffuse out of the catalyst quickly, which prevents further reaction of the chemicals.

### Effect of cosolvent on the reaction in scCO<sub>2</sub>

It is known that cosolvent may play a very important role in tuning the properties of SCFs.<sup>22,23</sup> The data in Table 2 show that the conversion of the reaction in butyric acid is much higher. Thus, it may be an effective cosolvent for the reaction in scCO<sub>2</sub>. The conversion and selectivity of the reaction in CO<sub>2</sub> + butyric acid are also given in Table 2. The data indicate that addition of small amount of butyric acid as a cosolvent can change the conversion and the selectivity considerably. To our knowledge, it is very difficult to give a precise explanation for this phenomenon. One of the main reasons may be that butyric acid affects the catalyst surface more significantly due to its strong polarity.

## Experimental

### Materials

Cyclohexane (C<sub>6</sub>H<sub>12</sub>), cyclohexanol (C<sub>6</sub>H<sub>12</sub>O), cyclohexanone (C<sub>6</sub>H<sub>10</sub>O), triethylamine (Et<sub>3</sub>N) and manganese acetate used

were analytical grade produced by Beijing Chemical Company. The catalyst MnAPO-5 (molecular sieve) was prepared by a hydrothermal crystallization method.<sup>24</sup> The molar ratios in the gel were: 0.96Al<sub>2</sub>O<sub>3</sub>:0.08MnO:1.5Et<sub>3</sub>N:40H<sub>2</sub>O. The details for the preparation of the catalyst have been given elsewhere.<sup>25</sup> Very briefly, the aluminium and phosphorus sources were aluminium hydroxide hydrate and phosphoric acid, respectively. Manganese acetate was used as the divalent metal source (Mn<sup>2+</sup>), and Et<sub>3</sub>N was used as a template agent. After stirring at room temperature for 2 h, the gel mixture was heated in a Teflon-lined bomb at 423 K for 48 h. The resultant crystalline products were washed with deionized water, and dried at room temperature. Subsequently the samples were calcined at 623 K for 5 h, and then stored in the desiccator before use.

### Apparatus and procedures

We only describe the apparatus and procedures for the reaction since those to determine the phase behavior have been described in detail previously.<sup>26,27</sup> The reaction was carried out in a stainless steel batch reactor of volume 23.75 ml. The reaction apparatus is shown in Fig. 1. Before an experiment the reactor was purged with CO<sub>2</sub> and measured amounts of catalyst (MnAPO-5), cyclohexane, oxygen and CO<sub>2</sub> were added to the reactor. The volume occupied by MnAPO-5 was corrected when the apparent density was calculated. Once the reactants and catalyst were charged, the reactor was installed in the constant temperature air bath as shown in Fig. 1. The driving motor (60 rpm) rotated the reactor. The temperature fluctuation of the air bath was ±0.1 K, which was controlled by a PID temperature controller made by Beijing Tianchen Electronic Company (Model SX/A-1). After the reaction had proceeded for the desired time, the reactor was placed in a freezer at about 250 K for 1 h, and then CO<sub>2</sub> and O<sub>2</sub> was released slowly. Experiments showed that the amount of reactants and products entrained by the gases was negligible. The products obtained were analyzed by GC (GC112, Shanghai Analytical Instrument Factory) with a FID detector, then cyclohexane conversion and the selectivities for products were obtained.

### Acknowledgement

This work was financially supported by Science and Technology of China (G2000048010), National Natural Science Foundation of China (20133030), and Office of Science and Technology of UK. The authors are also very grateful to Professor Martyn Poliakov for his suggestions and advice.

### References

- 1 L. Fan, Y. Nakayama and K. Fujimoto, *Chem. Commun.*, 1997, 1179.
- 2 M. Hartmann and L. Kevan, *Chem. Rev.*, 1999, **99**, 635.
- 3 U. Schuchardt, D. Cardoso, R. Sercheli, R. Pereira, R. S. da Cruz, M. C. Guerreiro, D. Mandelli, E. V. Spinace and E. L. Pires, *Appl. Catal., A*, 2001, **211**, 1.
- 4 T. Maschmeyer, R. D. Oldroyd, G. Sankar, J. M. Thomas, I. J. Shannon, J. A. Klepetko and A. F. Masters, *Angew. Chem., Int. Ed. Engl.*, 1997, **36**, 1639.
- 5 A. K. Suresh, T. Sridhar and O. E. Potter, *AIChE. J.*, 1990, **36**, 137.
- 6 D. Koch and W. Leitner, *J. Am. Chem. Soc.*, 1998, **120**, 13398.
- 7 C. A. G. Carter, R. T. Baker, W. Tumas and S. P. Nolan, *Chem. Commun.*, 2000, 347.

- 8 Z. S. Hou, B. X. Han, X. G. Zhang, H. F. Zhang and Z. M. Liu, *J. Phys. Chem B.*, 2001, **105**, 4510.
- 9 X. W. Wu, Y. Oshima and S. Koda, *Chem. Lett.*, 1997, 1045.
- 10 P. Srinivas and M. Mukhopadhyay, *Ind. Eng. Chem. Res.*, 1994, **33**, 3118.
- 11 M. Mukhopadhyay and P. Srinivas, *Ind. Eng. Chem. Res.*, 1997, **36**, 2066.
- 12 I. W. C. E. Arends, R. A. Sheldon, M. Wallau and U. Schuchardt, *Angew. Chem., Int. Ed. Engl.*, 1997, **36**, 1144.
- 13 J. D. Chen and R. A. Sheldon, *J. Catal.*, 1995, **153**, 1.
- 14 J. M. Thomas and R. Raja, *Chem. Commun.*, 2001, 675.
- 15 S. S. Lin and H. S. Weng, *Appl. Catal. A*, 1994, **118**, 21.
- 16 M. Dugal, G. Sankar, R. Raja and J. M. Thomas, *Angew. Chem., Int. Ed.*, 2000, **39**, 2310.
- 17 B. A. Stradi, M. A. Stadtherr and J. F. Brennecke, *J. Supercrit. Fluids.*, 2001, **20**, 1.
- 18 J. Ke, B. X. Han, M. W. George, H. K. Yan and M. Poliakoff, *J. Am. Chem. Soc.*, 2001, **123**, 3661.
- 19 D. Y. Peng and D. B. Robinson, *Ind. Eng. Chem. Fundam.*, 1976, **15**, 59.
- 20 C. L. Yaws, *Chemical Properties Handbook: Physical, thermodynamic, environmental, transport, safety, and health related properties for organic and inorganic chemicals*, McGraw-Hill Companies, Inc., New York, 1999.
- 21 S. K. Shibata and S. I. Sandler, *J. Chem. Eng. Data.*, 1989, **34**, 419.
- 22 A. K. Dillow, K. P. Hakner, S. L. J. Yun, F. Deng, S. G. Kazarian, C. L. Liotta and C. A. Eckert, *AIChE J.*, 1997, **43**, 515.
- 23 C. A. Eckert and K. Chandler, *J. Supercrit. Fluids*, 1998, **13**, 187.
- 24 B. Z. Wan and K. Huang, *Appl. Catal.*, 1991, **73**, 113.
- 25 V. P. Shiralkar, C. H. Saldarriaga, J. O. Perez, A. Clearfield, M. Chen, R. G. Anthony and J. A. Donohoe, *Zeolites*, 1989, **9**, 474.
- 26 H. F. Zhang, Z. M. Liu and B. X. Han, *J. Supercrit. Fluid.*, 2000, **18**, 185.
- 27 L. Gao, Z. S. Hou, H. F. Zhang, J. He, Z. M. Liu, X. G. Zhang and B. X. Han, *J. Chem. Eng. Data.*, 2001, **46**, 1635.



# Dimethyl carbonate and phenols to alkyl aryl ethers *via* clean synthesis

Samedy Ouk,<sup>a</sup> Sophie Thiébaud,<sup>\*a</sup> Elisabeth Borredon<sup>a</sup> and Pierre Le Gars<sup>b</sup>

<sup>a</sup> Laboratoire de Chimie Agro-industrielle, UMR 1010 INRA/INP-ENSIACET, 118 route de Narbonne, 31077 Toulouse cedex 4, France. E-mail: sophie.thiebaud@ensiacet.fr

<sup>b</sup> SNPE – Toulouse, Chemin de la Loge, 31078 Toulouse cedex, France

Received 4th April 2002

First published as an Advance Article on the web 2nd September 2002

The industrially important alkyl aryl ethers (ArOR) were selectively obtained in good yields from the O-alkylation of the corresponding phenols with the environmentally benign reagents, dimethyl carbonate or diethyl carbonate. The reactions were carried out under atmospheric pressure, in a homogenous process, without solvent and in the presence of potassium carbonate as catalyst.

## Introduction

The development of sciences and technologies have resulted in a substantial improvement of our lifestyles. These almost unbelievable achievements have, however, led to some impacts on the global environment and public awareness. In particular, chemistry has been contributing to this evolution. Through the combination of knowledge on molecular reactivity, design and other subdisciplines of chemistry and chemical engineering, green chemistry has been looked upon as a sustainable science which accomplishes both economical and environmental goals, simultaneously. With this objective, we developed an alternative process to obtain the industrially important aryl methyl ethers by O-methylation of phenols with dimethyl carbonate (DMC).

Alkyl methyl ethers are useful for the preparation of fragrances, pesticides, cosmetic products, dyes, *etc.*<sup>1</sup> By far the most common method of production is the O-methylation of phenols with dimethyl sulfate<sup>2–5</sup> or methyl halides.<sup>6–11</sup> These reagents are very harmful, and the need for a stoichiometric amount of base to neutralise the acid by-product results in large amounts of inorganic salts to be disposed of. Methanol has also been used as the methylating agent. However, the reaction needs a strong acid catalyst<sup>12–14</sup> or to be carried out at very high temperature (200–400 °C) using zeolite as catalyst.<sup>15–25</sup> Furthermore, the reaction was not selective. Due to these problems, DMC has been emerging as a potential methylating agent.<sup>26–29</sup>

The O-methylation of phenols with DMC can be carried out in an autoclave at a temperature between 120 and 200 °C, in the presence of catalysts such as alkali or organic bases in combination with an iodide,<sup>30</sup> tertiary amines or phosphines,<sup>31</sup> nitrogen-containing heterocyclic compounds (*e.g.* 4-(dimethylamino)pyridine),<sup>32</sup> pentaalkylguanidines<sup>33</sup> or cesium carbonate.<sup>34</sup>

Basic zeolites, aluminas or alumina-silica were described as good catalysts in a continuous-flow process. The reactions were conducted at a temperature range from 180 to 300 °C in the vapour phase. Although high yields of aryl methyl ethers were obtained, by-products of C-methylation were also observed.<sup>35,36</sup> Guaiacol and veratrole were synthesised by O-methylation of catechol over modified aluminas in a continuous-flow process at a temperature between 250 and 300 °C.<sup>37–39</sup> Selectivity towards either guaiacol<sup>38</sup> or veratrole<sup>39</sup> was obtained over alumina loaded with alkali hydroxide or alumina

loaded with potassium nitrate, respectively. Over the catalysts CrPO<sub>4</sub> and CrPO<sub>4</sub>-AlPO<sub>4</sub>, DMC was demonstrated to be more effective than methanol in the O-methylation of phenol.<sup>40</sup> Calcined Mg-Al hydrotalcite was also an efficient catalyst in the O-methylation of phenols with DMC. A maximum guaiacol yield was obtained at 300 °C under optimised conditions.<sup>41,42</sup> The continuous-flow process under gas/liquid phase transfer catalysis (GL-PTC) conditions, with polyethylene glycol (PEG) as phase transfer catalyst and potassium carbonate as base, has been widely reported.<sup>43–48</sup> The reactions were conducted at a temperature range from 160 to 180 °C. In such conditions, the reaction was O-selective and anisole was obtained in good yield. However, the reaction of high boiling point phenols might be difficult to carry out in a continuous-flow process. Other phase transfer catalysis processes were conducted in a solid/liquid system in the presence of catalysts composed of K<sub>2</sub>CO<sub>3</sub> and crown ether at 100 °C<sup>49</sup> or K<sub>2</sub>CO<sub>3</sub> and tetrabutylammonium bromide at reflux of DMC.<sup>50</sup> However, in these methods, the rate of ether formation per mole of catalyst was relatively low.

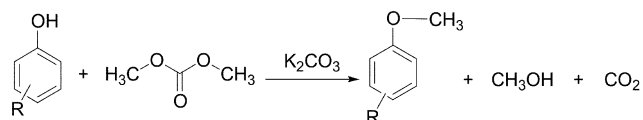
Due to their high boiling point, asymmetric carbonates have been used to accomplish the O-methylation of phenols under atmospheric pressure at a temperature between 120 and 150 °C, in the presence of potassium carbonate and a polar solvent. The selectivity of methylation *vs.* alkylation was better when DMF or triglyme was used as solvent. However, 100% selectivity towards methylation was not obtained.<sup>51</sup>

We report herein the development of an environmentally friendly process for O-methylation of phenol derivatives with DMC (Scheme 1). At 160 °C, under atmospheric pressure, without solvent, in the presence of catalytic amount of potassium carbonate alone, the O-methylation of phenols can be selectively achieved with an excellent conversion velocity, compared to the known processes.

## Green Context

The replacement of salt-forming reagents with more efficient systems is exemplified by the use of dimethyl carbonate (DMC) in place of *e.g.* methyl chloride. Here, DMC is successfully used to methylate phenols in good yield and with only (recyclable) methanol and CO<sub>2</sub> as co-products. Separation is relatively simple. *DJM*





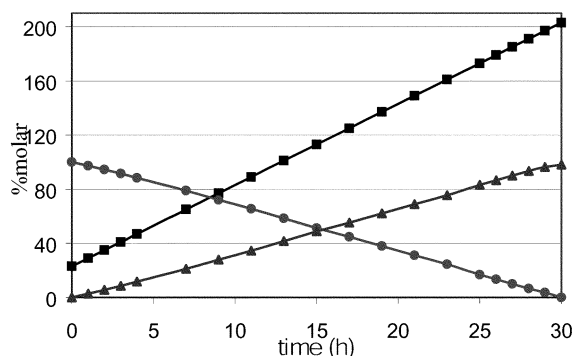
Scheme 1

## Results and discussion

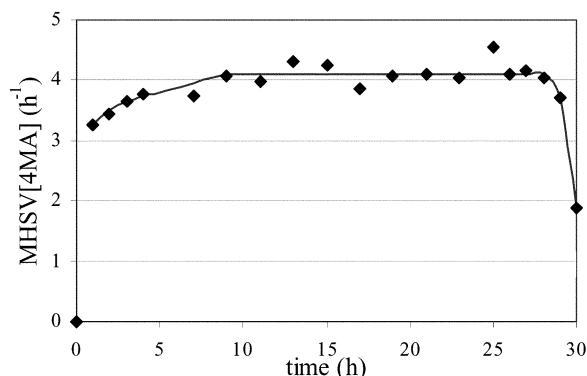
In this investigation, *p*-cresol (pC) was used to optimise the reaction conditions. Following the optimum conditions for the O-methylation of *p*-cresol, other phenols have also been tested.

We have reported that the reaction of phenols with DMC can easily be achieved in the presence of tetrabutylammonium bromide at 130 °C under atmospheric pressure. The performance of this reaction at a temperature higher than the boiling point of DMC can be achieved by progressive introduction of DMC into the reactor. Although excellent yields and rates of conversion were simultaneously obtained, the thermal stability of tetrabutylammonium bromide is a limitation.<sup>51,52</sup> To overcome this problem, we replaced the organic base by a mineral base, an alkaline carbonate, which is thermally more stable.

The reaction was carried out at 160 °C, in a semi-continuous process in which DMC was progressively fed into the pre-heated reactor already containing *p*-cresol and K<sub>2</sub>CO<sub>3</sub>. The pC/K<sub>2</sub>CO<sub>3</sub> molar ratio was 120. To maintain the reaction medium at 160 °C under atmospheric pressure, the low boiling point by-product (methanol) and the excess of DMC were progressively distilled from the reaction medium. After 30 h of the reaction, pC was totally converted into 4-methylanisole (Fig. 1). The molar hourly space velocity of 4-methylanisole (4MA) formation per mole of catalyst (herein, MHSV[4MA]) varied from 3.25 h<sup>-1</sup> at the beginning of the reaction to 4.1 h<sup>-1</sup> during the steady state (Fig. 2).



**Fig. 1** Progression of O-methylation of *p*-cresol with DMC. (■) Amount of DMC fed into the reactor; (●) amount of *p*-cresol, (▲) yield of 4-methylanisole.

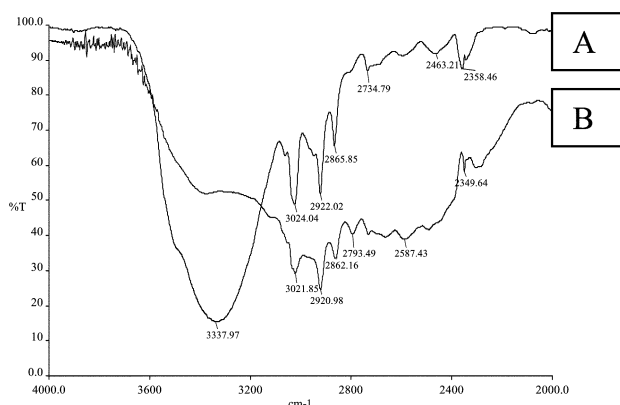


**Fig. 2** Evolution of molar hourly space velocity of 4MA formation per mole of catalyst, MHSV[4MA].

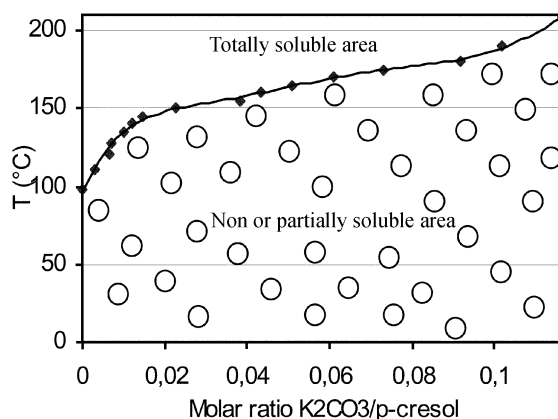
## Influence of substrate concentration

The reaction medium was homogeneous since during the pre-heating period, K<sub>2</sub>CO<sub>3</sub> was progressively dissolved in *p*-cresol. While nearly total conversion of pC was attained, the base reappeared in the solid state. This phenomena can be explained by the formation of CH<sub>3</sub>(C<sub>6</sub>H<sub>4</sub>)OK which is miscible with *p*-cresol. The formation of this potassium salt was confirmed by FTIR spectra (Fig. 3). The spectrum of the mixture of *p*-cresol and K<sub>2</sub>CO<sub>3</sub>, after heating to 160 °C, shows a decrease of intensity of a broad band characteristic of OH of *p*-cresol at 3338 cm<sup>-1</sup>. The degree of solubility depends on temperature as shown in Fig. 4. Therefore at 160 °C, the pC/K<sub>2</sub>CO<sub>3</sub> molar ratio should be >23 (or K<sub>2</sub>CO<sub>3</sub>/pC molar ratio <0.043) to ensure that the medium is homogeneous.

To reduce the reaction time, the pC/K<sub>2</sub>CO<sub>3</sub> molar ratio was decreased from 120 to 25. In the investigation of the effect of solvent, we found that the solvent does not influence the MHSV[4MA] (Table 1 entries 5–10). Meanwhile, the pC/K<sub>2</sub>CO<sub>3</sub> molar ratio has a slight influence on MHSV[4MA], because when the reaction medium is too concentrated in *p*-cresol (entries 1 and 4), MHSV[4MA] is slightly decreased. Hydrogen-bonding among molecules of *p*-cresol might disturb phenolate anion formation, and consequently the reaction kinetics are slowed down.



**Fig. 3** Comparison of FTIR spectra of pure *p*-cresol (A) and a mixture of *p*-cresol/K<sub>2</sub>CO<sub>3</sub> after being heated to 160 °C (B).



**Fig. 4** Relation between temperature and solubility of K<sub>2</sub>CO<sub>3</sub> in *p*-cresol.

## Influence of temperature of the reaction medium

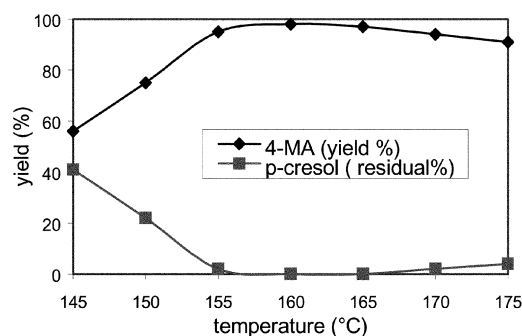
The temperature of the reaction is one of the most influential factors on the reaction kinetics. At 100 °C, the catalyst is totally

**Table 1** Effect of *p*-cresol concentration on yield and on MHSV[4MA] of the reaction

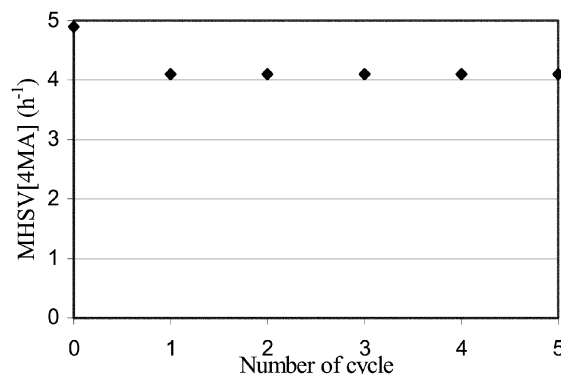
| Entry | Reaction conditions |                                     |                                   |                  |      |              |        | DMC flow/mol h <sup>-1</sup> | <i>p</i> C flow/mol h <sup>-1</sup> | Total DMC/mol | Total <i>p</i> C/mol | Yield (%) | Average MSHV[4MA]/h <sup>-1</sup> |
|-------|---------------------|-------------------------------------|-----------------------------------|------------------|------|--------------|--------|------------------------------|-------------------------------------|---------------|----------------------|-----------|-----------------------------------|
|       | <i>p</i> C/mol      | K <sub>2</sub> CO <sub>3</sub> /mol | DMC ( <i>t</i> <sub>0</sub> )/mol | Solvent Identity | Wt/g | <i>T</i> /°C | Time/h |                              |                                     |               |                      |           |                                   |
| 1     | 1.2                 | 0.01                                | 0.277                             | None             | 0    | 160          | 30     | 0.072                        | 0                                   | 2.437         | 1.2                  | 98        | 3.92                              |
| 2     | 0                   | 0.01                                | 0                                 | 4MA              | 50   | 160          | 26     | 0.096                        | 0.08 <sup>a</sup>                   | 2.496         | 1.2                  | 99        | 4.57                              |
| 3     | 0.3                 | 0.01                                | 0.1                               | 4MA              | 50   | 160          | 24     | 0.072                        | 0.06 <sup>a</sup>                   | 1.728         | 1.2                  | 99        | 4.97                              |
| 4     | 1.2                 | 0.01                                | 0.277                             | 4MA              | 50   | 160          | 26     | 0.072                        | 0                                   | 2.149         | 1.2                  | 99        | 4.55                              |
| 5     | 0.5                 | 0.02                                | 0.133                             | 4MA              | 50   | 160          | 5      | 0.120                        | 0                                   | 0.733         | 0.5                  | 97        | 4.85                              |
| 6     | 0.5                 | 0.02                                | 0.133                             | 4MA              | 25   | 160          | 5      | 0.120                        | 0                                   | 0.733         | 0.5                  | 96        | 4.8                               |
| 7     | 0.5                 | 0.02                                | 0.133                             | 4MA              | 12   | 160          | 5      | 0.120                        | 0                                   | 0.733         | 0.5                  | 98        | 4.9                               |
| 8     | 0.5                 | 0.02                                | 0.133                             | 4MA              | 6    | 160          | 5      | 0.120                        | 0                                   | 0.733         | 0.5                  | 97        | 4.85                              |
| 9     | 0.5                 | 0.02                                | 0.133                             | 4MA              | 3    | 160          | 5      | 0.120                        | 0                                   | 0.733         | 0.5                  | 98        | 4.9                               |
| 10    | 0.5                 | 0.02                                | 0.133                             | None             | 0    | 160          | 5      | 0.120                        | 0                                   | 0.733         | 0.5                  | 97        | 4.85                              |

<sup>a</sup> Over 15 h

insoluble in the reaction medium and the yield of 4MA is almost zero. The rate of conversion increases with increasing temperature and reaches a maximum at 160 °C (Fig. 5). At a temperature higher than 160 °C, the reaction medium becomes low in DMC under atmospheric pressure and the reaction is therefore slowed down.

**Fig. 5** Effect of temperature on reaction yield. Conditions: *p*C = 0.5 mol, K<sub>2</sub>CO<sub>3</sub> = 0.02 mol, DMC (*t*<sub>0</sub>) = 0.13 mol, flow rate of DMC = 0.12 mol h<sup>-1</sup>, time = 5 h.

conversion of *p*-cresol (in conditions of entry 10), the reaction medium was treated by distillation to obtain the pure 4-methylanisole. The catalyst was re-used consecutively five times without any decline in its reactivity though the reactivity of the recycled catalyst was slightly lower than the fresh catalyst (Fig. 6). DMC can be separated from methanol by extractive distillation<sup>53</sup> or on an ion exchanger.<sup>54</sup>

**Fig. 6** Reactivity of K<sub>2</sub>CO<sub>3</sub> according to the number of cycles.

### Influence of the catalyst nature

Among various catalysts tested, bases containing the potassium cation are more effective, in particular, potassium carbonate (Table 2).

**Table 2** Effect of the catalyst on yield of the reaction

| Catalyst                        | Yield of 4MA (%) |
|---------------------------------|------------------|
| KOH                             | 47               |
| KHCO <sub>3</sub>               | 69               |
| KNO <sub>3</sub>                | 0                |
| K <sub>2</sub> CO <sub>3</sub>  | 90               |
| Na <sub>2</sub> CO <sub>3</sub> | 21               |
| Cs <sub>2</sub> CO <sub>3</sub> | 63               |
| CaCO <sub>3</sub>               | 0                |
| No catalyst                     | 0                |

Reaction conditions: *p*-cresol = 0.5 mol, K<sub>2</sub>CO<sub>3</sub> = 0.02 mol, DMC (*t*<sub>0</sub>) = 0.13 mol; DMC continuous flow rate = 0.15 mol h<sup>-1</sup>; temperature = 160 °C time = 4 h.

### Catalyst and DMC recycling

To meet economical interest and the principles of clean synthesis the recycling of the catalyst was studied. After total

### Process generalisation

Table 3 shows the results of O-alkylation of various phenols with dialkyl carbonate by using the same procedure as for O-methylation of *p*-cresol with DMC. Therefore, the generalisation can easily be adopted to other phenols (entries 11–19) as well as to other alkyl carbonates (entries 20 and 21). Total conversion would be obtained if the reaction time is adequately extended. The reaction is totally O-selective except in the case of catechol in which various by-products were detected by gas chromatography analysis (entries 19).

### Conclusion

The combination of the use of dimethyl carbonate as reagent and potassium carbonate as recyclable catalyst avoids the use of conventional methylating agents. DMC is obviously more atom economic than MeI, MeBr or dimethyl sulfate (DMS). Furthermore, when DMC is used as the methylating agent, it only leads to methanol and carbon dioxide. These by-products can easily be separated from the alkyl aryl ethers and methanol can be re-used according to the principle of life cycle assessment. Compared with methanol, DMC is a better methylating agent

**Table 3** Results of the O-methylation of various phenols with DMC

| Entry | Substrate Identity            | Mol | Reaction conditions                     |                               | T/°C | Time/h | DMC flow/<br>mol h <sup>-1</sup> | DMC<br>total/mol | Yield<br>(%)    | Residual<br>substrate<br>(%) | Average<br>MSHV/<br>h <sup>-1</sup> |
|-------|-------------------------------|-----|---|-------------------------------|------|--------|----------------------------------|------------------|-----------------|------------------------------|-------------------------------------|
|       |                               |     | K <sub>2</sub> CO <sub>3</sub> /<br>mol | DMC (t <sub>0</sub> )/<br>mol |      |        |                                  |                  |                 |                              |                                     |
| 11    | Phenol                        | 0.5 | 0.02                                    | 0.1                           | 150  | 5      | 0.13                             | 0.75             | 70              | 26                           | 3.5                                 |
| 12    | 4-Chlorophenol                | 0.5 | 0.02                                    | 0.135                         | 160  | 4.5    | 0.15                             | 0.81             | 99              | 0                            | 5.5                                 |
| 13    | 4-Hydroxybenzophenone         | 0.5 | 0.02                                    | 0.175                         | 160  | 5      | 0.13                             | 0.82             | 52              | 44                           | 2.6                                 |
| 14    | 4'-Acetophenone               | 0.5 | 0.04                                    | 0.145                         | 160  | 9      | 0.88                             | 0.94             | 86              | 14                           | 1.2                                 |
| 15    | 2-Naphthol                    | 0.5 | 0.04                                    | 0.2                           | 160  | 6      | 0.1                              | 0.80             | 96              | 3                            | 2.0                                 |
| 16    | 4-Hydroxyphenylacetic acid    | 0.5 | 0.04                                    | 0.15                          | 160  | 11     | 0.1                              | 1.25             | 29              | 65                           | 0.33                                |
| 17    | Eugenol                       | 0.5 | 0.04                                    | 0.145                         | 170  | 6      | 0.12                             | 0.86             | 93              | 5                            | 1.9                                 |
| 18    | 2,4-Dihydroxybenzophenone     | 0.5 | 0.02                                    | 0.15                          | 160  | 10     | 0.1                              | 1.15             | 80 <sup>a</sup> | 15                           | 2.0                                 |
| 19    | Catechol                      | 0.5 | 0.04                                    | 0.15                          | 160  | 3      | 0.2                              | 0.75             | 48 <sup>b</sup> | 31                           | 2.0                                 |
| 20    | <i>p</i> -Cresol <sup>c</sup> | 0.5 | 0.02                                    | 0.17                          | 160  | 12     | 0.08                             | 1.13             | 94 <sup>d</sup> | 0                            | 1.9                                 |
| 21    | Phenol <sup>c</sup>           | 0.5 | 0.02                                    | 0.1                           | 155  | 8      | 0.08                             | 0.74             | 90 <sup>e</sup> | 8                            | 2.8                                 |

<sup>a</sup> Yield of 2-hydroxy-4-methoxybenzophenone. <sup>b</sup> Yield of guaiacol. <sup>c</sup> O-Ethylation with diethyl carbonate (DEC). <sup>d</sup> Yield of 4-ethoxytoluene. <sup>e</sup> Yield of phenetole.

due to its high reactivity and high selectivity. Therefore, waste of substrate can be avoided by using DMC. This process approaches to the twelve principles of green chemistry proposed by Anastas and Warner.<sup>55</sup>

## Experimental

The reaction was conducted in a 250 ml reactor equipped with a mechanical stirrer, a thermocouple linked to heater by an automatic regulator and a distillation column. The top of distillation column was equipped with a reflux system, enabling adjustment of the outlet flow rate of by-product. The reagents were fed into the reactor by a peristaltic pump (Scheme 2). At the end of the reaction, residual DMC can be separated from the product by distillation.

Dimethyl carbonate and diethyl carbonate were obtained from SNPE. Other reagents were commercially available in a purity of at least 97%.

The yield of each reaction was determined by gas chromatography on a Hewlett Packard™ 5890 with monochlorobenzene used as internal standard. The capillary column (BP1, 50 m × 0.25 mm × 0.25 μm) was temperature-programmed from 50 to 220 °C with a heating rate of 20 °C min<sup>-1</sup>. The injector and detector temperature were 240 and 260 °C, respectively. The column head pressure was 20 psi.

The products obtained were purified before being identified by <sup>13</sup>C and <sup>1</sup>H NMR on NMR Bruker™ AC 200 equipment

(CDCl<sub>3</sub> as solvent, 200 MHz for <sup>1</sup>H NMR and 50 MHz for <sup>13</sup>C NMR).

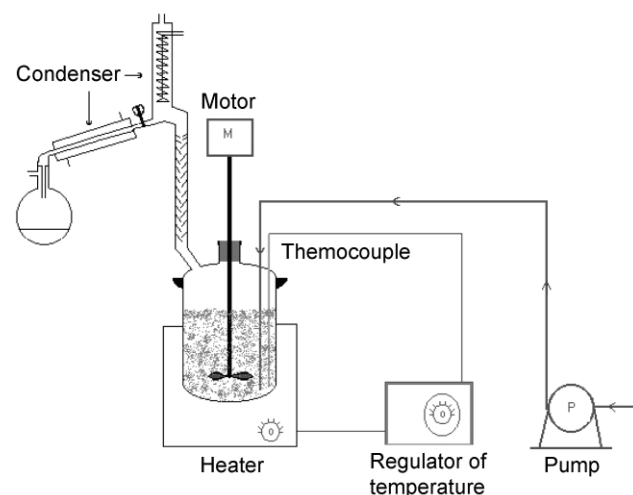
FT-IR spectra analysis: the mixture of *p*-cresol and K<sub>2</sub>CO<sub>3</sub> (4% molar of K<sub>2</sub>CO<sub>3</sub>) was heated to 160 °C with stirring and the mixture became homogeneous. After cooling down to room temperature, a brown solid was obtained which was analysed using a PERKIN ELMER™ Spectrum BX II FT-IR system.

## Acknowledgement

Dr F. Violleau, (Senior researcher at Laboratoire de Chimie Agro-industrielle) is gratefully acknowledged for his contribution. We also thank SNPE-Toulouse for their financial support.

## References

- H. Fiege, H. W. Voges, T. Hamamoto, S. Umamura, T. Iwata, H. Miki, Y. Fujita, H. J. Buysch and D. Garbe, *Ullmann's encyclopaedia of chemical industry*, 6th edn., 1999, electronic release.
- D. Achiet, D. Rochelle, I. Murengezi, M. Delmas and A. Gaset, *Synthesis*, 1986, 642–643.
- R. T. Winters, A. D. Sercel and H. D. H. Showalter, *Synthesis*, 1988, 712–714.
- M. L. Sharma and T. Chand, *Tetrahedron Lett.*, 1996, **37**, 2279–2280.
- A. Basak, M. K. Nayak and A. S. Chakraborti, *Tetrahedron Lett.*, 1998, **39**, 4883–4886.
- A. W. Williamson, *J. Chem. Soc.*, 1852, **4**, 106–112.
- R. A. W. Johnstone and M. E. Rose, *Tetrahedron*, 1979, **35**, 2169–2173.
- G. Brieger, D. Hachey and T. Nestrick, *J. Chem. Eng. Data.*, 1968, **13**, 581–582.
- B. A. Stoochnoff and N. Leo Benoiton, *Tetrahedron Lett.*, 1973, **1**, 21–24.
- W. E. Wymann, R. Davis, J. W. Patterson and J. R. Pfister, *Synth. Commun.*, 1988, **18**(12), 1379–1384.
- J. C. Lee, J. Y. Yuk and S. H. Cho, *Synth. Commun.*, 1995, **25**, 1367–1370.
- K. B. Wiberg and K. A. Saegbarth, *J. Org. Chem.*, 1960, **25**, 832–833.
- S. Oae and R. Kiritani, *Bull. Chem. Soc. Jpn.*, 1966, **39**, 611–614.
- P. Maggioni and F. Minisci, *UK Pat.*, 2085004, 1984, CAN 96:180960.
- N. M. Cullinane and W. C. Davies, *UK Pat.*, 600837, 1948, CAN 42:34392.
- A. B. Mossman, *US Pat.*, 4611084, 1986, CAN 105:193360.
- A. B. Mossman, *US Pat.*, 4638098, 1987, CAN 106:101880.
- S. Balsama, P. Beltrame, P. L. Beltrame, P. Carniti, L. Forni and G. Zuretti, *Appl. Catal.*, 1984, **13**, 161–170.
- V. Eshinazi, *US Pat.*, 4450306, 1984, CAN 101:90575.
- E. Santacesaria, D. Grasso, D. Gelosa and S. Carra, *Appl. Catal.*, 1990, **64**(1–2), 83–99.



**Scheme 2** Schematic plot of the reactor used in O-alkylation of phenols with DMC.

- 21 S. Furusaki, M. Matsuda, M. Saito, Y. Shiomi, Y. Nakamura and M. Tobita, *US Pat.*, 5189225, 1993, CAN 115:49082.
- 22 S. C. Lee, S. W. Lee, K. S. Kim, T. J. Lee, D. H. Kim and J. C. Kim, *Catal. Today*, 1998, **44**, 253–258.
- 23 Rajaram. Bal, K. Chaudhari and S. Sivasanker, *Catal. Lett.*, 2000, **70**, 75–78.
- 24 L. Calzolari, F. Cavani and T. Monti, *Acad. Sci. Paris, Sér. IIc*, 2000, **3**, 533–539.
- 25 V. V. Balasubramanian, A. Pandurangan, M. Palanichamy and V. Murugesan, *Indian J. Chem. Technol.*, 2000, **7**, 149–154.
- 26 S. Memoli, M. Selva and P. Tundo, *Chemosphere*, 2001, **43**, 115–121.
- 27 P. Tundo, P. Anastas, D. S. Black, J. Breen, T. Collins, S. Memoli, J. Miyamoto, M. Polyakoff and W. Tumas, *Pure Appl. Chem.*, 2000, **72**, 1207–1228.
- 28 F. Rivetti, *C. R. Acad. Sci. Paris, Sér. IIc*, 2000, **3**, 497–503.
- 29 Y. Ono, *Appl. Catal. A.*, 1997, **155**, 133–166.
- 30 G. Iori and U. Romano, *UK Pat.*, 2026484A, 1981, CAN 93:167894.
- 31 F. Merger, F. Tovae and L. Schroff, *US Pat.*, 4192949, 1980, CAN 92:6229.
- 32 Ralph Brewster Thompson, *Eur. Pat.*, 0104598, 1984, CAN 101:151578.
- 33 G. Barcelo, D. Grenouillat, J. P. Senet and G. Sennyey, *Tetrahedron*, 1990, **46**(6), 1839–1848.
- 34 Y. Lee and I. Shimizu, *Synlett*, 1998, 1063–1064.
- 35 Z. H. Fu and Y. Ono, *Catal. Lett.*, 1993, **21**, 43–47.
- 36 R. Rhodes and P. Nightingale, *World Pat.*, 86/03485, 1986, CAN 105:190655.
- 37 Y. Fu, T. Baba and Y. Ono, *Appl. Catal. A.*, 1998, **166**, 419–424.
- 38 Y. Fu, T. Baba and Y. Ono, *Appl. Catal. A.*, 1998, **166**, 425–430.
- 39 Y. Fu, T. Baba and Y. Ono, *Appl. Catal. A.*, 1999, **176**, 201–204.
- 40 F. M. Bautista, J. M. Campelo, A. Garcia, D. Luna, J. M. Marinas, A. A. Romero and M. R. Urbano, *React. Kinet. Catal. Lett.*, 1997, **62**(1), 47–54.
- 41 M. B. Talawar, T. M. Jyothi, P. D. Sawant, T. Raja and B. S. Rao, *Green Chem.*, 2000, **2**, 266–268.
- 42 T. M. Jyothi, T. Raja, M. B. Talawar and B. S. Rao, *Appl. Catal. A.*, 2001, **211**(11), 41–46.
- 43 A. Bomben, M. Selva, P. Tundo and L. Valli, *Ind. Eng. Chem. Res.*, 1999, **38**, 2075–2079.
- 44 P. Tundo, F. Trotta and G. Moraglio, *Reactive Polymers*, 1989, **10**, 185–188.
- 45 P. Tundo and M. Selva, *CHEMTECH*, 1995, **25**(5), 31–35.
- 46 M. Selva, F. Trotta and P. Tundo, *J. Chem. Soc., Perkin Trans. 2*, 1992, 519–522.
- 47 P. Tundo, G. Moraglio and F. Trotta, *Ind. Eng. Chem. Res.*, 1989, **28**, 881–890.
- 48 P. Tundo, F. Trotta, G. Moraglio and F. Ligorati, *Ind. Eng. Chem. Res.*, 1988, **27**, 1565–1571.
- 49 M. Lissel, S. Schmidt and B. Neumann, *Synthesis*, 1986, **5**, 382–383.
- 50 S. Ouk, S. Thiébaud, E. Borredon, P. Le Gars and L. Lecomte, *Tetrahedron Lett.*, 2002, **43**, 2661–2663.
- 51 A. Perosa, M. Selva, P. Tondo and F. Zordan, *Synlett*, 2000, **1**, 272–274.
- 52 S. Ouk, S. Thiébaud, E. Borredon and P. Le Gars, *Appl. Catal. A.*, 2002, accepted for publication.
- 53 F. J. Mais, P. Wagner and H. J. Buysch, *Eur. Pat.*, 0581115, 1994, CAN 121:111924.
- 54 I. Janisch, H. Landscheidt, W. Strüver and A. Klausener, *Eur. Pat.*, 0658536, 1995, CAN123:344112.
- 55 P. T. Anastas and J. C. Warner, *Green Chemistry: Theory and Practice*, Oxford University Press, Oxford, 1998.



# An eco-friendly approach for the synthesis of $\alpha$ -aminophosphonates using ionic liquids

J. S. Yadav,\* B. V. S. Reddy and P. Sreedhar

Division of Organic Chemistry, Indian Institute of Chemical Technology, Hyderabad 500 007, India. E-mail: yadav@iict.ap.nic.in

Received 23rd April 2002

First published as an Advance Article on the web 25th July 2002

Room-temperature ionic liquids are found to be efficient catalysts in promoting three component-coupling reactions of aldehydes, amines and diethyl phosphite in solvent-free conditions to afford the corresponding  $\alpha$ -aminophosphonates in high yields with high selectivity.

## Introduction

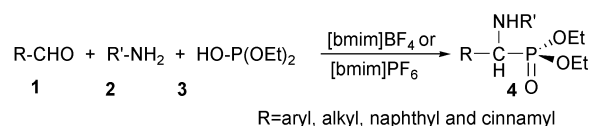
$\alpha$ -Aminophosphonates are an important class of biologically active compounds<sup>1</sup> and their synthesis has received a considerable amount of interest because of their structural analogy to  $\alpha$ -amino acids. They also act as peptide mimics,<sup>2</sup> enzyme inhibitors,<sup>3</sup> herbicides,<sup>4</sup> antibiotics and pharmacological agents.<sup>5</sup> Generally,  $\alpha$ -aminophosphonates are prepared by the addition of phosphorus nucleophiles to imines in the presence of either a base or an acid. A variety of reagents such as  $\text{SnCl}_4$ ,  $\text{BF}_3 \cdot \text{OEt}_2$ ,  $\text{ZnCl}_2$  and  $\text{MgBr}_2$  have been employed for this transformation.<sup>6,7</sup> However, these reactions can not be carried out in a one-pot operation with a carbonyl compound, amine and diethyl phosphite, because the amines and water that exist during imine formation can decompose or deactivate the Lewis acids.<sup>6</sup> In order to circumvent the problems associated with these methods, recently one-pot procedures have also been developed for this conversion using lanthanide triflates and indium trichloride as catalysts.<sup>8</sup> Although these procedures do not require the isolation of unstable imines prior to the reactions, long reaction times are required to obtain the desired products in good yields. In addition, the use of harmful organic solvents is undesirable from the view of today's environmental consciousness.

One of the prime concerns of industry and academia is the search for replacements to the environmentally damaging solvents used on a large scale, especially those that are volatile and difficult to handle. With the rapid development in the field of synthetic organic chemistry, researchers from both academia and industry, have started giving serious thought to the detrimental effect of non-green process chemicals on the environment. As a result, several environmentally benign procedures have successfully been developed to avoid, or at least minimize, these effects. Ionic liquids have recently gained recognition as possible environmentally benign alternative solvents in various chemical processes.<sup>9</sup> Room-temperature ionic liquids, especially those based on the 1-*n*-alkyl-3-methylimidazolium cation, have shown great promise as an attractive alternative to conventional solvents. They provide an eco-friendly reaction medium for a variety of organic transformations, as they are non-volatile, recyclable, non-explosive, easy to handle, thermally robust, and in addition, they are compatible with various organic compounds and organometallic reagents.<sup>10</sup> Because of the great potential of room-temperature ionic liquids as environmentally benign media for catalytic processes, much attention has been currently focused on organic reactions catalyzed by ionic liquids.<sup>11</sup> Several organic reactions catalyzed by ionic liquids have been reported with high performance.<sup>12</sup>

## Results and discussion

We wish to explore the use of ionic liquids as novel catalysts for the synthesis of  $\alpha$ -aminophosphonates under mild conditions (Scheme 1).

The treatment of benzaldehyde and aniline with diethyl phosphite in 1-butyl-3-methylimidazolium tetrafluoroborate ionic liquid resulted in the formation of the  $\alpha$ -aminophosphonate in 90% yield. In a similar fashion, various aldehydes and amines were treated with diethyl phosphite to afford the corresponding  $\alpha$ -aminophosphonates in high yields. The reactions proceeded smoothly at ambient temperature with high selectivity. No trace amounts of  $\alpha$ -hydroxyphosphonates are obtained as a result of the reaction between the aldehyde and diethyl phosphite under the present reaction conditions. However, in the absence of ionic liquids, the reaction did not yield any product even after a long reaction period (20 h). Furthermore, we have performed the reactions in polar organic solvents such as DMF and *N*-methylpyrrolidine to compare the efficiency of ionic liquids. The reactions did not proceed in these solvents even under heating conditions (75–80 °C). Several aromatic,  $\alpha,\beta$ -unsaturated, heterocyclic and aliphatic aldehydes reacted well in ionic liquids to produce the phosphonates in high yields. All the products were characterized by <sup>1</sup>H NMR, IR and mass spectral analysis and also by comparison with authentic samples.<sup>8a</sup> The reactions of various aldehydes, amines and diethyl phosphite were examined in hydrophilic

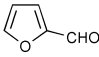
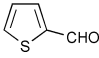
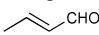
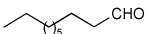


Scheme 1

## Green Context

The use of ionic liquids as alternative reaction media is becoming an established and vigorous theme in green chemistry. This paper describes a particularly advantageous use of these solvents in a three-component reaction. Not only do the ionic liquids support the reaction well, their use obviates the requirements for added promoters (base or acid is often required), makes the system water tolerant, and allows a one-pot coupling rather than the usual two-step method. DTM

**Table 1** Ionic liquid-promoted synthesis of  $\alpha$ -aminophosphonates<sup>a</sup>

| Entry | Aldehyde  | Amine  | [bmim]BF <sub>4</sub> |                        | [bmim]PF <sub>6</sub> |                        |
|-------|---|--|-----------------------|------------------------|-----------------------|------------------------|
|       |   |  | Time/h                | Yield <sup>b</sup> (%) | Time/h                | Yield <sup>b</sup> (%) |
| a     | C <sub>6</sub> H <sub>5</sub> CHO   | C <sub>6</sub> H <sub>5</sub> NH <sub>2</sub>      | 5.0                   | 90                     | 8.0                   | 84                     |
| b     | 4-FC <sub>6</sub> H <sub>4</sub> CHO  | C <sub>6</sub> H <sub>5</sub> NH <sub>2</sub>      | 6.5                   | 85                     | 9.0                   | 81                     |
| c     | C <sub>6</sub> H <sub>5</sub> CHO   | 4-MeC <sub>6</sub> H <sub>4</sub> NH <sub>2</sub>  | 4.5                   | 91                     | 10.0                  | 85                     |
| d     | 4-MeOC <sub>6</sub> H <sub>4</sub> CHO  | C <sub>6</sub> H <sub>5</sub> NH <sub>2</sub>      | 6.0                   | 93                     | 9.5                   | 80                     |
| e     | C <sub>6</sub> H <sub>5</sub> CHO   | 4-MeOC <sub>6</sub> H <sub>4</sub> NH <sub>2</sub> | 5.0                   | 91                     | 8.0                   | 83                     |
| f     | 4-NO <sub>2</sub> C <sub>6</sub> H <sub>4</sub> CHO                               | C <sub>6</sub> H <sub>5</sub> NH <sub>2</sub>      | 9.5                   | 80                     | 12.0                  | 71                     |
| g     | Ph-CH=CHCHO   | C <sub>6</sub> H <sub>5</sub> NH <sub>2</sub>      | 5.0                   | 90                     | 8.0                   | 85                     |
| h     | C <sub>6</sub> H <sub>5</sub> CHO   | 4-ClC <sub>6</sub> H <sub>4</sub> NH <sub>2</sub>  | 7.0                   | 88                     | 11.0                  | 81                     |
| i     | 4-ClC <sub>6</sub> H <sub>4</sub> CHO   | C <sub>6</sub> H <sub>5</sub> NH <sub>2</sub>      | 6.5                   | 85                     | 10.0                  | 78                     |
| j     |  | 4-FC <sub>6</sub> H <sub>5</sub> NH <sub>2</sub>   | 5.0                   | 91                     | 8.0                   | 87                     |
| k     |  | C <sub>6</sub> H <sub>5</sub> NH <sub>2</sub>      | 4.5                   | 90                     | 7.5                   | 83                     |
| l     | 2-Naphthal  | C <sub>6</sub> H <sub>5</sub> NH <sub>2</sub>      | 7.0                   | 87                     | 12.0                  | 79                     |
| m     |  | C <sub>6</sub> H <sub>5</sub> NH <sub>2</sub>      | 5.0                   | 85                     | 9.0                   | 80                     |
| n     |  | C <sub>6</sub> H <sub>5</sub> NH <sub>2</sub>      | 8.0                   | 81                     | 12.0                  | 75                     |

<sup>a</sup> All products were characterized by <sup>1</sup>H NMR, IR and mass spectra <sup>b</sup> Isolated and unoptimized yields after purification.

1-butyl-3-methylimidazolium tetrafluoroborate ([bmim]BF<sub>4</sub>) and hydrophobic 1-butyl-3-methylimidazolium hexafluorophosphate ([bmim]PF<sub>6</sub>) ionic liquids and the results were presented in Table 1. Among these ionic liquids, 1-butyl-3-methylimidazolium tetrafluoroborate ([bmim]BF<sub>4</sub>) was found to be superior in terms of yields and reaction rates. The advantage of the use of ionic liquids as novel reaction media for this transformation is that these ionic solvents were easily recovered and reused. Since the products were weakly soluble in the ionic phase, they were easily separated by simple extraction with ether. The remaining viscous ionic liquid was thoroughly washed with ether and reused in subsequent reactions without further purification. Although the products were obtained in the same purity as in the first run, the yields were gradually decreased in runs carried out using recycled ionic liquid. For example, the reaction of benzaldehyde, aniline and diethyl phosphite afforded the corresponding  $\alpha$ -aminophosphonate in 90, 87, 85 and 81% yields over four cycles. However, the activity of ionic liquid was consistent in runs and no decrease in yield was obtained when the recycled ionic liquid was activated at 80 °C under vacuum in each cycle. Finally, the catalytic performances of various quaternary ammonium salts were studied. The three-component condensation was not successful when *n*-tetrabutylammonium chloride (*n*-Bu<sub>4</sub>NCl) or 1-butyl-3-methylimidazolium chloride (bmimCl) was used as catalyst. This indicated that both cation and anion played an important role as the catalyst in this transformation.

## Conclusion

This paper describes a novel and efficient method for the synthesis of  $\alpha$ -aminophosphonates using environmentally safe ionic solvents. The simple operation combined with easy recovery and reuse of this novel reaction media makes this process economic, benign and a waste free route for the synthesis of  $\alpha$ -aminophosphonates. The use of ionic liquids as catalysts for this transformation allows avoiding the use of moisture-sensitive and heavy-metal Lewis acids.

## Experimental

1-Butyl-3-methylimidazolium tetrafluoroborate ([bmim]BF<sub>4</sub>) and 1-butyl-3-methylimidazolium hexafluorophosphate

([bmim]PF<sub>6</sub>) ionic liquids were prepared according to the procedures reported in the previous literature.<sup>13</sup>

## General procedure for the synthesis of $\alpha$ -aminophosphonate

Aldehyde (2 mmol), amine (2 mmol) and diethyl phosphite (2 mmol) in 1-butyl-3-methylimidazolium tetrafluoroborate or 1-butyl-3-methylimidazolium hexafluorophosphate (1 mL) were stirred at ambient temperature for an appropriate time (Table 1). After completion of the reaction, as indicated by TLC, the reaction mixture was washed with diethyl ether (3 × 10 mL). The combined ether extracts were concentrated *in vacuo* and the resulting product was directly charged on small silica gel column and eluted with a mixture of ethyl acetate–*n*-hexane (2:8) to afford the pure  $\alpha$ -aminophosphonate. The remainder of the viscous ionic liquid was further washed with ether and dried at 80 °C under reduced pressure to retain its activity in subsequent runs. Representative spectroscopic data for product **4a**: Liquid, <sup>1</sup>H NMR (CDCl<sub>3</sub>),  $\delta$  1.15 (t, *J* = 6.8 Hz, 3H), 1.25 (t, *J* = 6.8 Hz, 3H), 2.20 (br s, NH), 3.55 (d, *J* = 14.8 Hz, 1H), 3.70–4.18 (m, 6H), 7.20–7.45 (m, 10H). <sup>13</sup>C NMR (proton decoupled, CDCl<sub>3</sub>),  $\delta$  16.09, 16.2, 16.28, 16.40, 51.04, 51.38, 58.12, 61.17, 62.64, 62.79, 62.94, 127.05, 127.83, 128.26, 128.56, 128.68, 129.3, 130.05, 136.0, 146.7. <sup>31</sup>P NMR (CDCl<sub>3</sub>)  $\delta$ : 24.007. FAB Mass: *m/z*: 333 M<sup>+</sup>, 281, 196, 147, 123, 109, 91, 69, 55.

## Acknowledgements

B. V. S. and P. S. thank CSIR, New Delhi for the award of fellowships.

## References

- (a) S. C. Fields, *Tetrahedron*, 1999, **55**, 12237; (b) E. K. Fields, *J. Am. Chem. Soc.*, 1952, **74**, 1528; (c) C. Yuan and S. Chen, *Synthesis*, 1992, 1124; (d) D. R. More, *J. Org. Chem.*, 1978, **43**, 992; (e) R. Hirschmann, A. B. Smith III, C. M. Taylor, P. A. Benkovic, S. D. Taylor, K. M. Yager, P. A. Sprengler and S. J. Venkovic, *Science*, 1994, **265**, 234; (f) T. Yokomatsu, Y. Yoshida and S. Shibuya, *J. Org. Chem.*, 1994, **59**, 7930.
- P. Kafarski and B. Lejczak, *Phosphorus, Sulfur, Silicon Relat. Elem.*, 1991, **63**, 1993.

- 3 (a) M. C. Allen, W. Fuhrer, B. Tuck, R. Wade and J. M. Wood, *J. Med. Chem.*, 1989, **32**, 1652; (b) P. P. Giannousis and P. A. Bartlett, *J. Med. Chem.*, 1987, **30**, 1603.
- 4 A. Barder, *Aldrichim. Acta*, 1988, **21**, 15.
- 5 (a) F. R. Atherton, C. H. Hassal and R. W. Lambert, *J. Med. Chem.*, 1986, **29**, 29; (b) E. K. Baylis, C. D. Campbell and J. G. Dingwall, *J. Chem. Soc., Perkin Trans. 1*, 1984, 2845.
- 6 (a) S. Lashat and H. Kunz, *Synthesis*, 1992, 90; (b) J. S. Yadav, B. V. S. Reddy, K. Sarita Raj and K. Bhaskar Reddy, *Synthesis*, 2001, 2277.
- 7 J. Zon, *Pol. J. Chem*, 1981, **55**, 643.
- 8 (a) C. Qian and T. Huang, *J. Org. Chem.*, 1998, **63**, 4125; (b) K. Manabe and S. Kobayashi, *Chem. Commun.*, 2000, 669; (c) B. C. Ranu, A. Hajra and U. Jana, *Org. Lett.*, 1999, **1**, 1141; (d) S. Lee, J. H. Park and J. Kang, *Chem. Commun.*, 2001, 1698.
- 9 (a) Recent reviews on ionic liquids: T. Welton, *Chem. Rev.*, 1999, **99**, 2071; (b) P. Wasserscheid and W. Keim, *Angew. Chem., Int. Ed.*, 2000, **39**, 3772.
- 10 Catalytic reactions in ionic liquids: R. Sheldon, *Chem. Commun.*, 2001, 2399.
- 11 (a) Ionic liquids have already been described as catalysts: C. Wheeler, K. N. West, C. L. Liotta and C. A. Eckert, *Chem. Commun.*, 2001, 887; (b) J. Peng and Y. Deng, *Tetrahedron Lett.*, 2001, **42**, 5917.
- 12 Bronsted acidic ionic liquids as dual solvent and catalysts: A. C. Cole, J. L. Jensen, I. Ntai, K. L. T. Tran, K. J. Weaver, D. C. Forbes and J. H. Jr. Davis, *J. Am. Chem. Soc.*, 2002, **124**, 5962.
- 13 (a) Preparation of ionic liquids: S. Park and R. J. Kazlauskas, *J. Org. Chem.*, 2001, **66**, 8395; (b) P. Bonhôte, A. P. Dias, N. Papageorgiou, K. Kalyanasundaram and M. Grätzel, *Inorg. Chem.*, 1996, **35**, 1168.



# Reaction of silylalkylmono- and silylalkyldi-amines with carbon dioxide: evidence of formation of inter- and intra-molecular ammonium carbamates and their conversion into organic carbamates of industrial interest under carbon dioxide catalysis

Angela Dibenedetto,<sup>\*a</sup> Michele Aresta,<sup>a</sup> Carlo Fragale<sup>a</sup> and Marcella Narracci<sup>b</sup>

<sup>a</sup> University of Bari, Department of Chemistry and METEA Research Center, Via Celso Ulpiani, 27-Bari, Italy. E-mail: a.dibenedetto@chimica.uniba.it; Fax: +39 080 544 2083

<sup>b</sup> Istituto Sperimentale Talassografico 'A. Cerruti' – CNR, 74100 Taranto, Italy

Received 31st May 2002

First published as an Advance Article on the web 29th July 2002

The reactivity of industrially relevant silylalkylamines towards CO<sub>2</sub> and dialkyl/arylcarbonates is discussed. The kinetics of uptake of carbon dioxide at various temperatures shows that at 295 K, silylalkylmonoamines react with carbon dioxide in a 2 : 1 molar ratio, affording classic intermolecular ammonium carbamates of formula RNHCOO<sup>−</sup>+NH<sub>3</sub>R, while at 273 K, dimeric carbamic acids, (RNHCOOH)<sub>2</sub>, are formed. Conversely, silylalkyldiamines react at 297 K with carbon dioxide to afford zwitterionic intramolecular six-membered cyclic ammonium carbamates of formula RNH<sub>2</sub><sup>+</sup>CH<sub>2</sub>CH<sub>2</sub>NHCOO<sup>−</sup>, a unique example of CO<sub>2</sub> uptake by an amine with a 1 : 1 molar ratio. Such systems may have a potential application in CO<sub>2</sub> separation. The catalytic role of carbon dioxide in the carbamation of the above mentioned amines by reaction with organic carbonates is described.

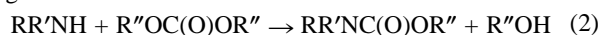
## Introduction

The reaction of amines with CO<sub>2</sub> is of great interest for two reasons: (i) amines are used for CO<sub>2</sub> separation from gases;<sup>1</sup> (ii) ammonium carbamates formed upon reaction of amines with CO<sub>2</sub> can undergo reaction with organic carbonates to afford organic carbamates. The use of monoethanolamine (MEA) for CO<sub>2</sub> separation from gases is a commercial process.<sup>1a,b</sup> Finding new amines<sup>1c</sup> or systems able to capture a higher amount of CO<sub>2</sub> per mole<sup>1d</sup> is also of great interest. Carbamates are used in pharmacology,<sup>2a</sup> agriculture,<sup>2b,c</sup> and the chemical industry.<sup>2d,e</sup> Their conventional synthesis is based on the use of phosgene, a toxic chemical which suffers from stringent transportation and stocking limitations. To substitute phosgene with less noxious starting materials may represent an important industrial target for the future, in addition to meet the raw material diversification goal. Carbon dioxide and organic carbonates are good candidates as phosgene substitutes.<sup>2f</sup>

The utilization of carbon dioxide in the synthesis of carbamate esters from amines and organic halides (eqn. (1)) has been investigated for long time.<sup>3</sup> Either crown-ethers<sup>3a,b</sup> or strong bases<sup>3c</sup> have been shown to promote the formation of carbamates. We have also described the recovery of crown-ethers<sup>3d</sup> that makes the synthesis of carbamates from amines, CO<sub>2</sub> and alkylating agents of practical interest.



Aminolysis of organic carbonates (eqn. (2), R, R' = H, alkyl or aryl; R'' = alkyl or aryl) is an alternative synthetic methodology that avoids the use of organic halides. As the carbonate itself can be used as solvent, the production of halogenated waste is eliminated.



The latter may become a methodology of general application in view of the fact that new non-phosgene processes for

dimethylcarbonate (DMC) have been recently developed based on the oxidative carbonylation of methanol.<sup>4</sup> Moreover, other organic carbonates can be prepared by transesterification of DMC with phenol or long-chain alcohols. The carboalkoxylation of aliphatic amines requires suitable catalysts such as AlCl<sub>3</sub>, SnCl<sub>2</sub>, ZnCl<sub>2</sub>, FeCl<sub>3</sub> or metal (Rh, Ru)<sup>5</sup> complexes in order to achieve high conversion rates and good selectivity. A major drawback may be the methylation of the amine. Recently, we have shown that carbon dioxide is an efficient catalyst for the synthesis of organic carbamates from aliphatic amines and DMC.<sup>6</sup> As this synthetic approach requires mild conditions, we made attempts to extend it to aminofunctional silanes,<sup>7</sup> as the corresponding carbamates are of industrial interest, as modulators of physico-mechanical properties of polymeric materials.<sup>8</sup> Moreover, silylalkylamines could be of interest as potential new CO<sub>2</sub> capturing agents from gas mixtures. In this paper, we describe the behaviour of silylalkylmono- and silylalkyldi- amines towards carbon dioxide, the different nature and thermal stability of the relevant ammonium carbamates, and the reactivity of the latter towards organic carbonates to afford organic carbamates under carbon dioxide catalysis.

## Green Context

The trapping of CO<sub>2</sub> by amines is well established in gas purification. Here novel amine trapping systems are discussed which can react readily with CO<sub>2</sub> under mild conditions to form carbamic acids and, with dimethyl carbonate, methyl carbamates. These latter compounds are very versatile synthons which are conventionally prepared from phosgene.

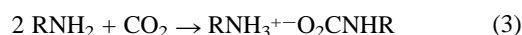
DJM



## Results and discussion

### Reactivity of aliphatic aminofunctional silanes towards carbon dioxide

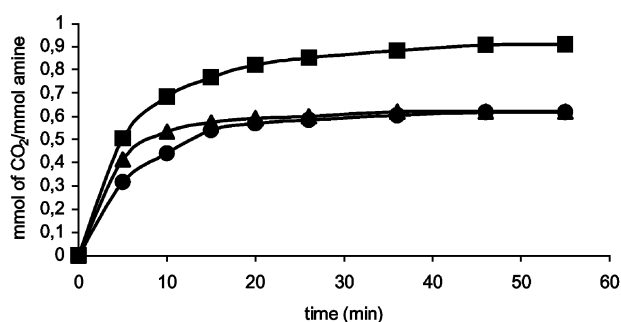
Aliphatic amines are known to react promptly with CO<sub>2</sub> (eqn. (3)) to afford an ammonium carbamate.<sup>6</sup>



We have investigated the behaviour of functionalised silylmonoalkylamines (silylamines for sake of brevity) such as H<sub>2</sub>N(CH<sub>2</sub>)<sub>3</sub>Si(OMe)<sub>3</sub> **I** and H<sub>2</sub>N(CH<sub>2</sub>)<sub>3</sub>Si(OEt)<sub>3</sub> **II** and silylalkyldiamines such as H<sub>2</sub>N(CH<sub>2</sub>)<sub>2</sub>NH(CH<sub>2</sub>)<sub>3</sub>Si(OMe)<sub>3</sub> **III** and H<sub>2</sub>NC(O)NH(CH<sub>2</sub>)<sub>2</sub>NH(CH<sub>2</sub>)<sub>3</sub>Si(OMe)<sub>3</sub> **IV** towards CO<sub>2</sub> at various temperatures.

**I** and **II** react rapidly with CO<sub>2</sub> at 297 ± 1 K in THF. Fig. 1(a) and (b) shows that the reaction is almost complete in 15 min and the amount of CO<sub>2</sub> taken up by the amine (*ca.* 0.55 mol/mol amine) indicates that one mole of CO<sub>2</sub> reacts with two moles of amine, as required by the stoichiometry of reaction (3), to afford ammonium carbamates (OMe)<sub>3</sub>Si(CH<sub>2</sub>)<sub>3</sub>NHCOO<sup>-</sup>H<sub>3</sub>N(CH<sub>2</sub>)<sub>3</sub>Si(OMe)<sub>3</sub> **V** (Fig. 1(a)) and (OEt)<sub>3</sub>Si(CH<sub>2</sub>)<sub>3</sub>NHCOO<sup>-</sup>H<sub>3</sub>N(CH<sub>2</sub>)<sub>3</sub>Si(OEt)<sub>3</sub> **VI** (Fig. 1(b)), respectively.

In both cases, the solution at the end of the reaction is cloudy due to a fine suspension of a white solid. IR spectra of the isolated compounds show the typical features of the ammonium

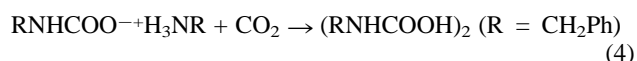


**Fig. 1** Kinetics of reactions of silylmonoamines with carbon dioxide: (a) silylmonoamine **I** at 298 K (●), (b) silylmonoamine **II** at 298 K (▲), (c) silylmonoamine **II** at 273 K (■).

carbamates usually isolated with other aliphatic amines (IR bands at 1535 cm<sup>-1</sup>). The <sup>1</sup>H and <sup>13</sup>C NMR spectra (Table 1), of compounds **V–VI** confirm their nature.

Similar to what we have observed in the case of other intermolecular ammonium carbamates,<sup>3a,b,d</sup> the proton NMR spectrum shows well defined signals for all the protons whose resonances, with the exception of those of the methylene group α to the carbamic and ammonium nitrogens, is very close to that of the parent amine. However, the perturbation of the electron distribution derived from the formation of the ammonium and carbamate moieties is felt only by the protons close to the nitrogen atom that is functionalised.

Interestingly, if the reaction is carried out at 273 K, the amount of CO<sub>2</sub> fixed by amine **II**, after a fast initial uptake of *ca.* 0.50 mol/mol, increases slowly to 1 mol/mol within less than 1 h (Fig. 1(c)). Amine **I** also shows a similar behaviour. This feature can be explained by assuming that at low temperature, the ammonium carbamate **V** or **VI** (RNHCOO<sup>-</sup>H<sub>3</sub>NR) slowly converts into the dimeric form of the corresponding carbamic (RNHCOOH)<sub>2</sub> acid. We have already shown that, under the same conditions, the carbamate/carbamic acid conversion<sup>9</sup> takes place with benzylamine and other N-compounds (eqn. (4)) In the case of C<sub>6</sub>H<sub>5</sub>CH<sub>2</sub>NH<sub>2</sub><sup>9a</sup> or the Co-complex of PhP(OCH<sub>2</sub>CH<sub>2</sub>)<sub>2</sub>NH<sup>9b</sup> the dimeric carbamic acid is not soluble and could be isolated and characterized by XRD. Conversely, if the dimeric carbamic acid is soluble, it may convert back into the amine and CO<sub>2</sub>. In fact, neat carbamic acid, RNHCOOH, is not stable and, like H<sub>2</sub>CO<sub>3</sub>, gives back CO<sub>2</sub>. We have not isolated the carbamic acid of **I** or **II** as a solid. In fact they are sticky liquids which are difficult to handle, that has prevented XRD characterization.



Carbamates **V** or **VI** heated *in vacuo* below 330 K do not lose carbon dioxide as demonstrated by <sup>1</sup>H NMR spectra; at higher temperatures, they undergo complex decomposition reactions. A different behaviour is shown by their aqueous solutions, that are able to release CO<sub>2</sub>. The different trend is due to the fact that ammonium hydrogencarbonate (EtO)<sub>3</sub>Si(CH<sub>2</sub>)<sub>3</sub>NH<sub>3</sub><sup>+</sup>HCO<sub>3</sub><sup>-</sup> is formed in water,<sup>1a</sup> that releases CO<sub>2</sub>.

**Table 1** <sup>1</sup>H and <sup>13</sup>C NMR data for free amines, ammonium carbamates and methyl carbamic esters

| Compound  | δ <sub>H</sub>                          |   |   |   |   |                              |                              |                      |                      |
|---|---|---|---|---|---|------------------------------|------------------------------|----------------------|----------------------|
|   | NH <sub>2</sub>                         | NHCO <sub>2</sub> CH <sub>3</sub>       | CH <sup>α</sup> <sub>2</sub>            | CH <sup>β</sup> <sub>2</sub>            | CH <sup>γ</sup> <sub>2</sub>            | CH <sup>δ</sup> <sub>2</sub> | CH <sup>ε</sup> <sub>2</sub> | OCH <sub>3</sub>     | C(O)OCH <sub>3</sub> |
| (CH <sub>3</sub> O) <sub>3</sub> SiCH <sup>γ</sup> <sub>2</sub> CH <sup>β</sup> <sub>2</sub> CH <sup>α</sup> <sub>2</sub> NH <sub>2</sub>   | 1.78                                    |   | 2.64                                    | 1.64                                    | 0.68                                    |                              |                              | 3.54                 |                      |
| (CH <sub>3</sub> O) <sub>3</sub> SiCH <sup>γ</sup> <sub>2</sub> CH <sup>β</sup> <sub>2</sub> CH <sup>α</sup> <sub>2</sub> NHCOO <sup>-</sup>  |   |   | 2.72 t                                  | 1.6 m, br                               | 0.66 m, br                              |                              |                              | 3.54                 |                      |
| (CH <sub>3</sub> O) <sub>3</sub> SiCH <sup>γ</sup> <sub>2</sub> CH <sup>β</sup> <sub>2</sub> CH <sup>α</sup> <sub>2</sub> NH <sub>3</sub> <sup>+</sup>  |   |   | 3.05 m, br                              | 1.6 m, br                               | 0.66 m, br                              |                              |                              | 3.54                 |                      |
| (CH <sub>3</sub> O) <sub>3</sub> SiCH <sup>γ</sup> <sub>2</sub> CH <sup>β</sup> <sub>2</sub> CH <sup>α</sup> <sub>2</sub> NHCOOCH <sub>3</sub>  |   | 2.01 s                                  | 3.02 m                                  | 1.44 m                                  | 0.48 m                                  |                              |                              | 3.42 s               | 3.51 s               |
| (CH <sub>3</sub> O) <sub>3</sub> SiCH <sup>ε</sup> <sub>2</sub> CH <sup>δ</sup> <sub>2</sub> CH <sup>γ</sup> <sub>2</sub> NHCH <sup>β</sup> <sub>2</sub> CH <sup>α</sup> <sub>2</sub> NH <sub>2</sub>   | 1.75                                    |   | 2.75                                    | 2.57                                    | 2.57                                    | 1.57                         | 0.63                         | 3.52                 |                      |
| (CH <sub>3</sub> O) <sub>3</sub> SiCH <sup>ε</sup> <sub>2</sub> CH <sup>δ</sup> <sub>2</sub> CH <sup>γ</sup> <sub>2</sub> NH <sub>2</sub> <sup>+</sup> CH <sup>β</sup> <sub>2</sub> CH <sup>α</sup> <sub>2</sub> NHCOO <sup>-</sup>   | 3.52                                    |   |   | 3.05                                    | 3.05                                    | 1.7                          | 0.65                         | 3.57                 |                      |
| (CH <sub>3</sub> O) <sub>3</sub> SiCH <sup>ε</sup> <sub>2</sub> CH <sup>δ</sup> <sub>2</sub> CH <sup>γ</sup> <sub>2</sub> NHCH <sup>β</sup> <sub>2</sub> CH <sup>α</sup> <sub>2</sub> NHCO <sub>2</sub> CH <sub>3</sub>   | 5.34                                    |   | 3.02                                    | 2.50                                    | 2.37                                    | 1.35                         | 0.40                         | 3.31                 | 3.39                 |
| Compound  | δ <sub>C</sub>                          |   |   |   |   |                              |                              |                      |                      |
|   | C <sup>α</sup> <sub>H<sub>2</sub></sub> | C <sup>β</sup> <sub>H<sub>2</sub></sub> | C <sup>γ</sup> <sub>H<sub>2</sub></sub> | C <sup>δ</sup> <sub>H<sub>2</sub></sub> | C <sup>ε</sup> <sub>H<sub>2</sub></sub> | OCH <sub>3</sub>             | C(O)OCH <sub>3</sub>         | C(O)OCH <sub>3</sub> |                      |
| (CH <sub>3</sub> O) <sub>3</sub> SiC <sup>γ</sup> <sub>H<sub>2</sub></sub> C <sup>β</sup> <sub>H<sub>2</sub></sub> C <sup>α</sup> <sub>H<sub>2</sub></sub> NH <sub>2</sub>  | 44.8                                    | 6                                       | 26.7                                    |   |   | 50.4                         |                              |                      |                      |
| (CH <sub>3</sub> O) <sub>3</sub> SiC <sup>γ</sup> <sub>H<sub>2</sub></sub> C <sup>β</sup> <sub>H<sub>2</sub></sub> C <sup>α</sup> <sub>H<sub>2</sub></sub> NHCOO <sup>-</sup>   | 43.8                                    | 6.2                                     | 25.1                                    |   |   | 50.2                         | 163                          |                      |                      |
| (CH <sub>3</sub> O) <sub>3</sub> SiC <sup>γ</sup> <sub>H<sub>2</sub></sub> C <sup>β</sup> <sub>H<sub>2</sub></sub> C <sup>α</sup> <sub>H<sub>2</sub></sub> NH <sub>3</sub> <sup>+</sup>   | 44.2                                    | 7.3                                     | 25.4                                    |   |   | 50.4                         |                              |                      |                      |
| (CH <sub>3</sub> O) <sub>3</sub> SiC <sup>γ</sup> <sub>H<sub>2</sub></sub> C <sup>β</sup> <sub>H<sub>2</sub></sub> C <sup>α</sup> <sub>H<sub>2</sub></sub> NHCOOCH <sub>3</sub>   | 43.22                                   | 6.11                                    | 23.00                                   |   |   | 50.37                        | 156.99                       | 51.71                |                      |
| (CH <sub>3</sub> O) <sub>3</sub> SiC <sup>ε</sup> <sub>H<sub>2</sub></sub> C <sup>δ</sup> <sub>H<sub>2</sub></sub> C <sup>γ</sup> <sub>H<sub>2</sub></sub> NHCH <sup>β</sup> <sub>H<sub>2</sub></sub> C <sup>α</sup> <sub>H<sub>2</sub></sub> NH <sub>2</sub>                               | 41.6                                    | 52.2                                    | 52.2                                    |   | 23                                      | 50.2                         |                              |                      |                      |
| (CH <sub>3</sub> O) <sub>3</sub> SiC <sup>ε</sup> <sub>H<sub>2</sub></sub> C <sup>δ</sup> <sub>H<sub>2</sub></sub> C <sup>γ</sup> <sub>H<sub>2</sub></sub> NH <sub>2</sub> <sup>+</sup> CH <sup>β</sup> <sub>H<sub>2</sub></sub> C <sup>α</sup> <sub>H<sub>2</sub></sub> NHCOO <sup>-</sup> |   | 38.2                                    | 38                                      | 5.8                                     | 20                                      | 50.5                         | 163                          |                      |                      |
| (CH <sub>3</sub> O) <sub>3</sub> SiC <sup>ε</sup> <sub>H<sub>2</sub></sub> C <sup>δ</sup> <sub>H<sub>2</sub></sub> C <sup>γ</sup> <sub>H<sub>2</sub></sub> NHCH <sup>β</sup> <sub>H<sub>2</sub></sub> C <sup>α</sup> <sub>H<sub>2</sub></sub> NHCOOCH <sub>3</sub>                          | 48.25                                   | 39.96                                   |   | 22.18                                   | 6.08                                    | 49.89                        | 156.88                       | 51.26                |                      |
| (CH <sub>3</sub> O) <sub>3</sub> SiC <sup>ε</sup> <sub>H<sub>2</sub></sub> C <sup>δ</sup> <sub>H<sub>2</sub></sub> C <sup>γ</sup> <sub>H<sub>2</sub></sub> N(COOCH <sub>3</sub> )C <sup>β</sup> <sub>H<sub>2</sub></sub> C <sup>α</sup> <sub>H<sub>2</sub></sub> NHCOOCH <sub>3</sub>       |   |   |   |   |   |                              | 156.83                       |                      |                      |
|   |   |   |   |   |   |                              | (primary)                    |                      |                      |
|   |   |   |   |   |   |                              | 162.57                       |                      |                      |
|   |   |   |   |   |   |                              | (secondary)                  |                      |                      |

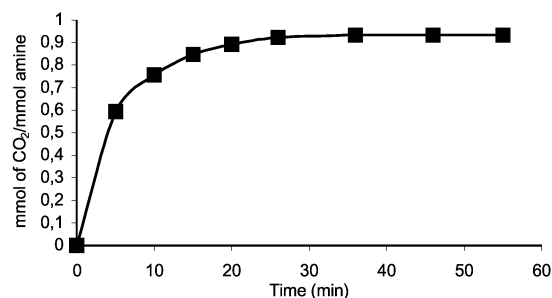


Fig. 2 Kinetics of reaction of diamine **III** with carbon dioxide at 298 K.

When diamine **III** is used, the CO<sub>2</sub> uptake curve (Fig. 2) at 295 K has a different shape with respect to that of monoamines.

In less than 20 min, diamine **III** takes up CO<sub>2</sub> with a 1:1 molar ratio, to afford a difficult to handle glassy material. The IR spectrum was taken on a film obtained by evaporating with a stream of CO<sub>2</sub> a solution deposited on a single KBr disk and shows the characteristic band at 1540 cm<sup>-1</sup> due to the carbamate RHNCOO<sup>-</sup> moiety. The liquid cannot be compressed between two disks as it acts as a sealing agent. This material behaves differently from either the intermolecular ammonium carbamate or the dimeric carbamic acid described above. CO<sub>2</sub> absorption quickly takes place also in absence of solvent if a thin film of the amine is used. In a bulk sample, the quantitative reaction of the amine with CO<sub>2</sub> is prevented by the fact that the carbamate occludes the amine that cannot undergo a complete conversion. The stoichiometry of the reaction shows that most likely a zwitterionic carbamate is formed. (Fig. 3).

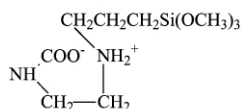
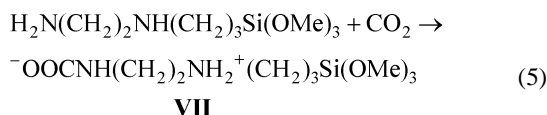


Fig. 3 Intramolecular ammonium carbamates.

We have carried out the CO<sub>2</sub> uptake in a NMR tube sealed under CO<sub>2</sub> (atmospheric pressure) and shown that the formation of the carbamate completely changes both the <sup>1</sup>H and <sup>13</sup>C spectra with respect to the starting amine (Table 1). Both the proton and the carbon-13 signals become very broad and low in intensity, features we have not observed previously, working with monoamines. Most likely, such a trend is due to rapid changes of configuration of the silylalkylamine with formation of a fluxional zwitterionic carbamate **VII** (eqn. (5)), with intramolecular, rather than intermolecular ion pairing (Fig. 3). Zwitterionic carbamates such as **VII** have not been described previously.

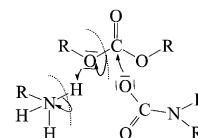


is completely released and the starting material **III** quantitatively recovered. The <sup>1</sup>H and <sup>13</sup>C NMR spectra of the recovered silyldiamine are identical with those of an authentic sample, showing that the -Si(OR)<sub>3</sub> moiety is intact. Diamine **III** can be reused several times in such a cyclic manner, demonstrating the potential it has for CO<sub>2</sub>-capture from gas mixtures, either neat or as a solid-gel.<sup>10</sup>

Differently from **III**, diamine **IV** scarcely reacts with carbon dioxide at room temperature and the yield of ammonium carbamate is very modest (<5%).

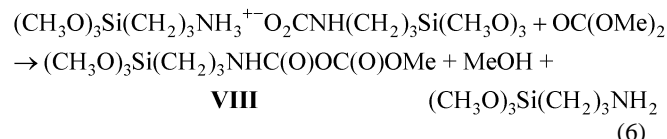
### Conversion of amines into organic carbamates

Silylamines **I–III** are converted into the relevant carbamates under CO<sub>2</sub>-catalysis by reaction with carbonates at 330 K. As

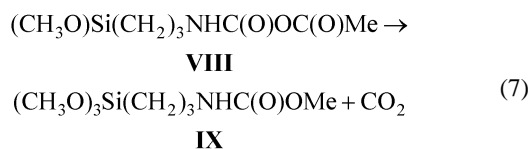


Scheme 1 Reactive step of the formation of carbamic-carbonic anhydride.

we have already shown for other amines,<sup>11–14</sup> the key reaction step<sup>13</sup> (Scheme 1) is the interaction of carbamate anion with the carbonate (eqn. (6)), which affords the mixed carbamic-carbonic anhydride **VIII**. This is a trimolecular reaction implying also the ammonium ion.<sup>13</sup>



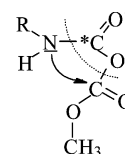
Subsequently, **VIII** decarboxylates to form the carbamate ester (**IX**). (eqn. (7))



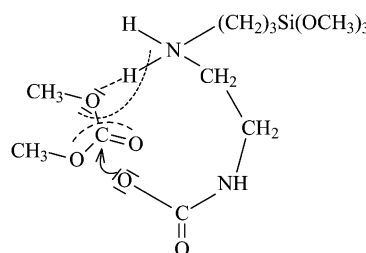
The CO<sub>2</sub> elimination is very regioselective,<sup>14</sup> and implies a nucleophilic attack by the nitrogen atom on the carbon of the carbonic ester moiety (Scheme 2). In fact, if the mixed anhydride (CH<sub>3</sub>O)<sub>3</sub>Si(CH<sub>2</sub>)<sub>3</sub>NH<sup>13</sup>C(O)<sup>12</sup>C(O)OCH<sub>3</sub> is allowed to decompose at room temperature only the unlabelled carbamate is obtained, (CH<sub>3</sub>O)<sub>3</sub>Si(CH<sub>2</sub>)<sub>3</sub>NH<sup>12</sup>COOCH<sub>3</sub>, with <sup>13</sup>CO<sub>2</sub> elimination.<sup>6</sup>

The reaction conditions are quite mild and the selectivity is 100%.

We have observed a faster reactivity of silyldiamine **III** with respect to silylmonoamines: this might be due to the fact that zwitterionic carbamate -O(O)CNH(CH<sub>2</sub>)<sub>2</sub>NH<sub>2</sub><sup>+</sup>(CH<sub>2</sub>)<sub>3</sub>Si(OR)<sub>3</sub> could be more reactive than the corresponding monoamine ammonium carbamates towards the organic carbonate, because of the lower molecularity of the reaction (Scheme 3) implying the intramolecular carbamate (bimolecular) with respect to the reaction of intermolecular carbamates (trimolecular).



Scheme 2 Regioselectivity in the CO<sub>2</sub> elimination step.



Scheme 3 Bimolecular reaction of intramolecular carbamate with DMC to afford CH<sub>3</sub>OH and the mixed anhydride (CH<sub>3</sub>O)<sub>3</sub>-Si(CH<sub>2</sub>)<sub>3</sub>NH(CH<sub>2</sub>)<sub>2</sub>NHC(O)OC(O)OCH<sub>3</sub>.

The fact that silylamine **IV** presents a low reactivity can be explained considering the deactivation of the amino-group produced by the carbonyl moiety.

The procedure described in this paper is quite useful for the synthesis of carbamates of functionalised amines where the silyl functional group is not attacked during the reaction. Moreover, the different reactivity of primary and secondary amino groups drives the regioselectivity of the reaction towards a single carbamation step under controlled temperature (below 335 K). Selectivity is lost at higher temperature (>340 K) and dicarbamates of amine **III** are also formed as demonstrated by the  $^{13}\text{C}$  NMR spectrum that shows resonances at 156.83 (terminal  $\text{COOCH}_3$ ) and 162.57 ppm (secondary amine  $\text{COOCH}_3$ ).

## Experimental

All reactions and manipulations were carried out under the specified atmosphere, by using vacuum line techniques. All solvents were dried as described in the literature,<sup>15</sup> and stored under dinitrogen. Silylalkylamines were Fluka products.

GC-MS analyses were carried out with a Shimadzu GCMS-QP5050 (MDN-5S capillary column: 60 m, 0.25  $\mu\text{m}$  film). IR Spectra were obtained with a Perkin Elmer 883 spectrophotometer.  $^1\text{H}$  and  $^{13}\text{C}$  NMR spectra were recorded with a Varian XL 200 or a Bruker AM 500 at 302 K.

## Uptake of $\text{CO}_2$

The uptake of  $\text{CO}_2$  was followed using a thermostated cell (19.4 mL), equipped with a septum for the injection of the amine, and connected to a gas-burette. The cell was thermostated at  $297 \pm 1$  K using a water bath, and at  $273 \pm 1$  K using a cryostat.

**General reaction of amines with  $\text{CO}_2$ .** 8 mL of THF was saturated with  $\text{CO}_2$  ( $P_{\text{CO}_2} = 0.1$  MPa) in the absorption cell and the liquid amine **I** (0.15 mL, 0.85 mmol, Fig. 1(a)), **II** (0.21 mL, 0.90 mmol, Fig. 1(b), (c)) or **III** (0.20 mL, 0.93 mmol, Fig. 2) was added through a rubber septum. The absorption of  $\text{CO}_2$  was monitored for 55 min, data are reported in Fig. 1 and 2.

Carbamates were isolated and characterized by  $^1\text{H}$ ,  $^{13}\text{C}$  NMR and analyses.

Anal. Calc. for  $\text{C}_{13}\text{H}_{34}\text{N}_2\text{O}_8\text{Si}_2$  (amine **I**): C, 38.78, H, 8.51, N, 6.95%. Found: C, 38.82, H, 8.55, N, 6.99%.

Anal. Calc. for  $\text{C}_{19}\text{H}_{46}\text{N}_2\text{O}_8\text{Si}_2$  (amine **II**): C, 44.33, H, 9.00, N, 5.44%. Found: C, 44.21, H, 9.11, N, 5.38%.

Anal. Calc. For  $\text{C}_9\text{H}_{22}\text{N}_2\text{O}_5\text{Si}$  (amine **III**): C, 43.14, H, 7.96, N, 10.05%. Found C, 43.08, H, 7.81, N, 9.98%.

## Carbamation of $\text{H}_2\text{N}(\text{CH}_2)_3\text{Si}(\text{OMe})_3$ with DMC in the presence of $\text{CO}_2$

A solution of amine  $\text{H}_2\text{N}(\text{CH}_2)_3\text{Si}(\text{OMe})_3$  (8.57 mmol) in DMC (10 mL) was prepared under nitrogen in an appropriate flask and, then, saturated with  $\text{CO}_2$  ( $P_{\text{CO}_2} = 0.1$  MPa). The system was heated at 333 K for 7 h. GC-MS analysis of the reaction mixture did show the formation of the carbamate as the only product. The reaction solution was dried under vacuum and the crude oil was distilled at reduced pressure to obtain the pure carbamate  $\text{CH}_3\text{OC}(\text{O})\text{NH}(\text{CH}_2)_3\text{Si}(\text{OMe})_3$ .

Anal. Calc. for  $\text{C}_8\text{H}_{19}\text{NO}_5\text{Si}$ : C, 44.21, H, 8.81, N, 6.44%. Found: C, 44.18, H, 8.75, N, 6.38%.

GC-MS: 237 [ $\text{M}^+$ ], 205, 164, 121, 102, 91, 59, 43.

$^1\text{H}$  NMR ( $\text{CDCl}_3$ , 500.138 MHz, 293 K): 0.48 (m,  $\text{SiCH}_2$ ), 1.44 (m,  $\text{CH}_2\text{CH}_2\text{CH}_2$ ), 2.01 (s,  $\text{NHCH}_2$ ), 3.02 (m,  $\text{NHCH}_2$ ), 3.42 (s,  $\text{SiOCH}_3$ ), 3.51 (s,  $\text{C}(\text{O})\text{OCH}_3$ ).

$^{13}\text{C}$  NMR ( $\text{CDCl}_3$ , 125.759 MHz, 293 K): 156.99 ( $\text{C}(\text{O})\text{O}$ ), 51.71 ( $\text{C}(\text{O})\text{OCH}_3$ ), 50.37 ( $\text{SiOCH}_3$ ), 43.22 ( $\text{NHCH}_2$ ), 23.00 ( $\text{SiCH}_2$ ), 6.11 ( $\text{CH}_2\text{CH}_2\text{CH}_2$ ).

## Carbamation of $(\text{CH}_3\text{O})_3\text{Si}(\text{CH}_2)_3\text{NH}(\text{CH}_2)_2\text{NH}_2$ **III** with DMC in the presence of $\text{CO}_2$

A solution of diamine  $\text{H}_2\text{N}(\text{CH}_2)_2\text{NH}(\text{CH}_2)_3\text{Si}(\text{OCH}_3)_3$  **III** ( $9.15 \times 10^{-3}$  mmol) in DMC (10 mL) was prepared under nitrogen as described above and then reacted with  $\text{CO}_2$  in the same operative conditions reported for the monoamine. After cooling to room temperature, the reaction mixture was filtered. The solvent was evaporated *in vacuo* and the residue distilled at reduced pressure to yield the pure carbamate  $\text{CH}_3\text{O}(\text{O})\text{CHN}(\text{CH}_2)_2\text{NH}(\text{CH}_2)_3\text{Si}(\text{OCH}_3)_3$  in a quantitative yield.

Anal. Calc. for  $\text{C}_{10}\text{H}_{24}\text{N}_2\text{O}_5\text{Si}$ : C, 46.13, H, 9.29, N, 10.75%. Found: C, 45.98, H, 9.18, N, 10.58%.

GC-MS: 281 [ $\text{M}^+$ ], 265, 249, 236, 217, 192, 160 (100), 130, 102, 91, 70, 59, 43.

IR Data,  $\nu(\text{neat})/\text{cm}^{-1}$ : 3339 (ms, br,  $\nu(\text{NH})$ ), 1719 (vs,  $\nu(\text{C}=\text{O})$ ).

At temperatures above 340 K, both amine groups reacted with DMC and a mixture of carbamates  $(\text{CH}_3\text{O})_3\text{Si}(\text{CH}_2)_3\text{NH}(\text{CH}_2)_2\text{NHCOOCH}_3$  and  $(\text{CH}_3\text{O})_3\text{Si}(\text{CH}_2)_3\text{N}(\text{COOCH}_3)(\text{CH}_2)_2\text{NHCOOCH}_3$  was obtained, as demonstrated by the  $^{13}\text{C}$  NMR spectrum (see Table 1). Mono- and dicarbamates were separated by column chromatography using diethyl ether-toluene (1:1 v/v) as eluent. The relative amount depends on the reaction time. After 7 h at 340 K, 16% of dicarbamate is formed and 84% of monocarbamate.

## Reaction of $\text{H}_2\text{NC}(\text{O})\text{NH}(\text{CH}_2)_2\text{NH}(\text{CH}_2)_3\text{Si}(\text{OMe})_3$ (**IV**) with DMC in the presence of $\text{CO}_2$

Aminosilane **IV** ( $9.15 \times 10^{-3}$  mmol) was reacted with DMC (10 mL) under the same conditions reported above. After 11 h, the mixture was worked up as already described and the carbamate  $\text{MeO}(\text{O})\text{CNHC}(\text{O})\text{NH}(\text{CH}_2)_2\text{NH}(\text{CH}_2)_3\text{Si}(\text{OMe})_3$  isolated in 4% yield. GC-MS analysis of the reaction mixture has shown an extended methylation of the starting amine (Parent ion at 265 and 279). These compounds were not further characterized.

Anal. Calc. for  $\text{C}_{10}\text{H}_{23}\text{N}_3\text{O}_6\text{Si}$ : C, 38.82, H, 7.49, N, 13.57%. Found C, 38.78, H, 7.37, N, 13.48%.

## Conclusions

Silylalkylmonoamines react with carbon dioxide affording classic ammonium carbamates of formula  $\text{RNHCOO}^-\text{H}_3\text{NR}$ , while silylalkyldiamines produce a six-membered cyclic carbamate, that has a zwitterionic structure. The latter easily releases carbon dioxide, while the former are more thermally stable. In presence of carbon dioxide, mono- and di-aminosilanes react with dimethylcarbonate to afford selectively the monocarbamate esters under controlled conditions. The primary amino group is reacted with 100% selectivity below 335 K. A carbon dioxide catalysis has been ascertained to drive the carbamation of the silylamines, that is very selective under controlled conditions of temperature and pressure. The formation of N-methyl species or ureas has not been observed. At temperatures

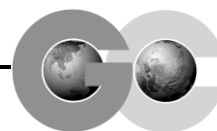
above 340 K, the diamine affords the mono- and di-carbamates.

## Acknowledgements

This work was supported by MURST, Project no. 9803026360 and MM03027791 and CNR-Rome Grant 98.01876.CT03. We thank ENIChem for a loan of DMC.

## References

- (a) S. H. Lin and C. T. Shyu, *Waste Manag.*, 1999, **19**, 255; (b) B. P. Mandal, M. Guha, A. K. Biswas and S. S. Bandyopadhyay, *Chem. Eng. Sci.*, 2001, **56**, 6217; (c) E. D. Bates, R. D. Mayton, I. Ntai and J. H. Davis, *J. Am. Chem. Soc.*, 2002, **124**, 926; (d) A. Dibenedetto, M. Aresta and M. Narracci, 223rd ACS National Meeting-Orlando, FL (April 7–11, 2002).
- (a) J. Barthelemy, *Lyon Pharm.*, 1986, **37**(6), 297; (b) T.-T. Wu, J. Huang, N. D. Arrington and G. M. Dill, *J. Agric. Food Chem.*, 1987, **35**, 817; (c) T. Kato, K. Suzuki, J. Takahashi and K. Kamoshita, *J. Pesticide Sci.*, 1984, **9**, 489; (d) P. Picardi, *Chim. Ind. (Milan)*, 1986, **68**(11), 108; (e) F. Rivetti, U. Romano and M. Sasselli, *US Pat.* 4514339, 1985; (f) M. Aresta and E. Quaranta, *CHEMTECH.*, 1997, **27**(3), 32.
- (a) M. Aresta and E. Quaranta, *J. Org. Chem.*, 1988, **53**, 4153; (b) M. Aresta and E. Quaranta, *Ital. Pat.*, 1198206, 1988; M. Aresta and E. Quaranta, *Ital. Pat. Appl.*, 22740 A/1989; (c) W. D. McGhee and D. P. Riley, *Organometallics*, 1992, **11**, 900; (d) M. Aresta and E. Quaranta, *Tetrahedron*, 1992, **48**, 1515; (e) I. Vauthey, F. Valot, C. Gozzi, F. Fache and M. Lemaire, *Tetrahedron Lett.*, 2000, **41**, 6347.
- (a) U. Romano and D. Delledonne, *Appl. Catal. A: Gen.*, 2001, **221**, 241 and references therein (b) K. Nishihira, S. Tanaka, Y. Nishida, N. Manada, T. Kurafuji and M. Marukami, *US Pat.*, 5 869 729, 1999 (Ube Industries).
- F. Porta, S. Cenini, M. Pizzetti and C. Crotti, *Gazz. Chim. Ital.*, 1985, **115**, 275.
- (a) M. Aresta and E. Quaranta, *Tetrahedron*, 1991, **47**, 9489; (b) M. Aresta and E. Quaranta, *Ital. Pat.*, 1237207, 1993.
- M. Aresta, A. Dibenedetto, E. Quaranta and B. Marciniak, *Appl. Organomet. Chem.*, 2000, **14**, 871.
- Organofunctional Silanes—Union Carbide (Organosilicon products, System, Services) 1991.
- (a) M. Aresta, D. Ballivet-Tkatchenko, D. Belli Dell'Amico, M. C. Bonnet, D. Boschi, F. Calderazzo, R. Faure, L. Labella and F. Marchetti, *Chem. Commun.*, 2000, **13**, 1099; (b) M. Aresta, D. Ballivet-Tkatchenko, M. C. Bonnet, R. Faure and H. Loiseleur, *J. Am. Chem. Soc.*, 1985, **107**, 2994.
- M. Aresta and A. Dibenedetto, *6th International Conference on Greenhouse Gas Control Technologies (GHGT-6)* 30th September–4th October 2002, Kyoto, Japan.
- M. Aresta, A. Dibenedetto and E. Quaranta, *Green Chem.*, 1999, **5**, 237.
- M. Aresta, A. Bosetti and E. Quaranta, *Ital. Pat. Appl.*, 002202, 1996.
- M. Aresta, A. Dibenedetto, E. Quaranta, M. Boscolo and R. Larsson, *J. Mol. Catal. A: Chem.*, 2001, **174**, 7.
- M. Aresta and A. Dibenedetto, *Chem.–Eur. J.*, 2002, **8**, 685.
- D. D. Perrin, W. L. F. Armarego and D. R. Perrin, *Purification of Laboratory Chemicals*, Pergamon Press, Oxford, England, 1986.



# Ionic liquids based on imidazolium, ammonium and pyrrolidinium salts of the dicyanamide anion

D. R. MacFarlane, S. A. Forsyth, J. Golding and G. B. Deacon

Centre for Green Chemistry, School of Chemistry, Monash University, Clayton, Victoria 3800, Australia

Received 11th June 2002

First published as an Advance Article on the web 29th July 2002

New families of salts, based on quaternary ammonium, 1-methyl-3-alkylimidazolium or *N*-methyl-*N*-alkylpyrrolidinium organic cations together with the dicyanamide (dca,  $N(CN)_2^-$ ) anion are reported. The salts are low melting compounds, all those reported are liquid at room temperature, for example 1-methyl-3-ethylimidazolium dicyanamide (mp  $-21\text{ }^\circ\text{C}$ ) and *N*-methyl-*N*-ethylpyrrolidinium dicyanamide (mp  $-10\text{ }^\circ\text{C}$ ). Some of the salts exhibit multiple crystalline phases below their melting points. Above their melting points they are stable to at least  $200\text{ }^\circ\text{C}$ . Many of the salts were found to be glass forming when cooled rapidly to  $-100\text{ }^\circ\text{C}$ . The room-temperature liquids exhibit very low viscosities, for example ethylmethylimidazolium dicyanamide:  $\eta = 21\text{ cP}$  at ambient temperature ( $25\text{ }^\circ\text{C}$ ).

## 1. Introduction

In our continued investigation of novel anions for use in ionic liquids for application both as solvents and in electrochemical devices we have recently focussed attention on ions which might offer particularly low viscosity and independently those that may offer a degree of donor solvent characteristics. In the field of green chemistry, in particular the use of ionic liquids, there has been much discussion and a number of syntheses in ionic liquids reported.<sup>1–5</sup> The viscosity of most chemically inert and otherwise useful ionic liquids remains substantially greater than the typical range of standard synthetic solvents. This is of extreme practical importance in developing synthetic uses of ionic liquids since the kinetics of solution based reactions can become diffusion limited in viscous media. At best this may simply slow the reaction down, at worst it may promote alternate, perhaps undesirable, reactions (*e.g.* unimolecular processes). One of the most fluid ionic liquids is 1-methyl-3-ethylimidazolium bis(trifluoromethanesulfonyl)amide [emIm][TFSA]<sup>6–8</sup> which has viscosity of  $34\text{ cP}$  at  $20\text{ }^\circ\text{C}$ . By comparison, the viscosity of water at  $20\text{ }^\circ\text{C}$  is  $1\text{ cP}$ , toluene =  $0.59\text{ cP}$ , cyclohexanol =  $68\text{ cP}$  and 1-methyl-3-ethylimidazolium tetrafluoroborate =  $67\text{ cP}$ .<sup>9</sup> Obviously elevated temperatures can be used to lower the viscosity, however this is not always preferred from the point of view of the reactants or the reaction involved. Low viscosity is also important in various synthetic procedures such as liquid–liquid extraction and filtration.

Thus it is of interest to develop ionic liquids of lower viscosity than the [TFSA] salts. In this work we have investigated a number of salts of a small anion that has been widely studied recently in a variety of organometallic compounds; the dicyanamide ion.<sup>10–12</sup> This anion bears a number of features in common with the [TFSA] anion in the sense that the charge is nominally centered on an amide nitrogen but delocalisation across the whole molecule is in fact likely and can be expected to produce weak ion–ion interactions. This is one of the features of ions that produce low melting point and low viscosity ionic liquids. However, as a substantially smaller ion than [TFSA], it can be expected that the greater (volumetric) cohesive energy density in the substance will to some extent counteract the effect of the delocalized charge.

The dicyanamide anion [1] is a ligand having Lewis basic properties.<sup>10–14</sup> This is in distinct contrast to many of the anions, such as  $[PF_6]$ ,  $[BF_4]$ , [TFSA],  $[CF_3SO_3]$ , typically present in ionic liquids, which are characterized as being very weak Lewis bases. It thus possesses the potential to provide ionic liquids which have powerful Lewis base donor solvent properties and therefore to have solvating properties for a range of metal ions that might otherwise be insoluble.

In recent reports from this laboratory<sup>15–20</sup> we have described the properties of a number of new families of ionic compounds arising from low symmetry quaternary ammonium cations and also from the pyrrolidinium cation. Many of these compounds possess plastic crystalline phases in their solid states, which are of interest because of their ionic transport properties. The potential for such phases to arise in the solid-state properties of the dicyanamide salts was also of interest.

In this paper, following on from our earlier report,<sup>21</sup> we describe in full the preparation and properties of a number of new salts of the dicyanamide anion [1], involving imidazolium [2], quaternary ammonium [3] and pyrrolidinium [4] cations (Fig. 1).

## 2. Experimental

The various alkyl iodides (Aldrich/BDH/Fluka), sodium dicyanamide ( $NaN(CN)_2$ , Aldrich), silver nitrate (Aldrich), tributylamine (Aldrich), triethylamine (Aldrich), 1-methylimidazole (Aldrich) and *N*-methylpyrrolidine (Aldrich) were used as

### Green Context

A series of new ionic liquids based on the dicyanamide anion are described. These have the advantage of being of very low viscosity, which is of benefit for heat and mass transport. The dicyanamide anion, while being relatively delocalised, still retains some Lewis basicity, a property which may also help these new solvents to find a niche in synthetic chemistry.

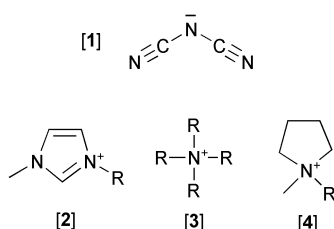
DJM

received. Differential scanning calorimetry (DSC) was carried out on a Perkin-Elmer DSC-7 and the sub-ambient temperature ranges were calibrated with cyclohexane ( $-87.0$  and  $6.5$  °C). Thermogravimetric analysis (TGA) was conducted using a STA1500 (Rheometric Scientific) in a nitrogen atmosphere between  $30$  and  $500$  °C with a temperature rate of  $10$  °C  $\text{min}^{-1}$ . The instrument was calibrated using four melting points (indium, tin, lead and zinc) and aluminium pans were used in all experiments.  $^1\text{H}$  and  $^{13}\text{C}$  NMR spectra were recorded on a Bruker DPX-300 MHz spectrometer, in  $d_6$ -DMSO. Tetramethylsilane (TMS) was used as an internal standard. IR spectra were recorded on a Perkin-Elmer FTIR 1600 instrument. Liquid samples were examined neat between sodium chloride plates. Electrospray mass spectroscopy was carried out on a Micromass Platform. Both positive and negative species were detected with an electrospray source. Samples were dissolved in a 1:1 methanol–water mixture. Electrochemistry was carried out under a nitrogen atmosphere (in a drybox) using a Maclab potentiostat, and Maclab software. Electrodes consisted of a glassy carbon working electrode, a platinum wire counter electrode and a silver wire pseudo-reference electrode. Viscosity was determined from the time for a fixed volume to flow through a narrow orifice in a calibrated glass viscometer. These measurements were carried out in a drybox.

For simplicity an acronym is used to describe the various cations prepared consisting of Im = imidazolium, P = pyrrolidinium and N = ammonium, along with a subscript indicating the number of carbons in each of the attached alkyl groups, e.g.  $\text{N}_{6222}$  corresponds to the *N,N,N*-triethyl-*N*-hexylammonium cation. Table 1 lists the compounds prepared and the acronyms applied.

### Synthesis and characterisation

The quaternized iodide salts of 1-methylimidazole, triethylamine, tributylamine and *N*-methylpyrrolidine were synthesized according to literature methods.<sup>6,7,22</sup>



**Fig. 1** Dicyanamide anion [1] with imidazolium [2], ammonium [3] and pyrrolidinium cations [4].

**Table 1** Thermal properties of dicyanamide salts

| Compound   | Abbrev.                    | $T_g$ /°C | $T_m$ /°C      | $\Delta S_f$ /<br>$\text{J K mol}^{-1}$<br>( $\pm 10\%$ ) | $T_{\text{decomp}}$ /<br>°C | $\rho$ /g $\text{cm}^{-3}$<br>( $\pm 5\%$ ) | $\eta$ /cP<br>( $20$ °C) |
|--|----------------------------|-----------|----------------|---|-----------------------------|---|--------------------------|
| <i>N</i> -Ethyl- <i>N</i> -methylpyrrolidinium dicyanamide     | [P <sub>12</sub> ][dca]    | —         | $-10$          | 75  | 250                         | —   | —                        |
| <i>N</i> -Propyl- <i>N</i> -methylpyrrolidinium dicyanamide    | [P <sub>13</sub> ][dca]    | —         | $-35$          | 5   | —                           | 0.92  | 45                       |
| <i>N</i> -Butyl- <i>N</i> -methylpyrrolidinium dicyanamide     | [P <sub>14</sub> ][dca]    | $-106$    | $-55^a$        | —   | —                           | 0.95  | 50                       |
| <i>N</i> -Hexyl- <i>N</i> -methylpyrrolidinium dicyanamide     | [P <sub>16</sub> ][dca]    | $-100$    | $-11$          | 95  | —                           | 0.92  | 45                       |
| <i>N</i> -Pentyl- <i>N,N,N</i> -triethylammonium dicyanamide   | [N <sub>5222</sub> ][dca]  | $-85$     | — <sup>b</sup> | —   | —                           | —   | —                        |
| <i>N</i> -Hexyl- <i>N,N,N</i> -triethylammonium dicyanamide    | [N <sub>6222</sub> ][dca]  | $-82$     | — <sup>b</sup> | —   | 230                         | —   | —                        |
| <i>N</i> -Hexyl- <i>N,N,N</i> -tributylammonium dicyanamide    | [N <sub>6444</sub> ][dca]  | —         | $-43^a$        | —   | —                           | —   | —                        |
| 1-Ethyl-3-methylimidazolium dicyanamide                        | [emIm][dca]                | $-104$    | $-21$          | 60  | 275                         | 1.06  | 21                       |
| 1-Ethyl-3-methylimidazolium bis(trifluoromethanesulfonyl)amide | [emIm][TF SA] <sup>c</sup> | —         | $-3$           | —   | 400                         | 1.56  | 34                       |

Note:  $T_g$  = glass transition temperature,  $T_m$  = onset of melting transition,  $\Delta S_f$  = approx. entropy of melting,  $T_{\text{decomp}}$  = onset of decomposition,  $\rho$  = density,  $\eta$  = viscosity.<sup>a</sup> In these cases the melting transition is weak and the reported value only approximate. <sup>b</sup> No melting transition observed. <sup>c</sup> Included as a comparison, data obtained by Bonhote *et al.*<sup>6</sup>

Metathesis for all halide salts to dicyanamide salts utilized the same general method. The synthesis of [P<sub>12</sub>][dca] is shown as an example.

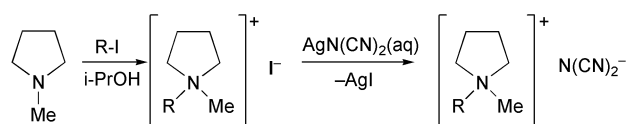
### General synthetic method

A slight excess of freshly prepared silver dicyanamide (filtered and washed with water from a solution of sodium dicyanamide and silver nitrate) was added to an aqueous solution of *N*-ethyl-*N*-methylpyrrolidinium iodide and gently heated ( $30$ – $40$  °C) and stirred for approximately 1 h (Scheme 1). The solid precipitate (AgI and excess  $\text{AgN}(\text{CN})_2$ ) was filtered off, and the water removed by rotary evaporation. The resultant sample was dissolved in dichloromethane to precipitate a small quantity of silver dicyanamide, which was filtered off, and the filtrate evaporated to dryness. *N*-Methyl-*N*-ethylpyrrolidinium dicyanamide was then dried *in vacuo* for 2 days.

The possible presence of residual  $\text{I}^-$  and  $\text{Ag}^+$  was examined *via* inspection of the appropriate mass regions of the respective mass spectra. The sensitivity of the mass spectrometry measurement to trace amounts of  $\text{I}^-$  was determined by spiking the ionic liquids with known iodide concentrations; the noise limited detection limit was thereby found to be  $0.5\%$  (w/w)  $\text{I}^-$ . No discernable  $\text{I}^-$  mass peaks were found in the [dca] salts, therefore indicating a residual  $\text{I}^-$  content of  $<0.5\%$  (w/w). The same considerations and lack of a detectable signal indicate residual  $\text{Ag}^+ < 0.5\%$  (w/w). It is known that impurities such as halides and water can have an effect on properties such as viscosity, though the effect of water in particular is expected to be more dramatic when the viscosity differs greatly from that of pure water.<sup>23,24</sup> All samples were dried similarly as evidenced by TGA.

### *N*-Ethyl-*N*-methylpyrrolidinium dicyanamide [P<sub>12</sub>][dca].

Metathesis of  $\text{AgN}(\text{CN})_2$  (2.08 g, 12 mmol) and  $\text{P}_{12}\text{I}$  (2.65 g, 11 mmol) gave  $\text{P}_{12}\text{N}(\text{CN})_2$  (1.92 g, 97%). IR (neat liquid):  $3484$  (w),  $3135$  (vw),  $2986$  (m),  $2361$  (w),  $2227$  (s),  $2191$  (s),  $2131$  (vs),  $1467$  (m),  $1304$  (s),  $1033$  (w),  $998$  (w),  $937$  (vw),  $904$  (w),  $810$  (vw)  $\text{cm}^{-1}$ .  $^1\text{H}$  NMR ( $d_6$ -DMSO)  $\delta$  1.27 (br t,  $\text{CH}_3$ ), 2.07 (br t,  $2 \times \text{CH}_2$ ), 2.95 (s,  $\text{CH}_3$ ), 3.36 (q,  $\text{CH}_2$ ), 3.42 (br m,  $2 \times \text{CH}_2$ ).  $^{13}\text{C}$  NMR ( $d_6$ -DMSO)  $\delta$  7.7 ( $\text{CH}_3$ ), 20.1 ( $2 \times \text{CH}_2$ ), 46.0 ( $\text{CH}_3$ ), 57.4 ( $\text{CH}_2$ ), 61.9 ( $2 \times \text{CH}_2$ );  $\text{N}(\text{CN})_2^-$  not observed.



**Scheme 1** Alkylation of *N*-methylpyrrolidine followed by metathesis with silver dicyanamide.

Electrospray MS: ES<sup>+</sup>:  $m/z$  114 [P<sub>12</sub><sup>+</sup>]. ES<sup>-</sup>:  $m/z$  66 [N(CN)<sub>2</sub><sup>-</sup>].

***N*-Propyl-*N*-methylpyrrolidinium dicyanamide [P<sub>13</sub>][dca].** Metathesis of AgN(CN)<sub>2</sub> (2.08 g, 12 mmol) and P<sub>13</sub>I (2.55 g, 10 mmol) gave P<sub>13</sub>N(CN)<sub>2</sub> (1.89 g, 97%). IR (neat liquid): 3484 (br m), 3020 (m), 2975 (m), 2883 (m), 2235 (s), 2196 (s), 2136 (vs), 1648 (w), 1471 (m), 1310 (m), 1040 (vw), 1003 (w), 971 (w), 940 (m), 905 (w), 758 (w) cm<sup>-1</sup>. <sup>1</sup>H NMR (d<sub>6</sub>-DMSO)  $\delta$  0.92 (t, CH<sub>3</sub>), 1.72 (m, CH<sub>2</sub>), 2.08 (br t, 2  $\times$  CH<sub>2</sub>), 2.97 (s, CH<sub>3</sub>), 3.24 (q, CH<sub>2</sub>), 3.43 (br m, 2  $\times$  CH<sub>2</sub>). <sup>13</sup>C NMR (d<sub>6</sub>-DMSO)  $\delta$  10.6 (CH<sub>3</sub>), 16.5 (CH<sub>2</sub>), 21.1 (2  $\times$  CH<sub>2</sub>), 47.6 (CH<sub>3</sub>), 63.4 (2  $\times$  CH<sub>2</sub>), 64.5 (CH<sub>2</sub>); N(CN)<sub>2</sub><sup>-</sup> not observed. Electrospray MS: ES<sup>+</sup>:  $m/z$  128 [P<sub>13</sub><sup>+</sup>]. ES<sup>-</sup>:  $m/z$  66 [N(CN)<sub>2</sub><sup>-</sup>].

***N*-Butyl-*N*-methylpyrrolidinium dicyanamide [P<sub>14</sub>][dca].** Metathesis of AgN(CN)<sub>2</sub> (2.08 g, 12 mmol) and P<sub>14</sub>I (2.70 g, 10 mmol) gave P<sub>14</sub>N(CN)<sub>2</sub> (1.73 g, 83%). IR (liquid film): 3488 (m), 2964 (m), 2876 (w), 2227 (s), 2191 (m), 2131 (vs), 1466 (m), 1340 (m), 1306 (m), 1004 (vw), 929 (w), 902 (vw), 830 (vw) cm<sup>-1</sup>. <sup>1</sup>H NMR (d<sub>6</sub>-DMSO)  $\delta$  0.92 (t, CH<sub>3</sub>), 1.31 (m, CH<sub>2</sub>), 1.67 (m, CH<sub>2</sub>), 2.06 (br t, 2  $\times$  CH<sub>2</sub>), 2.96 (s, CH<sub>3</sub>), 3.24 (q, CH<sub>2</sub>), 3.43 (br m, 2  $\times$  CH<sub>2</sub>). <sup>13</sup>C NMR (d<sub>6</sub>-DMSO)  $\delta$  13.8 (CH<sub>3</sub>), 19.6 (2  $\times$  CH<sub>2</sub>), 21.5 (CH<sub>2</sub>), 25.3 (CH<sub>2</sub>), 47.9 (CH<sub>3</sub>), 63.3 (CH<sub>2</sub>), 63.8 (2  $\times$  CH<sub>2</sub>); N(CN)<sub>2</sub><sup>-</sup> not observed. Electrospray MS: ES<sup>+</sup>:  $m/z$  142 [P<sub>14</sub><sup>+</sup>]. ES<sup>-</sup>:  $m/z$  66 [N(CN)<sub>2</sub><sup>-</sup>].

***N*-Hexyl-*N*-methylpyrrolidinium dicyanamide [P<sub>16</sub>][dca].** Metathesis of AgN(CN)<sub>2</sub> (2.08 g, 12 mmol) and P<sub>16</sub>I (3.2 g, 11 mmol) gave P<sub>16</sub>N(CN)<sub>2</sub> (2.42 g, 93%). IR (neat liquid): 3487 (br m), 2957 (m), 2930 (m), 2860 (w), 2228 (s), 2191 (m), 2131 (vs), 1466 (m), 1305 (m), 1052 (w), 996 (m), 934 (w), 903 (vw), 729 (w) cm<sup>-1</sup>. <sup>1</sup>H NMR (d<sub>6</sub>-DMSO)  $\delta$  0.88 (t, CH<sub>3</sub>), 1.31 (m, 3  $\times$  CH<sub>2</sub>), 1.68 (br m, CH<sub>2</sub>), 2.08 (br s, 2  $\times$  CH<sub>2</sub> (ring)), 2.98 (s, NCH<sub>3</sub>), 3.29 (m, NCH<sub>2</sub>), 3.45 (m, 2  $\times$  NCH<sub>2</sub> (ring)). <sup>13</sup>C NMR (JMOD) (d<sub>6</sub>-DMSO)  $\delta$  13.3 (CH<sub>3</sub>), 20.6 (2  $\times$  CH<sub>2</sub>), 21.3 (CH<sub>2</sub>), 22.3 (CH<sub>2</sub>), 25.0 (CH<sub>2</sub>), 30.1 (CH<sub>2</sub>), 48.2 (NCH<sub>3</sub>), 62.9 (CH<sub>2</sub>), 63.4 (2  $\times$  CH<sub>2</sub>); N(CN)<sub>2</sub><sup>-</sup> not observed. Electrospray MS: ES<sup>+</sup>:  $m/z$  170 [P<sub>16</sub><sup>+</sup>], 406 [P<sub>16</sub><sup>+</sup>]<sub>2</sub>[N(CN)<sub>2</sub><sup>-</sup>]<sup>+</sup>. ES<sup>-</sup>:  $m/z$  66 [N(CN)<sub>2</sub><sup>-</sup>], 302 [P<sub>16</sub><sup>+</sup>][N(CN)<sub>2</sub><sup>-</sup>]<sub>2</sub><sup>-</sup>.

***N*-Pentyl-*N,N*-triethylammonium dicyanamide [N<sub>5222</sub>][dca].** Metathesis of AgN(CN)<sub>2</sub> (2.08 g, 12 mmol) and N<sub>5222</sub>I (3.30 g, 11 mmol) gave N<sub>5222</sub>N(CN)<sub>2</sub> (2.54 g, 97%). IR (neat liquid): 3489 (br s), 3136 (w), 2959 (s), 2873 (s), 2363 (w), 2228 (s), 2192 (s), 2131 (s), 1638 (br w), 1487 (s), 1461 (s), 1396 (s), 1305 (s), 1228 (w), 1189 (w), 1165 (s), 1125 (w), 1088 (w), 1072 (w), 1010 (s), 942 (w), 903 (w), 796 (s), 734 (w) cm<sup>-1</sup>. <sup>1</sup>H NMR (d<sub>6</sub>-DMSO)  $\delta$  0.89 (t, CH<sub>3</sub>), 1.17 (m, 3  $\times$  CH<sub>3</sub>), 1.30 (m, 2  $\times$  CH<sub>2</sub>), 1.57 (m, CH<sub>2</sub>), 3.10 (m, NCH<sub>2</sub>), 3.23 (q, 3  $\times$  NCH<sub>2</sub>). <sup>13</sup>C NMR (JMOD) (d<sub>6</sub>-DMSO)  $\delta$  7.5 (3  $\times$  CH<sub>3</sub>), 14.1 (CH<sub>3</sub>), 21.0 (CH<sub>2</sub>), 22.0 (CH<sub>2</sub>), 28.3 (CH<sub>2</sub>), 52.4 (3  $\times$  CH<sub>2</sub>), 56.4 (CH<sub>2</sub>); N(CN)<sub>2</sub><sup>-</sup> not observed. Electrospray MS: ES<sup>+</sup>:  $m/z$  172 [N<sub>5222</sub><sup>+</sup>], 410 [(N<sub>5222</sub>)<sub>2</sub>N(CN)<sub>2</sub>]<sup>+</sup>. ES<sup>-</sup>:  $m/z$  66 [N(CN)<sub>2</sub><sup>-</sup>], 304 [N<sub>5222</sub><sup>+</sup>][N(CN)<sub>2</sub><sup>-</sup>]<sub>2</sub><sup>-</sup>.

***N*-Hexyl-*N,N*-triethylammonium dicyanamide [N<sub>6222</sub>][dca].** Metathesis of AgN(CN)<sub>2</sub> (2.08 g, 12 mmol) and N<sub>6222</sub>I (3.44 g, 11 mmol) gave N<sub>6222</sub>N(CN)<sub>2</sub> (2.65 g, 96%). IR (neat liquid): 3483 (w), 2956 (m), 2929 (m), 2860 (w), 2227 (s), 2190 (m), 2130 (vs), 1486 (m), 1396 (w), 1305 (m), 1164 (w), 1011 (w), 903 (w), 796 (w) cm<sup>-1</sup>. <sup>1</sup>H NMR (d<sub>6</sub>-DMSO)  $\delta$  0.88 (t, CH<sub>3</sub>), 1.17 (m, 3  $\times$  CH<sub>3</sub>), 1.30 (s, 3  $\times$  CH<sub>2</sub>), 1.57 (m, CH<sub>2</sub>), 3.10 (m, NCH<sub>2</sub>), 3.23 (m, 3  $\times$  NCH<sub>2</sub>). <sup>13</sup>C NMR (JMOD) (d<sub>6</sub>-DMSO)  $\delta$  7.7 (3  $\times$  CH<sub>3</sub>), 14.3 (CH<sub>3</sub>), 21.4 (CH<sub>2</sub>), 22.2 (CH<sub>2</sub>), 25.3 (CH<sub>2</sub>), 31.2 (CH<sub>2</sub>), 52.5 (3  $\times$  CH<sub>2</sub>), 58.2 (CH<sub>2</sub>); N(CN)<sub>2</sub><sup>-</sup> not observed. Electrospray MS: ES<sup>+</sup>:  $m/z$  186 [N<sub>6222</sub><sup>+</sup>]. ES<sup>-</sup>:  $m/z$  66 [N(CN)<sub>2</sub><sup>-</sup>], 318 [N<sub>6222</sub><sup>+</sup>][N(CN)<sub>2</sub><sup>-</sup>]<sub>2</sub><sup>-</sup>.

***N*-Hexyl-*N,N,N*-tributylammonium dicyanamide [N<sub>6444</sub>][dca].** Metathesis of AgN(CN)<sub>2</sub> (2.08 g, 12 mmol) and N<sub>6444</sub>I (4.39 g, 11 mmol) gave N<sub>6444</sub>N(CN)<sub>2</sub> (3.52 g, 95%). IR (neat liquid): 3463 (br m), 2965 (s), 2874 (s), 2228 (s), 2190 (s), 2130 (vs), 1653 (w), 1486 (m), 1394 (w), 1301 (m), 1172 (w), 1013 (w), 988 (w), 899 (w), 796 (w), 583 (vw) cm<sup>-1</sup>. <sup>1</sup>H NMR (d<sub>6</sub>-DMSO)  $\delta$  0.92 (t, 4  $\times$  CH<sub>3</sub>), 1.31 (s, 6  $\times$  CH<sub>2</sub>), 1.57 (m, 4  $\times$  CH<sub>2</sub>), 3.14 (m, 4  $\times$  NCH<sub>2</sub>). <sup>13</sup>C NMR (JMOD) (d<sub>6</sub>-DMSO)  $\delta$  13.5 (3  $\times$  CH<sub>3</sub>), 14.1 (CH<sub>3</sub>), 19.9 (3  $\times$  CH<sub>2</sub>), 21.4 (CH<sub>2</sub>), 22.2 (CH<sub>2</sub>), 23.1 (3  $\times$  CH<sub>2</sub>), 25.2 (CH<sub>2</sub>), 30.5 (CH<sub>2</sub>), 57.2 (3  $\times$  CH<sub>2</sub>), 57.8 (CH<sub>2</sub>); N(CN)<sub>2</sub><sup>-</sup> not observed. Electrospray MS: ES<sup>+</sup>:  $m/z$  270 [N<sub>6444</sub><sup>+</sup>]. ES<sup>-</sup>:  $m/z$  66 [N(CN)<sub>2</sub><sup>-</sup>], 402 [N<sub>6444</sub><sup>+</sup>][N(CN)<sub>2</sub><sup>-</sup>]<sub>2</sub><sup>-</sup>.

**1-Ethyl-3-methylimidazolium dicyanamide [emIm][dca].** Metathesis of AgN(CN)<sub>2</sub> (2.08 g, 12 mmol) and emImI (2.6 g, 11 mmol) gave emImN(CN)<sub>2</sub> (1.87 g, 96%). Microanalysis: Calculated for C<sub>8</sub>H<sub>11</sub>N<sub>5</sub>: C, 54.2; H, 6.3; N, 39.5%. Found C, 52.7; H, 6.3; N, 38.6%. IR (liquid film): 3489 (w), 3150 (s), 3106 (s), 2988 (s), 2365 (w), 2232 (vs), 2195 (vs), 2132 (vs), 1637 (w), 1573 (s), 1466 (m), 1427 (w), 1388 (w), 1170 (s), 1131 (s), 1088 (w), 1030 (w), 959 (w), 905 (w), 844 (w), 802 (w), 753 (m), 701 (w), 648 (m), 622 (s) cm<sup>-1</sup>. <sup>1</sup>H NMR (d<sub>6</sub>-DMSO)  $\delta$  1.42 (t, CH<sub>3</sub>), 3.84 (s, NCH<sub>3</sub>), 4.19 (q, NCH<sub>2</sub>), 7.67 (s, CH), 7.76 (s, CH), 9.10 (s, NCHN). <sup>13</sup>C NMR (JMOD) (d<sub>6</sub>-DMSO)  $\delta$  14.5 (CH<sub>3</sub>), 35.2 (CH<sub>3</sub>), 35.2 (CH<sub>3</sub>), 43.6 (CH<sub>2</sub>), 121.4 (CH), 123.0 (CH); N(CN)<sub>2</sub><sup>-</sup> and NCHN not observed. Electrospray MS: MS<sup>+</sup>:  $m/z$  111 [emIm<sup>+</sup>]. MS<sup>-</sup>:  $m/z$  66 [N(CN)<sub>2</sub><sup>-</sup>], 243 [emIm][N(CN)<sub>2</sub><sup>-</sup>]<sup>-</sup>.

### 3. Results and discussion

The thermal properties of the dicyanamide compounds are summarized in Table 1. A common ionic liquid, [emIm][TFSA], is included for comparison. All dicyanamide salts presented have melting points well below room temperature. The melting points are typically 20–30 °C below those of the corresponding [TFSA] salts, perhaps an unexpected result since charge delocalisation could be expected to be greater for [TFSA] than [dca], producing weaker ion–ion interactions. In fact, many are glass forming, with very low glass transition temperatures,  $T_g$ . Typical differential scanning calorimetry (DSC) traces are shown in Fig. 2. The [P<sub>12</sub>][dca] thermal trace is relatively simple showing only a melting transition of relatively high entropy of fusion ( $\Delta S_f$ ). The trace for [emIm][dca] shows a glass transition near -100 °C followed by an exotherm associated with the crystallization of the supercooled ionic liquid followed by melting. From Table 1 the very low  $\Delta S_f$  exhibited by [P<sub>13</sub>][dca] indicates the likely existence of a plastic phase which melts with only a small entropy of transition. A number of other [dca] salts having high symmetry

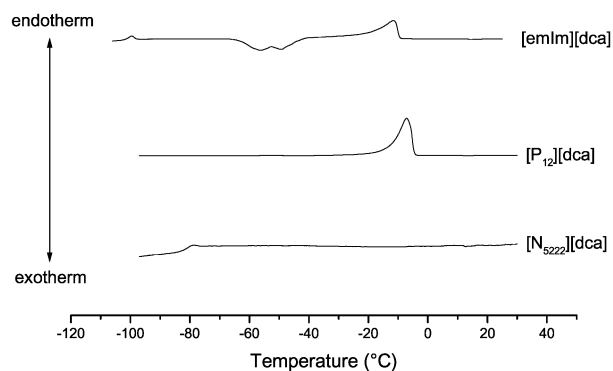


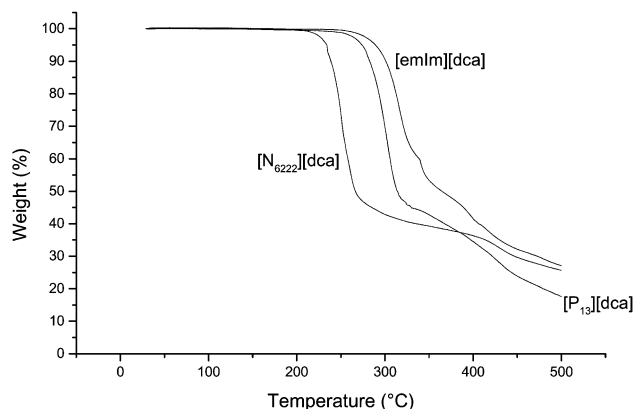
Fig. 2 DSC traces of selected imidazolium, pyrrolidinium and quaternary ammonium dicyanamide ionic liquids.

cations; [P<sub>11</sub>], [N<sub>1111</sub>], [N<sub>2222</sub>], [N<sub>3333</sub>], [N<sub>4444</sub>] have been prepared, and have higher melting points and exhibit plastic crystal properties. These solid materials are of interest in electrochemical applications and will be discussed elsewhere.

The thermogravimetric analyses of three representative [dca] ionic liquids are displayed in Fig. 3. The thoroughly dried compounds show no weight loss to at least 200 °C, providing a large, stable liquid range. The quaternary ammonium salt is the least thermally stable and decomposes at 230 °C. The pyrrolidinium salt decomposes at 250 °C while the imidazolium salt is the most thermally stable and decomposes at 275 °C. The [dca] ionic liquids are not as thermally stable as other salts of the same cation. For example [emIm][TFSA] decomposes at 400 °C<sup>6</sup> indicating thermal stability differences between anions. The alkali metal salts of the dicyanamide anion have much greater stability. Sodium dicyanamide is known to cyclotrimerise above 340 °C.<sup>25</sup> This suggests the decomposition of the [dca] ionic liquids involves interaction between anion and cation.

The viscosities of representative compounds (Table 1) are lower than those of the corresponding [TFSA] salts, *e.g.* 1-ethyl-3-methylimidazolium dicyanamide ( $\eta = 21$  cP) and [TFSA] ( $\eta = 34$  cP); *N*-butyl-*N*-methylpyrrolidinium dicyanamide ( $\eta = 50$  cP) and [TFSA] ( $\eta = 85$  cP). This rather useful trend is possibly related to the smaller size of the anion and parallels the lower melting points of the dicyanamide compounds. In practical terms, it is possible to filter a precipitate from a suspension in the lower viscosity dicyanamide ionic liquids at room temperature with a sintered glass frit under vacuum.

The series of dicyanamide room-temperature ionic liquids are hygroscopic and completely miscible with water. The dicyanamide ionic liquids are also soluble in most laboratory solvents; exceptions are hexane, toluene and light petroleum. This insolubility appears to be true for solvents with very low dielectric constants (less than 4). Diethyl ether is on the boundary of this solubility limit. Qualitative tests showed that a number of hydrated cobalt(II) and copper(II) salts are appreciably soluble in 1-ethyl-3-methylimidazolium dicyanamide [emIm][dca] at room temperature with enhanced solubility on heating to 75 °C. However, relatively little dissolution of nickel salts and CuCl occurs. By contrast, the dicyanamide-soluble CuCl<sub>2</sub>·2H<sub>2</sub>O and CoCl<sub>2</sub>·6H<sub>2</sub>O are insoluble in the corresponding [TFSA] liquid at room temperature and only dissolved slightly at 75 °C. The solubility of inorganic salts in the dicyanamide ionic liquid may be due to its donor ligand properties, consistent with the rich coordination chemistry that is known of the anion,<sup>10–12</sup> although the comparative insolubility of nickel salts is surprising. Organic compounds such as *p*-nitrotoluene, *p*-nitrobenzaldehyde, 2,2'-bipyridine, *N*-bromosuccinimide and triphenylphosphine have moderate to high solubility in dicyanamide ionic liquids. The solubility



**Fig. 3** Thermogravimetric traces for selected imidazolium, pyrrolidinium and quaternary ammonium dicyanamide ionic liquids.

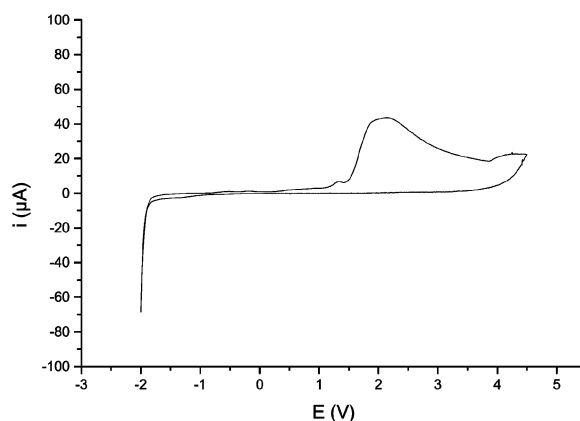
limits for organic compounds has not been fully investigated. However, one example, of some significance, is that unprotected saccharides such as glucose have relatively high solubility in dicyanamide ionic liquids, compared to traditional organic solvents and other ionic liquids. We have recently demonstrated the use of dicyanamide ionic liquids as effective solvents for the *O*-acetylation of alcohols and carbohydrates.<sup>26</sup> The *O*-acetylation reaction studied in that work also demonstrated a catalytic action of the dicyanamide anion, since the reaction proceeded without any additional base. It is not clear whether this action is a general base catalysis mechanism or whether it is a specific mechanism involving the amide nitrogen of the dicyanamide anion. This question is currently under further investigation; it illustrates the first example of intrinsically catalytic ionic liquids that are water stable,<sup>27</sup> unlike the well known tetrachloroaluminate based systems.

The electrochemical behaviour of these salts is illustrated by the example of the cyclic voltammogram of [emIm][dca] in Fig. 4. The liquid is stable to quite low potentials around  $-2$  V in common with other salts of this cation. There thus appears to be no reduction in stability associated with the dicyanamide anion. The stability in the oxidative range is reduced as compared to the [TFSA] ion, however. In fact the irreversible oxidation observed at *ca.* 2 V may be indicative of the formation of a neutral dimer (CN)<sub>2</sub>N–N(CN)<sub>2</sub>.

The existence of this species is suggested by analogy with a number of related compounds that exhibit pseudo-halide behaviour and which produce neutral dimers on oxidation; such anionic species include [SCN]<sup>–</sup>, [CN]<sup>–</sup>, [NO<sub>2</sub>]<sup>–</sup>, producing [NCS–SCN], [NC–CN], [O<sub>2</sub>N–NO<sub>2</sub>], respectively. The pseudo-halide characteristics of the dicyanamide anion have been noted previously.<sup>25</sup> Notably only the NO<sub>2</sub> case involves a nitrogen–nitrogen bond. It is also interesting that such a neutral dimer does not appear to easily form in the case of the [TFSA] anion. The significance of this reaction is that it limits somewhat the oxidative stability of the medium. This has consequences for both oxidative synthetic uses and electrochemical applications at high positive potentials.

## Conclusions

The dicyanamide ionic liquids presented have many properties that make them attractive as solvent replacements. The lower viscosity of dicyanamide ionic liquids compared to other ionic liquids provides a reaction medium that is easier to handle in a variety of standard experimental procedures (such as stirring



**Fig. 4** Cyclic voltammetry of neat 1-ethyl-3-methylimidazolium dicyanamide [emIm][dca] carried out at 100 °C under a nitrogen atmosphere (dry box), on a glassy carbon microelectrode, with a platinum counter electrode and Ag/Ag<sup>+</sup> pseudo reference electrode.



and filtering at ambient and sub-ambient temperatures). The dicyanamide ionic liquids are electrochemically stable from  $-2$  to  $+1.5$  V vs. Ag/Ag<sup>+</sup> and thermally stable to at least 200 °C. The donor solvent characteristics of dicyanamide ionic liquids provide remarkable solvating properties for a large range of organic and inorganic compounds.

## Acknowledgements

We are grateful for support from the Australian Research Council through Project funding and *via* the Special Research Centre for Green Chemistry.

## References

- 1 T. Welton, *Chem. Rev.*, 1999, **99**, 2071–2083.
- 2 M. J. Earle and K. R. Seddon, *Pure Appl. Chem.*, 2000, **72**, 1391–1398.
- 3 C. M. Gordon, *Appl. Catal., A: General*, 2001, **222**, 101–117.
- 4 R. A. Sheldon, *Chem. Commun.*, 2001, 2399–2407.
- 5 K. R. Seddon, *J. Chem. Technol. Biotechnol.*, 1997, **68**, 351–356.
- 6 P. Bonhote, A.-P. Dias, N. Papageorgiou, K. Kalyanasundaram and M. Graetzel, *Inorg. Chem.*, 1996, **35**, 1168–78.
- 7 J. Sun, D. R. MacFarlane and M. Forsyth, *eIonics*, 1997, **3**, 356–362.
- 8 J. Sun, M. Forsyth and D. R. MacFarlane, *J. Phys. Chem. B*, 1998, **102**, 8858–8864.
- 9 J. G. Huddleston, A. E. Visser, W. M. Reichert, H. D. Willauer, G. A. Broker and R. D. Rogers, *Green Chem.*, 2001, **3**, 156–164.
- 10 J. L. Manson, C. R. Kmety, Q. Huang, J. W. Lynn, G. M. Bendele, S. Pagola, P. W. Stephens, L. M. Liable-Sands, A. L. Rheingold, A. J. Epstein and J. S. Miller, *Chem. Mater.*, 1998, **10**, 2552–2560.
- 11 M. Kurmoo and C. J. Kepert, *New J. Chem.*, 1998, **22**, 1515–1524.
- 12 S. R. Batten, P. Jensen, B. Moubaraki, K. S. Murray and R. Robson, *Chem. Commun.*, 1998, 439–440.
- 13 P. Jensen, S. R. Batten, G. D. Fallon, D. C. R. Hockless, B. Moubaraki, K. S. Murray and R. Robson, *Solid State Chem.*, 1999, **145**, 387–393.
- 14 S. R. Batten, P. Jensen, B. Moubaraki and K. S. Murray, *Chem. Commun.*, 2000, 2331–2332.
- 15 J. Golding, N. Hamid, D. R. MacFarlane, M. Forsyth, C. Forsyth, C. Collins and J. Huang, *Chem. Mater.*, 2001, **13**, 558–564.
- 16 D. R. MacFarlane, P. Meakin, J. Sun, N. Amini and M. Forsyth, *J. Phys. Chem. B*, 1999, **103**, 4164–4170.
- 17 D. R. MacFarlane and M. Forsyth, *Adv. Mater.*, 2001, **13**, 957–966.
- 18 J. Huang, M. Forsyth and D. R. MacFarlane, *Solid State Ionics*, 2000, **136–137**, 447–452.
- 19 M. Forsyth, J. Huang and D. R. MacFarlane, *J. Mater. Chem.*, 2000, **10**, 2259–2265.
- 20 D. R. MacFarlane, J. Huang and M. Forsyth, *Nature*, 1999, **402**, 792–794.
- 21 D. R. MacFarlane, J. Golding, S. Forsyth, M. Forsyth and G. B. Deacon, *Chem. Commun.*, 2001, 1430–1431.
- 22 J. Sun, M. Forsyth and D. R. MacFarlane, *Molten Salt Forum*, 1998, **5–6**, 585–588.
- 23 K. R. Seddon, A. Stark and M.-J. Torres, *Pure Appl. Chem.*, 2000, **72**, 2275–2287.
- 24 J. T. Hamill, C. Hardacre, M. Nieuwenhuyzen, K. R. Seddon, S. A. Thompson and B. Ellis, *Chem. Commun.*, 2000, 1929–1930.
- 25 A. M. Golub, H. Kohler and V. V. Skopenko, *Chemistry of Pseudohalides*, Elsevier, Berlin, 1986.
- 26 S. A. Forsyth, D. R. MacFarlane, R. J. Thomson and M. von Itzstein, *Chem. Commun.*, 2002, 714–715.
- 27 Water solubility and the behaviour of acidic and basic solutes in dicyanamide ionic liquids are currently under investigation.



# Regioselectivity of phenol alkylation in supercritical water

Takafumi Sato, Gaku Sekiguchi, Tadafumi Adschiri, Richard L. Smith Jr. and Kunio Arai\*

Department of Chemical Engineering, Tohoku University, 07 Aoba, Aramaki-Aza, Aoba-ku, Sendai 980-8579, Japan. E-mail: karai@arai.che.tohoku.ac.jp; Fax: +81-22-217-7246; Tel: +81-22-217-7245

Received 19th July 2002

First published as an Advance Article on the web 8th August 2002

Regioselectivity of phenol alkylation with propionaldehyde could be controlled in supercritical water under non-catalytic conditions at 673 K by manipulating water density.

## Introduction

Toxicity and risk management of chemical processes can become simplified if environmental fluids such as water or carbon dioxide can be substituted for organic solvents in harmony with the philosophy of Green Chemistry. Water, in a state above its critical point ( $T_c$ : 647.3 K,  $P_c$ : 22.1 MPa) has many environmental and technological advantages.<sup>1</sup> In the supercritical region, water is completely miscible with many organics and provides a homogeneous reaction field.<sup>2</sup> The change of water density affects the reaction rate and reaction pathway by changing the contribution of ionic reaction pathways.<sup>2</sup> Organic syntheses such as dehydration, Diels–Alder reaction and rearrangements have been examined in supercritical water.<sup>1</sup> We have reported that non-catalytic alkylation of phenol with 2-propanol also occurs in supercritical water.<sup>3,4</sup>

Alkylphenols are important for industrial intermediates and the production of alkylphenols exceeds 450000 tonnes/year on a worldwide basis.<sup>5</sup> The vast majority of alkylphenols are used to synthesize derivatives for pharmaceuticals, antioxidants and polymers. The Friedel–Crafts reaction is one of the major methods for synthesis of alkylphenols and requires strong acids such as Lewis acids ( $\text{AlCl}_3$ ,  $\text{BF}_3$ ) and mineral acids ( $\text{HF}$ ,  $\text{H}_2\text{SO}_4$ ).<sup>6</sup> In the alkylation of phenol, the hydroxy group of phenol strongly activates the reactivity of both *ortho* and *para* positions.<sup>7</sup>

To control the regioselectivity of alkylation, base reagents or heterogeneous catalysis is used. Sartori *et al.*<sup>8</sup> reported that the ratio of *ortho* to *para* increased with increasing  $\text{PhOK}:\text{PhOH}$  ratio in  $\text{CHCl}_3$  solvent. Sato *et al.*<sup>9</sup> examined the *ortho*-selective alkylation of phenol with 1-propanol by  $\text{CeO}_2\text{-MgO}$ . Gray *et al.*<sup>10</sup> conducted the reaction of phenol with 2-propanol in supercritical  $\text{CO}_2$ . They reported that isopropyl phenyl ether was the main product and that the yield of *ortho* alkylphenols was always larger than that of the *para* products. In this work, we examined the regioselectivity of phenol alkylation when the ionic atmosphere of the water solvent was varied. As an example, we show alkylation of phenol with propionaldehyde in supercritical water solvent.

## Experimental

Experiments were conducted in stainless 316 tube-bomb reactors (6  $\text{cm}^3$ ) equipped with a high pressure shut-off valve.<sup>4</sup> For the reaction of propionaldehyde and phenol, 0.002 mol of propionaldehyde, 0.010 mol of phenol and 0.6–3 g of water

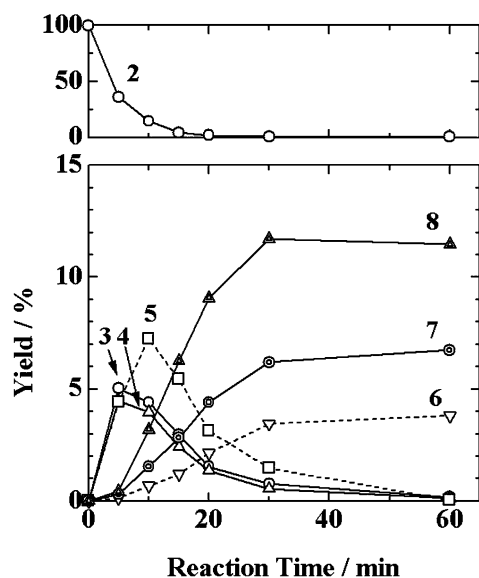
were loaded into the reactor. The amount of water corresponded to a water density of 0.1–0.5  $\text{g cm}^{-3}$ . We also conducted experiments without water (denoted as water densities of 0  $\text{g cm}^{-3}$ ). After loading samples and purging the reactor with argon, the reactor was submerged into a sand-bath controlled at 673 K. Heat-up time was within 4 min. After a given reaction time, the reactor was quenched in a water-bath. Liquid products were collected by combining the reacted mixtures with THF solvent in sufficient amounts such that a single phase mixture was formed. This allowed complete analysis of the liquid products. Products were identified by GC–MS and quantified by GC–FID. Gas products were analysed by GC–TCD by using a sampling loop attached to GC. The product yield was defined by on a propionaldehyde basis, as: yield (%) = (moles of carbon of the alkyl chains attached to the benzene ring)/(moles of carbon in propionaldehyde loaded)  $\times$  100.

## Results and discussion

Fig. 1 shows the yield of main products with reaction time for the reaction of phenol (1) and propionaldehyde (2) in supercritical water at 673 K at a water density of 0.5  $\text{g cm}^{-3}$ . From the experimental results, we propose the reaction pathway as Scheme 1. Propionaldehyde (2) was converted within 20 min and yielded 2-propenylphenol (3) and 4-propenylphenol (4) through the reaction with phenol (1). Then, cyclization of 2-propenylphenol (3) gave 2,3-dihydro-2-methylbenzofuran (5),<sup>11</sup> followed by the dehydrogenation to 2-methylbenzofuran (6). Hydrogenation of both 2-propenylphenol (3) and 4-propenylphenol (4) also occurred and yielded 2-propylphenol (7) and 4-propylphenol (8), respectively. Alkylphenols such as 2-cresol, 4-cresol, 2-ethylphenol and 4-ethylphenol were detected.

## Green Context

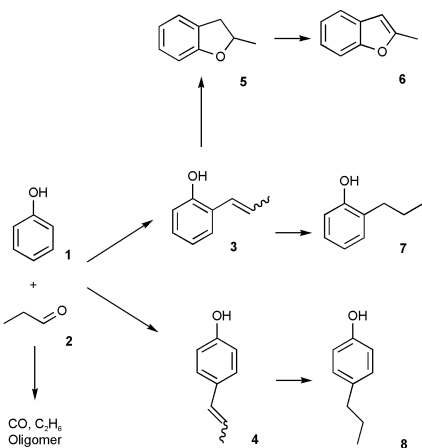
The ability of supercritical fluids to function as highly tunable solvents is remarkable. In addition to the normal solvent parameters, SCFs have the additional flexibility of variable density. While denser fluids are generally better solvents, the control of density can allow important changes in *e.g.* selectivity (see for example, C. Rayner, *Green Chem.*, 1999, 1(2), G44). Here the selectivity of phenol alkylation can be dramatically varied by simply controlling the density of the medium. Additionally, no catalyst was required to perform the operation. *DJM*



**Fig. 1** Yield of propionaldehyde (2), 2-propenylphenol (3), 4-propenylphenol (4), 2,3-dihydro-2-methylbenzofuran (5), 2-methylbenzofuran (6), 2-propylphenol (7) and 4-propylphenol (8) at  $0.5 \text{ g cm}^{-3}$  water density and 673 K.

The sum of the yield of the main liquid products was about 30% and almost constant. We conducted gas analyses and found that the main gas products were CO and  $\text{C}_2\text{H}_6$  as reported in the pyrolysis of propionaldehyde (2).<sup>12</sup> There was no solid after the reaction and byproducts from propionaldehyde (2), other than gas and alkylphenols, probably yielded oligomers through aldol condensation.<sup>13,14</sup>

We evaluated the product distribution at other ionic atmospheres by changing the water density to confirm the proposed mechanism of Scheme 1. Table 1 shows the product distribution

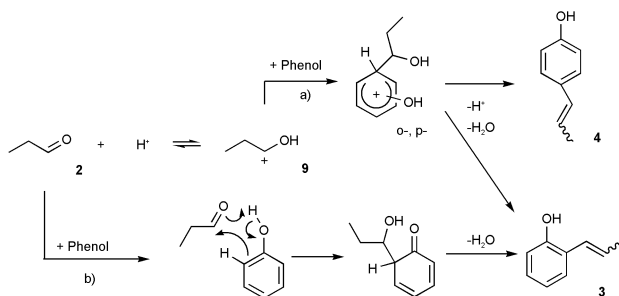


**Scheme 1** Reaction pathway for the reaction of phenol and propionaldehyde in supercritical water.

at 673 K and 60 min reaction time at water density of  $0\text{--}0.5 \text{ g cm}^{-3}$ . The ratio of *ortho* to *para* isomers was evaluated from the sum of the product yields of the alkyl side chain attached to the *ortho*-position of hydroxy group of phenol (3, 5, 6, 7) and to *para*-positions (4, 8). The sum of the yields of phenolic compounds increased with increasing water density. At 60 min reaction time, the yields of 2-propylphenol (7) and 4-propylphenol (8) were high, which means that these compounds were relatively stable. The reactivity at both *ortho* and *para* positions of the hydroxy group seemed to be enhanced in the region of high water density. The ratio of *ortho/para* product clearly decreased with increasing water density. These results provide strong evidence that the selectivity of the *para* position is a function of the ionic atmosphere of the water solvent.

The dielectric constant and ion product of water increase with increasing water density, which makes the reaction atmosphere have a greater ionic character.<sup>2</sup> Further, phenol dissociates in supercritical water and its dissociation constant increases with water density.<sup>15</sup> At 673 K, the dissociation constant of phenol increases from  $10^{-12}$  to  $10^{-11}$  with increasing water density from  $0.36$  to  $0.47 \text{ g cm}^{-3}$ .<sup>15</sup> This means that the proton concentration also increases with increasing water density. The high water density region provides an ionic atmosphere favorable for the formation of ionic species such as protons or carbonium ions.

From the experimental findings, we propose an alkylation mechanism as shown in Scheme 2. Propionaldehyde (2) and protons are in equilibrium with the 1-propanol cation  $\text{CH}_3\text{CH}_2\text{CH}^+\text{OH}$  (9) in aqueous solution. With increasing water density, this equilibrium probably shifts to the carbonium ion side through the contribution of solvating power for ionic species and proton concentration. In the experiments, both *ortho* and *para* substituents were formed in an ionic atmosphere due to the high water density. Under such conditions, the reaction proceeds through pathway (a). If 1-propanol cation (9) reacted with phenol, electrophilic substitution at the benzene ring of phenol should occur. The 1-propanol cation (9) attacked both *ortho* and *para* positions of phenol and yielded both *ortho* and *para* hydroxyalkylphenols in a similar manner as standard Friedel–Crafts reactions.<sup>6</sup> Hydroxyalkylphenols can be formed through the reaction of phenol and aldehyde in high temperature water.<sup>14</sup> The hydroxy group of aliphatic alcohols easily



**Scheme 2** Mechanism for alkylation of phenol with propionaldehyde in supercritical water.

**Table 1** Yield of main liquid products at various water densities (673 K, 60 min, propionaldehyde = 0.002 mol, phenol = 0.01 mol)

| Water density/ $\text{g cm}^{-3}$ | Yield (%) |              |     |     |             |     |      |      | Sum of alkyl phenols | <i>Ortho/para</i> ratio <sup>a</sup> |
|-----------------------------------|-----------|--------------|-----|-----|-------------|-----|------|------|----------------------|--------------------------------------|
|                                   | 2         | <i>Ortho</i> |     |     | <i>Para</i> |     | 8    |      |                      |                                      |
| 0                                 | 0.4       | 0.1          | 0.8 | 0.7 | 1.4         | 0.0 | 0.0  | 3.4  | $\gg 99^b$           |                                      |
| 0.1                               | 1.6       | 0.3          | 1.1 | 0.3 | 1.0         | 0.0 | 0.2  | 2.9  | 14.3                 |                                      |
| 0.3                               | 1.3       | 1.1          | 3.6 | 1.2 | 2.9         | 0.8 | 2.2  | 11.8 | 2.94                 |                                      |
| 0.5                               | 0.5       | 0.2          | 0.0 | 3.8 | 6.7         | 0.1 | 11.5 | 22.3 | 0.93                 |                                      |

<sup>a</sup>  $(3 + 5 + 6 + 7)/(4 + 8)$ ; <sup>b</sup> No *para* products observed.

dehydrates in high temperature water in the presence of phenol as well as acids.<sup>4</sup> The hydroxy group in the alkyl side chain of alkylphenols can be eliminated by dehydration and yielded the corresponding propenylphenols (**3**, **4**). In the low density region, the *ortho* substituent was the dominant product where the reaction atmosphere has less ionic character. Under these conditions, the equilibrium between propionaldehyde (**2**) and the 1-propanol cation (**9**) was shifted to the propionaldehyde (**2**) and the reaction proceeded through pathway (b). Sartori *et al.*<sup>16</sup> reported that the hydroxy group participates in the reaction mechanism in the catalytic alkylation of phenol. Under these conditions, phenol and propionaldehyde (**2**) probably react directly through the contribution of hydroxy group. Then, dehydration of hydroxyalkylphenol occurs, leading to the *ortho* product 2-propenylphenol (**3**).

In summary, the regioselectivity of phenol alkylation with propionaldehyde could be controlled in supercritical water under non-catalytic conditions. In the high density region of water, alkylation occurred at both *ortho* and *para* positions. A decrease in water density increased the product ratio of the *ortho* substituents.

### Acknowledgements

The authors are thankful for the Grant-in-Aid for Scientific Research on Priority Areas (09450281, 10555270, 11450295 and 11694921) the Ministry of Education, Culture, Sports, Science and Technology.

### References

- 1 P. E. Savage, *Chem. Rev.*, 1999, **99**, 603.
- 2 P. E. Savage, S. Gopalan, T. I. Mizan, C. J. Martino and E. E. Brock, *AIChE J.*, 1995, **41**, 1723.
- 3 T. Sato, G. Sekiguchi, T. Adschiri and K. Arai, *Chem. Commun.*, 2001, 1566.
- 4 T. Sato, G. Sekiguchi, T. Adschiri and K. Arai, *Ind. Eng. Chem. Res.*, 2002, **41**, 3064.
- 5 J. I. Kroschwitz and H.-G. Mary Kirk-Othmer, *Encyclopedia of Chemical Technology*, Wiley-Interscience, New York, 4th edn., 1991.
- 6 G. A. Olah, *Friedel-Crafts and related reactions*, Interscience Publishers, New York, 1963, vol. I.
- 7 F. J. Sowa, G. F. Hennion and J. A. Nieuwland, *J. Am. Chem. Soc.*, 1935, **57**, 709.
- 8 G. Sartori, F. Bigi, R. Maggi and A. Arienti, *J. Chem. Soc., Perkin Trans. 1*, 1997, **3**, 257.
- 9 S. Sato, R. Takahashi, T. Sodesawa, K. Matsumoto and Y. Kamimura, *J. Catal.*, 1999, **184**, 180.
- 10 W. K. Gray, F. R. Smail, M. G. Hitzler, S. K. Ross and M. Poliakoff, *J. Am. Chem. Soc.*, 1999, **121**, 10711.
- 11 L. Bagnell, T. Cablewski, C. R. Strauss and R. W. Trainor, *J. Org. Chem.*, 1996, **61**, 7355.
- 12 C. H. Bamford and C. F. H. Tipper, *Comprehensive Chemical Kinetics*, Elsevier, Amsterdam, 1972, vol. 5.
- 13 E. L. Coitino, J. Tomasi and O. N. Ventura, *J. Chem. Soc. Faraday Trans.*, 1994, **90**, 1745.
- 14 A. R. Katritzky, M. Balasubramanian and M. Siskin, *Energy Fuels*, 1990, **4**, 499.
- 15 K. Sue, K. Murata, Y. Matsuura, M. Tsukagoshi, T. Adschiri and K. Arai, *Fluid Phase Equilib.*, 2002, **194–197**, 1097.
- 16 G. Sartori, R. Maggi, F. Bigi, A. Arienti, C. Porta and G. Predieri, *Tetrahedron*, 1994, **50**, 10587.



# Green S as a prototype for an environmentally-degradable dye: the concept of a 'green dye' in future Green Chemistry†

Alexei U. Moozyckine<sup>a</sup> and D. Martin Davies<sup>\*b</sup>

<sup>a</sup> Department of Chemistry, University of Wales Swansea, Swansea, UK SA2 8PP

<sup>b</sup> Division of Chemical Sciences, School of Applied and Molecular Sciences, University of Northumbria at Newcastle, Newcastle upon Tyne, UK NE1 8ST.

E-mail: martin.davies@unn.ac.uk

Received 13th May 2002

First published as an Advance Article on the web 14th August 2002

The aqueous oxidation of Green S dye by hydrogen peroxide includes two alternative pathways: nucleophilic attack on the central carbon at near-neutral and high pH and the formation of N-oxide in the region of lower pH. This is indicative of a pH switch between nucleophilic and electrophilic reaction mechanisms for H<sub>2</sub>O<sub>2</sub> oxidation. The strong catalytic effect of chloride anion together with methyltrioxorhenium (MTO) on Green S oxidation by hydrogen peroxide has been observed, conforming to the staggered mechanism which involves the formation of free chlorine at a very low steady-state concentration. In terms of the observed first-order rate constants, the catalytic effect is estimated to be at least 2000 compared to the uncatalysed reaction, for an MTO concentration of  $3.0 \times 10^{-6}$  mol dm<sup>-3</sup> and Cl<sup>-</sup> concentration of 0.10 mol dm<sup>-3</sup> at pH 1.3.

## Introduction

The triarylmethane group of dyes is structurally related to an even larger family of diarylmethane (diphenylmethane) dyes and represents one of the oldest classes of synthetic dyes, many of which are still produced commercially today. Polyarylmethane dyes have been extensively used as colourants in photography, stationary and cosmetics, food and pharmaceutical industries.<sup>2</sup> Some of them are used in biomedical sciences as sterilizing and antimicrobial (antifungal) agents, biological stains, and to assay proteins;<sup>3</sup> many are deployed in analytical chemistry as indicators, colorimetric and complexing reagents.<sup>2</sup> They were employed as textile dyes for cotton, silk and wool, and used for preparation of inks and coloured paper.<sup>4</sup> More recent applications include dye-assisted laser inactivation of enzymes,<sup>4</sup> photochemotherapy,<sup>5</sup> use as sensitizers for solar cells and photoconductors.<sup>2,3</sup> The structure of triarylmethane dyes is non-coplanar and resembles a three-bladed propeller, where the aromatic rings forming the blades are tilted towards each other as a consequence of steric restrictions.<sup>3,4</sup>

Large amounts of wastewater from the manufacture and also from the consumption of polyarylmethane dyes have to be treated prior to entering the aquatic environment. The majority of these dyes are not easily biodegradable, as they possess antibiotic properties. Therefore, many of them are not amenable to conventional activated sludge treatment and might represent a serious threat to the environment and human health.<sup>2,6</sup> Currently, it is thought that around 12% of the synthetic textile dyes used yearly are lost to waste streams; it has been estimated that approx. 20% of these losses remain unchanged and find their way into rivers through effluents from wastewater treatment plants.<sup>2</sup> Although nowadays the polyarylmethane family of dyes is largely confined to non-textile applications, various estimates indicate that 1–2% of these dyes are lost during the manufacturing stage and up to 10% of di-(tri)-arylmethane dyes are lost to the aquatic environment at the user stage.<sup>2</sup>

Recently, we identified a type of triarylmethane dye that is very amenable to aqueous oxidation by dilute hydrogen peroxide at neutral pH.<sup>7</sup> The structure of this dye, Green S (Lissamine Green B, Acid Green 50, Wool Green S, C.I. 44090), is shown in Scheme 1. The characteristic feature that makes this dye behave differently from other substrates is the hydroxyaryl group positioned *ortho* to the central carbon. From the detailed analysis of the reaction of Green S dye and H<sub>2</sub>O<sub>2</sub>, we concluded that the ionized *ortho*-hydroxy group facilitates nucleophilic attack on the central carbon of the dye *via* intramolecular base catalysis.<sup>7</sup> We have found that the rate of Green S aqueous oxidation by hydrogen peroxide is comparable to those of enzymatic reactions.

In the hope that further analysis of Green S bleaching by H<sub>2</sub>O<sub>2</sub> would provide a better insight into the reaction mechanism and help to find new practical solutions, we attempted to expound some general trends that could be useful for environmental chemists dealing with polyarylmethane dyes. Thus, we extended our studies of Green S reactions with hydrogen

## Green Context

**Very large amounts of wastewater are produced from the manufacture and also from the consumption of polyarylmethane dyes. The majority of these dyes are not easily biodegradable and are not amenable to conventional activated sludge treatment. In fact it is believed that up to 10% of these dyes are lost to the aquatic environment. This paper describes studies on a triarylmethane dye that is amenable to aqueous oxidation using hydrogen peroxide. In particular, it is shown that the oxidation of the dye occurs at near neutral pH and remarkably rapidly and this can be further accelerated with a catalyst. The authors propose that the incorporation of an *ortho*-hydroxy group in to the structure of di- and triarylmethanes could lead to fast and effective oxidation of the dyes by dilute hydrogen peroxide. This could prove to be of considerable importance to the future design of 'greener dyes.'**

JHC

† Presented in part at the RSC International Conference *Green Chemistry—Sustainable Products and Technologies*, 3–6 April 2001, University of Wales Swansea.<sup>1</sup>

peroxide to the low pH region and also into the area of homogeneous catalysis, aiming for greater applicability of our previous findings to environmental water treatment. Characterizations of products and intermediates from  $\text{H}_2\text{O}_2$  aqueous oxidation of polyarylmethane dyes have been reported,<sup>6,8</sup> and the main pathways leading to deeper decomposition have been outlined, thus allowing for a general understanding of the processes involved. However, the exact pathways may vary significantly depending on the actual dye and the conditions, and these considerations are far beyond the scope of the present paper.

## Experimental

### Materials

The details for Green S (Lissamine Green B), EDTA, EDTMP (ethylenediaminetetramethylenephosphonic acid), hydrogen peroxide and other reagents used for preparing buffers were provided earlier.<sup>7</sup> All metal complexes tested as catalysts with hydrogen peroxide were of the best available grade, including methyltrioxorhenium  $\text{MeReO}_3$  (MTO), osmium oxide  $\text{OsO}_4$  and (5,10,15,20-tetrakis(pentafluorophenyl)-21*H*,23*H*-porphine)iron(III) chloride ( $\text{Fe}(\text{TPP})\text{Cl}$ ), all purchased from Aldrich and used as supplied. For the determination of the rate of Green S bleaching by free chlorine we used sodium hypochlorite solution (12%  $\text{Cl}_2$ ) obtained from BDH, the initial concentration of free chlorine in the solutions used for kinetic runs ranged from  $1.0 \times 10^{-3}$  to  $5.0 \times 10^{-3}$  mol  $\text{dm}^{-3}$ .

### Procedure

All reactions and measurements were carried out in buffered aqueous solutions described previously.<sup>7</sup> The ionic strength of the buffer in all cases was 0.10 mol  $\text{dm}^{-3}$ . All hydrogen peroxide solutions were prepared from a 0.800 mol  $\text{dm}^{-3}$  stock solution in distilled water. For standardising the concentration of  $\text{H}_2\text{O}_2$  stock solutions, we used a very accurate spectrophotometric method based on the colour reaction between  $\text{Ti}(\text{SO}_4)_2$  and  $\text{H}_2\text{O}_2$  at low pH.<sup>9</sup> Solutions of Green S were prepared from a  $1.00 \times 10^{-3}$  mol  $\text{dm}^{-3}$  stock solution. The concentration of Green S was  $1.25 \times 10^{-5}$  mol  $\text{dm}^{-3}$  while the hydrogen peroxide concentration ranged from  $5.0 \times 10^{-3}$  to 0.20 mol  $\text{dm}^{-3}$ . To suppress the background reactions occurring at low

pH and attributed to metal ion catalysis, we used the sequestering agents, EDTA and EDTMP, in concentrations ranging from  $4.0 \times 10^{-6}$  to  $2.5 \times 10^{-5}$  mol  $\text{dm}^{-3}$ .

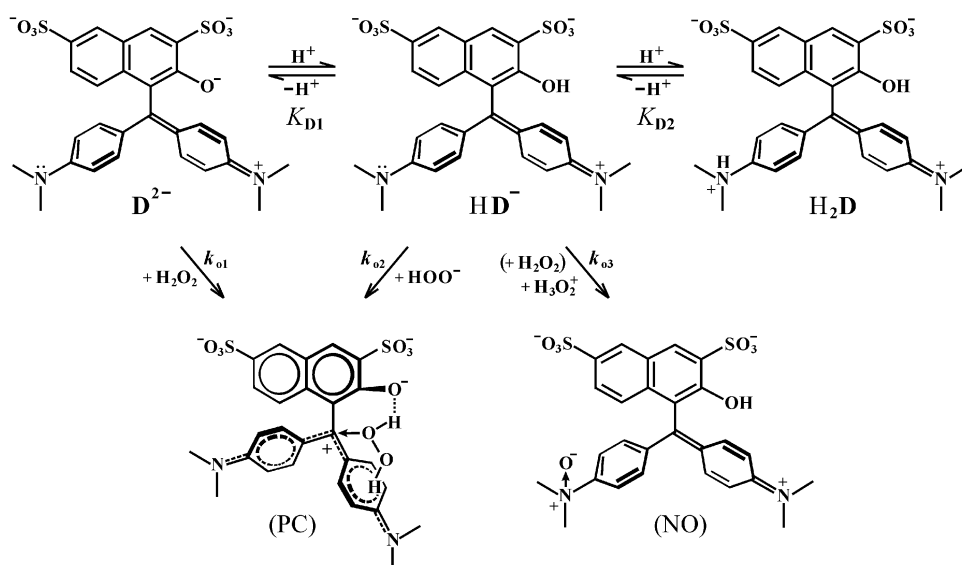
### Kinetic measurements

The UV/vis spectra were obtained using a Pharmacia Biotech Ultraspec 2000 spectrophotometer equipped with a thermostatted cell-holder and an Applied Photophysics SX-17MV stopped-flow spectrophotometer. For the pH measurements a Metrohm 702 SM Titrino pH-meter was used. When the stopped-flow instrument was used, one syringe contained Green S and a double strength buffer, whilst the second syringe contained hydrogen peroxide solution in distilled water, to avoid the decomposition of  $\text{H}_2\text{O}_2$ , especially with high pH buffers. All measurements were conducted at a temperature of  $25 \pm 0.2$  °C. The reaction was followed at a wavelength corresponding to the maximum of the main absorbance peak of Green S at the appropriate pH (between 615 and 635 nm). Pseudo-first-order rate constants were determined from non-linear regression of the mono-exponential decrease in absorbance with time, due to hydrogen peroxide bleaching of Green S. For each set of conditions used, rate constants were measured typically for at least six different concentrations of hydrogen peroxide. The observed second-order rate constants for  $\text{H}_2\text{O}_2$  bleaching were calculated from the quotient of the pseudo-first-order rate constants and hydrogen peroxide concentration. The initial rates method was used when the logarithmic plots of absorbance vs. time did not exhibit particularly well defined linearity. In these cases the first-order rate constants were obtained from the gradients of relative absorbance change,  $(A/A_0)$ , vs. time during the initial stage of reaction; the corresponding second-order rate constants were calculated from the quotient of  $(1/A_0)dA/dt$  and the concentration of the oxidizing agent (*i.e.* chlorine or hydrogen peroxide).

## Results

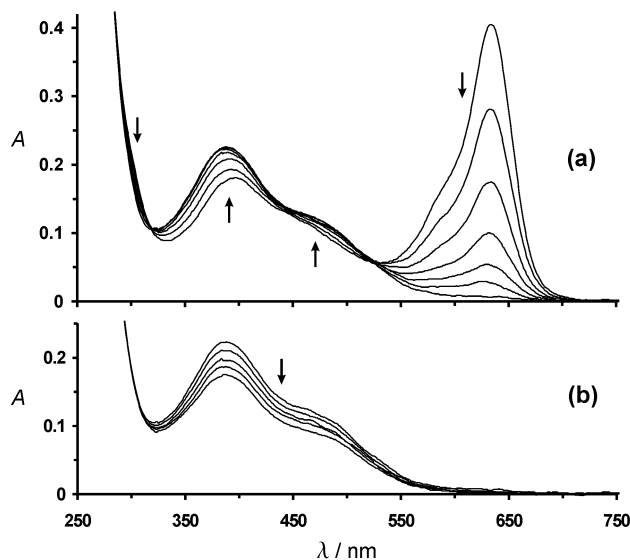
### Hydrogen peroxide bleaching of Green S

The spectral changes taking place during hydrogen peroxide bleaching of Green S at pH 1.1 are shown in Fig. 1. The intensity of the main visible band drops, whereas the absorbance at a

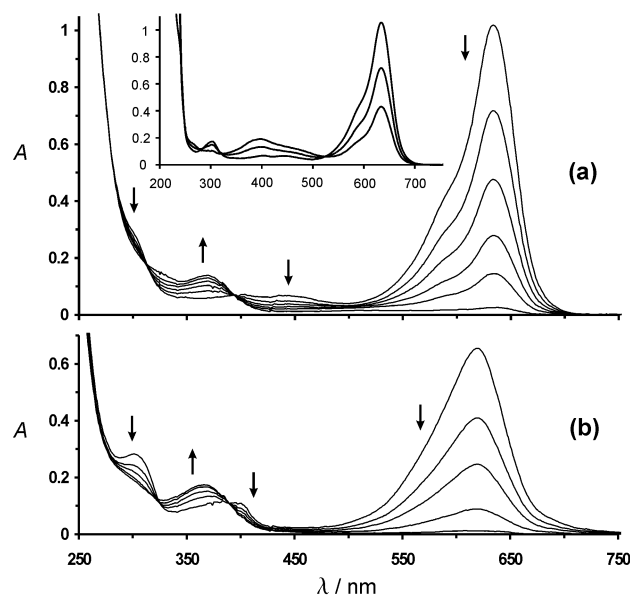


Scheme 1

lower frequency around 400–500 nm initially increases (Fig. 1(a)), with well defined isosbestic points at 319 and 526 nm. After the visible band at *ca.* 635 nm had almost disappeared, absorbance at all frequencies steadily falls (Fig. 1(b)) without showing any isosbestic points, for as long as it is possible to follow with no significant decomposition of hydrogen peroxide. All the area below 300 nm remains screened by hydrogen peroxide. As follows from Fig. 1, the H<sub>2</sub>O<sub>2</sub> oxidation of the dye at low pH exhibits only two spectrophotometrically distinguishable stages. Fig. 2 shows the spectral changes taking place during H<sub>2</sub>O<sub>2</sub> bleaching of Green S at pH 5.28 (a) and 8.08 (b).



**Fig. 1** Time-resolved changes in the absorption spectrum of  $1.25 \times 10^{-5}$  mol dm<sup>-3</sup> Green S during bleaching with 0.120 mol dm<sup>-3</sup> hydrogen peroxide at pH 1.12, ionic strength 0.10 mol dm<sup>-3</sup>, 25 °C. From the top to the bottom: (a) decrease in intensity of the band at *ca.* 630 nm: 0, 1, 2, 3, 4, 5, 10 h; (b) decrease in intensity of the band at *ca.* 390 nm: 10, 21, 39, 53, 69.5 h. Arrows indicate the direction of movement.



**Fig. 2** Changes in the absorption spectrum of  $1.25 \times 10^{-5}$  mol dm<sup>-3</sup> Green S during bleaching at 25 °C, ionic strength 0.10 mol dm<sup>-3</sup>, with (a) 0.120 mol dm<sup>-3</sup> hydrogen peroxide at pH 5.28, from the top to the bottom, on the band at *ca.* 635 nm: 0.1, 18, 39, 66, 99, 207 min; (b) 0.020 mol dm<sup>-3</sup> hydrogen peroxide at pH 8.08, from the top to the bottom, on the band at *ca.* 620 nm: 6, 54, 102, 198, 390 s. Arrows indicate the direction of movement. Inset: absorption spectrum of  $1.25 \times 10^{-5}$  mol dm<sup>-3</sup> Green S at 25 °C, ionic strength 0.10 mol dm<sup>-3</sup>, at the following pH values, in order of decreasing absorbance in the band at *ca.* 635 nm: 5.31, 1.56, 1.17.

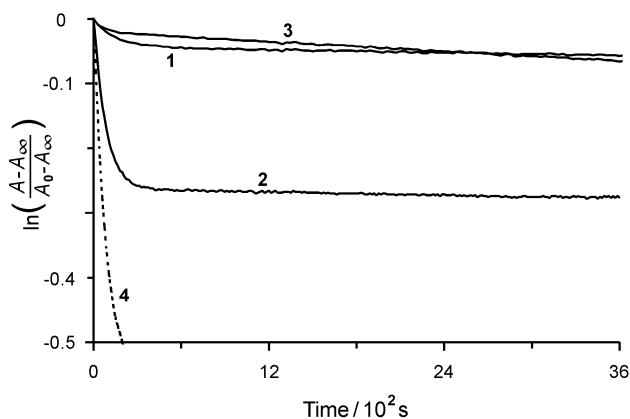
The inset shows the equilibrated spectra of Green S at different pH values.

### Catalytic oxidation of Green S by hydrogen peroxide

The concentration of the metal complexes in all studied solutions was  $3.0 \times 10^{-6}$  mol dm<sup>-3</sup> unless stated otherwise, except for Fe(TPP)Cl. The saturated solution of Fe(TPP)Cl, which we used due to its low solubility in water, was prepared by intensive stirring of the complex for 4 h at ambient temperature and subsequent filtration. All other solutions were prepared from stocks containing  $9.0 \times 10^{-6}$  mol dm<sup>-3</sup> of the metal complexes. Using the initial rates method, we estimated the second-order rate constant for Green S bleaching by free chlorine in the absence of catalysts to be  $9.5$  dm<sup>3</sup> mol<sup>-1</sup> s<sup>-1</sup> at pH 1.24 and ionic strength 0.1 mol dm<sup>-3</sup>. The corresponding pseudo-first-order rate constant obtained for the same uncatalysed reaction was  $2.86 \times 10^{-2}$  s<sup>-1</sup> at a concentration of chlorine of  $3.0 \times 10^{-3}$  mol dm<sup>-3</sup>.

Fig. 3 shows the absorbance changes during catalytic hydrogen peroxide bleaching of Green S in the presence of MTO catalyst. The first-order rate constants for the curves 1, 2, 3 and 4 (Fig. 3) were calculated from the initial rates, they are  $2.5 \times 10^{-4}$ ,  $2.1 \times 10^{-3}$ ,  $2.1 \times 10^{-4}$  and  $4.0 \times 10^{-3}$  s<sup>-1</sup>, respectively. The observed first-order rate constants obtained for MTO/H<sub>2</sub>O<sub>2</sub>/Cl<sup>-</sup> system and several other selected catalytic complexes are shown in Fig. 4. For all tested complexes the rate constants were determined using the initial rates technique, from the absorbance drop at *ca.* 635 nm during the initial period of the reaction (usually, about 120 s). Fig. 5 represents changes in absorbance during H<sub>2</sub>O<sub>2</sub> bleaching of Green S at pH 1.3 with MTO with and without Cl<sup>-</sup>. The curves show well defined first-order kinetics, the rate constants calculated from the slopes of logarithmic plots are  $3.1 \times 10^{-5}$ ,  $6.7 \times 10^{-3}$  and  $5.0 \times 10^{-3}$  s<sup>-1</sup> for the curves a, b and c, respectively.

Using three different concentrations of Green S (results not shown), we found that the reaction is independent of the initial concentration of the dye. Fig. 6 shows the dependence of the first-order rate constant for the reaction of Green S and H<sub>2</sub>O<sub>2</sub> on the concentration of chloride ion. The curve corresponds to the data fit into eqn. (1), using the best-fit values:  $m = 0.42 \pm 0.01$ ,  $k_1 = (1.7 \pm 0.1) \times 10^{-2}$  and  $a = (3.1 \pm 0.1) \times 10^{-5}$  s<sup>-1</sup>. Fig. 7 shows the dependence of the first-order rate constant for the reaction of Green S and H<sub>2</sub>O<sub>2</sub> on the concentration of MTO



**Fig. 3** Plot of the reaction progress for the reaction of H<sub>2</sub>O<sub>2</sub> (0.10 mol dm<sup>-3</sup>) and Green S ( $1.25 \times 10^{-5}$  mol dm<sup>-3</sup>) in the presence of MTO catalyst. Numbered curves correspond to an MTO concentration of  $3.0 \times 10^{-6}$  mol dm<sup>-3</sup> in buffer solutions at pH values: (1) 2.89 (NaH<sub>2</sub>PO<sub>4</sub> + HNO<sub>3</sub>); (2) 3.28 (KCl + HCl); (3) 3.80 (CH<sub>3</sub>COONa + CH<sub>3</sub>COOH) at 25 °C, ionic strength 0.10 mol dm<sup>-3</sup>. Curve (4) represents the conditions analogous to curve (2) for an MTO concentration of  $6.0 \times 10^{-6}$  mol dm<sup>-3</sup>. All absorbance changes were followed at 635 nm.

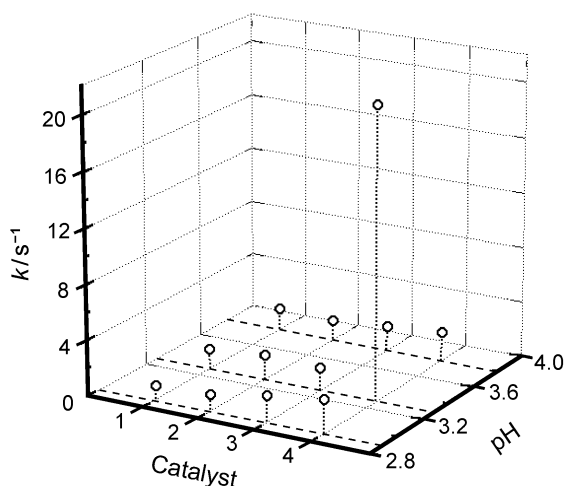
catalyst. The line corresponds to the data fit into eqn. (2), using best-fit values:  $k_2 = (6.5 \pm 0.1) \times 10^{-2} \text{ dm}^3 \text{ mol}^{-1} \text{ s}^{-1}$  and  $b = (1.7 \pm 0.2) \times 10^{-4} \text{ s}^{-1}$ .

$$k_{\text{obs}} = k_1[\text{Cl}^-]^m + a \quad (1)$$

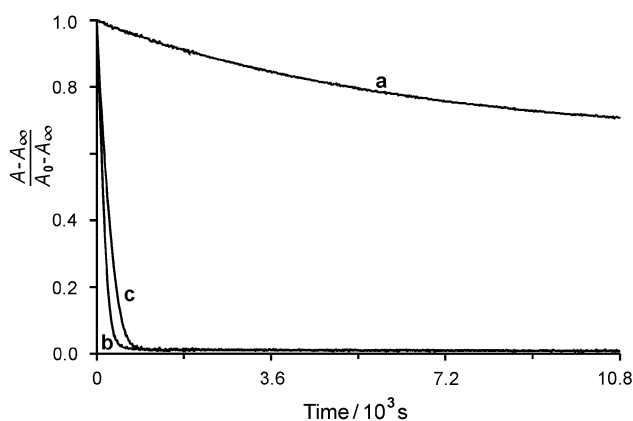
$$k_{\text{obs}} = k_2[\text{MTO}] + b \quad (2)$$

## Discussion

Admittedly, Green S represents a very convenient substrate for studies of aqueous oxidation reactions. Unlike many other triarylmethane dyes such as Victoria Blue R, Bromopyrogallol Red, *etc.* which tend to produce quite complicated kinetics (results not shown) due to various aggregation processes involved,<sup>4,10</sup> Green S has excellent solubility in water and in the spectrophotometrically feasible range of concentrations shows no sign of dimerization or trimerization.<sup>7</sup> For this reason we can recommend Green S as an ideal model substrate for under-



**Fig. 4** Comparative plot of first-order rate constants for the reaction of hydrogen peroxide ( $0.10 \text{ mol dm}^{-3}$ ) and Green S ( $1.25 \times 10^{-5} \text{ mol dm}^{-3}$ ), calculated from the initial rates for a selection of catalysts in buffer solutions at pH values 2.89, 3.28, 3.80 at  $25 \text{ }^\circ\text{C}$ , ionic strength  $0.10 \text{ mol dm}^{-3}$ . Buffer compositions are given in the caption to Fig. 3. The catalysts accorded numbers on the horizontal plane are: (1) blank solution; (2) Fe(TPP)Cl; (3)  $\text{OsO}_4$ ; (4) MTO.

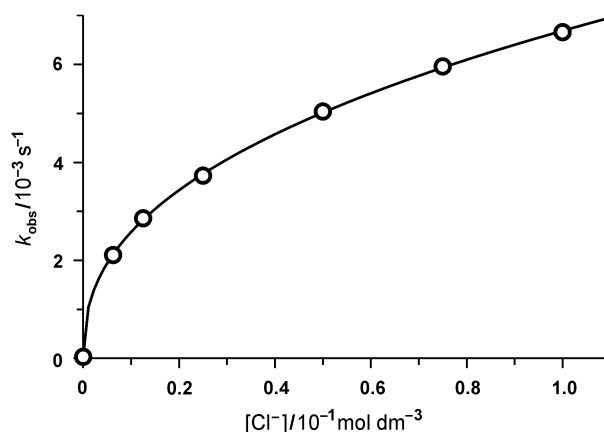


**Fig. 5** Plot of the reaction progress for the reaction of  $\text{H}_2\text{O}_2$  ( $0.10 \text{ mol dm}^{-3}$ ) and Green S ( $1.25 \times 10^{-5} \text{ mol dm}^{-3}$ ) in the presence of MTO catalyst ( $3.0 \times 10^{-6} \text{ mol dm}^{-3}$ ). The curves correspond to the following buffering solutions: (a)  $\text{HNO}_3$ ; (b)  $\text{HCl}$ ; (c) 1:1  $\text{HNO}_3/\text{KCl}$  at  $25 \text{ }^\circ\text{C}$ , ionic strength  $0.10 \text{ mol dm}^{-3}$ , pH 1.3. Absorbance changes were followed at 635 nm.

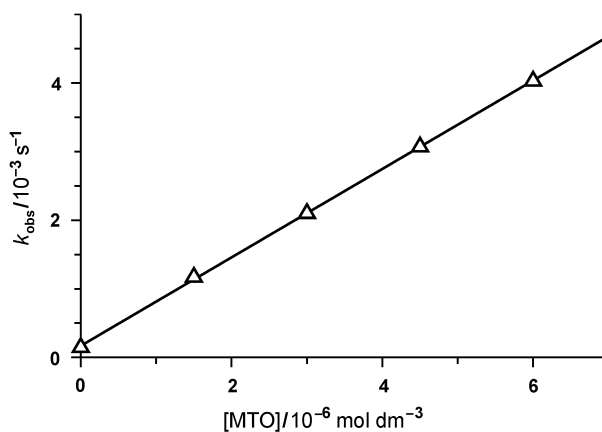
graduate studies—*dye bleaching by hydrogen peroxide*—in the context of environmental courses.

## A pH switch between N-oxidation and cleavage at the central carbon

Summarizing the changes in UV-vis spectrum of Green S during  $\text{H}_2\text{O}_2$  bleaching in different pH regions, we can describe them from Fig. 2, as follows: a steady drop on the main band and in the whole region above *ca.* 400 nm; a rise in quite a narrow region between *ca.* 320 and 390 nm; and a fall below *ca.* 310 nm. The corresponding isosbestic points are at 312 and 393 nm in the lower pH region (below pH 7.66) where  $\text{HD}^-$  (*q.v.* Scheme 1) species are predominant; and 323 and 389 nm in the region of higher pH values (above pH 7.66) where  $\text{D}^{2-}$  species are predominant. As we showed previously,<sup>7</sup> all this is commensurate with the nucleophilic attack on the central carbon. The changes in the spectra which are characteristic of N-oxidation at very low pH are very different (Fig. 1(a)), they closely resemble the spectrum of  $\text{H}_2\text{D}$  species with a broken chromophoric system (Fig. 2 inset) and can be described as follows: the absorbance drop on the main band above *ca.* 540 nm; a steady rise in a wide region between 319 and 525 nm;



**Fig. 6** Dependence upon chloride ion concentration of the observed first-order constant for hydrogen peroxide bleaching of Green S. Ionic strength  $0.10 \text{ mol dm}^{-3}$ ,  $[\text{Green S}] = 1.25 \times 10^{-5} \text{ mol dm}^{-3}$ ,  $[\text{MTO}] = 3.0 \times 10^{-6} \text{ mol dm}^{-3}$ , pH *ca.* 1.3. The curve represents best fit of eqn. (1) to the data points.



**Fig. 7** Dependence upon MTO catalyst concentration of the observed first-order constant for hydrogen peroxide bleaching of Green S. Ionic strength  $0.10 \text{ mol dm}^{-3}$ ,  $[\text{Green S}] = 1.25 \times 10^{-5} \text{ mol dm}^{-3}$ ,  $[\text{Cl}^-] = 0.10 \text{ mol dm}^{-3}$ , pH 3.28. The line represents best fit of eqn. (2) to the data points.



another drop below 319 nm. The corresponding isosbestic points are at 277, 326 and 522 nm. We demonstrated before<sup>7</sup> that the  $\text{H}_2\text{D}$  species is characterised by protonation occurring on one of the nitrogens. Now we can conclude that the initial stage of  $\text{H}_2\text{O}_2$  bleaching of Green S at very low pH is commensurate with N-oxidation occurring on one of dimethylamino groups, which breaks the chromophore by engaging the lone electron pair of the nitrogen. As it is possible to see from the comparison of timescales in Figs. 1 and 2, consistent with the observed rate profile given in the previous work,<sup>7</sup> the formation of N-oxide species (**NO**) greatly enhances the resistance of Green S dye to further fragmentation. The value of the observed rate constant calculated for the secondary oxidation processes for the reaction of Green S and  $\text{H}_2\text{O}_2$  at low pH, (Fig. 1(b)), is  $(1.13 \pm 0.02) \times 10^{-6} \text{ s}^{-1}$ .

For hydrogen peroxide oxidation of Green S a general idea of the reaction species and the initial pathways involved is reflected in Scheme 1. Here,  $\text{D}^{2-}$  corresponds to a bright-blue species with ionized hydroxy in *ortho* position to the central carbon,  $\text{HD}^-$  represents a teal-green species with protonated *ortho*-oxygen, and  $\text{H}_2\text{D}$  describes a yellowish species existing at low pH. The values<sup>7</sup> of  $\text{p}K_{\text{a}}$  for Green S species shown in Scheme 1 are 7.66 for  $\text{HD}^-$  (corresponding to  $K_{\text{D1}}$ ) and 1.31 for  $\text{H}_2\text{D}$  species (corresponding to  $K_{\text{D2}}$ ). The chromophoric structure of Green S is formed by a system of conjugated double bonds and the lone pair of electrons on nitrogen, whilst *ortho*-oxygen represents a relatively weak auxochrome and its protonation results in a slight hypsochromic shift of the main visible absorption band of the dye. The protonation of the dimethylamino nitrogen of the  $\text{H}_2\text{D}$  species breaks down the chromophore, and so does the N-oxidation occurring in a lower pH region with formation of (**NO**) species. Evidently, pH values necessary for both N-protonation and N-oxidation to take place are similar, both below 3. The precursor-type complex (**PC**), formed through the nucleophilic attack of hydrogen peroxide either on  $\text{D}^{2-}$  (Scheme 1,  $k_{\text{o1}}$ ) or on  $\text{HD}^-$  (Scheme 1,  $k_{\text{o2}}$ ) species, represents the main reaction pathway at higher pH. Upper limits of the bimolecular rate constants for parallel pathways,  $k_{\text{o1}}$  and  $k_{\text{o2}}$ , were determined from the observed rate constants as  $4.8 \times 10^{-1}$  and  $4.2 \times 10^3 \text{ dm}^3 \text{ mol}^{-1} \text{ s}^{-1}$ . On the basis of extensive kinetic analysis of  $\text{H}_2\text{O}_2$  and water bleaching of Green S dye,<sup>7</sup> we argued that the predominant pathway involves  $\text{D}^{2-}$  and  $\text{H}_2\text{O}_2$  reactive species, and not  $\text{HD}^-$  and  $\text{HOO}^-$ , so now we have a complete scheme of Green S species transformation across the whole range of pH. The upper limit for  $k_{\text{o3}}$  has been calculated as  $5.7 \times 10^{-6} \text{ dm}^3 \text{ mol}^{-1} \text{ s}^{-1}$  for the reaction of  $\text{HD}^-$  species and  $\text{H}_2\text{O}_2$ , and  $5.1 \times 10^2 \text{ dm}^3 \text{ mol}^{-1} \text{ s}^{-1}$  for  $\text{HD}^-$  and  $\text{H}_3\text{O}_2^+$ . The latter value represents a predominant pathway for the reaction of Green S with hydrogen peroxide at lower pH, commensurate with N-oxidation occurring on one of the nitrogens, as shown in Scheme 1. Thus, we have a compelling argument for the existence of a pH switch which regulates the predominant direction of the initial reaction between hydrogen peroxide and Green S: nucleophilic attack on the central carbon of the dye above pH 3, and the electrophilic attack resulting in N-oxidation of the dimethylamino group of the dye below this pH value. Apparently, similar pH switches regulating the direction of electrophilic/nucleophilic attack during  $\text{H}_2\text{O}_2$  oxidation exist for many other di-(tri-)arylmethane dyes carrying functional amino and alkylamino groups.

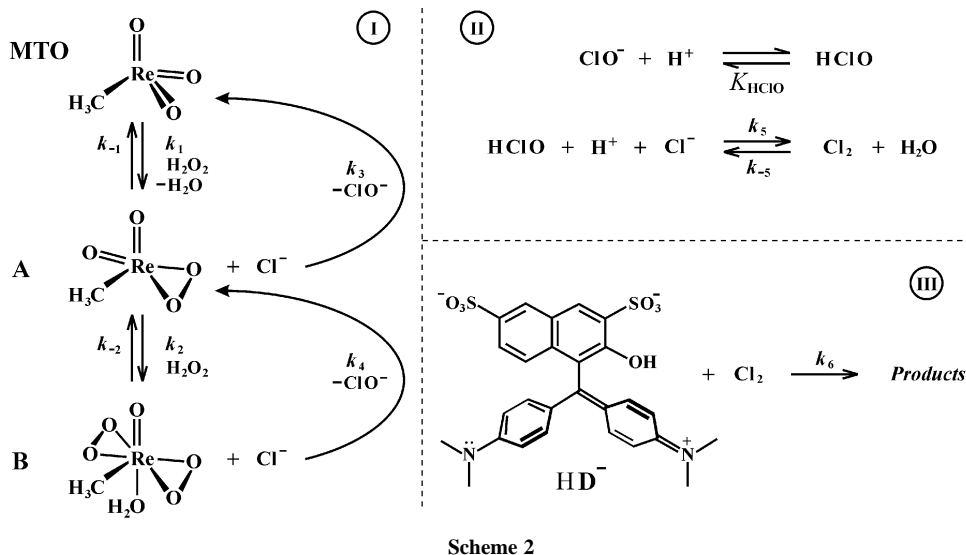
### Catalysis by the $\text{MTO}/\text{H}_2\text{O}_2/\text{Cl}^-$ system

The general pattern of the reactions observed for  $\text{H}_2\text{O}_2$  oxidation of Green S in the presence of small amounts of metal complexes is analogous to that demonstrated in curves 1 and 3 of Fig. 3. The rate constants were found to be more or less similar for all metal complexes tested, ranging from  $9.8 \times 10^{-5}$

to  $2.4 \times 10^{-4} \text{ s}^{-1}$ . This held to be true for all catalysts except MTO in the presence of chloride ion. The comparative magnitude of the catalytic effect of MTO in the presence of chloride ion can be seen in Fig. 4. The observed rate constant for the  $\text{MTO}/\text{H}_2\text{O}_2/\text{Cl}^-$  system reaches  $2.1 \times 10^{-3} \text{ s}^{-1}$ , clearly indicating that the mechanism of  $\text{MTO}/\text{Cl}^-$  catalysis is quite different from the 'normal' catalysis by other metal complexes, including MTO. The sharp slowdown in the observed rate after a short initial period shown in curves 2 and 4, Fig. 3, pertains to the increasing instability of  $\text{MTO}$ -peroxide complexes with elevated pH values at relatively high  $\text{H}_2\text{O}_2$  concentration.<sup>11</sup> The decomposition of MTO species, leading to the formation of  $\text{ReO}_4^-$ , can be considerably suppressed by increasing the acidity of the solution; this can be demonstrated by comparing curves b, c (Fig. 5) and 2, 4 (Fig. 3).

The real extent of the catalytic effect can be estimated by comparing the observed first-order rate constant for the uncatalysed reaction of Green S dye bleaching with that catalysed by the  $\text{MTO}/\text{H}_2\text{O}_2/\text{Cl}^-$  system (the latter case is illustrated by Fig. 5). For an MTO concentration of  $3.0 \times 10^{-6} \text{ mol dm}^{-3}$  and stoichiometric excess of chloride ion, the magnitude of the effect appears to be at least 2000 times. Taking into account some recent works,<sup>11-14</sup> the reaction of Green S dye with hydrogen peroxide, catalysed by MTO (or, rather, two peroxorhenium species  $\text{CH}_3\text{Re}(\text{O})_2(\eta^2\text{-O}_2)$ , **A**, and  $\text{CH}_3\text{Re}(\text{O})(\eta^2\text{-O}_2)_2(\text{H}_2\text{O})$ , **B**, present in its  $\text{H}_2\text{O}_2$  solutions)<sup>11,13</sup> with bromide ion would be expected to be even faster than with chloride. Our qualitative tests using small amounts of NaBr added to the buffering solutions showed that indeed this is the case. However, from the environmental viewpoint the presence of free bromine in water, even at very low levels, could cause considerable damage to the aquatic ecology, and thus is absolutely unacceptable. Therefore, we restricted our studies of Green S oxidation by the  $\text{MTO}/\text{H}_2\text{O}_2$  system to reactions catalysed by chloride ion, the latter being normally present in significant concentrations in the aquatic environment. It is commonly known that chloride is the third major inorganic solute in natural groundwater, and the average concentration of  $\text{Cl}^-$  in rivers exceeds  $1.6 \times 10^{-4} \text{ mol dm}^{-3}$ .<sup>15</sup> From Fig. 6 and eqn. (1) it follows that to be sufficiently effective for the oxidation of Green S and similar dye structures, the concentration of chloride ion must be at least  $0.01 \text{ mol dm}^{-3}$ ; this feature makes the system  $\text{MTO}/\text{H}_2\text{O}_2/\text{Cl}^-$  particularly suitable for the treatment of polyarylmethane dye pollutions in sea and saline waters. The methods of wastewater treatment using sodium hypochlorite solutions are known and sometimes used in pharmaceutical practices for quick oxidation of triarylmethane dyes.<sup>16</sup> However, these methods require the presence of relatively high concentrations of free chlorine in solution, which apart from being harmful in itself leads to the formation of secondary organochlorine products in appreciable concentrations.<sup>16</sup> The advantages of using the  $\text{MTO}/\text{H}_2\text{O}_2/\text{Cl}^-$  system in cases like these are self-evident.

Scheme 2 shows the mechanism of the process detailed in stages I-III, where stage I corresponds to the reaction of MTO with  $\text{H}_2\text{O}_2$  and consecutive oxidation of chloride ion; stage II represents the association of hypochlorite and its reaction with chloride ion with the formation of free chlorine at very low steady-state concentration; stage III demonstrates the successive reaction of the free chlorine with Green S dye. In Scheme 2, **A** and **B** represent  $\eta^2$ -peroxo complexes of rhenium(vii), usually both present in MTO solutions in appreciable concentrations;<sup>11</sup> in diperoxo complex, **B**, rhenium adopts the structure of a pentagonal bipyramid with axial oxo- and aqua-groups and with a methyl group and four peroxo oxygens positioned equatorially. The  $\text{p}K_{\text{a}}$  value of  $\text{HClO}$  is 7.40.<sup>17</sup> The Scheme can be assessed with the aid of Table 1, showing the values for the rate and equilibrium constants compiled from several works. The observed second-order rate constant for the oxidation of Green S by hydrogen peroxide using  $\text{MTO}/\text{Cl}^-$  catalytic



**Table 1** Partial rate constants for the reactions shown in Scheme 2 and the corresponding equilibrium constants calculated from the forward and reverse rate constants:  $K_n = k_n/k_{-n}$  and  $K_{-n} = k_{-n}/k_n$

| $n$ | $k_n/s^{-1}$         | $k_n/dm^3 \text{ mol}^{-1} s^{-1}$ | $k_n/dm^6 \text{ mol}^{-2} s^{-1}$ | $K_n/dm^3 \text{ mol}^{-1}$ | $K_n/mol^2 \text{ dm}^{-6}$ | Ref.  |
|-----|----------------------|------------------------------------|------------------------------------|-----------------------------|-----------------------------|-------|
| 1   |                      | $4.22 \times 10^1$                 |                                    | $1.61 \times 10^1$          |                             | 13    |
| -1  | $2.62 \times 10^0$   |                                    |                                    |                             |                             | 13,14 |
| 2   |                      | $5.2 \times 10^0$                  |                                    | $1.32 \times 10^2$          |                             | 13,14 |
| -2  | $3.9 \times 10^{-2}$ |                                    |                                    |                             |                             | 13    |
| 3   |                      | $5.9 \times 10^{-2}$               |                                    |                             |                             | 13    |
| 4   |                      | $1.24 \times 10^{-1}$              |                                    |                             |                             | 13    |
| 5   |                      |                                    | $1.8 \times 10^4$                  |                             |                             | 17,18 |
| -5  | $1.1 \times 10^1$    |                                    |                                    |                             | $6.0 \times 10^{-4}$        | 17,18 |

system, relevant to  $k_6$ , was estimated as  $6.7 \times 10^{-2} \text{ dm}^3 \text{ mol}^{-1} \text{ s}^{-1}$ , which is very close to the values of  $k_3 = 5.9 \times 10^{-2}$  and  $k_4 = 1.24 \times 10^{-1} \text{ dm}^3 \text{ mol}^{-1} \text{ s}^{-1}$ , determined by Hansen and Espenson<sup>13</sup> for species **A** and **B**. This, together with the consideration of the eqns. (1) and (2) suggests that stage I of Scheme 2 might represent the rate limiting step. Scheme 2 does not show a pathway involving the formation of singlet oxygen from the reaction of HOCl and  $\text{H}_2\text{O}_2$  since the question concerning participation of singlet and triplet oxygen in a similar reaction has been extensively discussed and, essentially, ruled out by Espenson.<sup>13</sup>

## Conclusions

We have shown that due to the presence of the *ortho*-aryloxide moiety and the intramolecular base catalysis pertaining to it, the oxidation of Green S dye at near-neutral pH occurs unusually rapidly.<sup>7</sup> Now, we present the evidence that the homogeneous oxidation of Green S by  $\text{H}_2\text{O}_2$  can be accelerated much further, even at low pH, by applying MTO catalyst in the presence of chloride ion.

We propose that the incorporation of the hydroxy group into the structure of di-(tri-)arylmethane dyes in *ortho* position to the central carbon will result in a very easy and effective oxidation of the dye by dilute  $\text{H}_2\text{O}_2$  at moderate pH. We believe that this is a universal principle that can be used by synthetic chemists working on the design of future environmentally-friendly polyarylmethane dyes. As all dyes of this type are synthetically produced, the effect of the *ortho*-hydroxy group on the colouristic properties of the dye can be easily counterbalanced by the choice of another appropriate substituent. If for safety,

environmental or other reasons the acidic reaction of the aqueous solution of such a dye is essential and cannot be neutralized, the dye can still be easily oxidized by hydrogen peroxide, deploying MTO catalyst in the presence of chloride ion.

## References

- A. U. Moozyckine and D. M. Davies, RSC International Conference, *Green Chemistry—Sustainable Products and Technologies*, 3–6 April 2001, University of Wales Swansea, Abstracts, o-6.
- Kirk-Othmer Encyclopedia of Chemical Technology*, ed. J. I. Kroschwitz and M. Howe-Grant, Wiley-Interscience, New York, vol. 8, 1993, p. 763; vol. 24, 1997, pp. 551–572 and references therein.
- D. F. Duxbury, *Chem. Rev.*, 1993, **93**, 381–433.
- L. M. Lewis and G. L. Indig, *Dyes Pigm.*, 2000, **46**, 145–154.
- M. S. Baptista and G. L. Indig, *J. Phys. Chem.*, 1998, **102**, 4678–4688; J. A. Bartlett and G. L. Indig, *Dyes Pigm.*, 1999, **43**, 219–226.
- I. A. Salem, *Appl. Catal. B*, 2000, **28**, 153–162; D. R. Doerge, H. C. Chang, R. L. Divi and M. I. Churchwell, *Chem. Res. Toxicol.*, 1998, **11**, 1098–1104.
- D. M. Davies and A. U. Moozyckine, *J. Chem. Soc., Perkin Trans. 2*, 2000, 1495–1503.
- X. Li, G. Liu and J. Zhao, *New J. Chem.*, 1999, **23**, 1193–1196; K. M. Thompson, W. P. Griffith and M. Spiro, *J. Chem. Soc., Faraday Trans.*, 1993, **89**, 1203–1209; L. Jurasek, L. Křištofová, Y. Sun and D. S. Argyropoulos, *Can. J. Chem.*, 2001, **79**, 1394–1401; I. A. Salem, *Chemosphere*, 2001, **44**, 1109–1119.
- N. L. Gil-Ad and A. M. Mayer, *FEMS Microbiol. Lett.*, 1999, **176**, 455–461; F. D. Snell and C. T. Snell, *Colorimetric Methods of Analysis*, Vol. II, D. Van Nostrand Co., New York, 1949.
- H. B. Lueck, B. L. Rice and J. L. McHale, *Spectrochim. Acta., Part A*, 1992, **48**, 819–828; J. A. Bartlett and G. L. Indig, *Photochem.*

- Photobiol.*, 1999, **70**, 480–498; M. Sarkar and S. Poddar, *J. Colloid Interf. Sci.*, 2000, **221**, 181–185.
- 11 J. H. Espenson, *Chem. Commun.*, 1999, 479–488.
- 12 C. C. Romão, F. E. Kühn and W. A. Herrmann, *Chem. Rev.*, 1997, **97**, 3197–3246; T. H. Zauche and J. H. Espenson, *Inorg. Chem.*, 1998, **37**, 6827–6831; J. H. Espenson, Z. Zhu and T. H. Zauche, *J. Org. Chem.*, 1999, **64**, 1191–1196.
- 13 P. J. Hansen and J. H. Espenson, *Inorg. Chem.*, 1995, **34**, 5839–5844.
- 14 J. H. Espenson, O. Pestovsky, P. Hutson and S. Staudt, *J. Am. Chem. Soc.*, 1994, **116**, 2869–2877.
- 15 J. F. Pankow, *Aquatic Chemistry Concepts*, Lewis Publishers, Chelsea, Mich., 1991; W. Stumm and J. J. Morgan, *Aquatic Chemistry*, Wiley, New York, 1981; F. M. M. Morel and J. G. Hering, *Principles and Applications of Aquatic Chemistry*, Wiley, New York, 1993; V. L. Snoeyink and D. Jenkins, *Water Chemistry*, Wiley, New York, 1980.
- 16 M. Jank, H. Köser, F. Lücking, M. Martiensen and S. Wittchen, *Environ. Technol.*, 1998, **19**, 741–747.
- 17 L. C. Adam, I. Fábrián, K. Suzuki and G. Gordon, *Inorg. Chem.*, 1992, **31**, 3534–3541.
- 18 M. Eigen and K. Kustin, *J. Am. Chem. Soc.*, 1962, **84**, 1355–1361.



# The selective oxidation of benzyl alcohol using a novel catalytic membrane reactor

David W. Hall,<sup>a</sup> Georgia Grigoropoulou,<sup>a</sup> James H. Clark,<sup>\*a</sup> Keith Scott<sup>b</sup> and Roshan J. J. Jachuck<sup>b</sup>

<sup>a</sup> Clean Technology Centre, Department of Chemistry, University of York, York, UK YO10 5DD. E-mail: jhc1@york.ac.uk

<sup>b</sup> Process Intensification and Innovation Centre, Department of Chemical and Process Engineering, University of Newcastle, Merz Court, Newcastle upon Tyne, UK

Received 13th May 2002

First published as an Advance Article on the web 23rd August 2002

A silica–polyethylene membrane has been chemically modified to produce ion-exchangeable onium sites, which are more active than their homogeneous analogues in a membrane reactor. The resulting catalytic membrane reactor is compact and energy efficient and provides an excellent low-waste method for the selective oxidation of benzyl alcohol.

## Introduction

The membrane reactor approach to phase-transfer catalysis is a cleaner more intensified process than conventional mixer/settler methods, reducing energy requirements and waste.<sup>1</sup> We have previously demonstrated this in the context of oxidation reactions whereby a PTFE microporous membrane was successfully used to maintain separation of the organic (substrate, product and catalyst) and aqueous (hypochlorite and salt) layers.<sup>2</sup> The obvious limitation to this process is the homogeneous catalyst, which requires separation from the organic layer. Furthermore, being soluble in the organic layer, must mean that the catalyst is not concentrated at the interface where it is needed to accelerate the organic reaction. Clearly, if we can fix the phase transfer catalyst to the membrane while maintaining its activity, we can anticipate both a cleaner, less plant and energy, intensive process and more efficient use of the catalyst species. Here we describe the first successful demonstration of this, which we believe opens the door to an exciting new area of green chemistry utilising both heterogeneous catalysis and process intensification.

## Experimental

Benzyl alcohol, sodium hypochlorite solution and trimethoxysilylpropyltri-*n*-butylammonium bromide were commercial samples used as such. Empore® membrane was obtained from the 3M company and Entek® membrane from Entek International.

The membranes were functionalised by refluxing in a solution of the silane (1 g) in methanol (100 cm<sup>3</sup>) for 6 h. The presence of the onium functions after chemical surface modifications was confirmed by elemental analysis and using a Kratos HSi imaging X-ray photoelectron spectrometer.

Oxidation reactions were carried out with the chemically modified membranes in a specially designed cell (Fig. 1) with starting solutions of 0.05 M of benzyl alcohol in dichloromethane on one side and 0.5 M aqueous hypochlorite solution on the other. The pH of the aqueous hypochlorite solution was adjusted to pH 9 prior to the addition to the reactor. Samples were periodically removed and analysed by GC showing a steady build up of benzaldehyde only. Benzoic acid was not observed on either side of the membrane reactor. No change in

the reaction kinetics was observed in reuse experiments, which were carried out by recharging the cell with fresh substrate and oxidant.

## Results and discussion

The design of the cell used in this study is shown in Fig. 1. The two sides of the cell have independent temperature controls enabling, for example, a higher temperature to be used on the organic side (for faster reactions), while keeping the aqueous side cool so as to minimise destructive decomposition of the oxidant. Although we used PTFE membranes in our original work with homogeneous catalysts,<sup>2,3</sup> it is not a suitable material for chemical modification. Two alternative materials were identified, which met the criteria for adequate mass transport and chemical resistance:

- Empore® Anion-SR, which is made up of a particulate poly(styrenedivinylbenzene) copolymer modified with quater-

## Green Context

The selective oxidation of organic compounds presents some of the most challenging goals for the green chemist. Problems of over-oxidation, disposal of aqueous chloride waste, and appropriate design of multiphase reactor systems are just some of the problems that may be encountered. These authors have chosen to improve multiphase reactor chemistry and engineering by preparing a novel membrane material that contains a covalently-incorporated phase transfer catalyst derived from a silylpropyltri-*n*-butylammonium bromide. In contrast to a soluble phase transfer catalyst, this membrane-bound catalyst avoids contamination of either the aqueous layer (containing the oxidant) or the organic layer (containing the benzyl alcohol substrate). In addition, the concentration of the phase transfer catalyst is maintained exclusively at the interfacial boundary where it is needed. This latter effect is believed to explain the high catalyst turnover numbers in this study relative to previous work with soluble phase transfer catalysts. The new membrane material allows ready catalyst preservation and re-use.

JKB

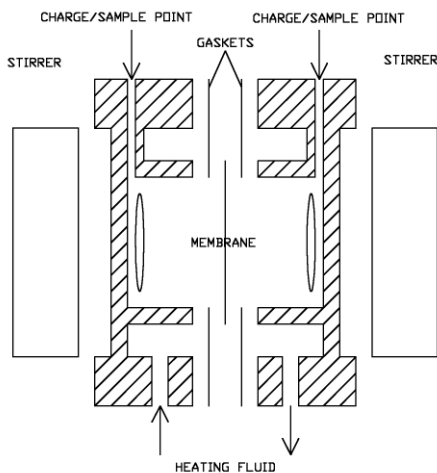


Fig. 1 Diffusion cell design.

nary ammonium groups within a PTFE matrix. This was anion exchanged to the  $\text{HSO}_4^-$  form, which is known to be more active in homogeneous reactions.<sup>3</sup>

• Entek®, which is a silica-impregnated polyethylene. This was chemically modified by reaction with trimethoxysilylpropyl-tri-*n*-butylammonium bromide to give a typical loading of *ca.* 0.002 mmol  $\text{N}^+/\text{cm}^2$  membrane. Thus, for a membrane with an area of 7  $\text{cm}^2$ , the amount of catalyst available to the reaction was 1/30th of that used in the previous homogeneous catalyst membrane reactor.<sup>2,3</sup>

We first tested the diffusion capabilities of the two membranes in a simple diffusion cell with pure solvent on one side and a solution of a PTC on the other. The results were compared to those using a conventional Gore-Tex® microfiltration membrane (Fig. 2). While the new membrane showed poorer mass transport, the results were not unreasonable. Using a steady-state approximation, the rate of diffusion was found to follow the relationship:

$$d(C_{\text{left}} - C_{\text{right}})/dt = D'\beta(C_{\text{right}} - C_{\text{left}})$$

where  $\beta$  is a geometric cell constant specific to the diaphragm cell used:

$$\beta = (AH/L)[(1/V_{\text{right}}) - (1/V_{\text{left}})]$$

( $H$  is a partition coefficient and is a function of the membrane structure;  $A$  is the membrane area;  $L$  is the membrane thickness;  $V_{\text{right}}$  and  $V_{\text{left}}$  are the volume of the two sides of the cell).

We then calculated the steady-state effective mass transfer coefficients:

$$\text{Gore-Tex® } 7.6 \times 10^{-6} \text{ m s}^{-1}$$

$$\text{Empore® } 7.1 \times 10^{-6} \text{ m s}^{-1}$$

$$\text{Modified-Entek® } 4.3 \times 10^{-6} \text{ m s}^{-1}$$

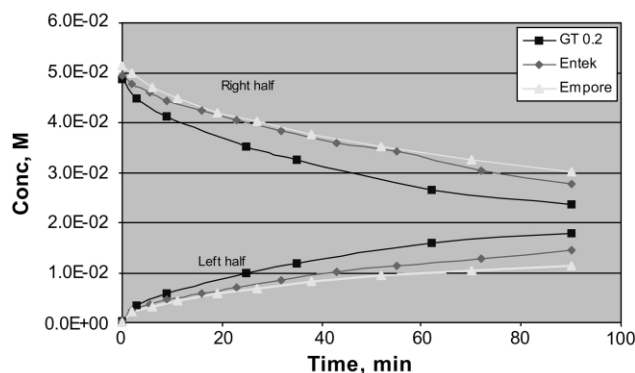


Fig. 2 Membrane diffusion measurements.

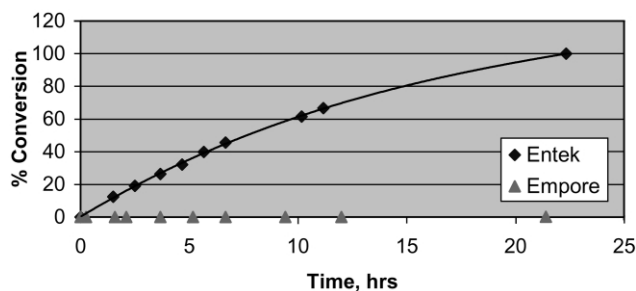


Fig. 3 Conversion of benzyl alcohol ( $T = 20^\circ\text{C}$ ;  $V_{\text{org}} = 25 \text{ ml}$ ;  $[\text{C}_6\text{H}_5\text{CH}_2\text{OH}]_0 = 0.05 \text{ M}$ ;  $V_{\text{aq}} = 25 \text{ ml}$ ;  $[\text{NaOCl}]_0 = 0.5 \text{ M}$ ).

This indicated that of the two onium-functionalised materials, the Empore® might be expected to be more active in a membrane reactor. However, when we tested the two in the reactor for the oxidation of benzyl alcohol, their performances were dramatically different with the Empore® showing little if any activity, while the Modified-Entek® performed very well (Fig. 3). We believe that this is due to the design of the Empore® material, which is a two-layer film of PTFE with the functionalised copolymer particles (90% by weight of the material) trapped in between. While the organic layer will be able to penetrate the hydrophobic PTFE film to access the catalytic species, the aqueous oxidant will not. In contrast, the modified Entek® materials are not hydrophobic and both organic and aqueous layers can freely access the catalyst enabling the oxidation reaction to occur. The quaternary ammonium catalyst immobilised on the membrane extracts the hypochlorite anion, which is believed to be the active oxidant. The active  $\text{R}_4\text{N}^+\text{OCl}^-$  catalyst ion pair oxidises the organic substrate. The reaction rate profile shows first order kinetics with a rate constant of  $0.0935 \text{ h}^{-1}$ . Further runs with the same membrane show no reduction in the rate of reaction, demonstrating excellent stability to leaching or fouling. For comparison, we ran a reaction using a non-functionalised Gore-Tex® membrane and homogeneous tetrabutylammonium hydrogen-sulfate as catalyst at 30 times the concentration of onium species used in the catalytic membrane reactions. The reaction conditions were otherwise identical. We observed a similar reaction profile with a rate constant of  $0.222 \text{ h}^{-1}$ . The much higher catalyst turnover numbers that can be achieved with the catalytic membrane can be attributed to the location of the active species at the system interface, whereas the bulk of the homogeneous catalyst will be in one half of the cell from where mass transport must take place before reaction can occur.

In conclusion, we have demonstrated for the first time how highly efficient phase transfer catalysis can be achieved in a catalytic membrane reactor using simply modified materials. The process offers simultaneous reaction and separation of phases with the added advantage of isolating and preserving the catalyst. There are excellent opportunities to expand the scope of this innovative technology to other oxidation reactions and beyond.

## Acknowledgements

We thank the EPSRC for supporting this work and other members of the York Green Chemistry–Newcastle Process Intensification collaboration for helpful discussions.

## References

- 1 T. J. Stanley and J. A. Quin, *Chem. Eng. Sci.*, 1987, **42**, 2313.
- 2 G. Grigoropoulou, J. H. Clark, D. W. Hall and K. Scott, *Chem. Commun.*, 2001, 547.
- 3 G. Grigoropoulou, Ph. D. thesis, University of York, UK, 2001.



# Conjugate addition of unmodified aldehydes: recycle of heterogeneous amine catalyst and ionic liquid

Hisahiro Hagiwara,<sup>\*a</sup> Tsuji Sayuri,<sup>b</sup> Tomoyuki Okabe,<sup>a</sup> Takashi Hoshi,<sup>b</sup> Toshio Suzuki,<sup>b</sup> Hiromasa Suzuki,<sup>a</sup> Ken-ichi Shimizu<sup>a</sup> and Yoshie Kitayama<sup>b</sup>

<sup>a</sup> Graduate School of Science and Technology, Niigata University, 8050, 2-nocho, Ikarashi, Niigata 950-2181, Japan. E-mail: hagiwara.gs.niigata-u.ac.jp

<sup>b</sup> Faculty of Engineering, Niigata University, 8050, 2-nocho, Ikarashi, Niigata 950-2181, Japan

Received 21st February 2002

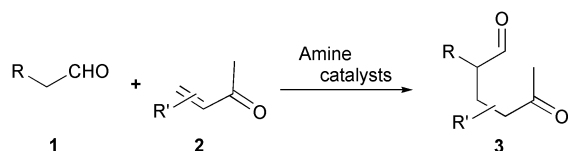
First published as an Advance Article on the web 19th August 2002

Unmodified aldehydes add to vinylketones in 1,4-manner in ionic liquid, [bmim]PF<sub>6</sub>, in the presence of a catalytic amount of propylamine grafted on silica. The ionic liquid involving the catalyst has been recycled intact without loss of efficiency.

## Introduction

Room temperature ionic liquids have attracted continuous attention<sup>1</sup> as recyclable and thus green media in organic syntheses mainly because of low volatility, low lipophilicity and low hydrophobicity. In view of the development of more advanced recycle systems in organic syntheses, reaction in ionic liquids with heterogeneous catalysts is the best combination providing that the catalyst suspends only in ionic liquid layer. By recycling the reaction, turnover number of the catalyst could be multiplied and such a system is considered to be a sustainable reactor. As a part of our efforts in this area, we focused on our newly developed 1,4-conjugate addition of unmodified aldehydes.

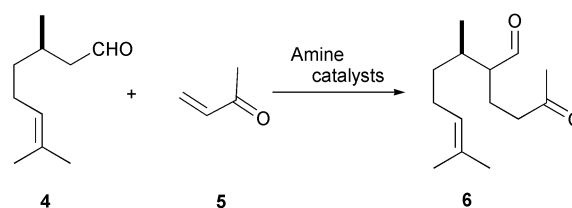
Aldehydes have been employed as excellent electrophiles in nucleophilic reactions. On the other hand, aldehydes have rarely been used as a nucleophiles due to the shortage of efficient methods to generate enolates or enols quantitatively. In order to function as a nucleophile, aldehydes must be transformed into the corresponding trimethylsilylenol ether<sup>2</sup> or enamine<sup>3</sup> which is reacted with an electrophile. We recently reported the 1,4-conjugate addition reaction of unmodified aldehyde **1** to vinylketone **2** in the presence of a catalytic amount of diethylaminotrimethylsilane (DEATMS)<sup>4,5</sup> or diethylamine (DEA)<sup>6</sup> to afford 5-ketoaldehyde **3** in acceptable yield (Scheme 1). The procedure is very simple.<sup>4</sup> Evaporation of the solvent followed by distillation or chromatography of the residue provided the product **3**. No aqueous work up is required. Based on these results as well as our own experience<sup>7</sup> toward ionic liquids as recyclable media for organic reactions prompted us to investigate the 1,4-conjugate addition of unmodified aldehyde **1** to vinylketone **2** in an ionic liquid. We disclose herein a more efficient protocol enabling recycling of an ionic liquid and a heterogeneous amine catalyst (Scheme 1). These 5-ketoaldehydes **3** are useful synthons for natural products such as perfumery ingredients or terpenoids.<sup>8</sup>



## Results and discussion

Reaction of citronellal **4** and 3-penten-2-one (MVK) **5** was employed as a probe to find an appropriate catalyst (Scheme 2). As ionic liquid, [bmim]PF<sub>6</sub>, was chosen because of low lipophilicity which allows easy separation of organic solvent from ionic liquid phase during partition of the product.

The reaction was carried out at 80 °C under nitrogen atmosphere. At room temperature, the reaction resulted in complete recovery of citronellal **4**. The product **6** was isolated by trituration with diethyl ether several times. After evaporation of the combined ether layers, the residue was purified by medium pressure LC. The results are summarized in Table 1. Without amine, citronellal **4** was recovered completely (entry 1). Then the secondary amine, grafted on a silica support such as *N*-methyl-3-aminopropylated FSM16 mesoporous silica (FSM16)<sup>9</sup> or *N*-methyl-3-aminopropylated silica (NMAP)<sup>10</sup> was tested, with recycling of the catalyst in mind. Though the reaction catalyzed by FSM16 was slow and gave a low yield



## Green Context

The development of alternative solvent systems to replace VOCs and of heterogenised catalysts to replace soluble acids and bases have been two of the most widely studied areas in the context of green chemistry. It is clear however, that it will be a combination of cleaner technologies that will often be required to make a technically viable step change in manufacturing methods. Here a non-volatile ionic liquid solvent is successfully combined with a solid base to effect an organic reaction. The solvent-catalyst system is fully recyclable

JHC

**Table 1** 1,4-Addition of citronellal **4** to MVK **5** in [bmim]PF<sub>6</sub><sup>a</sup>

| Entry | Amine (0.2 equiv.) | Time/h    | Yield (%) |
|-------|--------------------|-----------|-----------|
| 1     | —                  | Overnight | 0         |
| 2     | FSM16 <sup>b</sup> | Overnight | 20        |
| 3     | NMAP <sup>c</sup>  | 4         | 62        |
| 4     | DEA                | 2         | 71        |
| 5     | DEATMS             | 2         | 85        |

<sup>a</sup> Reaction was carried out at 80 °C under nitrogen. <sup>b</sup> Nitrogen content per gram of the support was 0.5 mmol g<sup>-1</sup>. <sup>c</sup> Nitrogen content per gram of the support was 0.8 mmol g<sup>-1</sup>.

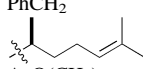
(entry 2), the reaction catalyzed by NMAP provided a satisfactory result (entry 3). The yield was improved further when DEA or DEATMS was used (entries 4 and 5).

The reaction was applied to the several other aldehydes to expand the generality of the reaction conditions. Though DEATMS gave a higher yield in the reaction of citronellal **4** (Table 1, entry 5), reaction with other aldehydes gave by-products resulting in lower yields. Then, DEA was used for further reactions and results are compiled in Table 2, in which yields are comparable to the reaction in THF or toluene.<sup>6</sup> It is noteworthy that the low volatility of [bmim]PF<sub>6</sub> enabled direct isolation of the products by bulb-to-bulb distillation under reduced pressure as shown in entries 1 and 2. The reaction conditions were so mild that acid- or base-sensitive protecting groups survived under the reaction conditions as shown in entries 5 to 7. In spite of the volatile nature of DEA, the reaction was carried out simply in test tube with a rubber septum. The sealed tube technique used was no different from the previous experiments<sup>6</sup> in organic solvents.

The utility of the ionic liquid was further exemplified by employing the additional Michael acceptors as shown in Table 3. Though yields were rather modest, a variety of 1,4-addition products of unmodified aldehydes were obtained.

Then, recycling of the ionic liquid as a solvent was investigated to give reproducible yields as shown in Table 4. In this case DEA was freshly added for each recycle. Purification

**Table 2** 1,4-Addition of representative aldehydes to MVK **5**<sup>a</sup>

| Entry | <b>1</b> (R)  | <b>3</b> Yield (%)   |
|-------|---|----------------------|
| 1     | <i>i</i> -Pr  | 50 <sup>b</sup>      |
| 2     | CH <sub>3</sub> (CH <sub>2</sub> ) <sub>7</sub>                                     | 61 (58) <sup>b</sup> |
| 3     | PhCH <sub>2</sub>   | 60                   |
| 4     |  | 71                   |
| 5     | AcO(CH <sub>2</sub> ) <sub>8</sub>  | 56                   |
| 6     | THPO(CH <sub>2</sub> ) <sub>8</sub>   | 68                   |
| 7     | TBMSO(CH <sub>2</sub> ) <sub>8</sub>  | 75                   |

<sup>a</sup> Reaction was carried out with 0.2 equiv. of DEA at 80 °C for 1–3 h.

<sup>b</sup> Product was distilled directly from [bmim]PF<sub>6</sub> *in vacuo*.

**Table 3** 1,4-Addition with other Michael acceptors<sup>a</sup>

| Entry          | Aldehyde <b>1</b>    | Acceptor <b>2</b>                      | Time/h | Yield of <b>3</b> (%) |
|----------------|----------------------|--|--------|-----------------------|
| 1              | Citronellal <b>4</b> | Acrylonitrile                          | 18.5   | 16                    |
| 2              | Citronellal <b>4</b> | 4-Penten-3-one                         | 9      | 74                    |
| 3 <sup>b</sup> | Decanal              | 4-Penten-3-one                         | 4      | 43                    |
| 4              | Decanal              | Nitrostyrene                           | 3      | 45                    |
| 5 <sup>c</sup> | Decanal              | 2-Methylenecycloheptanone <sup>d</sup> | 29     | 37                    |

<sup>a</sup> Reaction was carried out with 0.2 equiv. of DEA at 80 °C. <sup>b</sup> Reaction was carried out with 0.2 equiv. of NMAP. <sup>c</sup> Reaction was carried out with 2.4 equiv. of DEATMS at room temperature. <sup>d</sup> Generated *in situ* by treatment of 2-mesyloxymethylcycloheptanone with DEATMS.

**Table 4** Recycling of [bmim]PF<sub>6</sub> in 1,4-addition of citronellal **4** to MVK **5**<sup>a</sup>

| Cycle | Yield (%) |
|-------|-----------|
| 1     | 62        |
| 2     | 65        |
| 3     | 68        |
| 4     | 70        |
| 5     | 71        |

<sup>a</sup> Reaction was carried out at 80 °C for 4 h; each time 0.2 equiv. of fresh DEA was added.

**Table 5** Recycling of the catalyst system in 1,4-addition of citronellal **4**<sup>a</sup>

| Cycle | Yield (%) |
|-------|-----------|
| 1     | 49        |
| 2     | 46        |
| 3     | 59        |
| 4     | 57        |

<sup>a</sup> Reaction was carried out with 0.2 equiv. of NMAP at 80 °C for 4 h in [bmim]PF<sub>6</sub>.

of [bmim]PF<sub>6</sub> such as washing with water or drying by evacuation was not required.

Since successful recycling of the ionic liquid had been confirmed, our attention then focused on recycling both the amine catalyst and the ionic liquid, by employing a secondary amine grafted on silica (NMAP).<sup>10</sup> The 1,4-conjugate addition products were obtained in acceptable yields during several recycles as shown in Table 5. No isolation of the catalyst from the ionic liquid by filtration was required. Neither was activation of the catalyst by washing the suspension with alkaline water needed. Such features along with the simple operation<sup>11</sup> are environmentally important features.

In summary, we have demonstrated an efficient and environmentally benign recyclable method for the 1,4-conjugate addition of unmodified aldehydes **1** to vinylketones **2** to provide 5-ketoaldehydes **3**. The present procedure would be easier to scale up and recycle by employing a secondary amine grafted on silica as the catalyst. This system could find use as a sustainable process.

## Acknowledgements

We thank Sasaki Environmental Technology Foundation for partial financial support.

## Notes and references

- 1 T. Welton, *Chem. Rev.*, 1999, **99**, 2071; P. Wassersheid and W. Keim, *Angew. Chem., Int. Ed.*, 2000, **39**, 3773; R. Sheldon, *Chem. Commun.*, 2001, 2399; C. M. Gordon, *Appl. Catal. A, General*, 2001, **222**, 101.
- 2 P. Duhamel, L. Hennequin, J. M. Poirier, G. Tavel and C. Vottero, *Tetrahedron*, 1986, **42**, 4777.
- 3 G. Stork, A. Brizzolara, H. Landesman, J. Szmuszkovicz and R. Terrell, *J. Am. Chem. Soc.*, 1963, **85**, 207; M. Brown, *J. Org. Chem.*, 1968, **33**, 162.
- 4 H. Hagiwara, N. Komatsubara, H. Ono, T. Okabe, T. Hoshi, T. Suzuki, M. Ando and M. Kato, *J. Chem. Soc., Perkin Trans. 1*, 2001, 316.
- 5 H. Hagiwara, N. Komatsubara, T. Hoshi, T. Suzuki and M. Ando, *Tetrahedron Lett.*, 1999, **40**, 1523; H. Hagiwara, H. Ono, N. Komatsubara, T. Hoshi, T. Suzuki and M. Ando, *Tetrahedron Lett.*, 1999, **40**, 6627.

- 6 H. Hagiwara, T. Okabe, K. Hakoda, T. Hoshi, H. Ono, V. P. Kamat, T. Suzuki and M. Ando, *Tetrahedron Lett.*, 2001, **42**, 2705.
- 7 H. Hagiwara, Y. Shimizu, T. Hoshi, T. Suzuki, M. Ando, K. Ohkubo and C. Yokoyama, *Tetrahedron Lett.*, 2001, **42**, 4349.
- 8 H. Hagiwara, T. Okabe, H. Ono, V. P. Kamat, T. Hoshi, T. Suzuki and M. Ando, *J. Chem. Soc., Perkin Trans. 1*, 2002, 895.
- 9 S. Inagaki, Y. Fukushima and K. Kuroda, *J. Chem. Soc., Chem. Commun.*, 1993, 680.
- 10 A. Cauvel, G. Renard and D. Brunel, *J. Org. Chem.*, 1997, **62**, 749; D. J. Macquarrie, J. H. Clark, A. Lambert, J. E. G. Mdoe and A. Priest, *React. Funct. Polym.*, 1997, **35**, 153.
- 11 *Typical experimental procedure*: a solution of citronellal **4** (181  $\mu\text{L}$ , 1 mmol), 3-penten-2-one **5** (125  $\mu\text{L}$ , 1.5 mmol) and NMAP (200 mg, 0.8 mmol  $\text{g}^{-1}$ , 0.16 mmol) in [bmim]PF<sub>6</sub> (1 mL) was stirred at 80 °C for 2 h under nitrogen atmosphere. The product was extracted 15 times with diethyl ether by vigorous stirring followed by decantation of the upper ether layer. Evaporation of the combined organic layers and subsequent medium pressure LC purification of the residue (eluent: AcOEt–*n*-hexane = 1:3) afforded the 5-ketoaldehyde **6** (110 mg, 49%) as a mixture of 1:1 diastereomers. The ionic liquid layer was heated at 80 °C for 1 h before subsequent re-use.





# Microwave-enhanced tritium–hydrogen exchange: application to radioactive waste reduction

John R. Jones,<sup>\*a</sup> Paul B. Langham<sup>b</sup> and Shui-Yu Lu<sup>a</sup>

<sup>a</sup> Department of Chemistry, School of Physics and Chemistry, University of Surrey, Guildford, Surrey, UK GU2 7XH. E-mail: J.R.Jones@surrey.ac.uk

<sup>b</sup> AWE plc, Aldermaston, Reading, Berkshire, UK RG7 4PR

Received 30th April 2002

First published as an Advance Article on the web 15th August 2002

A microwave-enhanced, Raney nickel catalysed, tritium–hydrogen exchange procedure has been developed with considerable potential in the radioactive waste reduction area, as exemplified by the detritiation of a commercial oil.

## Introduction

The growth in the use of tritium labelled compounds in recent years has been accompanied by an increasing appreciation of the need to devise new and improved tritiation procedures which lead to better isotopic incorporation (compounds of higher specific activity) and the production of less radioactive waste.<sup>1</sup> Microwave-enhanced procedures provide such opportunities and all of the main tritiation procedures (hydrogen isotope exchange, hydrogenation, borohydride reduction and aromatic dehalogenation) with the exception of methylation reactions have benefited from this particular development.<sup>2–7</sup> New, more stringent, radioactive waste legislation, together with the increased costs associated with the storage and removal of radioactive material points to the need for progress to be also made in this area and here we report on such a development.

Of the above mentioned reactions only hydrogen isotope exchange is truly reversible<sup>8</sup> and it seemed sensible therefore to take advantage of this opportunity and investigate whether the benefits of microwave irradiation as previously observed for H/T exchange could also be observed for T/H exchange. Carrying out the reactions in a good microwave solvent with exchangeable hydrogens such as H<sub>2</sub>O makes it possible for a tritiated compound or mixture of compounds to be ‘decontaminated’ and the HTO formed used in further tritiation studies, even if it is at a reduced specific radioactivity. If the latter requirements are not too demanding the whole labelling/detritiation cycle can be repeated several times, thereby making much better use of the tritiated water.

In deciding on which compound/mixture to use we benefited from the experience gained in two previous studies, one dealing with shale oils<sup>9</sup> and the other with engine basestocks.<sup>10</sup> In both cases the <sup>3</sup>H and <sup>1</sup>H NMR spectra of the oils are deceptively simple, each signifying a preponderance of aliphatic CH<sub>2</sub> and CH<sub>3</sub> groups, both of which are difficult to exchange when present in unactivated positions. The harsh tritiation conditions—metal-catalysed H/T exchange at high temperature for extended periods of time—gave good isotopic incorporation and radio-gas chromatography studies revealed the complex nature of the mixtures.

Of the three oils used in the present study two had been exposed to a harsh tritium rich environment for a considerable time and had a level of radioactivity in the 2.1–2.2 KBq mg<sup>-1</sup> range. The inactive oil, as represented by its <sup>1</sup>H NMR spectrum, had an identical composition and was tritiated using a Raney nickel catalysed procedure to generate a radioactive model

compound. The combination of microwave irradiation and parallel exchange procedures<sup>11</sup> showed, very quickly, that this particular catalyst was the best for inducing H/T exchange in such a mixture.

## Experimental

An inactive oil sample (Oil-1) and two radioactive oils (Oil-2A and Oil-2B) were supplied by AWE plc. Other chemicals were used as supplied without further treatment or purification. NMR spectra were recorded on a Bruker AC300 spectrometer. Liquid scintillation counting was performed using a Packard Tri-Carb 1500 liquid scintillation analyser. The microwave oven was a Matsui 169BT (750 W) multimode unit.

Our customary tritiation procedures are dictated by safety and radiochemical considerations and invariably involve preliminary deuterium studies under thermal and/or microwave-enhanced conditions prior to performing the corresponding tritiations. Only details of the tritiations are reported here.

### Tritiation of Oil-1 by thermal heating

Oil-1 (1.1 g) was placed in a 5 cm<sup>3</sup> Pyrex glass tube containing Raney nickel (ethanol washed, 869 mg), followed by tritiated water (15 μl, specific activity 185 GBq cm<sup>-3</sup>). The contents were frozen in liquid nitrogen and the tube evacuated, and then flame sealed. The contents were heated at 120 °C for 48 h. After cooling the tritiated oil was taken up in diethyl ether (30 cm<sup>3</sup>). The organic layer was washed with water (3 × 5 cm<sup>3</sup>), and dried

## Green Context

Isotopic labelling is an increasingly valuable methodology but it also requires a particularly high level of application of the principles of green chemistry. High cost and particularly demanding safety requirements mean that both very efficient and very low-waste synthesis is needed. Then, very efficient removal of the isotope will be required ideally in a truly recyclable way via a suitable transfer agent. Here, the combination of these requirements is demonstrated for T/H exchange to follow original H/T exchange with the transfer agent being the highly recyclable HTO

JHC

over anhydrous  $\text{Na}_2\text{SO}_4$ . Removal of solvent afforded the tritiated oil (1.1 g). Liquid scintillation counting in Ecosint A scintillator showed that a total of 164 MBq of radioactive oil had been produced, equating to  $149 \text{ KBq mg}^{-1}$ . The  $^3\text{H}$  NMR spectrum ( $^1\text{H}$  decoupled) of  $^3\text{H}$ -Oil-1 was recorded in  $\text{CDCl}_3$ .

### Detritiation of $^3\text{H}$ -labelled oil by thermal heating

Typically, a Pyrex tube containing  $^3\text{H}$ -Oil-1 (15.2 mg), Raney nickel (50 mg) and  $\text{H}_2\text{O}$  (80  $\mu\text{l}$ ) was frozen in liquid nitrogen, evacuated, and then flame sealed. The contents were heated at a predetermined temperature (*e.g.* 180  $^\circ\text{C}$ ) for a fixed time (*e.g.* 48 h). After cooling and opening the tube the oil was taken up in diethyl ether (15  $\text{cm}^3$ ). The ether layer was washed with water ( $3 \times 5 \text{ cm}^3$ ) and dried over anhydrous  $\text{Na}_2\text{SO}_4$ . Removal of solvent using a rotary evaporator afforded the detritiated oil (14.8 mg). The radioactivity was determined by liquid scintillation counting. Similar experiments were performed at different temperatures and for various times.

### Detritiation of $^3\text{H}$ -labelled oil by a microwave-enhanced procedure

Typically, a mixture of  $^3\text{H}$ -Oil-1 (9.7 mg), water (150  $\mu\text{l}$ ) and Raney nickel (40 mg) was placed in an pear-shaped glass flask (25  $\text{cm}^3$ ) fitted with a silicone rubber septum disc as a pressure release device. The contents were kept over  $\text{N}_2$ . The vessel was then irradiated in the microwave oven at power level 1 for 5 pulses, each pulse lasting 2 min. After cooling the oil was extracted into diethyl ether (10  $\text{cm}^3$ ). The organic layer was washed with water ( $3 \times 10 \text{ cm}^3$ ) and dried over anhydrous  $\text{Na}_2\text{SO}_4$ . Removal of the solvent using a rotary evaporator afforded the detritiated oil (9.3 mg). Similar experiments were performed using different pulse sequences.

## Results and discussion

The  $^1\text{H}$  NMR,  $^{13}\text{C}$  NMR and  $^{13}\text{C}$  DEPT-135 NMR spectra of Oil-1 in  $\text{CDCl}_3$  are shown in Fig. 1. The  $^1\text{H}$  NMR spectrum shows signals characteristic of aliphatic chains, but no sign of either aromatic or unsaturated presence. Terminal and branched methyl hydrogens ( $-\text{CH}_3$ ,  $\delta < 1 \text{ ppm}$ ), methylene hydrogens in straight or branched hydrocarbon chains ( $-\text{CH}_2-$ ,  $\delta 1.2\text{--}1.3 \text{ ppm}$ ), and cyclic methylene hydrogens ( $\delta 1.1\text{--}1.8 \text{ ppm}$ ) are among the most important contributions. There are also signs of methine hydrogens ( $-\text{CHR}-$ ,  $\delta 1.6\text{--}2.0 \text{ ppm}$ ) and hydrogens attached to carbons connected to other elements (O, N,  $\delta 2.0\text{--}2.5 \text{ ppm}$ ) being present, but the concentrations of these hydrogens are far lower than for the other hydrogens. The  $^{13}\text{C}$  NMR spectrum contains more than two dozen discernible signals. The DEPT-135 spectrum differentiates the methyl and methine protons (positive) from the methylene protons (negative). Essentially the  $^{13}\text{C}$  NMR analysis supports the information obtained from the  $^1\text{H}$  NMR spectra.

The  $^1\text{H}$  NMR spectrum of a tritiated oil (Fig 2(A)) is essentially the same as that of the unlabelled version (Fig. 1(A)) as the percentage tritium incorporation is low as a consequence of the low specific activity of the tritiated water used. This is one of the main differences from the deuterium work where the high percentage deuterium incorporation leads to important changes in the  $^1\text{H}$  NMR spectrum.

The  $^3\text{H}$  ( $^1\text{H}$  decoupled) NMR spectrum shows that the tritium has been incorporated randomly in all positions in the complex oil mixture. The broader than usual signals, which were also observed for the oil shale<sup>9</sup> and engine basestock,<sup>10</sup> are characteristic of randomly tritiated polymer chains.

The thermal detritiation of the oils (Table 1) requires elevated temperatures over an extended period of time, consistent with the conditions required for the tritiation of Oil-1. The marked improvement in detritiation efficiency when using microwave irradiation is immediately apparent—what required between 48 and 66 h under thermal conditions was now achieved in 10 min, representing  $\sim 97\%$  saving in time.

Further improvements in detritiation efficiency can be achieved by increasing the water/oil ratio (Fig. 3) but this has

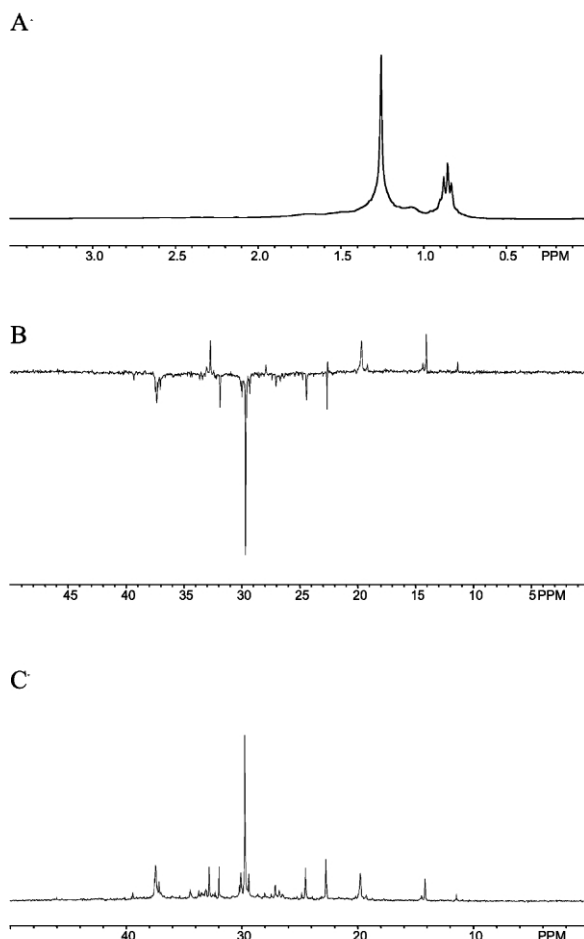


Fig. 1  $^1\text{H}$  (A),  $^{13}\text{C}$  DEPT (B) and  $^{13}\text{C}$  (C) NMR spectra of untreated Oil-1 in  $\text{CDCl}_3$

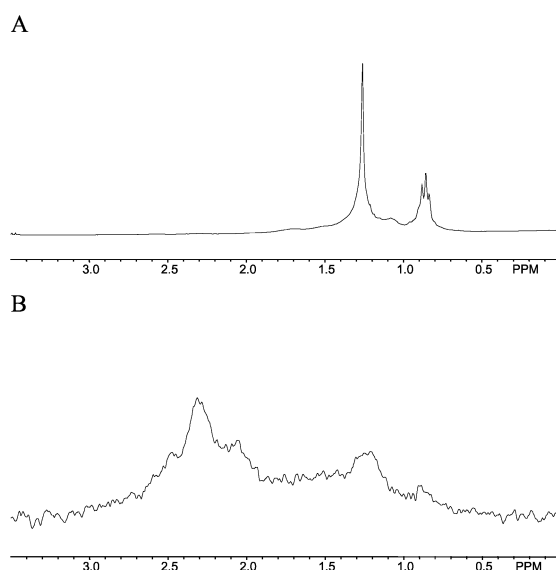


Fig. 2  $^1\text{H}$  (A) and  $^3\text{H}$  ( $^1\text{H}$  decoupled) NMR (B) spectra of  $^3\text{H}$ -Oil-1B.

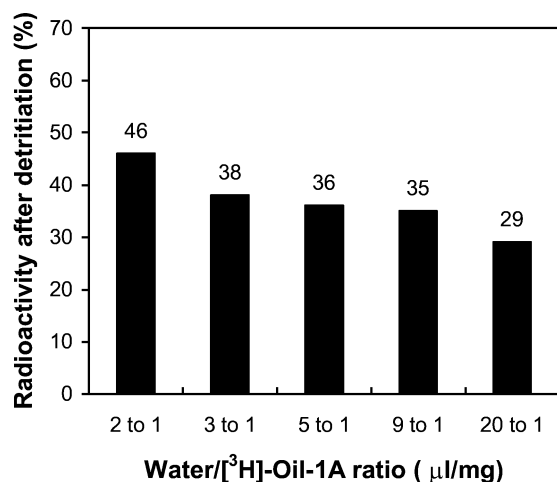
the potentially adverse effect of decreasing the specific activity of the tritiated water formed, which may be used for further tritiation studies.

Finally, the detritiation can be taken to complete either by (a) increasing the temperature (Fig 4) or (b) by separating the oil from the tritiated water formed and repeating the experiment, preferably under microwave-enhanced conditions. Whilst the present studies have been performed using low volumes of reactants the development of new instrumentation and, particularly flow systems, will greatly increase the attractions of emerging microwave-enhanced technologies.

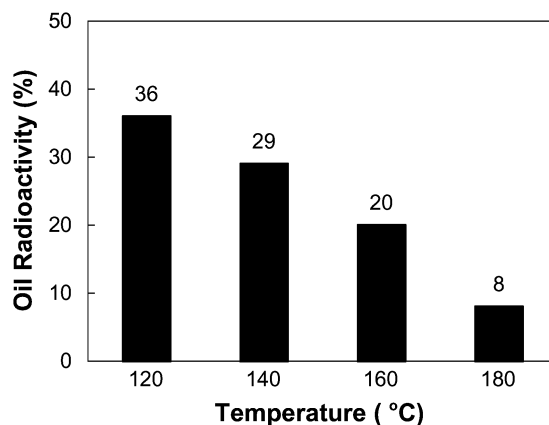
**Table 1** Detritiation results

| [ <sup>3</sup> H]-Oil | Original radioactivity/<br>kBq mg <sup>-1</sup> | Thermal detritiation |        | Microwave detritiation <sup>a</sup> |          |
|-----------------------|---|----------------------|--------|-------------------------------------|----------|
|                       |   | Detritiation %       | Time/h | Detritiation %                      | Time/min |
| <b>1A</b>             | 149   | 62 <sup>b</sup>      | 48     | 60                                  | 5 × 2    |
| <b>1B</b>             | 1128  | 89 <sup>c</sup>      | 48     | 87                                  | 5 × 2    |
| <b>2A</b>             | 2.1   | 60 <sup>c</sup>      | 66     | 43                                  | 5 × 2    |
| <b>2B</b>             | 2.2   | 70 <sup>c</sup>      | 66     | 71                                  | 5 × 2    |

<sup>a</sup> Microwave power set at level I (25%). <sup>b</sup> At 120 °C. <sup>c</sup> At 180 °C.



**Fig. 3** Graphical representation of detritiation efficiency as a function of water/[<sup>3</sup>H]-Oil-1A ratio (standard thermal heating procedure at 120 °C, time = 48 h).



**Fig. 4** Graphical representation of detritiation efficiency as a function of temperature (standard thermal heating procedure, fixed time of 48 h).

## Acknowledgement

We are grateful to AWE plc, Aldermaston for financial support.

## References

- 1 M. Saljoughian and P. G. Williams, *Curr. Pharm. Des.*, 2000, **6**, 1029.
- 2 J. R. Jones, W. J. S. Lockley, S. Y. Lu and S. P. Thompson, *Tetrahedron Lett.*, 2001, **42**, 331.
- 3 N. Elander, S. Stone-Elander, J. R. Jones and S. Y. Lu, *Chem. Soc. Rev.*, 2000, **29**, 239.
- 4 T. Grobosch, L. Frederiksen, J. R. Jones, S. Y. Lu and C. C. Zhao, *J. Chem. Res. (S)*, 2000, 42.
- 5 S. Anto, G. S. Getvoldsen, J. R. Harding, J. R. Jones, S. Y. Lu and J. C. Russell, *J. Chem. Soc., Perkin Trans. 2*, 2000, 2208.
- 6 W. T. Erb, J. R. Jones and S. Y. Lu, *J. Chem. Res. (S)*, 1999, 728.
- 7 J. M. Barthez, A. V. Filikov, L. B. Frederiksen, M. L. Huguet, J. R. Jones and S. Y. Lu, *Can. J. Chem.*, 1998, **76**, 726.
- 8 J. R. Jones, *Isotopes: Essential Chemistry and Applications, II*, The Royal Society of Chemistry, London, 1988.
- 9 L. Carroll, J. R. Jones and P. Shore, *J. Labelled Compd. Radiopharm.*, 1986, **24**, 763.
- 10 D. S. Farrier, J. R. Jones, J. P. Bloxidge, J. A. Elvidge and M. Saieed, *J. Labelled Compd. Radiopharm.*, 1982, **19**, 213.
- 11 J. R. Jones and S. Y. Lu, unpublished results.



# Synthesis of dimethyl carbonate using CO<sub>2</sub> and methanol: enhancing the conversion by controlling the phase behavior

Zhenshan Hou, Buxing Han,\* Zhimin Liu,\* Tao Jiang and Guanying Yang

Center for Molecular Science, Institute of Chemistry, The Chinese Academy of Sciences, Beijing 100080, China. E-mail: Hanbx@infoc3.icas.ac.cn

Received 27th March 2002

First published as an Advance Article on the web 4th September 2002

The critical parameters and phase behavior of the multi-component system CO<sub>2</sub>-CH<sub>3</sub>OH-CH<sub>3</sub>I-H<sub>2</sub>O-CH<sub>3</sub>OC(O)OCH<sub>3</sub> (dimethyl carbonate, DMC) were determined. The concentrations of the components were selected in such a way that they simulated the compositions of the reaction system at different conversions for synthesizing DMC using CO<sub>2</sub> and methanol in a batch reactor. The critical density of the reaction system decreases with the conversion of methanol. The critical temperature and critical pressure of the reaction system increase with the conversion. Based on the determined critical parameters and phase behavior, DMC synthesis using CO<sub>2</sub> and methanol was run at various pressures that corresponded to conditions in the two-phase region, the critical region as well as the single-phase supercritical region. The original ratios of the reactants CO<sub>2</sub>:CH<sub>3</sub>OH were 8:2 and 7:3, and the corresponding reaction temperatures were 353.2 and 393.2 K, respectively, which were slightly higher than the critical temperatures of the reaction systems. The results indicate that the phase behavior affects the equilibrium conversion of methanol significantly and the conversion reaches a maximum in the critical regions of the reaction system. At 353.2 K, the equilibrium conversion in the critical region is about 7%, and can be about three times as large as those in other phase regions. At 393.15 K, the equilibrium conversion in the critical region is also much higher and can be twice as large as those in other phase regions.

## Introduction

Development of environmentally benign industrial processes utilizing carbon dioxide, which is a cheap and safe C<sub>1</sub> resource as well as a nontoxic reaction medium, has received much interest.<sup>1-5</sup> One of the most attractive reactions is the synthesis of dimethyl carbonate (DMC) from CO<sub>2</sub> and methanol. The reaction is reversible and can be expressed by eqn. (1):



Some compounds, such as Bu<sub>2</sub>Sn(OMe)<sub>2</sub>, phosphoric acid on zirconia, and potassium carbonate, have been employed as catalysts for the one-step synthesis process.<sup>6-9</sup> In these studies, it was doubtful in which phase region the reaction took place because the critical parameters and the phase behavior were not studied at the experimental conditions. For this reaction, the main problem is the low conversion because of thermodynamic limitation. How to increase the methanol conversion is a challenging problem.

In recent years, increasing numbers of chemists have begun to study reaction chemistry in supercritical fluids (SCFs).<sup>10-18</sup> There are some unique advantages in conducting chemical reactions in SCFs, such as the conversion and selectivity may be tuned by pressure.<sup>18</sup> In recent years, many papers concerning chemical reactions in SCFs have been published, including review papers.<sup>19-22</sup> Most reaction systems are complex mixtures and the compositions change with conversion. Conducting a reaction at supercritical conditions means that the reaction system should be in the supercritical state. Thus, how to control the reaction system at the supercritical state is a crucial question, and critical parameters and the related phase equilibrium data require clarification.

The study of phase equilibrium and critical parameters is a long established field.<sup>23-28</sup> However, nearly all studies were restricted to mixtures of less than three components, and were not for reaction systems. As discussed above, reaction mixtures

differ from those which are normally studied because their chemical composition changes with reaction time. Hence, their critical parameters and phase behavior change with reaction conversion. Researchers often approximately assume that the reactions take place under supercritical condition when the reaction temperature and pressure are higher than the critical temperature and critical pressure of the solvent (or the main component) because the related phase behavior data are not available. This assumption is reasonable when the concentrations of the reactants or the products are very low. However, the critical parameters of a reaction system may differ from those of the solvent significantly when the concentrations of the reactants and the products are large enough. In practice, most reaction systems contain more than three components and the concentrations of the reactants and the products are not low during the reaction processes. Thus, the related phase behavior is a key for exploring the advantages of the reactions under supercritical conditions. Recently, several articles have been published to discuss the phase behavior and critical parameters in reaction processes.<sup>29-32</sup>

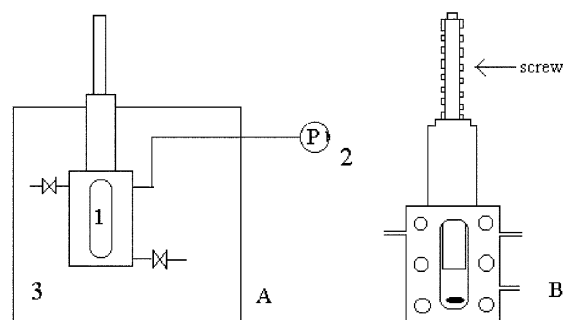
Phase behavior is directly related with intermolecular interactions, which may influence the conversion and selectivity of the reactions. Tuning the conversion or selectivity of chemical reactions by controlling the phase behavior is an

## Green Context

The use of dimethyl carbonate as a reagent is becoming more popular. This paper deals with its synthesis from the methanol and carbon dioxide, and seeks to answer some questions relating to the phase behaviour during synthesis. Control over phase behaviour is shown to have a significant impact on the progress of the reaction

DJM

interesting research area, especially near the critical points of reaction systems. In this work, we carry out the first study on critical parameters and the phase behavior of the reaction system for DMC synthesis using  $\text{CO}_2$  and methanol, and then reactions are studied in the two-phase region, and in the supercritical region. This work aims at three questions. First, how the critical parameters and phase behavior of the reaction system change with conversion of the reactants; second, how the critical parameters and phase behavior of the reaction system affect the equilibrium conversion of methanol; finally, how the desiccant affects the conversion of the reaction in different phase regions. A schematic diagram of the apparatus to measure the phase behavior and critical points of the reaction system is shown in Fig. 1.

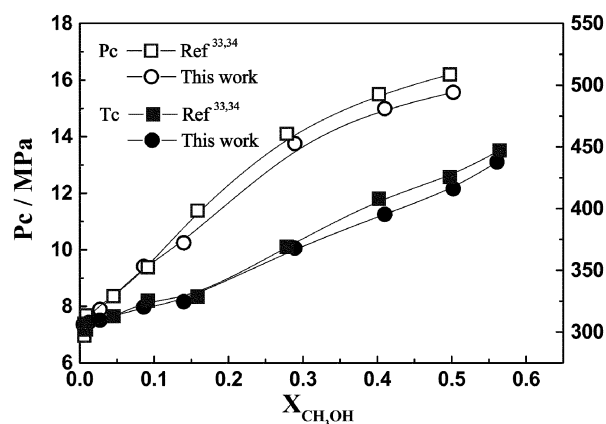


**Fig. 1** (A) Schematic diagram of the apparatus to measure the phase behavior and critical points. 1. High-pressure optical cell (shown in detail in (B)); 2. pressure sensor; 3. constant temperature air bath.

## Results and discussion

### Phase equilibria of the reaction system

The critical parameters of  $\text{CO}_2$ - $\text{CH}_3\text{OH}$  binary system were first determined, and the data agreed reasonably with those reported by Brunner *et al.*<sup>33,34</sup> which is shown in Fig. 2. Then, we determined the critical parameters and phase behavior of the reaction system for synthesizing DMC from  $\text{CO}_2$  and methanol by simulating the compositions of the reaction system at different methanol conversions in the absence of catalyst.  $\text{CH}_3\text{I}$  was used as promoting agent. Thus, for the phase behavior study, there were three components in the reaction system before reaction,  $\text{CO}_2$ ,  $\text{CH}_3\text{OH}$ , and  $\text{CH}_3\text{I}$ , and there were five components during the reaction process,  $\text{CO}_2$ ,  $\text{CH}_3\text{OH}$ ,  $\text{CH}_3\text{I}$ , DMC and  $\text{H}_2\text{O}$ . The composition of the reaction system was a function of the original molar ratio (before reaction)

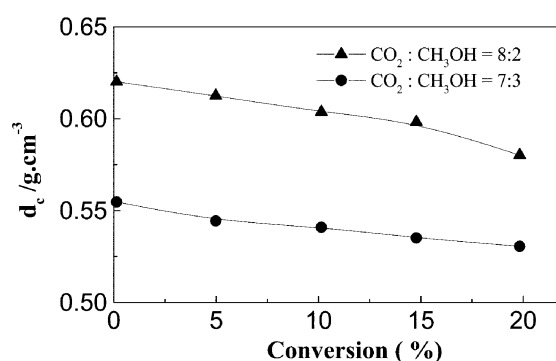


**Fig. 2** The dependence of critical temperature and critical pressure on the mole fraction of methanol for the  $\text{CO}_2$ - $\text{CH}_3\text{OH}$  binary system.

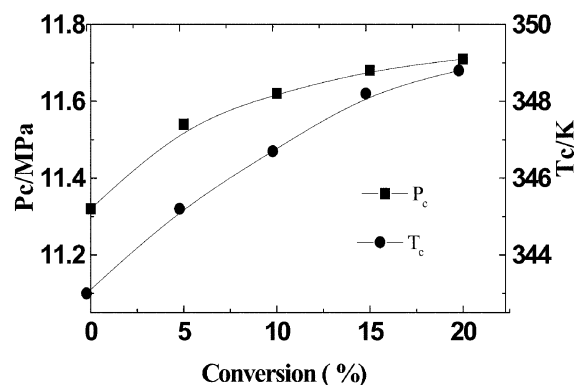
$\text{CO}_2$ : $\text{CH}_3\text{OH}$ : $\text{CH}_3\text{I}$  and the conversion of methanol. In other words, the composition of the reaction system at a fixed original ratio could be easily calculated based on methanol conversion, and thus the phase behavior and critical parameters at the methanol conversion could be determined by preparing the mixtures using the pure chemicals.

Figs. 3–5 show the dependence of the critical temperature, critical pressure and critical density of the reaction system on methanol conversion, for original molar ratios  $\text{CO}_2$ : $\text{CH}_3\text{OH}$ : $\text{CH}_3\text{I} = 8:2:0.25$  and  $7:3:0.36$ , respectively. The data are also listed in Table 1. It is estimated that the accuracies of  $T_c$ ,  $P_c$  and  $d_c$  values are  $\pm 0.5$  K,  $\pm 0.05$  MPa, and  $\pm 0.003$   $\text{g}\cdot\text{cm}^{-3}$ , respectively.

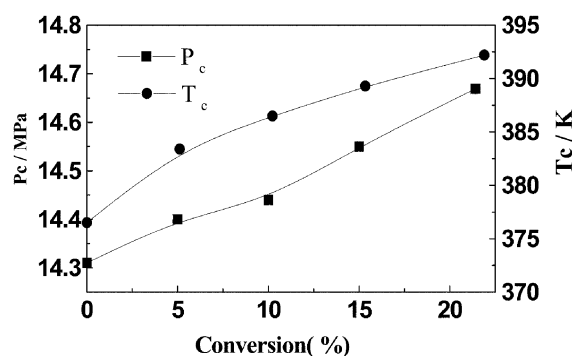
Fig. 3 illustrates that the critical density of the reaction system decreases slightly with increasing methanol conversion for both original ratios of the reactants. At and above the critical temperature, pressure and density of a mixture it becomes homogeneous. Both critical temperature and critical pressure increase with methanol conversion, as shown in Fig. 4 and 5.



**Fig. 3** Effect of methanol conversion on the critical density ( $d_c$ ) at different initial ratios of  $\text{CO}_2$  to  $\text{CH}_3\text{OH}$



**Fig. 4** The effect of methanol conversion on the critical properties of the reaction system at an initial ratio  $\text{CO}_2$ : $\text{CH}_3\text{OH} = 8:2$ .



**Fig. 5** The effect of methanol conversion on the critical properties of reaction system at an initial ratio  $\text{CO}_2$ : $\text{CH}_3\text{OH} = 7:3$ .

The reaction experiments were also conducted at these two original ratios of the reactants and data in Fig. 3–5 allowed us to choose suitable reaction conditions, where the reaction system existed in two-phase and supercritical regions at equilibrium.

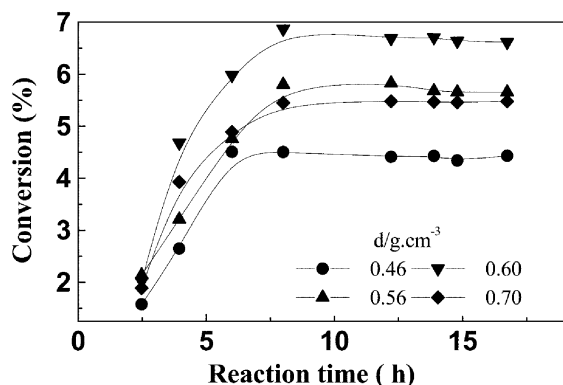
### Synthesis of DMC in different phase regions

The reactions were carried out at temperatures slightly above the critical temperatures of the reaction system in the pressure range from the two-phase region to supercritical region, *i.e.*, the apparent density varied from much less than the critical density to higher than the critical density. This allowed us to study how the phase behavior affects the conversion. Experiments illustrated that the amount of the by-products was negligible.

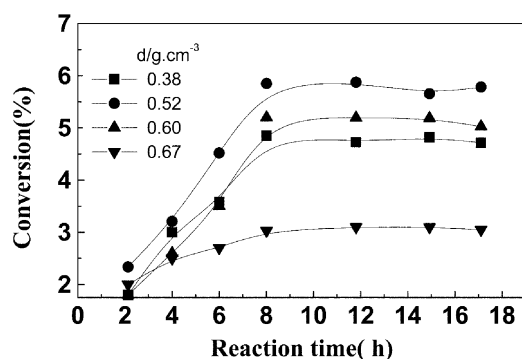
Figs. 6 and 7 show methanol conversion as a function of reaction time at an original ratio  $\text{CO}_2:\text{CH}_3\text{OH}:\text{CH}_3\text{I} = 8:2:0.25$  and  $\text{CO}_2:\text{CH}_3\text{OH}:\text{CH}_3\text{I} = 7:3:0.36$  at some typical apparent densities, and the reaction temperatures are 353.2 and 393.2 K, respectively. The original molar ratios of

**Table 1** The critical parameters of reaction mixtures at different methanol conversions and initial molar ratios  $\text{CO}_2:\text{CH}_3\text{OH} = 8:2$  and  $7:3$

|  | Conversion (%) | $P_c/\text{MPa}$ | $T_c/\text{K}$ | $d_c/\text{g cm}^{-3}$ |
|--|----------------|------------------|----------------|------------------------|
| $\text{CO}_2:\text{CH}_3\text{OH} = 8:2$ | 0              | 11.32            | 342.0          | 0.625                  |
|  | 5              | 11.54            | 345.2          | 0.615                  |
|  | 10             | 11.62            | 346.7          | 0.604                  |
|  | 15             | 11.68            | 348.2          | 0.598                  |
|  | 20             | 11.71            | 348.8          | 0.580                  |
| $\text{CO}_2:\text{CH}_3\text{OH} = 7:3$ | 0              | 14.31            | 376.5          | 0.555                  |
|  | 5              | 14.40            | 383.4          | 0.544                  |
|  | 10             | 14.44            | 386.5          | 0.541                  |
|  | 15             | 14.55            | 389.3          | 0.535                  |
|  | 20             | 14.65            | 392.2          | 0.531                  |



**Fig. 6** Plot of methanol conversion vs. reaction time at various apparent densities ( $d$ ) at 353.2 K with initial ratio  $\text{CO}_2:\text{CH}_3\text{OH} = 8:2$ .

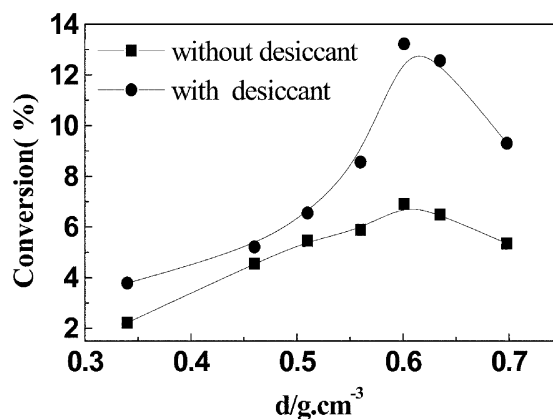


**Fig. 7** Plot of methanol conversion vs. reaction time at various apparent densities ( $d$ ) at 393.2 K with initial ratio  $\text{CO}_2:\text{CH}_3\text{OH} = 7:3$ .

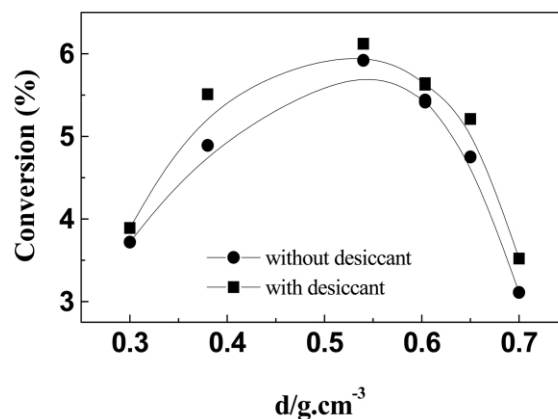
$\text{CH}_3\text{OH}:\text{K}_2\text{CO}_3 = 64:1$ . Obviously, the reaction reaches equilibrium after about 8 h. It is also seen that the reaction rate is faster at the critical density or higher. In the following sections, we use the data for a reaction time of 12 h to discuss the effects of original reactant ratio, apparent density (pressure), and phase behavior on the equilibrium conversion of methanol.

Figs. 8 and 9 show the effect of apparent density on equilibrium methanol conversion at 353.2 K (initial  $\text{CO}_2:\text{CH}_3\text{OH}:\text{CH}_3\text{I} = 8:2:0.25$ ) and 393.2 K (original  $\text{CO}_2:\text{CH}_3\text{OH}:\text{CH}_3\text{I} = 7:3:0.36$ ), respectively. Figs. 3, 8, and 9 indicate that there is a maximum in each conversion vs. apparent density curve, which corresponds to the critical density of the reaction system. In other words, the equilibrium conversion of methanol increases with increasing pressure in the two-phase region, and decreases with increasing pressure in the supercritical region (one phase region). At 393.2 K, the equilibrium conversion near the critical point is also much higher. This can be attributed mainly to the special intermolecular interactions near the critical point. It is very difficult to give a detailed discussion on this, although this is a very interesting and important topic.

The effect of 4A molecular sieves, which behaves as a desiccant (mass ratio of methanol to molecular sieve = 25), on the equilibrium conversion of methanol is investigated, and the results are also shown in Figs 8 and 9. It can be seen that at 353.2 K methanol conversion is enhanced significantly in the presence of molecular sieves, especially in the critical region. This is because the desiccant can absorb the water produced and the chemical equilibrium is shifted. The equilibrium conversion is as high as 13.4% near the critical point. However, at 393.2 K the effect of the desiccant on the conversion is much smaller. One



**Fig. 8** Plot of equilibrium conversion of methanol vs. apparent density ( $d$ ) at 353.2 K at an initial ratio  $\text{CO}_2:\text{CH}_3\text{OH} = 8:2$ .



**Fig. 9** The relationship between apparent density ( $d$ ) and equilibrium conversion of methanol at 393.2 K with initial ratio  $\text{CO}_2:\text{CH}_3\text{OH} = 7:3$ .

of the reasons may be that the ability of the molecular sieve to absorb water is weaker at the higher temperature.

## Experimental

### Materials

Methanol, iodomethane and potassium carbonate were A.R grade reagents produced by Beijing Chemical Reagent Factory. CO<sub>2</sub> was supplied by Beijing Analytical Instrument Factory with a purity of better than 99.95%.

### Apparatus and procedures for phase behavior measurements

The apparatus was similar to that described previously,<sup>35</sup> and is shown schematically in Fig. 1. The apparatus consists of a high-pressure view cell, a constant-temperature air-bath, a high-pressure pump, a pressure gauge and a magnetic stirrer.

The high-pressure view cell was composed of a stainless steel body, a stainless steel piston and two windows. The piston could be moved up and down by the screw, and the volume of the cell could be changed in the range from 20 to 50 cm<sup>3</sup> by moving the piston. The cell was installed in a constant temperature air-bath, which was controlled by a temperature controller (model SX/A-1) made by Beijing Tianchen Electronic Company, and the temperature was measured by accurate mercury thermometers with an accuracy of better than ± 0.1 K. The pressure gauge was composed of a pressure transducer (FOXBORO/ICT) and an indicator, which was accurate to ± 0.025 MPa in the pressure range 0–20 MPa.

The experimental procedure was similar to that described elsewhere.<sup>32</sup> In a typical experiment, the air in the view cell was replaced by CO<sub>2</sub>. A desired amount of liquid chemicals (such as methanol, DMC, H<sub>2</sub>O) were charged into the cell. A suitable amount of CO<sub>2</sub> was then introduced into the cell with a CO<sub>2</sub> sample bomb of 41 ml. The temperature of the air-bath was controlled at a suitable value. The pressure was adjusted by moving the piston in the cell and the system equilibrated for at least 4 h. The phase behavior could be seen through the windows of the cell. The volume of the system was known by the position of the piston, which was calibrated before the experiments. The density of the mixture was calculated on the basis of the masses of all components and the volume of the system. At the critical point of a mixture, strong opalescence can be observed, and the mixture changes from a single phase to about 50 vol% liquid phase and 50 vol% vapor phase as the pressure was reduced slightly.

The catalyst (K<sub>2</sub>CO<sub>3</sub>) was not involved during the phase behavior measurements for two reasons. First, the fluid mixtures cannot dissolve the catalyst (K<sub>2</sub>CO<sub>3</sub>) solid at our experimental conditions, and thus it is not necessary to consider it when studying the phase behavior. Second, the reaction can be avoided in the absence of the catalyst, which is important for the phase behavior measurement.

### Apparatus and procedure of reaction

A batch reactor made of stainless steel with a volume of 23.75 ml was used. The temperature fluctuation of the air bath was ± 0.1 K, which was controlled by a PID temperature controller made by Beijing Tianchen Electronic Company (model SX/A-1).

In a typical experiment, the catalyst (potassium carbonate) was loaded into the reactor. The reactor was purged with CO<sub>2</sub>, then the desired amount of iodomethane and methanol was charged into the reactor by a syringe. A suitable amount of CO<sub>2</sub>

was introduced into the reactor with a CO<sub>2</sub> sample bomb. The molar ratios of methanol to potassium carbonate (CH<sub>3</sub>OH:K<sub>2</sub>CO<sub>3</sub> = 64:1) and the molar ratio of methanol to iodomethane (CH<sub>3</sub>OH:CH<sub>3</sub>I = 8:1) were kept constant for all the experiments. The molar ratio of CO<sub>2</sub> to methanol was chosen to be 8:2 or 7:3. The experiments were performed at different densities by changing the amount of the loaded chemicals. Obviously, the amounts of K<sub>2</sub>CO<sub>3</sub> and CH<sub>3</sub>I in the reaction system were different when the density of the reaction mixture was changed. After all the chemicals had been charged, the reactor was installed in a constant temperature air-bath and the reaction allowed to take place. After the reaction had proceeded for a desired time, the reactor was placed in a freezer at about 250 K for 1 h, and then the CO<sub>2</sub> was released slowly. Experiments showed that the amount of reactants and products entrained by CO<sub>2</sub> was negligible. The mixture in the reactor was analyzed by a gas chromatograph (GC112, Shanghai Analytical Instrument Factory) with a FID detector. In this work, the apparent density is defined as the mass of the fluids in the reactor divided by its volume, and the volume occupied by K<sub>2</sub>CO<sub>3</sub> was taken into account since it was not soluble in the reaction mixture. Obviously, the apparent density was equal to the density of the fluid in the single phase region.

## Acknowledgment

This work was financially supported by the National Natural Science Foundation of China (20073056), National Key Basic Research Project (G2000048010), UK–China R & D Program. The authors are also very grateful to Professor Martyn Poliakoff for his valuable suggestions.

## References

- 1 W. Leitner, *Angew. Chem., Int. Ed. Engl.*, 1995, **34**, 2207.
- 2 A.-A. Shaikh and S. Sivaram, *Chem. Rev.*, 1996, **96**, 951.
- 3 M. E. Paulaitis and G. C. Alexander, *Pure Appl. Chem.*, 1987, **59**, 61.
- 4 C. Vieville, Z. Mouloungui and A. Gaset, *Ind. Eng. Chem. Res.*, 1993, **32**, 2065.
- 5 X. Wu, Y. Oshima and S. Koda, *Chem. Lett.*, 1997, 1045.
- 6 T. Sakakura, J. C. Choi, Y. Saito, T. Masuda, T. Sako and T. Oriyama, *J. Org. Chem.*, 1999, **64**, 4506.
- 7 J. C. Choi, T. Sakakura and T. Sako, *J. Am. Chem. Soc.*, 1999, **121**, 3793.
- 8 K. Tomishige, T. Sakaihori, Y. Ikeda and K. Fujimoto, *Catal. Lett.*, 1999, **58**, 225.
- 9 Y. Ikeda, T. Sakaihori, K. Tomishige and K. Fujimoto, *Catal. Lett.*, 2000, **66**, 59.
- 10 G. Kaupp, *Angew. Chem., Int. Ed.*, 1994, **33**, 1452.
- 11 P. G. Jessop, T. Ikariya and R. Noyori, *Science*, 1995, **269**, 1065.
- 12 P. G. Jessop, Y. Hsiao, T. Ikariya and R. Noyori, *J. Am. Chem. Soc.*, 1996, **118**, 344.
- 13 H. Kawanami and Y. Ikushima, *Chem. Commun.*, 2000, 2089.
- 14 M. G. Hitzler and M. Poliakoff, *Chem. Commun.*, 1997, 1667.
- 15 F. Loeker and W. Leitner, *Chem. Eur. J.*, 2000, **6**, 2011.
- 16 C. Bolm, O. Beckmann and O. A. G. Dabard, *Angew. Chem., Int. Ed.*, 1999, **38**, 907.
- 17 M. J. Burk, S. Feng, M. F. Gross and W. Tumas, *J. Am. Chem. Soc.*, 1995, **117**, 8277.
- 18 C. A. Eckert, B. L. Knutson and P. G. Debenedetti, *Nature*, 1996, **383**, 313.
- 19 O. Kajimoto, *Chem. Rev.*, 1999, **99**, 355.
- 20 J. F. Brennecke and J. E. Chateaufneuf, *Chem. Rev.*, 1999, **99**, 433.
- 21 P. G. Jessop, T. Ikariya and R. Noyori, *Chem. Rev.*, 1999, **99**, 475.
- 22 J. A. Darr and J. M. Poliakoff, *Chem. Rev.*, 1999, **99**, 495.
- 23 C. P. Hicks and C. L. Young, *Chem. Rev.*, 1975, **75**, 119.
- 24 G. M. Schneider, *Pure. Appl. Chem.*, 1983, **55**, 479.
- 25 M. L. McGlashan, *Pure. Appl. Chem.*, 1985, **57**, 89.

- 26 R. J. Sadus, *AICHE. J.*, 1994, **40**, 1376.
- 27 J. S. Rowlinson and F. L. Swinton, *Liquids and Liquids Mixture*, Butterworth, London, 3rd edn., 1982.
- 28 A. Kordikowski, D. G. Robertson, A. I. Aguiar-Ricardo, V. K. Popov, S. M. Howdle and M. Poliakoff, *J. Phys. Chem.*, 1996, **100**, 9522.
- 29 J. Ke, J. B. X. Han, M. W. George, H. K. Yan and M. Poliakoff, *J. Am. Chem. Soc.*, 2001, **123**, 3661.
- 30 B. A. Stradi, J. P. Kohn, M. A. Stadtherr and J. F. Brennecke, *J. Supercrit. Fluids*, 1998, **12**, 109.
- 31 B. A. Stradi, M. A. Stadtherr and J. F. Brennecke, *J. Supercrit. Fluids*, 2001, **20**, 1.
- 32 Z. S. Hou, B. X. Han, X. G. Zhang, H. F. Zhang and Z. M. Liu, *J. Phys. Chem. B*, 2001, **105**, 4510.
- 33 E. Brunner, W. Hultenschmidt and G. Schlichthaerle, *J. Chem. Thermodyn.*, 1987, **19**, 273.
- 34 E. Brunner, *J. Chem. Thermodyn.*, 1985, **17**, 671.
- 35 H. F. Zhang, Z. M. Liu and B. X. Han, *J. Supercrit. Fluids*, 2000, **18**, 185.





# Allylboration of carbonyl compounds in ionic liquids

George W. Kabalka,\* Bollu Venkataiah and Bhaskar C. Das

Departments of Chemistry and Radiology, The University of Tennessee, Knoxville, TN 37996-1600, USA. E-mail: kabalka@utk.edu; Fax: (865)974-2997; Tel: (865)974-3260

Received 30th April 2002

First published as an Advance Article on the web 2nd September 2002

Room-temperature ionic liquids are suitable reaction media for the allylboration of carbonyl compounds. A wide variety of aldehydes and ketones react with allyldiisopropoxyborane in butylmethylimidazolium bromide at room temperature to yield homoallylic alcohols.

## Introduction

In recent years, a number of synthetic methodologies have been developed which utilize room-temperature ionic liquids.<sup>1</sup> These solvents are of growing interest because of their low environmental load (lack of vapour pressure, ease of reuse, and the absence of flammability). Allylboranes react with carbonyl compounds to form homoallylic alcohols<sup>2</sup> which are important intermediates in the synthesis of natural products and in the pharmaceutical industry.<sup>3</sup> Brown *et al.* studied the effect of solvent on the allylation of carbonyl compounds and found that poorly coordinating solvents enhance the rate of allylboration reactions.<sup>2b</sup> Since ionic liquids are poorly coordinating solvents and have been utilized in allylmetal addition reactions,<sup>1a,4</sup> we examined the use of ionic liquids in allylboration reactions. We wish to report the results of our study.

## Results and discussion

In a continuation of our investigation of boron reactions in ionic liquid media,<sup>5</sup> we discovered that butylmethylimidazolium bromide (bmimBr), butylmethylimidazolium tetrafluoroborate (bmimBF<sub>4</sub>), ethylmethylimidazolium tetrafluoroborate (emimBF<sub>4</sub>) and ethyl ammonium nitrate (EAN) are effective media for the allylboration of carbonyl compounds as illustrated for the reactions of benzaldehyde with allyldiisopropoxyborane (Scheme 1 and Table 1).

The reaction of a variety of aromatic aldehydes and ketones with allyldiisopropoxyborane were carried out in bmimBr and

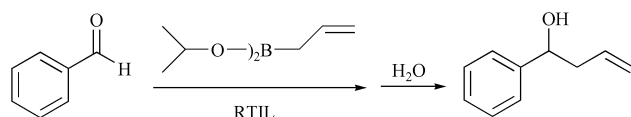
produced high yields of the expected products (Table 2). In a typical experiment, the carbonyl compound is dissolved in the ionic liquid and allyldiisopropoxyborane is added. The reaction mixture becomes homogeneous during the course of the reaction. The product is readily isolated by extraction or distillation and the yields are comparable to reactions carried out in conventional solvents.<sup>2</sup>

Ferrocene carbaldehyde (Table 2, entry 6) affords 1-ferrocenyl-1,3-butadiene<sup>6</sup> which is formed *via* allylation followed by dehydration due to conjugation with ferrocene. 2-Phenylpropionaldehyde (Table 2, entry 7) produces the *syn* diastereomeric product predominantly. The diastereofacial selectivity is greater than that observed in conventional solvents.<sup>2a</sup> The diastereoisomers are readily differentiated using <sup>1</sup>H NMR spectroscopy and the chemical shifts of the methyl groups are identical to the values reported in the literature.<sup>7</sup> It is noteworthy that, after extraction of the products, the ionic liquids can be reused. The NMR spectra of the recovered ionic liquid solvents show no evidence of degradation, and little variation in reaction yield<sup>8</sup> is observed using recovered ionic liquids.

In summary, the allylboration of carbonyl compounds can be successfully conducted in room-temperature ionic liquids.<sup>9</sup> The procedure permits recycling of the solvent without significant loss in activity.

## Experimental

Carbonyl reagents and emimBF<sub>4</sub> were obtained from commercial sources (Aldrich Chemical Co.) and used as received. bmimBr,<sup>10</sup> bmimBF<sub>4</sub>,<sup>10</sup> EAN,<sup>11</sup> and *B*-allyldiisopropoxyborane<sup>2b</sup> were prepared according to literature procedures. The ionic liquids could be recycled after the product was extracted (see below) by dissolving them in ethyl acetate or methylene chloride, drying over anhydrous magnesium sulfate, and evaporating the solvent after filtration.



Scheme 1

**Table 1** Reaction of benzaldehyde with allyldiisopropoxyborane in ionic liquids

| Entry | Ionic liquid        | Isolated yield (%) |
|-------|---------------------|--------------------|
| 1     | bmimBr              | 87                 |
| 2     | bmimBF <sub>4</sub> | 89                 |
| 3     | emimBF <sub>4</sub> | 88                 |
| 4     | EAN                 | 85                 |

## Green Context

The development of a wide range of chemistry in ionic liquids continues. This contribution demonstrates the use and reuse of ionic liquids in the functionalisation of aldehydes and ketones. The transfer of allyl groups to give homoallyl alcohols proceeds smoothly and in very good yield using ionic liquids. Reuse of the solvent is possible. *DJM*

**Table 2** Reaction of carbonyl compounds with allyl diisopropoxyborane in bmimBr

| Entry | Carbonyl compound | Product | Isolated yield (%) |
|-------|-------------------|---------|--------------------|
| 1     |                   |         | 87                 |
| 2     |                   |         | 86                 |
| 3     |                   |         | 86                 |
| 4     |                   |         | 86                 |
| 5     |                   |         | 84                 |
| 6     |                   |         | 82                 |
| 7     |                   |         | 85                 |
| 8     |                   |         | 82                 |
| 9     |                   |         | 83                 |

### General procedure

The carbonyl compound (1 mmol) and bmimBr (300 mg) are placed in a 10 mL round-bottomed flask. Allyl diisopropoxyborane (170 mg, 1 mmol) is added and the mixture stirred at r.t. for 3 h. The mixture is hydrolyzed with water (2 drops) and the product extracted into diethyl ether (3 × 5 mL), the extracts combined, dried (anhydrous MgSO<sub>4</sub>), the solvent removed under reduced pressure, and the product isolated by silica gel column chromatography.

### Acknowledgments

We thank the U.S. Department of Energy and the Robert H. Cole Foundation for financial support of this study.

### References

- (a) T. Welton, *Chem. Rev.*, 1999, **99**, 2071; (b) R. Sheldon, *Chem. Commun.*, 2001, 2399.
- (a) Y. Yamamoto, T. Komatsu and K. Maruyama, *J. Am. Chem. Soc.*, 1984, **106**, 5031; (b) H. C. Brown, U. S. Racherla and P. Pellechia, *J. Org. Chem.*, 1990, **55**, 1868; (c) Z. Wang, X.-J. Meng and G. W. Kabalka, *Tetrahedron Lett.*, 1991, **32**, 1945; (d) Z. Wang, X.-J. Meng and G. W. Kabalka, *Tetrahedron Lett.*, 1991, **32**, 4619; (e) Z. Wang, X.-J. Meng and G. W. Kabalka, *Tetrahedron Lett.*, 1991, **32**, 5677; (f) G. W. Kabalka, C. Narayana and N. K. Reddy, *Tetrahedron Lett.*, 1996, **37**, 2181.
- (a) W. R. Roush, A. D. Palkowitz and K. Ando, *J. Am. Chem. Soc.*, 1990, **112**, 6348; (b) M. V. R. Reddy, J. P. Rearick and P. V. Ramachandran, *Org. Lett.*, 2001, **3**, 19.
- (a) C. M. Gordon and A. McCluskey, *Chem. Commun.*, 1999, 1431; (b) C. M. Gordon and C. Ritchie, *Green Chem.*, 2002, **4**, 124; (c) M. C. Law, K.-Y. Wong and T. H. Chan, *Green Chem.*, 2002, **4**, 161.
- (a) G. W. Kabalka and R. R. Malladi, *Chem. Commun.*, 2000, 2191; (b) G. W. Kabalka and B. Venkataiah, *Tetrahedron Lett.*, 2002, **43**, 3703; (c) R. M. Pagni, G. W. Kabalka, C. Lee, R. R. Malladi, B. Collins and N. Conley, unpublished results.
- S.-J. Jong and J.-M. Fang, *J. Org. Chem.*, 2001, **66**, 3533.
- C. K. Z. Andrade and N. R. Azevedo, *Tetrahedron Lett.*, 2001, **42**, 6473.
- The reaction of benzaldehyde in recycled bmimBr, bmimBF<sub>4</sub>, emimBF<sub>4</sub> and EAN afforded the desired product in 87, 88, 86, and 80% yields, respectively.
- It is interesting to note that no reaction occurs in the absence of ionic liquid solvents.
- S. Park and R. J. Kazlauskas, *J. Org. Chem.*, 2001, **66**, 8395.
- D. Mirejovsky and E. M. Arnett, *J. Am. Chem.*, 1983, **105**, 1112.



# Synthesis of methylpseudoionones by activated hydrotalcites as solid base catalysts

M. J. Climent, A. Corma, S. Iborra and A. Velty

*Instituto de Tecnología Química, UPV-CSIC, Universidad Politécnica de Valencia, Avda. de los Naranjos s/n, 46022 Valencia, Spain. E-mail: acorma@itq.upv.es; Fax: 34 96 3877809; Tel: 34 96 3877800*

Received 7th June 2002

First published as an Advance Article on the web 17th September 2002

Preparation of methylpseudoionones (precursors of methylionones) has been carried out by aldol condensation between citral and methyl ethyl ketone (Mek) using an amorphous aluminophosphate (ALPO), KF–Alumina and differently activated Al–Mg hydrotalcites as solid base catalysts. Activated hydrotalcites (calcined or calcined–rehydrated hydrotalcites) exhibited the best activity and selectivity to obtain methylpseudoionones. The effect of the chemical composition of the calcined hydrotalcites as well as the effect of the water content of the rehydrated samples have been studied. The main process variables such as reaction temperature and Mek: citral molar ratio have been studied on these different activated catalysts, and in general it has been found that an increase of reaction temperature increases in rate of formation of methylpseudoionones, whereas the influence of the reaction temperature on the selectivity to this compound strongly depends on the type of activated hydrotalcite used. Owing to basicity/adsorption differences between calcined and rehydrated hydrotalcite, a different behaviour of reaction rate and selectivity to the desired product *versus* Mek: citral ratio is observed, which should be attributed to the different nature and distribution of basic sites existing for both samples.

## Introduction

Ionones are cyclic terpenoids that occur in many essential oils and are known for their extensive uses in enhancing the organoleptic properties of consumable materials such as medicinal products, fragrance material and as intermediates in vitamin A synthesis.<sup>1</sup> Methylionones is a term used in perfumery to designate ionones whose preparation involve the aldol condensation of citral with methyl ethyl ketone on a basic catalyst followed by cyclization of the acyclic precursors (called methylpseudoionones) over acid catalysts such as sulfuric and phosphoric acid.<sup>2,3</sup>

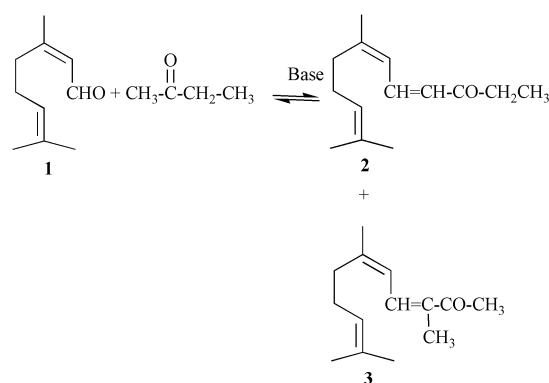
When the aldehyde group of citral (**1**) reacts with the methyl group of methyl ethyl ketone, *n*-methylpseudoionone (**2**) is obtained, whereas reaction with the methylene group will lead to the formation of isomethylpseudoionone (**3**) (Scheme 1). Both compounds can be converted in the presence of acids into the corresponding methylionones. It is known that the isomethylionone isomer is the most desirable as a perfume ingredient, and consequently more attention has been given to the preparation of isomethylpseudoionone. It was found<sup>1</sup> that

the ratio of the two methylpseudoionone isomers in a mixture depends on the catalyst employed and the reaction conditions.

Aqueous alkali metal hydroxide solutions, alcoholates in alcohol or benzene solvents which lead to waste streams, are used for the preparation of methylpseudoionones in the commercial production processes.<sup>2,4,5</sup> The yield of the cross-condensation compound obtained in this process is variable and strongly depends on the type of catalyst and reaction conditions such as, catalyst concentration, molar ratio of reagents and reaction temperature.

The substitution of the homogeneous bases by solid catalysts is environmentally highly desirable, and solid bases such as modified aluminas<sup>6</sup> alkaline exchanged zeolites,<sup>7</sup> clays and hydrotalcites have been tested recently<sup>8–14</sup> as basic catalysts in aldol condensation. Heterogeneous catalysts are easy to separate from the reaction media by filtering, avoiding the formation of by-products and the neutralization step, moreover it allows the unreacted excess ketone to be recovered in a substantial anhydrous state facilitate recycling.

In previous work we have studied the condensation of citral with acetone and found that whereas heterogeneous acid catalysts such as Beta and Y zeolites were not successful for producing the ionones in one step, solid base catalysts such as



Scheme 1

## Green Context

While much attention is being paid to the development of solid acids, there exist a large number of base-catalysed reactions which also would benefit from the provision of solid base catalysts, avoiding the generation of salt waste upon reaction quenching. Here, the use of a range of basic catalysts is investigated in an important industrial reaction type. Key observations of structure–activity are made which are useful for the further development of this process, as well as being of a more general applicability. *DJM*

MgO and activated hydrotalcites, exhibited excellent activity and selectivity for the synthesis of pseudoionones.<sup>15</sup> Now, we describe here, the preparation of methylpseudoionones by aldol condensation between citral and methyl ethyl ketone using different basic catalysts. Thus, KF on alumina, a high surface area MgO, differently activated hydrotalcites, and an acid–base bifunctional catalyst such as amorphous aluminophosphate (ALPO), have been tested here as catalysts for this reaction. Since the nature of the catalyst and the reaction conditions are important factors controlling the yield and selectivity to methylpseudoionone, an in depth study of the reaction conditions and the influence of basic strength of the catalyst have been made.

## Experimental

### Materials

The amorphous aluminophosphate (AIPO) with a P:Al ratio of 1.0 was prepared following the method proposed by Lindblad *et al.*<sup>16</sup> The MgO samples were prepared by thermal decomposition of magnesium oxalate at 873 K in vacuum for 6 h<sup>17</sup> and the textural properties are given in Table 1. The KF–Al<sub>2</sub>O<sub>3</sub> sample was provided by Aldrich (40 wt% impregnated on alumina).

Al–Mg hydrotalcites were prepared from gels produced by mixing two solutions: A and B. Solution A contains (3 – *x*) moles of Mg(NO<sub>3</sub>)<sub>2</sub>·6H<sub>2</sub>O and *x* moles of Al(NO<sub>3</sub>)<sub>3</sub>·9H<sub>2</sub>O in the (Al + Mg) concentration of 1.5 mol l<sup>-1</sup> for a range of Al:Al + Mg ratios between 0.20 to 0.29. Solution B is formed by (6 + *x*) moles of NaOH and 2 moles of Na<sub>2</sub>CO<sub>3</sub> dissolved in the same volume as solution A. Both solutions were co-added at a rate of 1 mL min<sup>-1</sup> under vigorous mechanical stirring at room temperature. The suspension was left for 12 hours at 60 °C. The hydrotalcite was filtered and washed until pH = 7, and the solids were dried at 60 °C.

The hydrotalcite was activated by calcining at 723 K in a dry flow of N<sub>2</sub> (99.99%). The temperature was raised at a rate of 2 °C min<sup>-1</sup> to reach 723 K and maintained for 6 h. The solid was then cooled to room temperature. The calcined hydrotalcite (HTc) was rehydrated at room temperature under a flow of nitrogen saturated with water vapour, free of CO<sub>2</sub>. The flow of wet nitrogen (40 mL min<sup>-1</sup>) was maintained for 24 hours. In other experiments, hydrotalcites were rehydrated by direct water addition on the freshly calcined catalysts just before reaction. Analyses of Mg and Al were performed using atomic absorption. The main characteristics of the hydrotalcite samples are summarised in Table 1.

X-Ray diffraction measurements were recorded with a Philips X'PERT (PN 3719) diffractometer (CuK $\alpha$  radiation provided by a graphite monochromator) equipped with an automatic variable divergence slit and working in the constant irradiated area mode.

N<sub>2</sub> and Ar adsorption–desorption isotherms were performed at 77 and 87 K, respectively, in an ASAP 2010 apparatus from Micromeritics, after pre-treating the samples under vacuum at 673 K overnight and the BET surfaces were obtained using the BET methodology.

**Table 1** Main characteristic of the base catalysts

| Catalyst                          | Al:(Al + Mg) | S <sub>BET</sub> /m <sup>2</sup> g <sup>-1</sup> |
|-----------------------------------|--------------|--|
| HT-1                              | 0.20         | 220  |
| HT-2                              | 0.25         | 227  |
| HT-3                              | 0.29         | 247  |
| MgO                               | 0            | 246  |
| KF–Al <sub>2</sub> O <sub>3</sub> | —            | 14.8   |
| ALPO                              | —            | 211  |

### Reaction procedure

Commercial citral, a mixture of *cis* and *trans* isomers (geranial and neral) with a proportion of 25 and 75 wt% respectively was used without purification. Methyl ethyl ketone was supplied by Aldrich.

Typically, a mixture of citral (6.8 mmol), methyl ethyl ketone (71.4 mmol) and the catalyst (555 mg) were added to a three necked-round bottomed flask equipped with a condenser system. The resultant suspension was heated up to 357 K under vigorous stirring in an oil bath equipped with an automatic temperature control system. Samples were taken at regular time periods and analysed by gas chromatography (GC) using a FID detector and a Tracer-wax column (15 m × 0.32 mm × 0.25  $\mu$ m). Nitrobenzene was used as internal standard. At the end of the reaction, after cooling, the reaction mixture was filtered to remove the catalyst. The response factors were calculated for each reactive agent from pure samples. Reaction products were identified by GC-MS (Hewlett-Packard 5988 A) and by <sup>1</sup>H-NMR spectroscopy (Varian VXR-400S, 400 MHz).

## Results and discussion

### Citral condensation with methyl ethyl ketone on different solid catalysts

Condensation reactions between citral and Mek were carried out at 357 K on different heterogeneous catalysts (Table 2) using a molar ratio Mek : citral of 10.6, and 8.3 wt% (with respect to the total amount of reagents) of catalyst. In all experiments, a mixture of *cis*–*trans* isomers of *n*-methylpseudoionone (7,11-dimethyldodeca-4,6,10-trien-3-one) (**2**) and isomethylpseudoionone (3,6,10-trimethylundecan-3,5,9-trien-2-one) (**3**) were obtained. Products **2** and **3** come from the condensation of the Mek through the methyl or methylene groups, which correspond to the kinetic and thermodynamic products respectively (Scheme 1). In Table 2 yields and selectivities of methyl plus isomethylpseudoionone obtained with the different catalysts, after 5 hours reaction time are summarised. No  $\beta$ -hydroxyl ketones derived from Mek or methylpseudoionones were detected under these conditions. However, other condensation products coming from the self-condensation of Mek, self-condensation of citral, and oligomers derived from citral were detected in the reaction mixture.

Kinetically, the attack on the carbonyl group of citral by the carbanion generated from the methyl group of the methyl ethyl ketone, appears to be favoured since the methyl group is less sterically hindered. However, it was found that reaction temperature, reaction time and the catalyst employed have a profound influence on the ratio of the two isomeric methylpseudoionones (**2** and **3**).<sup>1</sup>

In all the experiments, the kinetic product **2** is the predominant compound obtained. This is not only due to the higher steric hindrance of the methylene group, but also to the different acidity of the hydrogens in the methyl and methylene groups. Indeed, we have calculated the relative density of positive

**Table 2** Condensation of citral with Mek using different heterogeneous basic catalysts

| Catalyst                          | Conversion      | Yield <b>2</b> + <b>3</b> | Selectivity <b>2</b> + <b>3</b> | Ratio <b>2</b> : <b>3</b> |
|-----------------------------------|-----------------|---------------------------|---------------------------------|---------------------------|
| KF–Al <sub>2</sub> O <sub>3</sub> | 99 <sup>a</sup> | 50                        | 50                              | 1.5                       |
| ALPO                              | 23              | 16                        | 70                              | 4.2                       |
| MgO                               | 70              | 9                         | 13                              | 2.3                       |
| HT-2                              | 90              | 80                        | 89                              | 5.2                       |

Reaction conditions: molar ratio Mek:citral = 10.6; 8.3% (wt%) of catalyst; 5 h reaction at 357 K. <sup>a</sup> At 1 h reaction time.

charge of the hydrogens, the results show that the hydrogens in the methyl group have a density of positive charge of +0.12, while those of the methylene group have +0.09.

With respect to the catalytic activity, results from Table 2 indicate that the order of activity is  $\text{KF-Al}_2\text{O}_3 > \text{HT-2} > \text{MgO} > \text{ALPO}$ . While the relatively high activity of KF-alumina is not surprising considering the strong basic character of this material, however it has low selectivity to methylpseudoionones (50%). ALPO exhibits a higher selectivity to methylpseudoionones (70%), being the subproducts oligomers of the citral. MgO shows an unexpected low activity and selectivity to methylpseudoionones giving mainly citral polymerization. This could be due to strong adsorption of citral on this material in competition with that of methyl ethyl ketone resulting in a decrease of the amount of intermediates able to produce the desired condensation products. The disappointing results obtained with MgO are surprising if we consider previously obtained results with this catalyst for the condensation of citral with acetone under similar reaction conditions.<sup>15</sup> The higher activity and selectivity to the condensation product found with acetone using MgO as a catalyst, could be attributed to the higher polarity of the acetone with respect to the Mek. Indeed if one considers that the reagent present in excess (the ketone) acts as a solvent, an increase in the polarity of the solvent should help to desorb the citral, minimizing the self-condensation of citral as well as the extension of other side reactions.

Results from Table 2 clearly show that the calcined Mg–Al hydrotalcite is the material which presents the best catalytic behaviour from the point of view of activity and selectivity. Owing to this, and in order to select the best reaction conditions to obtain methylpseudoionones, a kinetic study of the reaction was performed on catalysts based on calcined hydrotalcites.

Mg–Al hydrotalcites are Mg–Al hydroxycarbonates with lamellar structure. The isomorphous substitution of  $\text{Mg}^{2+}$  by  $\text{Al}^{3+}$  produces layers with an excess of positive charges which are compensated by carbonate anions located in the interlamellar space. Thermal decomposition above 723 K involves successive dehydration, dehydroxylation and decarbonization which result in the formation of a highly active Mg–Al-oxide solid solution which is potentially a basic catalyst for a variety of organic transformations such as self-condensation of acetone<sup>18</sup> and the condensation of formaldehyde and acetone.<sup>19</sup> Recently, it has been presented that the calcined product can be activated by rehydration at room temperature by contacting with a stream of nitrogen saturated with water vapour during long periods of time.<sup>13</sup> It is a general belief that the basic sites produced by calcination are oxygen anions of low co-ordination, which correspond to Lewis basic sites, and when the hydrotalcite is rehydrated these basic sites are converted to hydroxyls or basic Brønsted sites which become the compensating interlayer anions.<sup>13</sup> Taking this into consideration both type of catalysts, *i.e.* calcined hydrotalcite and the rehydrated form will be studied here.

### Condensation of citral and methyl ethyl ketone on calcined hydrotalcites. Influence of the reaction temperature and molar ratio Mek : citral

It has been recently presented<sup>20</sup> that rehydrated hydrotalcites were very active for the condensation of acetone and citral at temperatures of 273 K. The authors found that with a molar acetone : citral ratio of 20 (10 wt% of citral) the desired condensation reaction did not take place, while when the amount of citral was decreased to 1 wt% both acetone self condensation and citral–acetone condensation occurred. The authors claimed that a negative reaction order in citral takes place, and the inhibition of citral could be due to strong adsorption of citral on the catalyst surface. However, considering that the adsorption is an exothermic process, the inhibition

should decrease when working at higher reaction temperatures. In fact, in previous work<sup>15</sup> using calcined hydrotalcites as catalysts, we found that when the condensation of citral with acetone was performed at 333 K it is possible to achieve high conversions and selectivities to pseudoionone (90%) at relatively low acetone : citral ratios ( $\sim 4$ ). Taking into account the results obtained previously with the aldol condensation between acetone and citral it becomes mandatory to study the influence of the reaction temperature and the molar ratio of reagents on the activity and selectivity of the calcined hydrotalcite for the condensation of Mek and citral to produce methylpseudoionones.

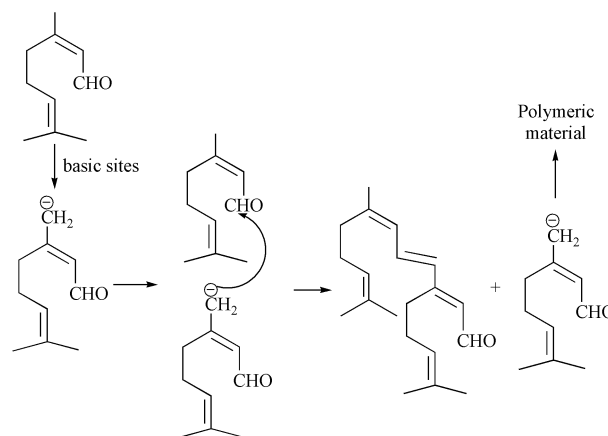
The study of the influence of the reaction temperature on the condensation reaction between Mek and citral was performed in the presence of 8.3 wt% of a calcined hydrotalcite sample (HT-2), using a molar ratio Mek : citral of 10.6 at 333, 345 and 357 K. In Table 3 the conversion of citral, yield and selectivity to methylpseudoionones are presented. As expected, at 333 K, the reaction was slow and it was possible to obtain after 5 h reaction time a yield of 43% with a selectivity of 66% to methylpseudoionones. When the reaction temperature was increased to 345 K a considerable improvement of yield and selectivity to (2 + 3) (98%) can be obtained. These results indicate that at low reaction temperatures the strong adsorption of citral on the catalyst surface favour side reactions, such as oligomerization (Scheme 2), instead of the desired cross condensation between Mek and citral. As can be seen in Table 3, a further increase of temperature to 357 K leads to a higher yield of methylpseudoionones. However, at the same level of conversion the selectivity to products (2 + 3) slightly decreased with temperature, while the 2 : 3 ratio remains practically constant. This result indicates that working at reaction temperatures higher than 357 K, secondary reactions, such as methylpseudoionone polymerization, will be favoured.

From these results it is clear that working at 357 K reaction temperature it is possible to achieve an excellent yield and selectivity to methylpseudoionones and, because of that, we have selected this reaction temperature to study the influence of the molar ratio of the reagents on the conversion and selectivity.

**Table 3** Condensation of citral with Mek using calcined hydrotalcite as catalyst (HT-2) at different reaction temperatures

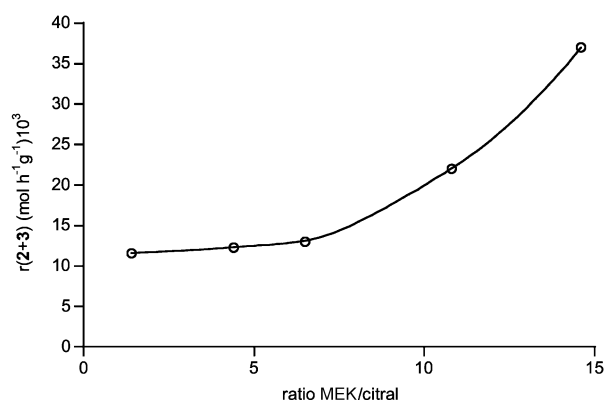
| T/K | Conversion of <b>1</b> (%) | Yield (%) of (2 + 3) | Ratio 2 : 3 | Selectivity (%) to 2 + 3 |
|-----|----------------------------|----------------------|-------------|--------------------------|
| 333 | 66 <sup>a</sup>            | 43                   | 4.5         | 66                       |
| 345 | 68 <sup>a</sup>            | 67                   | 5.0         | 98                       |
| 357 | 68                         | 60                   | 5.0         | 88                       |
|     | 90 <sup>a</sup>            | 80                   | 5.2         | 89                       |

<sup>a</sup> At 5 h reaction time; catalyst 8.3 wt%; molar ratio Mek : citral 10.6



**Scheme 2**

In order to do this, the aldol condensation was carried out at 357 K using a calcined hydrotalcite catalyst (HT-2), 53 wt% with respect to citral with molar ratios Mek: citral of 2.5, 4.4, 6.5, 10.8 and 14.5 mol mol<sup>-1</sup>. In Fig. 1, the initial rates of 2 + 3 determined from the experimental curves of yield *versus* time, are plotted *versus* molar ratios of Mek: citral. The results show that the rate of formation of methylpseudoionones increases when the Mek: citral molar ratio increases, being more pronounced for Mek: citral molar ratios between 6.5 and 14.5. Concerning the influence of Mek: citral molar ratio on the selectivities to methylpseudoionones, we can see (Table 4) that for molar ratios higher than 6 it is possible to achieve selectivities of methylpseudoionones of nearly 90%. However, we have to point out that better yields and selectivities of methylpseudoionones are obtained when the Mek: citral molar ratio is further increased. On the other hand, the ratio 2:3 increases when increasing the Mek: citral molar ratio up to 5 and remains constant for a further increase of the ratio of the reactants (Fig. 2). The fact that the formation of the methylpseudoionone (2) is favoured when the Mek: citral ratio increases, could be explained taking into account the different acidity and accessibility of the hydrogens at the methyl and methylene group which compete for the same basic sites. Thus, when the concentration of Mek increases it should be expected that the fraction of basic sites occupied by the most acidic hydrogens increases up to a certain concentration of Mek for which surface saturation will occur. The preferential adsorption through the most acidic hydrogens will afford a higher surface concentration of the carbanion species leading to product 2. These results, along with those obtained in the study of the reaction temperature are supporting the inhibiting effect of the citral concentration during this condensation reaction. Nevertheless the inhibiting effect can be minimised by increasing the Mek: citral ratio or even better by increasing the reaction temperature. When this was done, it was possible to achieve yields and selectivities of methylpseudoionones which are reasonable from an industrial application point of view.

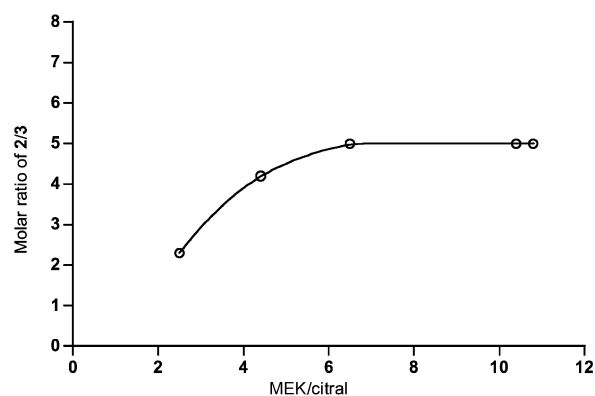


**Fig. 1** Influence of the Mek: citral molar ratio on the initial rate of formation of methylpseudoionones (mol h<sup>-1</sup>g<sup>-1</sup>) at 357 K in the presence of hydrotalcite HT-2 (53 wt% with respect to citral).

**Table 4** Influence of the Mek: citral molar ratio on the yield and selectivity to methylpseudoionones

| Mek: citral | Conversion (%)  | Yield (%) of (2 + 3) | Selectivity (%) to (2 + 3) |
|-------------|-----------------|----------------------|----------------------------|
| 2.5         | 92 <sup>a</sup> | 43                   | 47                         |
| 4.4         | 95 <sup>a</sup> | 61                   | 65                         |
| 6.5         | 88 <sup>b</sup> | 70                   | 80                         |
| 10.8        | 93 <sup>b</sup> | 81                   | 87                         |
| 14.5        | 94 <sup>b</sup> | 83                   | 88                         |

<sup>a</sup> 2 h reaction time; <sup>b</sup> 3 h reaction time; catalyst (HT-2) 53 wt% with respect to citral, at 357 K.

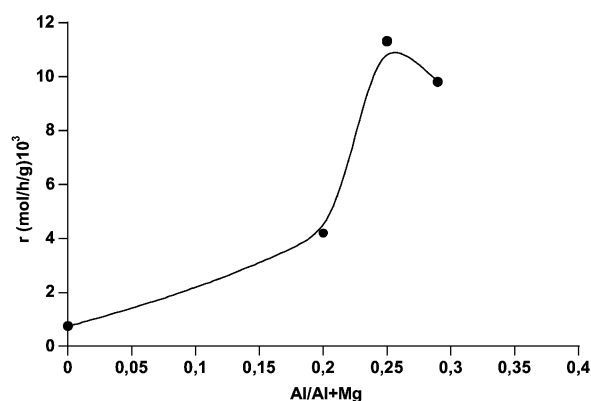


**Fig. 2** Influence of the Mek: citral molar ratio on the ratio of methylpseudoionones (2:3) at 357 K in the presence of hydrotalcite HT-2 at 3 h of reaction time.

### Influence of the chemical composition of the hydrotalcite and catalyst concentration on the condensation reaction

It is known that the base properties of calcined hydrotalcites depend on the Al:(Al + Mg) ratio. Thus, when the amount of aluminium increases, the total number of basic sites decreases, but the proportion of the stronger ones increases.<sup>8</sup> If this is so, we may expect to find a maximum in activity for a given base catalyzed reaction at a given Al:(Al + Mg) ratio. The position of the maximum will depend then on the base strength needed to activate the particular reagent. In order to find the optimum chemical composition of the hydrotalcite for this reaction, the condensation between citral and Mek was performed using a molar ratio Mek: citral of 10.6, at 357 K using different calcined hydrotalcites with Al:(Al + Mg) ratios ranging from 0.20 to 0.29. In Fig. 3, the initial reaction rates are plotted *versus* the chemical composition of the mixed oxides (Al:(Al + Mg)), and a maximum in activity occurs for an Al:(Al + Mg) ratio of 0.25.

When the influence of the catalyst chemical composition on the selectivity to methylpseudoionones at different reaction temperatures is analyzed (Table 5) one can see that at 333 K the selectivity is very similar for the three samples. Assuming that the main cause for decreasing selectivity to methylpseudoionones is the strong adsorption of citral on the active sites and the consequent oligomerization of the  $\alpha,\beta$ -unsaturated aldehyde, the results indicate that at low reaction temperature the citral adsorption on the catalyst should be highly favoured, independently of the basic strength of the active sites on the catalyst. However, when the reaction temperature is increased up to 345



**Fig. 3** Influence of the Al:(Al + Mg) ratio on the initial rate of formation of methylpseudoionones when the aldol condensation was carried out at 357 K using a Mek: citral molar ratio of 10.6 in the presence of a series of hydrotalcites (8.3 wt%).

**Table 5** Influence of chemical composition of the calcined hydrotalcite and reaction temperature on the yield and selectivity to methylpseudoionones

| T/K | Catalyst Al:(Al + Mg) | Conversion <sup>a</sup> of <b>1</b> (%) | Yield (%) of ( <b>2</b> + <b>3</b> ) | Selectivity (%) to ( <b>2</b> + <b>3</b> ) |
|-----|-----------------------|---|--------------------------------------|--|
| 333 | 0.20                  | 59                                      | 35                                   | 60   |
|     | 0.25                  | 66                                      | 43                                   | 66   |
|     | 0.29                  | 57                                      | 37                                   | 65   |
| 345 | 0.20                  | 66                                      | 43                                   | 66   |
|     | 0.25                  | 68                                      | 67                                   | 98   |
|     | 0.29                  | 54                                      | 45                                   | 83   |
| 357 | 0.20                  | 74                                      | 53                                   | 72   |
|     | 0.25                  | 90                                      | 80                                   | 89   |
|     | 0.29                  | 73                                      | 56                                   | 77   |

<sup>a</sup> At 5 h reaction time; molar ratio Mek:citral = 10.6, catalyst 8.3 wt%.

It is clearly observed that there is a minimum of selectivity for the sample with a Al:(Al + Mg) of 0.20. These results could indicate that catalysts containing a large number of basic sites with low basic strength favour the adsorption of citral affording then low selectivity to methylpseudoionones. This hypothesis will be consistent with the results previously obtained with MgO. At 345 K, the hydrotalcite with an Al:(Al + Mg) ratio of 0.25 exhibits the maximum selectivity to products (**2** + **3**) indicating that this is the optimum in the number and basic strength of the active sites which allows minimization of the citral adsorption. Finally, when increasing the Al:(Al + Mg) up to a ratio of 0.29, for which the total number of basic sites is lower but the proportion of the stronger ones is higher, a decrease in selectivity is observed. This indicates that an excessive basic strength of the active sites also favors citral adsorption and side reactions. This hypothesis agrees with the results of selectivity to methylpseudoionone found when a strong basic catalyst such as KF-alumina is used to catalyze this condensation (see Table 2). Similar argumentation can be totally valid for the results found at 357 K, although the differences in selectivity for the three samples are lower than those found at 345 K.

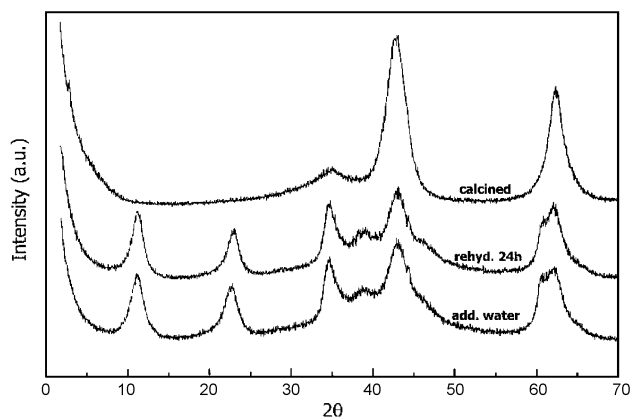
From these results one can conclude that independently of the reaction temperature, at least above 333 K, the chemical composition of the heterogeneous catalyst, *i.e.*, the strength distribution and concentration of basic sites, has a strong influence on the activity and selectivity to methylpseudoionones.

#### Condensation of citral and methyl ethyl ketone on calcined-rehydrated hydrotalcites. Influence of pre-treatment of hydrotalcite on the catalytic activity

As it was said above, two types of solids can be obtained according to the pre-treatment of the original layered hydrotalcite sample: a Lewis base by a calcination-decarbonation process (HT calcined) and a Brønsted base by further rehydration.<sup>13</sup>

To study the influence of the pre-treatment on the catalytic activity, two hydrotalcite derived samples activated by different procedures were used for the aldol condensation of citral and Mek. One of them was a hydrotalcite sample (HT-2) calcined at 723 K (HTc), and the second was this same calcined sample rehydrated by contacting with a stream of nitrogen saturated with water vapour for 24 h (which corresponds to a total 36 wt% water with respect to the solid catalyst) (HTr).<sup>13</sup>

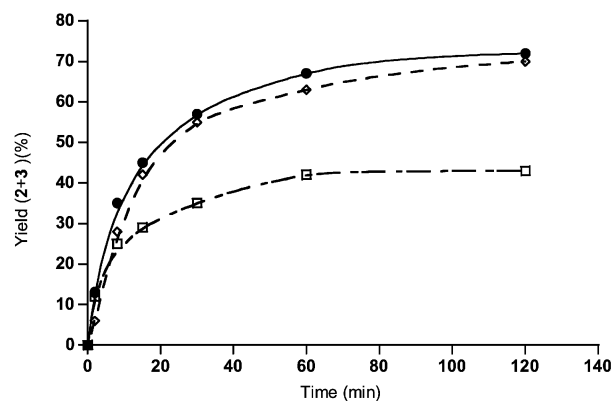
The X-ray diffraction of the material is displayed in Fig. 4. After calcination of the hydrotalcite at 723 K the structure of the resultant material corresponds to that of a mixed Al<sub>2</sub>O<sub>3</sub>-MgO oxide, while after rehydration the original laminar structure was partially restored.



**Fig. 4** Powder X-ray diffraction patterns of hydrotalcites.

The reactions were carried out with these two catalysts at 357 K using a molar ratio Mek:citral = 2.3 and 16 wt% of catalyst. The results from Fig. 5 show that the rehydrated hydrotalcite sample exhibits higher activity than the calcined (HTc) sample. These results are in good agreement with those reported previously,<sup>13</sup> and would agree with the view that Brønsted basic sites are active for this condensation.

It has been reported in the literature<sup>20</sup> from CO<sub>2</sub> adsorption measurements that only 5% of the total available basic sites in the rehydrated calcined hydrotalcite, are accessible for the condensation reactions, and these sites are most likely localised at the edges of HT-platelets. Then it is not unreasonable to suppose that the most accessible basic sites could be activated in a similar way by adding water directly on fresh calcined HT. This procedure should avoid the tedious and time consuming rehydration procedure reported. Meanwhile, with this method there is the possibility that the heat liberated by the fast rehydration of the mixed-oxides may cause the particles to break, increasing in this way the number of accessible OH basic sites. In order to study this, the condensation reaction was performed using a calcined hydrotalcite and adding at once all the water required for rehydration. We name this sample as water added hydrotalcite (HTa), in contrast to rehydrated (HTr) in which the water was added continuously during a 24 h period. A comparison (Fig. 5) between the previous samples (calcined hydrotalcite (HTc), rehydrated (HTr) and water added hydrotalcite (HTa) showed that the calcined HT was much less active than the rehydrated samples. The results of the initial rates of formation of **2** + **3** and the yields are similar for both rehydrated samples regardless of the procedure by which the water was added (see Fig. 5). However the selectivity to methylpseudoionones (**2** + **3**) after two hours of reaction time on HTc,



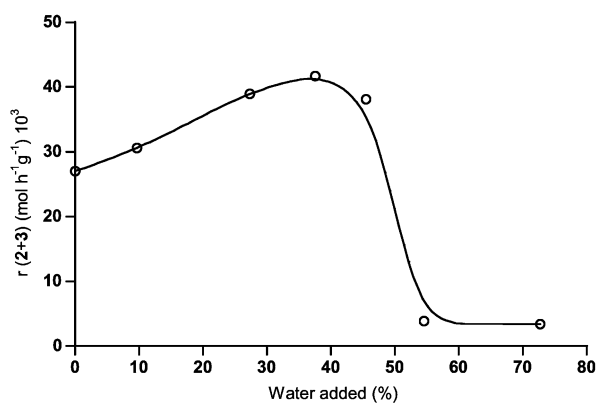
**Fig. 5** Results of aldol condensation between methyl ethyl ketone and citral molar ratio = 2.3, 16 wt% catalyst with respect to the total amount of reagents at 357 K, in the presence of calcined hydrotalcite (□); 24 h rehydrated (36 wt% water) (●); and with 36 wt% water added (◇).

HTa and HTr were 47, 70 and 80% for citral conversions of 43, 70 and 72% respectively. Since it is known that Brönsted sites are more selective than Lewis basic sites, these results would imply that the ratio Brönsted–Lewis basic sites is larger in HTr than in HTa. This however is not supported by the XRD results, since no differences were observed for the level of regeneration of the lamellar structure with both samples (see Fig 4). Therefore, we cannot confirm with our experiments that the activity is only due to the Brönsted basic sites of the regenerated hydrotalcite.

### Influence of the degree of rehydration on the rate of formation of methylpseudoionones

The role of the water on the catalytic process is complex since it reacts with the solid to produce Brönsted basic sites and it is also one of the reaction products. Then, considering that the aldol condensation is a reversible reaction, one should be careful with the amount of water added, since an excess of water over the HTc catalyst should shift the reaction equilibrium towards the formation of citral. Therefore it should be expected that a maximum in activity should occur for an optimum amount of water added to the catalyst. In order to study this parameter we have carried out the condensation reactions at 357 K with a molar ratio Mek: citral = 2.3, and adding different percentages of water directly on HTc. From the results given in Fig. 6, it can be seen that a maximum in activity can be found when the percentage of water added on the hydrotalcite was between 27 and 40 wt% (with respect to the amount of catalyst).

Owing to the rehydration of HTc, a change of the nature of the basic sites occurs and, one should also expect a change of the adsorption properties, and consequently taking into account the results presented above with the calcined hydrotalcites the influence of the temperature and molar ratio of Mek: citral should also be explored on the rehydrated samples.



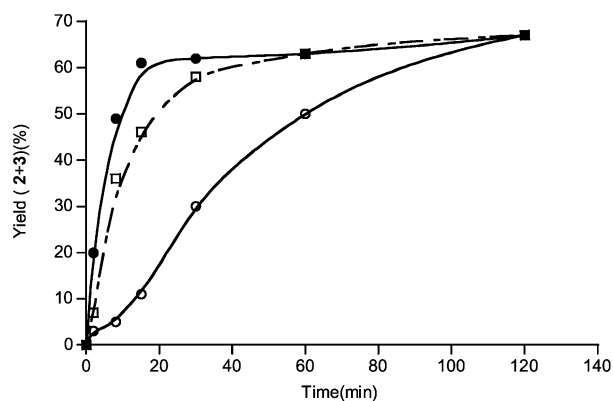
**Fig. 6** Influence of the water added to calcined hydrotalcite on the initial rate of formation of methylpseudoionones, using a molar ratio Mek: citral = 2.3, 16 wt% (with respect to the total amount of reagents), and at 357 K.

### Influence of reaction temperature on the condensation reaction using calcined-rehydrated hydrotalcites as catalysts

We have shown that there is a benefit on catalyst activity when water is directly added to the fresh calcined hydrotalcite and it is possible to achieve a similar yield in a similar reaction time, compared to the hydrotalcite rehydrated using a flow of nitrogen saturated with water. Thus, using the direct rehydration procedure for modifying the catalyst, the influence of the reaction temperature was studied by working at 333, 357 and 373 K using a molar ratio Mek: citral of 2.3 and a calcined

rehydrated hydrotalcite (HTa) with an Al:(Al + Mg) ratio of 0.25 as a catalyst. As could be expected, an increase in activity is observed when increasing the reaction temperature (see Fig. 7). Meanwhile, the selectivities at 333, 357 and 373 K were 78, 80 and 58% for citral conversions of 70, 73 and 86% respectively. It is interesting to notice that even working at a very low molar ratio of reactants (2.3) an increase of reaction temperature from 333 up to 357 K practically does not affect the selectivity to methylpseudoionones, indicating that on the rehydrated hydrotalcites samples, the adsorption of the citral on the catalyst surface should be less than on the calcined samples (see Table 3). On the other hand, a similar molar ratio 2:3 of ~ 2, was found at the three reaction temperatures.

Apparent activation energies were calculated from the Arrhenius expression, and the values obtained were 41.9 kJ mol<sup>-1</sup> for the calcined hydrotalcite and 50.34 kJ mol<sup>-1</sup> for the rehydrated samples. The differences observed in the values could be due to differences in the heat of adsorption of the reactant on the stronger basic sites of the rehydrated hydrotalcites. However if one compares the activation energy values obtained on calcined and rehydrated hydrotalcites with the 106.5 kJ mol<sup>-1</sup> obtained in homogeneous phase using NaOH as catalyst,<sup>21</sup> it can be concluded that the process may very well be controlled by diffusion of reactants in the solid. Notice that Shi Yukui *et al.* have also obtained low activation energy values (37.5 kJ mol<sup>-1</sup>) for this aldol condensation using NaOH as catalyst but working in a two phase system.



**Fig. 7** Yield of methylpseudoionones versus reaction time obtained in the aldolisation reaction using a Mek: citral = 2.3, in the presence of hydrotalcite HT-2 (16 wt% with respect to the total amount of reagents) with 36 wt% water added at 333 K (○); 357 K (□); and 373 K (●).

### Influence of the molar ratio Mek: citral on the rate of formation of methylpseudoionones on calcined-rehydrated materials

As we have shown above with calcined hydrotalcites, the molar ratio of reagents is an important parameter in the rate of formation of methylpseudoionones. Thus, the condensation reaction was performed in the presence of a HTa sample with 36 wt% water added using different Mek: citral ratios at 357 K. From the kinetic curves obtained for each Mek: citral molar ratio tested in this study we observed that for low molar ratios (2.3 and 4.5) higher initial rates are obtained than for higher molar ratios (10.8 and 14), in clear contrast with the results obtained using calcined hydrotalcite (see Fig. 1). Moreover the increase of the Mek: citral ratio has significant influence on the selectivity to methylpseudoionones, in such a way that working at molar ratios higher than 10 it is possible to obtain selectivities of methylpseudoionones above 90% after 1 h reaction time (Table 6). These selectivity results are in good agreement with those obtained using calcined HT sample (see Table 4).



**Table 6** Influence of the molar ratio Mek:citral on the yield and selectivity of methylpseudoionones

| Mek:citral | Conversion of <b>1</b> (%) | Yield (%) of ( <b>2</b> + <b>3</b> ) | Ratio <b>2</b> : <b>3</b> | Selectivity (%) to ( <b>2</b> + <b>3</b> ) |
|------------|----------------------------|--------------------------------------|---------------------------|--|
| 2.3        | 97                         | 69                                   | 2.4                       | 71   |
| 4.5        | 98                         | 81                                   | 2.1                       | 81   |
| 10.8       | 95                         | 89                                   | 2.1                       | 94   |
| 14         | 85                         | 83                                   | 2.3                       | 98   |
|            | 97 <sup>a</sup>            | 96                                   | 2.3                       | 99   |

Reaction conditions: catalyst: HTa (water added 36 wt%), 54 wt% respect to citral, 1 h reaction time at 357 K.<sup>a</sup> At 2 h reaction time.

Nevertheless, it is interesting to point out that working at lower Mek:citral ratios, the reconstructed hydrotalcite gives, at shorter reaction times, higher yields and selectivities to methylpseudoionones than those obtained using calcined hydrotalcites. These results indicate that the inhibiting effect of the citral is less on the catalyst containing hydroxyl groups as basic sites.

From these results we can conclude that a decrease of the citral concentration decreases the initial rate of the cross-condensation and, at the same time, this lower concentration of citral improves the performance and selectivity of the rehydrated hydrotalcite, probably due to a minor adsorption of the citral on the catalyst surface, avoiding side reactions and catalyst decay.

It is interesting to point out that the ratio **2**:**3** is not affected by the Mek:citral molar ratio in clear contrast with the results obtained when calcined HT (HTc) was used as basic catalyst (see Fig. 2). These results could be attributed to the fact that in HTc a wide range of basic strengths probably exist, due to the presence of basic sites associates to O<sup>2-</sup> with different coordination numbers. However, in the case of rehydrated HT samples, the basic Brønsted sites (OH groups) have a narrow distribution of the basic strength, and moreover only a low percentage of the total available basic sites are accessible to the reagents. Then the different distribution of basic strength along with the different accessibility of the Mek to the basic sites in both samples could be responsible for the lack of selectivity towards one of the methylpseudoionones (**2** or **3**) in the case of rehydrated hydrotalcites.

## Conclusions

The condensation reaction between citral and methyl ethyl ketone has been carried out using different solid basic catalysts: an amorphous aluminophosphate, KF-alumina and differently activated aluminium-magnesium hydrotalcites. Calcined or calcined-rehydrated hydrotalcites showed the best catalytic activity and selectivity to obtain methylpseudoionones. The study of the chemical composition of the calcined hydrotalcites showed that there is a maximum in activity and selectivity to methylpseudoionones which corresponds to samples with an Al:(Al + Mg) ratio of 0.25.

While calcined hydrotalcites are very active for this condensation, reaction rate and selectivity to pseudoionones can be improved by rehydrating the calcined sample. The process of rehydration is successfully carried out by directly adding water to the calcined solid, the optimum catalyst obtained by adding 36 wt% water. This sample exhibited similar catalytic activity to a rehydrated sample obtained by treatment with water in a nitrogen stream for 24 hours (36 wt% of water), however better selectivity to methylpseudoionones is obtained with the latter sample. Moreover, it has been found that working with calcined

hydrotalcites, low reaction temperature (333 K) increases side reactions, possibly due to a strong adsorption of citral on the catalyst surface, giving rise to low yield and selectivity to methylpseudoionones, whereas at 345 K a maximum in selectivity is found. In contrast, working with rehydrated hydrotalcite samples, similar selectivity to methylpseudoionones is found at 333 and 357 K what can be related to a minor adsorption of citral on the rehydrated samples. Finally, we have found that working with calcined hydrotalcites the reaction rate increases with the Mek:citral molar ratio showing the inhibiting effect of the citral concentration. Different behaviour is observed working with rehydrated hydrotalcites where a decrease of the initial reaction rate is observed using high molar ratios of reagents (10.8 and 14). However, concerning the selectivity to methylpseudoionones, similar behaviour is found for the two differently activated hydrotalcites, *i.e.*, the selectivity increases with the molar ratio of Mek:citral. Nevertheless, working at lower Mek:citral molar ratios (between 2.5 and 10.8), hydrotalcites activated by water addition give, at shorter reaction times, higher yields and selectivity to methylpseudoionones than those obtained using calcined samples. These results indicate that the inhibiting effect of the citral is lower on the catalyst containing hydroxyl groups as basic sites.

## Acknowledgements

The authors thank the Spanish Comisión Interministerial de Ciencia y Tecnología, CICYT (MAT2000-1392) for the financial support.

## References

- 1 K. Bauer, D. Garbe and H. Surburg, in *Common Fragrances and Flavors Materials*, 2nd ed. 1990, VCH, New York.
- 2 P. S. Gradelf and N. J. Andover, 3,840,601, 1974.
- 3 K. Steiner and H. Tiltcher, EP 628544A1, 1995.
- 4 J. Lothar, W. Hoffmann, A. Lothar, M. Stroezel and H. J. Scheiper, US4431844, 1984.
- 5 P. W. D. Mitchell, US 4874900, (1987).
- 6 P. A. Vatakencherry and K. N. Pushpakumari, *Chem. Ind.*, 1987, **5**, 163.
- 7 H. Tsuji, F. Yagi, H. Hattori and H. Kita, *J. Catal.*, 1994, **148**, 759.
- 8 M. J. Climent, A. Corma, S. Iborra and J. Primo, *J. Catal.*, 1995, **151**, 60.
- 9 R. Tessier, D. Tichit, F. Figueras and J. Kervenal, FP 95 00094, 1995.
- 10 D. Tichit, M. H. Lhouty, A. Guida, B. H. Chiche, F. Figueras, A. Auroux, D. Bartalini and E. Garrone, *J. Catal.*, 1995, **151**, 50.
- 11 J. C. A. A. Roelofs, A. J. van Dillen and K. P. de Jong, *Catal. Lett.*, 2001, **74**, 91.
- 12 A. Guida, M. H. Lhouty, D. Tichit, F. Figueras and P. Geneste, *Appl. Catal. A*, 1997, **164**, 251.
- 13 K. K. Rao, M. Gravelle, J. Sanchez and F. Figueras, *J. Catal.*, 1998, **173**, 115.
- 14 M. Lakshmi Kantam, B. M. Choudary, Ch. Venkat Reddy, K. Koteswara Rao and F. Figueras, *Chem. Commun.*, 1998, 1033.
- 15 M. J. Climent, A. Corma, S. Iborra and A. Velty, *Catal. Lett.*, 2002, **79**, 157.
- 16 I. Lindblad, B. Rebenstorf, Y. Zhi-Guang, S. Lars and I. Andersson, *Appl. Catal. A*, 1984, **112**, 187.
- 17 P. Putanov, E. Kis and G. Boskovic, *Appl. Catal.*, 1991, **73**, 17.
- 18 N. T. Reichle, S. Y. Kang and D. S. Everhardt, *J. Catal.*, 1986, **101**, 352.
- 19 E. SuzuKi and Y. Ono, *Bull. Chem. Soc. Jpn.*, 1988, **61**, 1008.
- 20 J. C. A. A. Roelofs, A. J. van Dillen and K. P. de Jong, *Catal. Today*, 2000, **60**, 297.
- 21 Yukui. Shi and Qiwei. Gu, *Huaxue Fanying Gongcheng Yu Gongyi*, 1993, **9**, 353.



# Eco-friendly synthesis of *p*-nitrobenzonitrile by heterogeneously catalysed gas phase ammoxidation

Andreas Martin,<sup>\*a</sup> Narayana V. Kalevaru,<sup>a</sup> Bernhard Lücke<sup>a</sup> and Jürgen Sans<sup>b</sup>

<sup>a</sup> Institut für Angewandte Chemie Berlin-Adlershof e.V, Richard-Willstätter-Str. 12, D-12489 Berlin, Germany

<sup>b</sup> Degussa AG, Dr. Albert-Frank-Str. 32, D-83308 Trostberg, Germany

Received 1st May 2002

First published as an Advance Article on the web 16th September 2002

Ammoxidation of *p*-nitrotoluene (PNT) to *p*-nitrobenzonitrile (PNB) has been carried out over some bulk and supported vanadium phosphate (VPO) catalysts and also on supported V<sub>2</sub>O<sub>5</sub> catalysts for the first time. The solid PNT was successfully metered over the catalyst bed using a saturator by maintaining the temperature in the saturator above the melting point of PNT and with simultaneous bubbling of a known amount of nitrogen gas as a carrier to the PNT vapours. PNT has been observed to undergo some kind of thermal decomposition at temperatures higher than 623 K even in the absence of catalyst as was evidenced from blank tests. Hence all the catalytic runs had to be restricted to a reaction temperature of 623 K and below. A maximum PNB selectivity of 77% was obtained over a bulk VPO catalyst with a P/V ratio of 1.2 at a conversion of 13% with a high carbon balance of 100%. The lowest PNB selectivity and the carbon balance were given by the catalyst with the lowest P/V ratio (0.5 P/V). The high non-selectivity of this catalyst can be explained on the basis that it contains excess of highly active lattice oxygen and also due to less stabilisation of reduced vanadium species because of the presence of less phosphorus content in the catalyst. In general, the lower activities and selectivities obtained over the studied catalysts have been attributed to the presence of the strongly deactivating –NO<sub>2</sub> group on the aromatic ring.

## Introduction

Aromatic as well as hetero aromatic nitriles are valuable intermediates and reactants in the fine chemical sector used for the synthesis of several pharmaceuticals, dyestuffs and pesticides, respectively.<sup>1</sup> Most of the industrial processes of some commodities are performed by the vapour phase ammoxidation such as production of benzonitrile, terephthalodinitrile or nicotinonitrile;<sup>2–5</sup> otherwise small scale products and specialities (higher substituted aromatics) are manufactured mostly using traditional routes of organic chemistry.<sup>5</sup> The production of *p*-nitrobenzonitrile may belong to the latter. The nitrile yields of these traditional synthesis methods are sometimes quite high but a number of hazardous reagents, expensive feed components and solvents are used, moreover, a lot of waste is produced such as harmful side-products, salts and others.<sup>6</sup> The following summarises some examples: (i) *p*-nitrobenzonitrile could be manufactured by liquid phase conversion of *p*-nitrobenzaldehyde in tetrahydrofuran in the presence of iodine and ammonia,<sup>7</sup> in acetonitrile containing NaN<sub>3</sub> and TiCl<sub>4</sub><sup>8</sup> or in NH<sub>4</sub>OAc–NH<sub>2</sub>OH–HCl solutions under microwave irradiation.<sup>9</sup> Yields between 70 and 95% are reported. (ii) Similar high yields can be obtained by the dehydration method using *p*-nitrobenzamide heated in 1,2-dimethoxyethane in the presence of P<sub>2</sub>O<sub>5</sub>.<sup>10</sup> (iii) *p*-Nitrobenzonitrile is formed in a reaction of *p*-nitrobenzoyl chloride with sulfonamide in tetrahydrothiophene 1,1-dioxide at ca. 423 K.<sup>11</sup> (iv) Another synthesis method describes the nitration of benzonitrile using HNO<sub>3</sub> on zeolite Hβ. Besides the desired *p*-compound the other isomers are also formed.<sup>12</sup> (v) One of the most classical routes is the substitution of halogens by cyanides (KOLBE-synthesis); 92% yield is reached using ZnCN in the presence of tetrakis(triphenylphosphine)palladium(0) in DMF at 353 K.<sup>13</sup> (vi) Last but not least, is the SANDMEYER-reaction that enables the formation of nitriles

by the conversion of diazonium salts in presence of copper cyanides.

Another process for the preparation of nitriles in a single step reaction is the so-called vapour phase ammoxidation, which is the most simple, ecologically and economically profitable route,<sup>1,3</sup> as mentioned above. The conversion of organics containing an  $\alpha$ -activated methyl (alkyl) group (olefins, methyl (alkyl) aromatics and hetero aromatics) in the presence of ammonia and oxygen (air) leads to a variety of nitriles.<sup>1</sup> The reaction is normally carried out on transition metal oxide catalysts (*e.g.* V–TiO, V–MoO, *etc.*) used as bulk systems or supported on alumina or silica at ca. 573–673 K, in multi-tube or fluidised bed reactors. However, high reaction temperatures, oxidation sensitivity of more substituted reactants as well as parallel and consecutive oxidations of reactants and intermediates and/or products towards total oxidation final products like carbon oxides and water limit the number of industrial applications so far.

## Green Context

**While aromatic nitriles are valuable synthetic intermediates in the manufacture of many high-value products, including pharmaceuticals and dyestuffs, their synthesis can be problematic, hazardous or environmentally damaging. Known routes to the important *p*-nitrobenzonitrile, for example, involve azides, strong acids or cyanides. Vapour phase ammoxidation is, by comparison, a very attractive route in terms of simplicity, safety and waste-minimisation. Here probably the first example of the effective use of this procedure to the synthesis of *p*-nitrobenzonitrile is described.**

JHC

Vanadium phosphates (VPO) are well known as catalysts for the oxidation of *n*-butane to maleic anhydride (*e.g.* refs. 14,15 and references therein). In addition to their application as oxidation catalysts VPO solids can also be successfully employed as highly active and selective catalysts in the heterogeneously catalysed ammoxidation of toluene and other substituted methyl aromatics and hetero aromatics (*e.g.* refs. 16–19).

In the present state of our knowledge, there is not even a single published source of information either in open literature or in patent literature (in English language) on the gas phase ammoxidation of *p*-nitrotoluene (PNT) to *p*-nitrobenzotrile (PNB) (Scheme 1). But we have come across a review article by Rizayev *et al.*,<sup>19</sup> in which two early Russian references<sup>20,21</sup> from the Suvorov group were quoted for the vapour phase ammoxidation of PNT to PNB, where a maximum PNB selectivity of *ca.* 30% is reported by the authors over V–Ti-oxide catalysts. However, the reaction conditions, dosing of PNT, conversion and other details are not known from this reference. Nevertheless, this low selectivity (*ca.* 30%) of PNB has been explained by the authors due to the intensive oxidation of the substituted toluene along the carbon attached to the –NO<sub>2</sub> group.

The aim of the present study was to investigate the activity and selectivity behaviour of some available bulk and supported VPOs and also a few supported V<sub>2</sub>O<sub>5</sub> catalysts for the vapour phase ammoxidation of PNT to PNB for the first time.

## Experimental

### Catalysts preparation

Bulk VPO precursors with different P/V ratios of 0.5, 0.95 and 1.2 [mainly consisting of VOHPO<sub>4</sub>·0.5H<sub>2</sub>O (VHP) phase] were prepared in an organic medium as described below. 52.5 g of V<sub>2</sub>O<sub>5</sub> (UH-2862) was suspended in a mixture of 315 ml of butan-2-ol (Merck, Germany) and 210 ml of benzyl alcohol (Merck, Germany) and the suspension was stirred continuously under reflux for 3 h, then cooled to room temperature and left stirring at room temperature overnight before the addition of *o*-H<sub>3</sub>PO<sub>4</sub>. Then an appropriate amount of 85% *o*-H<sub>3</sub>PO<sub>4</sub> (quantity depends upon the P/V ratio) was added slowly and the solution was again heated and maintained under reflux with constant stirring for 2 h. Then the slurry was cooled to room temperature, filtered, washed with ethyl alcohol. The precursor (VHP) obtained was oven dried at 393 K for 24 h and finally calcined at 723 K for 3 h in nitrogen.

The supported VPO catalysts [P/V = 0.95 with α-Al<sub>2</sub>O<sub>3</sub>, γ-Al<sub>2</sub>O<sub>3</sub> and TiO<sub>2</sub> (rutile, anatase)] were prepared using 0.95 P/V bulk precursors by the solid–solid wetting method. Appropriate quantities of VPO precursors and support materials were mixed thoroughly and ground in an agate mortar and then transferred to a grinding machine where the powders were electrically mixed thoroughly for ~5 minutes. The resulting solid mixture was pelletised, crushed and sieved to the required particle size (1.0 to 1.25 mm) and then calcined at 723 K for 3 h.

Supported vanadia catalysts were prepared by wet impregnation technique by contacting support particles with required

amounts of ammonium metavanadate (Aldrich) dissolved in aqueous oxalic acid solution. The excess water, in the impregnated samples was evaporated to dryness on a water bath. The catalyst precursors were oven dried at 393 K for 16 h and finally calcined at 723 K for 6 h in air.

### Characterisation of catalysts

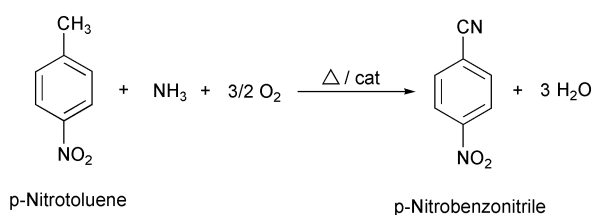
The X-ray powder diffraction (XRD) measurements were carried out using a STADI P (STOE) set-up (Debye-Scherrer geometry, Ge-primary-monochromator, Cu-Kα<sub>1</sub>). The XRD patterns were scanned in the 2θ range of 5–60° (step width: 0.5°, 100 s per step) and were recorded with a STOE position sensitive detector (PSD). Data interpretation was carried out using the software X-POW (STOE) and the database of Powder Diffraction Files (PDF) of the International Centre for Diffraction Data (ICDD).

Catalyst surface areas were determined by N<sub>2</sub>-adsorption according to the BET method at 77 K (Gemini III 2375, Micromeritics). The samples were pre-treated at 423 K for 2 h under vacuum.

### Catalytic runs

Ammoxidation runs were carried out by means of continuous, fixed bed tubular glass reactor, made of Pyrex glass (16 mm id and 250 mm length) and heated in an electrical furnace. Air, NH<sub>3</sub> and N<sub>2</sub> supplied were commercially available gases from compressed gas cylinders. The flow rates of these gases were measured using mass flow controllers. The liquid water was pumped using high precision HPLC pump (LC 9A, Shimadzu) and was vaporised in a preheating zone provided on the top of the catalyst bed. *p*-Nitrotoluene is basically a solid material (mp = *ca.* 325 K) and hence it is very difficult to pump it as a heated liquid. Therefore, we have successfully overcome this difficulty of dosing solid PNT by the use of a heated double walled saturator (made up of Pyrex glass). It can be operated at temperatures up to *ca.* 523 K using silicon oil as heating medium. In the present study the temperature in the saturator was constantly maintained above the melting point of solid PNT (*i.e.* 403 K) such that it is melted and becomes present in a liquid state, through which a known amount of nitrogen gas as a carrier was bubbled to obtain desired flow rates of PNT throughout the catalytic runs. In fact, two separate lines were used for the passage of the nitrogen gas, one is for nitrogen bubbling through the saturator and the other is used for maintaining constant space velocities and residence times throughout the runs. The exact amount of PNT fed is separately determined from GC analysis prior to the actual catalytic runs. Two thermocouples were positioned one at the centre of the catalyst bed to indicate reaction temperature and the other one was attached to the furnace through the temperature indicator cum controller to monitor the temperature of the reaction. 2 g of the catalyst particles (1.0 to 1.25 mm size) mixed with corundum crystals were loaded in the reactor for catalytic runs. For some blank tests, the reactor was loaded with glass beads in equal amounts as catalyst particles and operated under identical conditions to the real catalytic experiments. The product stream was collected every half-an-hour and analysed by gas chromatography (GC 17A, Shimadzu, Japan with auto sampler) equipped with an FID module using a capillary column (FS-SE-54). The carbon oxides were continuously monitored by an on-line non-dispersive infrared analyser (Rosemount, BINOS 100 2M, Germany).

The start up procedure for every test, prior to performing the real tests, is that, PNT was metered from the saturator (maintained at 403 K) for one hour with nitrogen bubbling at a flow rate of 2 L h<sup>-1</sup> at an oven (reaction) temperature of 473 K

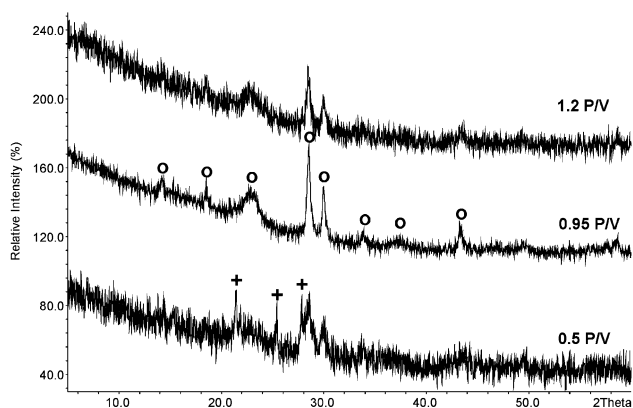


Scheme 1

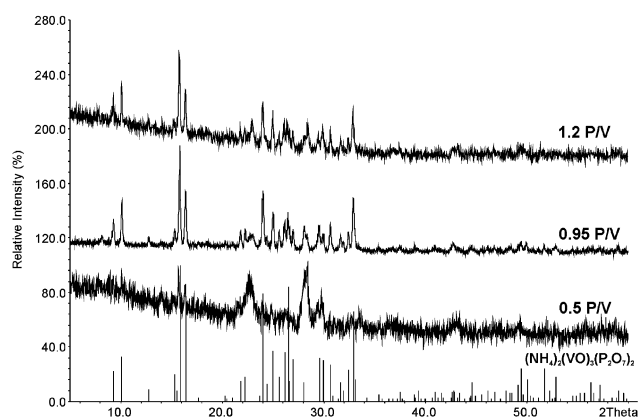
and then PNT is collected from the reactor outlet for half-an-hour and analysed by GC to know the exact amount of PNT, that is coming out from the saturator. The same amount is used for further calculations of conversion (ratio of reacted moles of organic compound related to concentration in feed), selectivities (moles of formed product divided by moles of reacted compound, multiplied by carbon number of product and divided by that of reactant, to get stoichiometric corrected values) and carbon balance. It is also confirmed that no reaction took place at 473 K oven temperature at which PNT was collected prior to actual catalytic tests.

## Results and discussion

XRD patterns of both fresh and used (bulk) VPO catalysts are shown in Figs. 1 and 2. All the three parent samples except the one with the lowest P/V ratio (0.5 P/V) have exhibited only crystalline  $(\text{VO})_2\text{P}_2\text{O}_7$  phase (hereinafter called as VPP) [ASTM card no: 34-1381] with principal  $2\theta$  values of 22.96, 28.43, 29.94 and 43.41 that correspond to crystal planes (020), (204), (221) and (008). The catalyst with the lowest P/V ratio (0.5 P/V) has exhibited traces of a V(v)-containing  $\gamma\text{-VOPO}_4$  phase in addition to the major VPP phase [ASTM card no: 47-950]. All these samples calcined in  $\text{N}_2$  atmosphere appear to be less crystalline compared to the XRD patterns of their corresponding parent bulk precursors. The most probable reason for the exhibition of amorphous nature by all the calcined samples appears to be due to the performance of calcination at low temperatures (723 K) and in  $\text{N}_2$  atmosphere. All the precursors in the present investigation were prepared through an organic medium using alcohols as reducing agents. Therefore,



**Fig. 1** XRD patterns of the parent bulk VPO catalysts (0.5 P/V, 0.95 P/V, 1.2 P/V); o- $(\text{VO})_2\text{P}_2\text{O}_7$ , +  $\gamma\text{-VOPO}_4$ .



**Fig. 2** XRD patterns of the used bulk VPO catalyst samples showing the formation of  $(\text{NH}_4)_2(\text{VO})_3(\text{P}_2\text{O}_7)_2$  besides the remaining  $(\text{VO})_2\text{P}_2\text{O}_7$  phase.

the presence of organic alcohols trapped between the layers of precursor is believed to modify the mechanism of the phase transformation from precursor to active phase during calcination. The transformation to the active phase does not seem to occur in the absence of gaseous oxygen because the trapped alcohols are to be removed only in the form of  $\text{CO}_2$  and therefore the presence of gaseous oxygen is essential for this process of removal of alcohols. Otherwise, when the samples are calcined under anaerobic conditions *i.e.* in  $\text{N}_2$  atmosphere, this removal of alcohols as  $\text{CO}_2$  occurs probably due to removal of lattice oxygen from the catalyst structure, which makes the sample amorphous in nature. According to this interpretation, the process of alcohol release in the absence of gaseous oxygen is a very slow process and hence causes further reduction in the catalysts during the course of release of alcohols with simultaneous phase transformation. This also resulted in the reduction of the average oxidation state of vanadium below +4 in the catalysts that contain high P/V ratios.<sup>22</sup>

A careful examination of the results of the XRD studies of used (bulk) VPO catalysts (Fig. 2) would reveal that the severe reaction conditions have brought about drastic changes in surface characteristics of the V-oxide species in these catalysts. The phase transformation from VPP to crystalline  $(\text{NH}_4)_2(\text{VO})_3(\text{P}_2\text{O}_7)_2$  (ASTM card no: 47-804) (herein after called, AVP) has been found to occur partly in all the used catalysts. But interestingly, complete phase transformation from VPP to AVP is not observed in any of the catalysts under the present study and the amount of AVP depended mainly on the duration of the catalytic tests. It can also be seen from Fig. 2 that this phase transformation from VPP to AVP is much more pronounced in the cases of 0.95 P/V and 1.2 P/V used (bulk) VPO catalysts as they were tested for longer times. However, this transformation has no effect on the catalytic performance of the catalyst. This kind of transformation (VPP into AVP) has also been observed and reported in more detail elsewhere.<sup>23,24</sup>

Relative intensities of XRD reflections (with background correction) correspond to AVP and VPP phases and the changes in surface areas between fresh and used (bulk) VPO catalysts are presented in Table 1. It is evident that the surface areas of all the fresh catalysts were observed to decrease after use owing to the phase transformation from VPP into AVP. The remarkable decrease in the surface area of used 0.95 P/V bulk VPO catalyst is due to the reason that this catalyst has been tested for a longer period of time compared to the other two catalysts and hence the phase transformation from VPP into AVP is also significantly higher in this catalyst.

Prior to ammoxidation runs, some blank tests (in the absence of catalyst particles) have been carried out over a wide range of reaction temperatures from 463 K to 678 K under identical conditions as used for real catalytic tests to check the oxidation stability and the thermal decomposition of PNT, if any.

The PNT flow rates vs. reaction temperature during blank tests are shown in Fig. 3. It is evident that the flow rate of PNT is found to be consistent and maintained more or less constant ( $2.26 \text{ mmol h}^{-1}$ ) up to a temperature of 618 K and then the amount of PNT is decreased from  $2.26 \text{ mmol h}^{-1}$  to  $1.61 \text{ mmol h}^{-1}$  with a further increase in temperature from 618 K to 678 K.

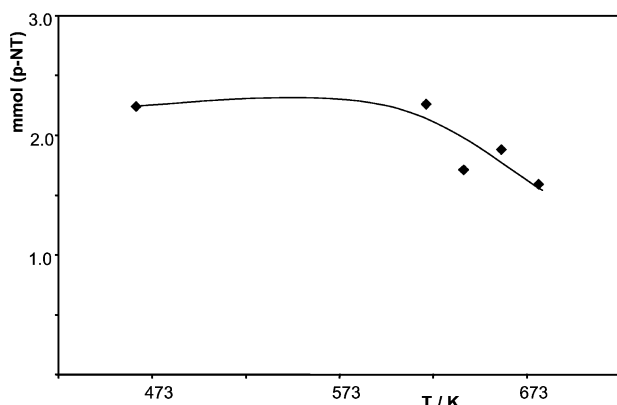
**Table 1** Relative intensities of XRD reflections of used VPO catalysts (with background correction) correspond to  $(\text{NH}_4)_2(\text{VO})_3(\text{P}_2\text{O}_7)_2$  (AVP) and  $(\text{VO})_2\text{P}_2\text{O}_7$  (VPP) phases and surface areas of fresh and used VPO catalysts.

| Catalyst | Rel. int. AVP | Rel. int. VPP | BET surface area/ $\text{m}^2 \text{g}^{-1}$ |      |
|----------|---------------|---------------|--|------|
|          |               |               | Fresh  | Used |
| 0.5 P/V  | 66            | 100           | 14.6   | 10.5 |
| 0.95 P/V | 100           | 14            | 40.0   | 5.3  |
| 1.2 P/V  | 100           | 35            | 28.2   | 9.7  |

It is surprising to note that there is a loss of *ca.* 30% in the recovered PNT portion with increase in temperature. It seems likely that PNT is undergoing some kind of thermal decomposition even in the absence of catalyst at temperatures higher than *ca.* 623 K. This might also be one of the more probable and main reasons for obtaining lower carbon balances when experiments were performed at higher temperatures above 623 K. After observing the *ca.* 30% loss of PNT at 678 K, the temperature is again reduced back to the minimum temperature (*i.e.* 463 K) where the first sample is collected and again collected a sample for comparison under identical conditions and gas flows and obtained the same amount of PNT (2.26 mmol h<sup>-1</sup>) as found earlier.

Hence, we have restricted all our experiments to a reaction temperature below 623 K, though the conversions are rather low at these temperatures. We have also achieved higher conversions of *ca.* 90% at higher temperatures in the range from 653 K to 683 K but the carbon balances are very bad and, therefore, these results are not included.

The results obtained in the ammoxidation of PNT over bulk VPO catalysts are shown in Table 2. It can be seen that the selectivity of PNB is observed to increase with increase in P/V ratio of the catalysts. A maximum selectivity of 77% was exhibited by the VPO catalyst with a P/V ratio of 1.2 at a conversion of 13% with a good carbon balance of 100% at a reaction temperature of 603 K. The maximum activity (47% conversion) was obtained on 0.95 P/V catalyst which is close to the stoichiometric P/V ratio of (VO)<sub>2</sub>P<sub>2</sub>O<sub>7</sub> but the selectivity towards nitrile was only 24%, with a carbon balance of 81%, at a reaction temperature of 603 K. This result points to an oxidative decomposition of PNT and/or PNB. A similar poor C-balance was found on 0.5 P/V catalyst that might be the most active system due to the surplus of VO<sub>x</sub> species and hence the lower selectivity of nitrile. However, the conversion on the 0.5 P/V catalyst is rather low and that could point to an easier deactivation of this catalyst. The ammoxidation reaction on all these bulk VPO catalysts was carried out under an identical molar ratio, PNT:H<sub>2</sub>O:NH<sub>3</sub>:air:N<sub>2</sub> = 1:15:6:30:46–55; with space velocity (GHSV) in the range of 2290–2985 h<sup>-1</sup> and



**Fig. 3** Variation of flow rate of *p*-nitrotoluene with temperature during blank tests.

**Table 2** Activity and selectivity behaviour of various bulk VPO catalysts in the ammoxidation of *p*-nitrotoluene

| Catalyst <sup>a</sup> | T/K | Conversion (%) (PNT) | Selectivity (%) (PNB) | C-balance (%) |
|-----------------------|-----|----------------------|-----------------------|---------------|
| 0.5 P/V               | 623 | 28                   | 10                    | 78            |
| 0.95 P/V              | 563 | 12                   | 50                    | 98            |
|                       | 603 | 47                   | 24                    | 81            |
| 1.2 P/V               | 603 | 13                   | 77                    | 100           |

<sup>a</sup> Molar ratio of PNT:H<sub>2</sub>O:NH<sub>3</sub>:air:N<sub>2</sub> = 1:15:6:30:46–55; GHSV = 2290–2985 h<sup>-1</sup>; CT = 1.21–1.57 sec.

contact time in the range of 1.21 to 1.57 sec. The major products identified were only PNB and total oxidation products (*i.e.* CO and CO<sub>2</sub>). No other by-products were identified during the course of entire period of these investigations.

Similar observations of decreasing activity and increasing selectivity with increase in phosphorus content (*i.e.* P/V ratio) of the catalysts were also made from our earlier investigations during ammoxidation of other organic substrates. The role of phosphorus is mainly to stabilise reduced vanadium species [*i.e.* V(IV)] in the catalysts. The increase in phosphorus content beyond the stoichiometric P/V ratio (*i.e.* > 1) causes further stabilisation of reduced vanadium species and hence, excess phosphorus inhibits the reoxidation of the bulk, which in turn causes a decrease in the activity of the catalysts. The decrease in the catalytic activity of the catalysts with increase in P/V ratios might also be due to the reason that the catalysts with higher P/V ratios produce larger crystallites, and exhibit different phase compositions and morphologies compared to the ones with the lower P/V ratios. Another reason for decrease in catalytic activity is that the number of active sites (vanadium-containing species) is also supposed to be decreased with an increase in phosphorus content because of dilution of active sites with excess phosphorus especially at higher P/V ratios. All these factors collectively influence the overall performance and decrease the catalytic activity of the catalysts in general with increase in phosphorus content.

The catalyst with the lowest P/V ratio of this series gave the lowest selectivity of PNB and the carbon balance. The high non-selectivity of this catalyst can be explained on the basis that it contains an excess of highly active lattice oxygen and also due to less stabilisation of reduced vanadium species because of less phosphorus content in the catalyst.

The results of ammoxidation runs on some supported VPO catalysts are depicted in Table 3. The data demonstrate that anatase (TiO<sub>2</sub>) supported VPO catalyst exhibited better selectivity compared to all other supported catalysts investigated in the present study. It has exhibited a maximum conversion of 26% with a nitrile selectivity of 26% (carbon balance 90%) at a reaction temperature of 608 K. The same catalyst at a low conversion (6%) exhibited as high as 100% selectivity of nitrile with 100% carbon balance. The reaction was carried out on these supported catalysts at a molar ratio of PNT:H<sub>2</sub>O:NH<sub>3</sub>:air:N<sub>2</sub> = 1:15:6:35:46–51, GHSV = 2242 to 3356 h<sup>-1</sup> and a contact time in the range from 1.07 to 1.47 seconds. Rutile (TiO<sub>2</sub>) and α-Al<sub>2</sub>O<sub>3</sub> supported catalysts have exhibited very low conversions (<5%) compared to all other catalysts. However, the supported VPO catalysts were not effective as expected to improve the catalytic performance of bulk VPO samples.

Activity and selectivity behaviour of supported vanadium(V) oxide catalysts are presented in Table 4. The reaction was carried out in the range from 563 to 608 K, at a molar ratio of PNT:H<sub>2</sub>O:NH<sub>3</sub>:air:N<sub>2</sub> = 1:15:6:35:46–56, with GHSV = 2500 to 2900 h<sup>-1</sup> and contact time = 1.24 to 1.44 seconds. Among all the catalysts screened, the anatase supported V<sub>2</sub>O<sub>5</sub>

**Table 3** Activity and selectivity behaviour of supported VPO catalysts (P/V = 0.95 solid was used) in the ammoxidation of *p*-nitrotoluene

| Catalyst <sup>a</sup>                | T/K | Conversion (%) (PNT) | Selectivity (%) (PNB) | C-balance (%) |
|--------------------------------------|-----|----------------------|-----------------------|---------------|
| VPO/γ-Al <sub>2</sub> O <sub>3</sub> | 603 | 7                    | 36                    | 97            |
|                                      | 623 | 19                   | 24                    | 88            |
| VPO/α-Al <sub>2</sub> O <sub>3</sub> | 583 | 4                    | 20                    | 97            |
| VPO/TiO <sub>2</sub> (anatase)       | 588 | 6                    | 100                   | 100           |
|                                      | 608 | 26                   | 26                    | 90            |
| VPO/TiO <sub>2</sub> (rutile)        | 583 | 1                    | 43                    | 99            |
|                                      | 603 | 2                    | 43                    | 99            |

<sup>a</sup> 25 wt% VPO and 75 wt% support; molar ratio of PNT:H<sub>2</sub>O:NH<sub>3</sub>:air:N<sub>2</sub> = 1:15:6:35:46–51; GHSV = 2442–3356 h<sup>-1</sup>; CT = 1.07–1.47 sec.

**Table 4** Activity and selectivity behaviour of supported vanadia catalysts in the ammoxidation of *p*-nitrotoluene

| Catalyst <sup>a</sup>   | T/K | Conversion (%) (PNT) | Selectivity (%) (PNB) | C-balance (%) |
|---|-----|----------------------|-----------------------|---------------|
| 10% V <sub>2</sub> O <sub>5</sub> /Al <sub>2</sub> O <sub>3</sub> | 563 | 11                   | 30                    | 95            |
|   | 588 | 22                   | 27                    | 96            |
| 10% V <sub>2</sub> O <sub>5</sub> /TiO <sub>2</sub> (rutile)      | 603 | 8                    | 16                    | 94            |
| 10% V <sub>2</sub> O <sub>5</sub> /TiO <sub>2</sub> (anatase)     | 593 | 27                   | 62                    | 98            |
|   | 608 | 63                   | 17                    | 68            |

<sup>a</sup> Molar ratio of PNT:H<sub>2</sub>O:NH<sub>3</sub>:air:N<sub>2</sub> = 1:15:6:35:46–56; GHSV = 2500–2900 h<sup>-1</sup>; CT = 1.24–1.44.

catalyst is found to exhibit good activity and selectivity giving 27% conversion of PNT with 62% PNB selectivity. The same catalyst has also exhibited a high conversion of 63% at a reaction temperature of 608 K, but the selectivity has been dropped to only 17%. The results showed that the presence of anatase had a great influence on the activity and selectivity of the catalysts. It is well known and well documented in the literature that the anatase modification of TiO<sub>2</sub> is more suitable as a support and enhances the activity of especially the vanadium-based catalysts. Such enhancement has also been observed in the selective oxidation *o*-xylene,<sup>25</sup> the oxidation of toluene<sup>26</sup> and the ammoxidation of toluene.<sup>27</sup> This effect of enhancement in the activity is mainly due to active phase-support interaction and various explanations have been proposed in the literature. The rutile form of titania is not suitable as a good support due to the weak active phase-support interaction, which results in poor dispersion and also the formation of crystalline V<sub>2</sub>O<sub>5</sub> phase even at lower loadings.

One of the main reasons for limited nitrile selectivity at higher conversions could be found in substituent effects and charge stabilisation of intermediates through the entire reaction. The dispersal or concentration of the charge due to electron release or electron withdrawing nature of the substituent groups greatly influences the reactivity of the aromatic ring. It is well known that a group attached to a benzene ring would affect the stability of the intermediate carbocation either by dispersing or intensifying the positive charge depending upon electron releasing or withdrawing nature of the substituent group. The electron releasing nature of a –CH<sub>3</sub> group neutralises the positive charge of the ring and becomes more positive itself, in turn dispersing the charge and stabilising the carbocation. In a similar manner, the inductive effect stabilises the developing positive charge in the transition state and thus leads to a faster reaction. On the other hand, the presence of a –NO<sub>2</sub> group, which has an electron withdrawing inductive effect, tends to intensify the positive charge, and destabilises the carbocation, which in turn causes a slower reaction. It is widely accepted that a group that releases electrons activates the ring and a group that withdraws electrons deactivates the ring. This is the same situation, which is expected to operate well with *p*-nitrotoluene due to the presence of a strong electron withdrawing –NO<sub>2</sub> group that remarkably destabilise the intermediate carbocation, which in turn significantly reduces the reactivity of the molecule. There is indeed an influence of three highly electronegative atoms (1 N and 2 O from –NO<sub>2</sub> group) on the aromatic ring. This appears to be a more probable reason for exhibiting lower activities and selectivities of the catalysts for the present reaction of study. However, at lower conversion rates high nitrile selectivity was reached. Nevertheless, the results of the present investigation indicate that there is an ample scope for further development and improvement in the activity and selectivity behaviour of various catalysts to obtain higher yields of PNB.

## Conclusions

The vapour phase ammoxidation is the most ecological and economical synthesis route to *p*-nitrobenzotrile starting from *p*-nitrotoluene. V<sub>2</sub>O<sub>5</sub>/TiO<sub>2</sub> (anatase) is found to exhibit good catalytic performance with a nitrile selectivity of 62% at 27% conversion. Using VPO catalysts, a maximum nitrile selectivity of 77% at 13% conversion was obtained over a bulk VPO catalyst with a P/V ratio of 1.2. However, at low conversion up to ca. 10%, a nitrile selectivity of almost 100% can be reached. The strong electron withdrawing effect of the nitro group leads to an increased destabilisation of the aromatic ring of reaction intermediates that can be easily attacked by oxygen. Hence, the catalyst performance is mainly limited by oxidative destruction reactions of the reactant at reaction temperatures above 623 K.

## Acknowledgement

The authors thank Mrs J. Kubias and Mrs H. French for experimental assistance.

## References

- 1 A. Martin and B. Lücke, *Catal. Today*, 2000, **57**, 61.
- 2 B. Lücke and A. Martin, *Ammoxidation of aromatic side-chains in: Fine Chemicals through Heterogeneous Catalysis*, eds. R. Sheldon and H. van Bekkum, VCH-Wiley, Weinheim, 2001, p. 527.
- 3 K. Weissermel and H.-J. Arpe, *Industrielle Organische Chemie*, VCH, Weinheim, 1994, 4. Aufl., pp. 207, 330, 430.
- 4 B. V. Suvorov, *Ammoxidation of Organic Compounds*, Nauka, Alma-Ata, 1971 (Russ.).
- 5 R. K. Grasselli, *Catal. Today*, 1999, **49**, 141.
- 6 *Ullmann's Encyclopedia of Industrial Chemistry*, 5th Completely Revised Edition, vol. 17A, VCH, Weinheim, 1991, p. 371.
- 7 S. Talukdar, J.-L. Hsu, T.-C. Chou and J.-M. Fang, *Tetrahedron Lett.*, 2001, **42**, 1103.
- 8 H. Suzuki, Y. S. Hwang, C. Nataya and Y. Matano, *Synthesis*, 1993, **12**, 1218.
- 9 B. Das, C. Ramesh and P. Madhusudhan, *Synlett.*, 2000, **11**, 1599.
- 10 D. A. Kaiser, P. T. Kaye, L. Pillay and G. H. P. Roos, *Synth. Commun.*, 1984, **14**, 883.
- 11 A. Hulkenberg and J. J. Troost, *Tetrahedron Lett.*, 1982, **23**, 1505.
- 12 K. Smith, T. Gibbins, R. W. Millar and R. P. Claridge, *J. Chem. Soc., Perkin Trans. 1*, 2000, **16**, 2753.
- 13 D. M. Tschaen, R. Desmond, A. O. King, M. C. Fortin and B. Pipik, *Synth. Commun.*, 1994, **24**, 887.
- 14 E. Bordes, *Catal. Today*, 1987, **1**, 499.
- 15 G. Centi, *Catal. Today*, 1993, **16**, 1.
- 16 A. Martin, B. Lücke, H. Seeboth, G. Ladwig and E. Fischer, *React. Kin. Catal. Lett.*, 1989, **38**, 33.
- 17 A. Martin, B. Lücke, H. Seeboth and G. Ladwig, *Appl. Catal.*, 1989, **49**, 205.
- 18 I. Matsuura, *Stud. Surf. Sci. Catal.*, 1992, **72**, 247.
- 19 R. G. Rizayev, E. A. Mamedov, V. P. Vislovskii and V. E. Sheinin, *Appl. Catal. A: General*, 1992, **83**, 103.
- 20 N. R. Bukeikhanov and B. V. Suvorov, in *Khim. Monomeroi i Polimeroi*, Nauka, Alma-Ata, 1980, p. 3.
- 21 P. V. Vorobyev, N. R. Bukeikhanov, A. G. Lyubarskii, O. N. Satnikova, A. G. Gorelik and B. V. Suvorov, *Izv. Akad. Nauk Kaz. SSR Ser. Khim.*, 1983, (No.5), 34.
- 22 G.-U. Wolf, unpublished results.
- 23 Y. Zhang, A. Martin, G. Wolf, S. Rabe, H. Worzala, B. Lücke, M. Meisel and K. Witke, *Chem. Mater.*, 1996, **8**, 1135.
- 24 A. Martin, L. Wilde and U. Steinike, *J. Mater. Chem.*, 2000, **10**, 2368.
- 25 A. Andersson and S. Hansen, *J. Catal.*, 1988, **114**, 332.
- 26 A. J. van Hengstum, J. G. van Ommen, H. Bosch and P. J. Gellings, *Appl. Catal.*, 1983, **8**, 369.
- 27 F. Cavani, E. Foresti, F. Trifirò and G. Busca, *J. Catal.*, 1987, **106**, 251.



# A solvent-free method for preparing improved quality ion-selective electrode membranes

Thierry Le Goff,<sup>a</sup> James Marsh,<sup>b</sup> Jim Braven,<sup>a</sup> Les Ebdon<sup>\*a</sup> and David Scholefield<sup>c</sup>

<sup>a</sup> Department of Environmental Sciences, Plymouth Environment Research Centre, University of Plymouth, Drake Circus, Plymouth, UK PL4 8AA. E-mail: lebdon@plymouth.ac.uk

<sup>b</sup> Imerys, John Keay House, St. Austell, Cornwall, UK PL25 4DJ

<sup>c</sup> Institute of Grassland and Environmental Research, North Wyke, Okehampton, Devon, UK EX20 2SB

Received 12th July 2002

First published as an Advance Article on the web 26th September 2002

A solvent-free method for making hot-pressed ion-selective membranes has been developed. The method not only overcomes the expensive use and recovery of organic solvents but also gives rise to superior quality tougher and longer-lived membranes. As described the method has been applied to an established nitrate selective ion exchange electrode membrane. The technique however should have a much wider general applicability in membrane technology. The method used a combination of milling technology with a clay-based filler (PoleStar™ 200R). *N,N,N*-triallyl leucine betaine (nitrate sensor), polystyrene-*block*-polybutadiene-*block*-polystyrene (SBS polymer), 2-nitrophenyl octyl ether (solvent mediator), dicumyl peroxide (free radical initiator) and PoleStar™ 200R (filler) which were mixed using a rolling mill without solvent. After cross-linking and appropriate conditioning, the resulting rubbery membrane exhibited a linear response from 1400 to 0.07 ppm nitrate-N with a slope of  $-58.5$  mV per decade. The limit of detection was 0.01 ppm nitrate-N and the selectivity coefficient for nitrate against chloride,  $K^{\text{Pot}}_{\text{NO}_3^-, \text{Cl}^-}$ , was  $4.0 \times 10^{-3}$ . A field evaluation in agricultural drainage waters of the resulting clay-based membrane was performed for 15 weeks. The nitrate levels determined with the novel nitrate-ISE compared favourably with the standard method using a nitrate-ISE previously developed by our group ( $R^2 = 0.96$ ,  $y = 1.1x + 0.55$ ). Clay based membranes had an approximately threefold improvement in both tensile strength and resistance to penetration relative to the clay free membranes. Field performance was also improved by at least a 20% increase in lifetime.

## Aim of investigation

Numerous nitrate sensors have been reported<sup>1</sup> most of which are based upon tris(1,10-phenanthroline)nickel(II)<sup>2</sup> or hydrophobic quaternary ammonium salts.<sup>3</sup> Their mechanism of action is based on ion exchange following a Hofmeister-type selectivity.<sup>4,5</sup> It is well recognised that ion selective electrodes (ISEs) often perform well under laboratory conditions but suffer from a lack of stability when used in the environment.<sup>6</sup> Nitrate-ISEs are commercially available and are generally based upon a membrane having the sensor trapped in an inert polymer matrix such as poly(vinyl chloride) (PVC). A variation on this principle had involved immobilising the nitrate sensor by covalent attachment to a polymer.<sup>7,8</sup>

Recently a novel class of nitrate sensors based upon *N,N,N*-triallyl  $\alpha$ -amino acid betaine salts was reported by the present group.<sup>9</sup> *N,N,N*-Triallyl leucine betaine yielded an ISE having a limit of detection (LOD) of 0.005 ppm nitrate-N and a selectivity coefficient for nitrate against chloride,  $K^{\text{Pot}}_{\text{NO}_3^-, \text{Cl}^-}$ , of  $3.4 \times 10^{-3}$ . The low LOD, good stability, rapid response, acceptable lifetimes and a working pH range of 2–8 made these electrodes the most suitable ever reported for use in environmental nitrate monitoring. This was demonstrated later by their evaluation in continuous use in drainage waters for 5 months with no re-calibration or maintenance.<sup>10</sup> Over a large nitrate concentration range (0.47–16 ppm nitrate-N) there was an excellent correlation ( $R^2 = 0.99$ ) between the ISEs and the laboratory-based method. The regression line had a gradient (0.95) that did not differ significantly from 1 at the 95% confidence level indicating that there was no systematic error. The electrode performance showed that the method was capable of replacing laboratory-based spot sample analyses and offered

a novel continuous method of monitoring nitrate in environmental freshwater.

Preparation of polystyrene-*block*-polybutadiene-*block*-polystyrene (SBS)-based membranes followed that of previous studies.<sup>11,12</sup> The uncross-linked paste was obtained by dissolving all the membrane components in tetrahydrofuran (THF) and subsequent evaporation of the solvent. This step is also commonly used for the preparation of PVC-based membranes by solvent casting,<sup>13</sup> a process which is expensive in solvent, time demanding, generates hazardous waste and gives a two-sided membrane response.<sup>14</sup> THF is a commonly used polymer

## Green Context

We have seen an increasing use of solvent-free chemical processing reported in this journal. It is important to realise that the technology is not restricted to the more familiar synthesis of organic compounds but can also be applicable to materials synthesis, for example. Here we see the use of solvent-free chemistry applied to the preparation of ion-selective electrode membranes. These materials often suffer from poor performance when used in the environment due to a lack of stability. This paper describes a milling method for making polymeric membranes. The methodology shows several advantages compared to traditional methods notably being solvent-free, fast, relatively inexpensive and significantly giving more stable materials. The resulting materials show increased tensile strength and improved longevity.

JHC

solvent. Overexposure to it can cause irritation of eyes, nausea, dizziness, headache and skin irritation.<sup>15</sup>

In the present paper, we report a solvent-free method for fabricating liquid polymeric membranes for ISEs. This method, based upon the use of a clay-based filler combined with milling technology, was used to produce SBS-based membranes containing a covalently bound nitrate sensor. Clay-based fillers find use in a variety of applications in the polymer industry, *e.g.* they facilitate homogeneous mixing of a polymer with other components, especially non-volatile liquids and also impart excellent electrical insulation and improve the robustness of rubber-based products. The use of these procedures in the present project offered the prospect of mixing rapidly all the membrane components without solvent and producing membranes of improved robustness. *N,N,N*-Triallyl leucine betaine chloride was used as nitrate sensor and two different grades of clay-based filler, PoleStar™ 200R and PoleStar™ 400, were evaluated for the production of nitrate-selective membranes using a milling process.

A field evaluation of the new membranes was undertaken in drainage waters from a 1 ha grassland lysimeter plot at the Institute of Grassland and Environmental Research (IGER) station on the Rowden Moor site.<sup>16</sup> The present group had already used this experiment site for previous field trials<sup>10</sup> and the drainage water was known to cover a wide nitrate concentration range (1–20 ppm nitrate-N) which is ideal for evaluation of the nitrate-ISEs.

## Experimental

### Apparatus and reagents

The potential measurements in the laboratory were made using a high impedance voltmeter (HI 931402 Microprocessor, Hanna Instruments Ltd., Beds, UK). The electrode assembly was composed of a nitrate-ISE based upon a commercially available electrode body IS560 (Philips Analytical, Cambridge, UK) and a double junction reference electrode (model 90-02, Orion Research, Cambridge, MA, USA).

The basic field instrument used in this work has been previously described.<sup>10</sup> The one used for the present study comprised one set of two nitrate ISEs (one containing a clay-based membrane and the other clay-free), one reference electrode, connected through a pre-amplifier to a data-logger (CR10X1, Campbell Scientific, UK) and a 12 V battery supply (NP24-12B, YUASA Corporation, Taiwan). This set-up allowed the two ISEs to be compared under identical conditions in order to assess their reproducibility.

The equipment used for the milling was a twin roll mill having a face length of 30 cm, a roll diameter of 15 cm and was running at a friction ratio of 1.25:1. The clay-based fillers, PoleStar™ 200R (particle size: 2 µm) and Polestar™ 400 (particle size: 4 µm) were manufactured by Imerys (Imerys Minerals Ltd., St. Austell, UK) and produced by heating highly refined kaolins to temperatures above 1000 °C. They were selected because they were chemically inert and gave low levels of mill striking when used with polymers.

The SBS polymer was obtained from Aldrich (Gillingham, Dorset, UK). THF (Rathburn Chemicals, Walkburn, Scotland) was refluxed over potassium metal and freshly distilled prior to use. Dicumyl peroxide (DCP) and 2-nitrophenyloctyl ether (2-NPOE) were obtained from Fluka (Selectophore grade, Fluka, Glossop, Derbyshire, UK) and were used as received. Potassium nitrate, potassium chloride, ammonium sulfate, sodium hydroxide, citric acid, trisodium citrate and potassium dihydrogen orthophosphate were obtained from BDH Chemicals (AnalaR, Dorset, UK). Pure water was obtained using a Milli-Q water system (Milli-Q, Millipore (UK) Ltd., Watford,

UK). A commercial nitrate-ISE (ELITE, Merck Ltd, Lutterworth, Leicestershire, UK) was used for performance comparison purposes.

### Membrane preparation using the THF-based method

The membranes were composed of SBS (0.565 g, 43.5% m/m) dissolved in freshly distilled THF (6 ml), free radical initiator, DCP (0.13 g, 10% m/m), solvent mediator, 2-NPOE (0.52 g, 40%) and *N,N,N*-triallyl leucine betaine salt as nitrate sensor molecule (0.085 g, 6.5% m/m). The suspension was then shaken until dissolution was complete. The solvent was then evaporated by drying to constant weight in a vacuum oven at room temperature (5 days) over phosphorus pentoxide. The hot pressing process was used to ensure covalent binding of the sensor moiety into a cross-linked co-polymer. The resulting membrane was 7 cm in diameter and 0.3 mm in thickness.

### Membrane preparation using the solvent-free method

The rolling mill was pre-heated at 140 °C and the SBS was melted and milled to form a sheet (23.9 g, 32.6% m/m) followed by small additions of Polestar 200R (18.3 g, 25% m/m) and 2-NPOE (22.0 g, 30.0% m/m). After 5 min the milling produced a homogeneous mixture of the three components and DCP (5.5 g, 7.5% m/m) was quickly added. Because of the large scale of the milling process (69.7 g), *N,N,N*-triallyl leucine betaine chloride (0.064 g, 4.9% m/m) was then added to a sample of the uncross-linked paste (1.236 g, 95.1% m/m) and manually mixed without the use of solvent in an agate pestle and mortar. The resulting uncross-linked paste (1.3 g) was then hot-pressed as described in the THF-based method. The membranes were 7 cm in diameter and 0.3 mm in thickness.

### Membrane electrochemical evaluation

Discs of 7 mm diameter were punched from hot pressed master membranes and conditioned in 0.1 mol dm<sup>-3</sup> potassium nitrate solution for seven days. The conditioned membrane was assembled into the tip of the electrode containing an equimolar mixture of potassium nitrate and potassium chloride (0.1 mol dm<sup>-3</sup>). The electrode assembly was completed with a double junction reference electrode having an outer filling solution composed of ammonium sulfate (0.04 mol dm<sup>-3</sup>). Potassium nitrate standards were prepared using Milli-Q water and contained 0.01 mol dm<sup>-3</sup> potassium dihydrogen orthophosphate solution as ionic strength adjustment buffer (ISAB). The potential measurements were made at 25 ± 0.5 °C in stirred solutions for reproducibility purposes.

The slope of the calibration curve is a linear function of the logarithm of nitrate ion concentration and was measured as the gradient of the observed linear range.<sup>17</sup> The range of linear response was measured over the region of the calibration curve exhibiting a Nernstian slope.

The LOD was measured from the experimental data as the point of the intersection between a linear extrapolation of the Nernstian slope, and the horizontal part of the upper curve where the cell potential is a constant value.<sup>17</sup>

Selectivity coefficients ( $K^{\text{pot}}_{\text{NO}_3^-, \text{Cl}^-}$ ) were determined accordingly to IUPAC recommendations<sup>18</sup> for ions of same charges using the fixed interferent method (FIM) with a constant level of interfering anion (0.01 mol dm<sup>-3</sup>).

The pH dependency experiments were performed using 50 mmol dm<sup>-3</sup> citric acid/trisodium citrate/sodium hydroxide buffer solutions containing 1 mmol dm<sup>-3</sup> potassium nitrate. The pH was monitored with a pH electrode (Gelplas, General Purpose Combination, Merck, Lutterworth, UK) and a high



impedance pH meter (model 290, Pye Unicam, Cambridge, UK).

Speed of response ( $t_{90}$ ) was determined accordingly to IUPAC recommendations<sup>19</sup> by measuring the time required by the ISE to reach 90% of the equilibrium potential value. This was performed by measuring the time required for the ISE to equilibrate in a solution of 0.14 ppm nitrate-N solution having been previously immersed in a 0.014 ppm nitrate-N solution.

### Membrane robustness evaluation

Two different sets of experiments were carried out to compare the robustness of the membranes with and without PoleStar™ 200R. Firstly, membrane direct stress ( $s$ ) was determined using an electro-mechanical testing machine (Instron model 1026, Instron Ltd, High Wycombe, Buckinghamshire, UK) which had a force measuring system, provided by a load cell/weighbeam (0 to 50 kN in tension). Direct stress measurement is a good indicator of the robustness of a material and can be defined as the internal force a material exerts per unit area ( $A$ ), when it resists an external axial force ( $W$ ). In this experiment the axial force was tensile and therefore was positive. Direct stress can be calculated as shown in eqn. (1). The greater the value  $s$  the more robust is the material.

$$s = W \times A^{-1} \quad (1)$$

where  $A$  is the cross section in  $m^2$  and  $W$  is the external axial force in N

In a second experiment, the force required to puncture the membrane was determined. This was achieved by an electro-mechanical testing machine (Instron model 4301, Instron Ltd, High Wycombe, Buckinghamshire, UK) which had a force measuring system, provided by a load cell/weighbeam (0–5 kN in compression). A needle was fitted to the upper part of the testing machine and compressed against the membrane directly fitted in the ISE body. The force required to go through the membrane was measured.

### Exposure of membranes to sunlight

To test the effects of exposure to sunlight, membranes were exposed to a Suntest CPS xenon lamp which emitted radiation at environmentally realistic wavelengths. Radiation was emitted from a 1.8 kW xenon arc installed horizontally in a parabolic reflector and fitted with a UV filter, the radiation limit in the UV range was 290 nm, corresponding to natural sunlight. Before membrane irradiation, the lamp was switched on for an hour to allow the lamp to reach its maximum radiation intensity which was measured and the membranes were subjected to an average radiation intensity of  $700 \text{ W m}^{-2}$ . Membranes were irradiated for 50, 100, 295 and 545 min and conditioned for 15 days prior to electrochemical evaluation.

### Nitrate measurements in drainage waters

Our previous communication,<sup>10</sup> described in detail the field evaluation of a nitrate-ISE using membranes prepared with the THF-based method. Nitrate results obtained with the ISEs compared very favourably ( $R^2 = 0.99$ ,  $y = 0.95x + 0.01$ ) with those obtained with a laboratory standard method<sup>20</sup> using a segmented-flow instrument with spectrophotometric detection (SAN Plus Segmented Flow Analyser containing a SA4000/SA20000 Chemistry Unit; Skalar UK Ltd., York, UK).

In the present work, the same site and field instrument were used to compare membranes prepared, respectively, with the solvent-free and THF-based methods. The experiment was run from 16/02/00 to 31/05/00 and nitrate measurements were recorded at hourly intervals using a data-logger. Calibration checks were carried out every three weeks.

## Results and discussion

### Clay-based filler effect on membrane electrochemical parameters

An initial study was performed to investigate the effect of clay-based fillers when used in the fabrication of SBS membranes. This experiment was carried out by adding some clay in various proportions to a THF solution containing all the membrane components. Table 1 shows the composition of the membranes evaluated in this initial study. Membrane S0 was clay-free and of the type used in previous publications.<sup>9,10</sup> Membranes S1–S5 contained various amounts of PoleStar 200R, however S1 and S2 were free of sensor and membranes S6, S7 and S8 were fabricated using PoleStar 400. After drying, hot pressing and appropriate conditioning, the membranes were evaluated for linear range, slope and  $K^{\text{pot}}_{\text{NO}_3^-, \text{Cl}^-}$  determined as described in the experimental section. Table 2 shows that blank membranes S1 and S2 fabricated respectively with 10 and 25% m/m Polestar 200R exhibited sub-Nernstian slopes ( $-22.0 \text{ mV decade}^{-1}$  for S1 and  $-11.0 \text{ mV decade}^{-1}$ ) over a very narrow linear range (1400–14 ppm nitrate-N). This response was observed only for a short time and disappeared after approximately two weeks. This confirms that the response obtained from the clay-based membranes was obtained from the sensor and not due to the presence of the filler. Table 2 also shows that all the clay-based membranes containing the betaine sensor (S3–S8) had a similar performance to those fabricated without clay (S0). However, some differences in the membrane performance were observed between those using PoleStar 200R and PoleStar 400. Generally, membranes fabricated with PoleStar 200R gave better results for sensitivity and selectivity than those fabricated with PoleStar 400R. Membranes S3 and S4 fabricated respectively with 10 and 25% PoleStar 200R had a linear Nernstian range of 1400–0.07 and 1400–0.05 ppm nitrate-N with a slope of  $-59.25$  and  $-58.5 \text{ mV decade}^{-1}$ . This

**Table 1** Composition of membranes containing various amounts of clay-based filler (PoleStar 200R and PoleStar 400) and *N,N,N*-triallyl leucine betaine as nitrate sensor (S3–S8) compared with clay-free membrane (S0) and sensor-free membranes (S1 and S2)

| Membrane | 2-NPOE<br>(% m/m) | Sensor<br>(% m/m) | SBS<br>(% m/m) | DCP<br>(% m/m) | Calcined<br>clay (% m/m) |
|----------|-------------------|-------------------|----------------|----------------|--------------------------|
| S0       | 40.0              | 6.5               | 43.5           | 10.0           | 0.0                      |
| S1       | 38.5              | 0.0               | 41.9           | 9.6            | PoleStar 200R (10.0)     |
| S2       | 32.0              | 0.0               | 34.9           | 8.1            | PoleStar 200R (25.0)     |
| S3       | 36.0              | 5.9               | 39.1           | 9.0            | PoleStar 200R (10.0)     |
| S4       | 30.0              | 4.9               | 32.6           | 7.5            | PoleStar 200R (25.0)     |
| S5       | 20.0              | 3.25              | 21.75          | 5.0            | PoleStar 200R (50.0)     |
| S6       | 36.0              | 5.9               | 39.1           | 9.0            | PoleStar 400 (10.0)      |
| S7       | 30.0              | 4.9               | 32.6           | 7.5            | PoleStar 400 (25.0)      |
| S8       | 20.0              | 3.25              | 21.75          | 5.0            | PoleStar 400 (50.0)      |

**Table 2** Electrochemical performance of membranes S3–S8 compared with a commercial nitrate-ISE, a membrane without clay (S0) and sensor-free membranes (S1 and S2)

| Membrane number | Slope/mV decade <sup>-1</sup> | Linear Nernstian range/ppm nitrate-N | $K^{\text{pot}}_{\text{NO}_3^-, \text{Cl}^-}$ |
|-----------------|-------------------------------|--------------------------------------|---|
| S0              | -59.1                         | 1400–0.07                            | $3.4 \times 10^{-3}$                          |
| S1              | -22.0                         | 1400–14                              | N.D   |
| S2              | -11.0                         | 1400–14                              | N.D   |
| S3              | -59.25                        | 1400–0.07                            | $3.5 \times 10^{-3}$                          |
| S4              | -58.5                         | 1400–0.05                            | $4.0 \times 10^{-3}$                          |
| S5              | -56.75                        | 1400–0.07                            | $8.0 \times 10^{-3}$                          |
| S6              | -59.4                         | 1400–0.07                            | $4.0 \times 10^{-3}$                          |
| S7              | -53.25                        | 1400–0.14                            | N.D   |
| S8              | -54.875                       | 1400–0.14                            | N.D   |
| Commercial      | -59.0                         | 1400–0.14                            | $5.5 \times 10^{-3}$                          |

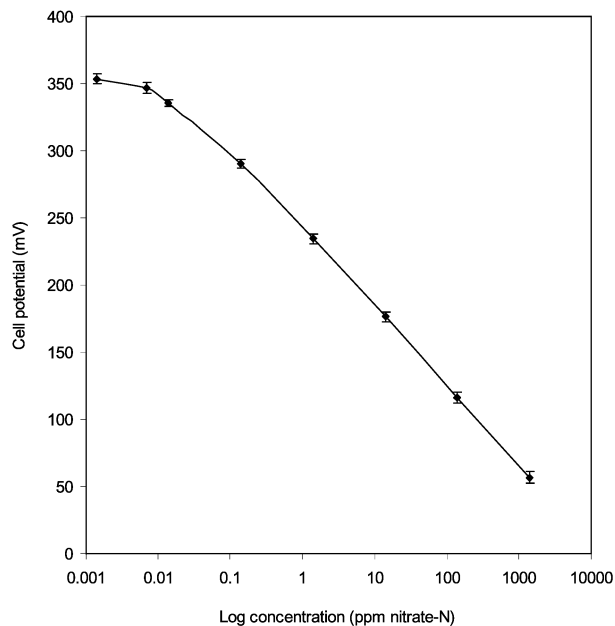
N.D: not determined

compared very favourably with membrane S0 (clay-free membrane) which exhibited a linear response between 1400–0.07 ppm nitrate-N with a slope of  $-59.1 \text{ mV decade}^{-1}$ . The selectivity coefficients for nitrate against chloride,  $K^{\text{pot}}_{\text{NO}_3^-, \text{Cl}^-}$ , were also very similar with values of  $3.5 \times 10^{-3}$  and  $4.0 \times 10^{-3}$ , respectively, determined with membranes S3 and S4 compared to  $3.4 \times 10^{-3}$  obtained with membrane S0. It was also noted that they exhibited better selectivity and sensitivity than the commercial nitrate-ISE. The speed of response ( $t_{90}$ ) was 30 s at low concentrations as described in the Experimental section and almost instantaneous at higher concentrations. The pH range of the membranes containing clay was also unchanged compared to clay-free membranes (2–8) which is satisfactory for freshwater monitoring. To conclude, PoleStar 200R (25% m/m) appeared an excellent candidate for being used as filler in the milling process because all the characteristics of the membrane were retained.

## Evaluation of nitrate-selective membranes milled with 25% m/m PoleStar 200R

### Laboratory evaluation

Membranes were fabricated using the solvent-free method as described in the experimental section. The results of the electrochemical evaluation obtained with the milled membranes S9 are shown in Fig. 1 and Table 3. As observed in the initial study, milled membranes S9 containing 25% m/m PoleStar 200R exhibited similar electrochemical characteristics to those obtained with membrane S0 (clay-free membrane). Membrane S9 yielded an ISE having a linear response from 1400 to 0.07 ppm nitrate-N, with a slope of  $-58.5 \text{ mV decade}^{-1}$ , which compared favourably with the linear range (1400–0.07 ppm nitrate-N) and the slope ( $-59.1 \text{ mV decade}^{-1}$ ) obtained with membrane S0. The selectivity coefficients for nitrate against chloride,  $K^{\text{pot}}_{\text{NO}_3^-, \text{Cl}^-}$ , were also very similar with values of  $4.0 \times 10^{-3}$  determined with membrane S9 compared to  $3.4 \times 10^{-3}$  obtained with membrane S0. The temperature dependency of membrane S9 was almost identical to that observed with membrane S0. Therefore, the temperature correction algorithm previously developed for the field evaluation<sup>10</sup> could also be used for membrane S9. The temperature dependency was studied by calibrating the nitrate-ISEs from 0 to 25 °C. For membrane S9, the slope varied by  $-0.155 \text{ mV decade}^{-1} \text{ } ^\circ\text{C}^{-1}$  and the potential of a  $0.1 \text{ mol dm}^{-3}$  nitrate (1400 ppm nitrate-N) standard varied by  $+0.31 \text{ mV } ^\circ\text{C}^{-1}$ . In theory, according to the Nernst equation, the temperature coefficient slope should be  $-0.1984 \text{ mV decade}^{-1} \text{ } ^\circ\text{C}^{-1}$  and the potential of the  $0.1 \text{ mol dm}^{-3}$  nitrate (1400 ppm nitrate-N) standard should vary by



**Fig. 1** Response obtained with four membranes (S9), milled and containing 25% m/m PoleStar 200R over a concentration range from 1400 to 0.0014 ppm nitrate-N.

**Table 3** Electrochemical properties of the milled membrane (S9) compared to membrane S0 (free of clay) and a commercial nitrate-ISE

| Membrane   | Slope/mV decade <sup>-1</sup> | Linear Nernstian range/ppm nitrate-N | $K^{\text{pot}}_{\text{NO}_3^-, \text{Cl}^-}$ | LOD/ppm nitrate-N |
|------------|-------------------------------|--------------------------------------|---|-------------------|
| S0         | -59.1                         | 1400–0.07                            | $3.4 \times 10^{-3}$                          | 0.005             |
| S9         | -58.5                         | 1400–0.07                            | $4.0 \times 10^{-3}$                          | 0.01              |
| Commercial | -59.0                         | 1400–0.14                            | $5.5 \times 10^{-3}$                          | 0.098             |

$+0.1984 \text{ mV } ^\circ\text{C}^{-1}$ . The slight difference observed especially for the  $0.1 \text{ mol dm}^{-3}$  nitrate standard is probably due to the temperature dependency of ion activity coefficient, solubility of the salts and complexes and electrode junction potentials. However, this showed that the nitrate-ISEs are capable of operating over the temperature range 0–25 °C without adaptation other than temperature compensation. The LOD however was slightly increased with a value of 0.01 ppm nitrate-N obtained with membrane S9 compared to a LOD value of 0.005 ppm nitrate-N for membrane S0. Generally, an increase in the LOD can be caused by a perturbation of the interfacial sample concentration due to a release of a low amount of analyte or competing ion from the membrane.<sup>21,22</sup> However, PoleStar 200R was formed at temperatures above 1000 °C which would decompose most salts, therefore a contamination from the clay was unlikely to occur. However this increase in the LOD would not affect membrane S9 evaluation in agricultural drainage waters because the ISE still exhibited a wide linear measuring range from 1400 to 0.07 ppm nitrate-N which is sufficient for most environmental freshwaters.

### Membrane robustness

The maximum tensile stress,  $s_{\text{max}}$ , of membranes S9 (25% m/m PoleStar 200R) and S0 (0% m/m PoleStar 200R) was found to be respectively  $251 \pm 23 \text{ kN m}^{-2}$  ( $n = 3$ ) and  $83 \pm 6 \text{ kN m}^{-2}$  ( $n = 3$ ). The  $s_{\text{max}}$  increase of threefold for membranes S9 compared to membranes S0 shows that PoleStar 200R increased the resistance to extension and rupture. Similarly the force required to puncture membranes S9 was also three times greater

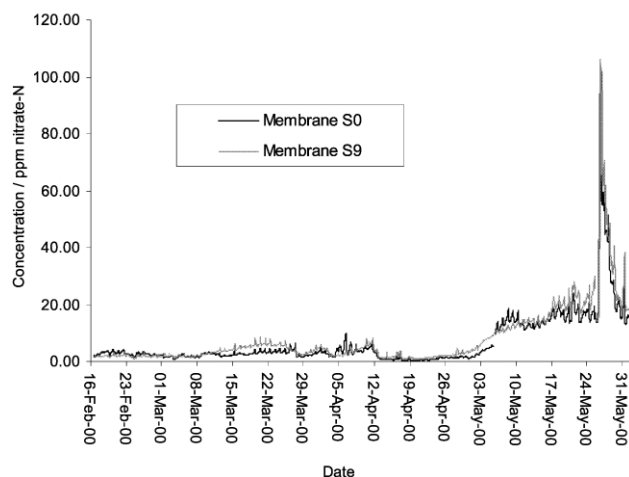
( $1.5 \pm 0.0$  N) compared to membrane S0 ( $0.5 \pm 0.0$  N). Both experiments showed that the PoleStar 200R was a very successful additive for SBS-based polymeric membranes increasing both their membrane resistance to tensile stress and to puncture about three times.

### Effect of sunlight on membrane performance

Membrane S0 (0% m/m PoleStar 200R) exhibited a sub-Nernstian response (slope =  $-41.3$  mV decade $^{-1}$ ) after 295 min of exposure whereas membrane S9 (25% m/m PoleStar 200R) exhibited a Nernstian response over the concentration range 140–0.14 ppm nitrate-N with a slope of  $-54.9$  mV decade $^{-1}$  after 545 min of exposure. This shows that the addition of the clay-based filler in the membrane composition improves the resistance to degradation upon exposure to sunlight. It should be noted that this experiment tends to exaggerate the field conditions. In reality, the radiation intensity encountered in the field is much weaker. The electrodes would normally be kept in a light-proof enclosure to exclude rainwater and prevent algal growth and more generally the electrodes would be inverted in the water where the radiation intensity is not very important.

### Field evaluation

The field evaluation of the clay-based membrane was undertaken by continuous immersion over a period of 15 weeks in agricultural drainage weirs. During this period, clay-based membrane (S9) and clay-free membrane (S0) were used to determine nitrate at hourly intervals. Fig. 2 shows that membranes S0 and S9 gave very similar results during the period of the field trial (16th February to 31st May). The temperature (6.7–14.1 °C) varied significantly during the field trial but membranes S0 and S9 were still performing without loss of response. Over a concentration range from 0.3 to 101.0 ppm nitrate-N, the correlation coefficient ( $R^2$ ) between the two ISEs gave a value of 0.96. The regression line had a gradient of 1.1 indicating that there was only a small systematic error. The discrepancy observed in Fig. 2 between the two ISEs from 11th March to 27th March corresponded to a period of extremely low rainfall resulting in stagnant water in the drainage weir which could have interfered with the electrodes due to the absence of stirring in the small enclosed structure of the weir. In early May a connection fault developed for membrane S0 and after replacement of the faulty lead, the two ISEs gave almost identical nitrate levels for the rest of the experiment.

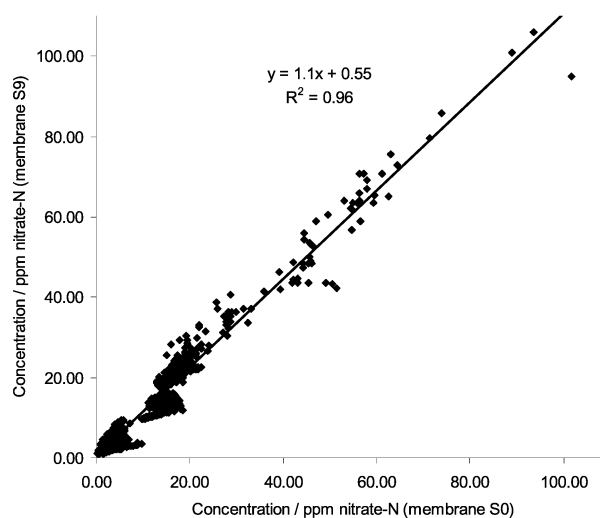


**Fig. 2** Concentration of nitrate-N measured over the 15 weeks period in drainage waters by a THF-based membrane (S0) and a clay-based membrane (S9).

The same membranes were used during the total period of the field evaluation. As observed previously for S0,<sup>10</sup> no degradation or fouling occurred for membranes S9. The field experiment was continued beyond May 31<sup>st</sup> but membrane S0 developed a potential drift indicating a decline in performance relative to S9. The clay based membrane continued to perform satisfactorily for a further 3 weeks when the field study was terminated. It would appear therefore that the presence of clay results in an improved membrane lifetime.

### Conclusion

A milling method for the preparation of SBS membranes containing covalently bound nitrate sensor was developed using a clay-based filler. The membrane was composed of SBS (32.6% m/m), 2-NPOE (30.0% m/m), DCP (7.5% m/m), *N,N,N*-triallyl leucine betaine (4.9% m/m) and PoleStar 200R (25% m/m). The resulting rubbery membrane exhibited a linear response from 1400 to 0.07 ppm nitrate-N with a slope of  $-58.5$  mV per decade. The LOD was 0.01 ppm nitrate-N and the selectivity coefficient for nitrate against chloride,  $K^{pot}_{NO_3^-, Cl^-}$ , was  $4.0 \times 10^{-3}$ . These results were better than those obtained with a commercial nitrate-ISE. The advantages of the milling compared to a solvent-based protocol are: (1) environmentally friendly (no toxic solvent used), (2) faster (no need to wait for the evaporation of the THF), (3) cheaper (replacement of expensive chemicals by PoleStar 200R and no THF used), (4) possibility of large scale fabrication (5) an increased tensile strength and resistance to penetration of clay containing milled membranes, each of them of about three times compared to PoleStar 200R free membranes, and (6) an improved longevity of use with milled membranes. This solvent-free method could also be used for preparing PVC-based selective membranes because PoleStar 200R is already used to fabricate PVC products and it did not affect the electrochemical parameters of SBS membranes. It is also important to note that the present group is currently developing a phosphate-ISE based upon an immobilised heterocyclic macrocycle ionophore. Its immobilisation to SBS and the use of PoleStar 200R did not affect its electrochemical performance compared to the trapped one in PVC, however, its long-term stability was improved. Ionophores are commonly used in the fabrication of ISEs<sup>23</sup> and the fact that the developed method is applicable for this class of sensors extends its use for the fabrication of more ISE products. It would appear that this methodology is applicable to a wide range



**Fig. 3** Correlation and regression between the nitrate levels measured with a THF-based membrane (S0) and a clay-based membrane (S9) in drainage waters over a period of 15 weeks.

of ISEs, both cation and anion sensing and both ionophore and ion-exchanger based.

None of the electrodes prepared required maintenance or recalibration over a period of 15 weeks. The nitrate levels determined with the clay-based nitrate-ISE compared favourably ( $R^2 = 0.96$ ,  $y = 1.1x + 0.55$ ) with the standard method using a nitrate-ISE previously tested under the same conditions (Fig. 3).<sup>10</sup>

## Acknowledgements

The authors wish to express their gratitude for financial support to the Environment Agency (R & D programme).

## References

- 1 T. Bühner, P. Gehrig and W. Simon, *Anal. Sci.*, 1988, **4**, 547.
- 2 J. E. W. Davies, G. J. Moody and J. D. R. Thomas, *Analyst*, 1972, **97**, 87.
- 3 F. Zuther and K. Cammann, *Sens. Actuators B*, 1994, **18–19**, 356.
- 4 D. Wegmann, H. Weis, D. Ammann, W. E. Morf, E. Pretsch, K. Sugahara and W. Simon, *Mikrochim. Acta*, 1984, **3**, 1.
- 5 F. Hofmeister, *Arch. Experiment. Pathol. Pharmacol.*, 1888, **24**, 247.
- 6 J. H. MacDuff, S. C. Jarvis, C.-M. Larsson and P. Oscarson, *J. Exp. Bot.*, 1993, **44**, 1475.
- 7 L. Ebdon, J. Braven and N. C. Frampton, *Analyst*, 1990, **115**, 189.
- 8 L. Ebdon, J. Braven and N. C. Frampton, *Analyst*, 1991, **116**, 1005.
- 9 T. Le Goff, J. Braven, L. Ebdon and D. Scholefield, *Anal. Chem.*, 2002, **74**, 2596–2602.
- 10 T. Le Goff, J. Braven, L. Ebdon, D. Scholefield and J. Wood, *Analyst*, 2002, **127**, 507.
- 11 L. Ebdon, A. T. Ellis and G. C. Corfield, *Anal. Proc.*, 1982, **22**, 354.
- 12 L. Ebdon, B. A. King and G. C. Corfield, *Analyst*, 1985, **107**, 288.
- 13 A. Craggs, G. J. Moody and J. D. R. Thomas, *J. Chem. Educ.*, 1974, **51**, 541.
- 14 N. C. Frampton, Ph. D. Thesis, University of Plymouth, 1992.
- 15 The Merck Index, *An encyclopedia of chemicals, drugs and biologicals*, ed. S. Budavari, Merck & Co., Inc., Whitehouse Station, New Jersey, 1996, p. 1574.
- 16 D. Scholefield, E. A. Gardwood and N. M. Titchen, in *Nitrogen efficiency in agricultural soils; the plot of management practices for reducing losses of nitrogen from grazed pastures*, ed. D. S. Jenkinson and K. A. Smith, Elsevier, London, 1988, pp. 20–231.
- 17 D. Ammann, in *Ion-selective microelectrodes-Principle, Design and Application*, ed. Springer-Verlag, Berlin, 1986, p. 33.
- 18 IUPAC recommendations prepared by Y. Umezawa, K. Umezawa and H. Sato, *Pure Appl. Chem.*, 1995, **67**, 507.
- 19 IUPAC recommendations prepared by G. G. Guilbault, *Ion-Selective Electrode Rev.*, 1979, **1**, 139.
- 20 E. Callaway, in *Standard methods for examination of water and wastewater: Nitrogen (Nitrate)*, ed. A. D. Eaton, L. S. Clesceri and A. E. Greenberg, American Public Health Association, 19th edn., 1995, pp. 85–91.
- 21 E. Bakker, P. Bühlmann and E. Pretsch, *Chem. Rev.*, 1997, **90**, 3083.
- 22 E. Bakker, M. Nägele, U. Schaller and E. Pretsch, *Electroanalysis*, 1994, **7**, 817.
- 23 P. Bühlmann, E. Pretsch and E. Bakker, *Chem. Rev.*, 1998, **98**, 1593.



# Mild catalytic multiphase hydrogenolysis of benzyl ethers

Alvise Perosa,\*<sup>a</sup> Pietro Tundo\*<sup>a</sup> and Sergei Zinovyev<sup>b</sup>

<sup>a</sup> Dipartimento di Scienze Ambientali, Università Ca' Foscari, Dorsoduro 2137, 30123, Venezia, Italy. E-mail: [alvise@unive.it](mailto:alvise@unive.it); Fax: +39-041-2348620

<sup>b</sup> Consorzio Interuniversitario 'la Chimica per l'Ambiente', Via della Libertà 5/12, 30175, Marghera (VE), Italy

Received (in Cambridge, UK) 12th July 2002

First published as an Advance Article on the web 25th September 2002

A preliminary study was conducted on the multiphase (aqueous KOH–isooctane–Aliquat® 336) hydrogenolysis of benzyl methyl ether using Pd/C, Pt/C and Raney-Ni as catalysts, under mild conditions ( $T = 50\text{ }^{\circ}\text{C}$ ,  $p_{\text{H}_2} = 1\text{ atm}$ ). Using ethanol as solvent, the Pd/C system is very efficient, while the same catalyst under multiphase conditions is almost inactive. With Pt/C, the reaction is always sluggish, and ring hydrogenation kicks in under multiphase conditions. The Raney-Ni system has an opposite behavior, while debenzoylation is slow in ethanol, under multiphase conditions the reaction is quite fast. Other *O*-benzyl protected substrates undergo debenzoylation with Raney-Ni as well, with varying chemoselectivity.

## Introduction

The multiphase system<sup>1</sup> made by hydrogen, an aqueous phase, isooctane, a phase transfer (PT) agent (*e.g.* Aliquat® 336, A336), and a heterogeneous catalyst (*e.g.* Pd/C, Pt/C) allows a variety of reduction reactions to be conducted under mild conditions ( $T = 50\text{ }^{\circ}\text{C}$ ,  $p_{\text{H}_2} = 1\text{ atm}$ ), *e.g.*: hydrodehalogenation of aryl halides,<sup>2–6</sup> hydrogenation of carbonyls,<sup>7</sup> hydrogenolysis of hydroxyls,<sup>7</sup> up to aromatic hydrogenation.<sup>7,8</sup> For substrates liable to multiple reductions, selectivity can be achieved by tuning the multiphase system, in order to favor one over the other of the possible reaction pathways.<sup>9,10</sup> Recently Raney-Ni was found to be active for hydrodehalogenation and hydrogenation reactions under multiphase conditions as well.<sup>11</sup> The multiphase system proves advantageous over monophasic ones, as demonstrated in a number of instances,<sup>10</sup> in particular for the case of Raney-Ni, where in the absence of A336, or of the alkaline aqueous phase, the reactions are inhibited.<sup>11</sup>

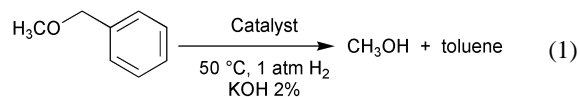
From the green chemistry standpoint, heterogeneous catalysis is an attractive synthetic tool, particularly: when it allows to selectively (chemo-, regio-, stereo-) conduct different transformations by tuning some simple reactions parameters, when the reaction conditions are easily accessible (*e.g.* low temperature and pressure), when the catalyst system can be conveniently recovered and recycled, and when the product can be easily separated. The positive features of heterogeneous catalysis can be improved by using an aqueous–organic biphasic solvent mixture.<sup>12</sup> Such mixtures provide a built-in method for product isolation and catalyst recycling (phase separation instead of distillation), resulting in fewer by-products. When the substrate forms a separate organic phase, the need for an organic solvent can be eliminated altogether, and aqueous–organic biphasic processes allow tuning of selectivity by proper manipulation of the pH of the aqueous phase. Further advantages for biphasic heterogeneous catalytic systems can be obtained by modifying the heterogeneous catalyst with phase transfer (PT) agents. In fact, in such a multiphase catalytic reduction system it is possible to conduct a variety of reduction reactions under mild conditions and with interesting chemo-, regio- and stereo-selectivities.

## Results and discussion

To expand the synthetic applicability of this multiphase reduction system, we carried out a preliminary exploration of

the hydrogenolysis of benzyl ethers, in view of its use for the selective deprotection of benzyl (Bn) protected alcohols. One common method for the cleavage of Bn protected hydroxyl groups is catalytic hydrogenolysis.<sup>13</sup> Palladium on charcoal (Pd/C)<sup>14–17</sup> and Raney-Ni<sup>14,18</sup> are among catalysts used, the solvent is generally ethanol, and the hydrogen pressures are often high for Raney-Ni.<sup>14</sup> Selectivity is an issue since other reduction-sensitive functional groups present in the molecule may be hydrogenated.

Benzyl methyl ether was chosen as the model substrate (eqn. (1)), to compare the activity of different catalysts (Pd/C, Pt/C, Raney-Ni), with and without A336, under the standard multiphase conditions.<sup>10,11</sup>



The results are reported in Table 1. In the usual hydrogenolysis conditions, with ethanol as solvent, Pd/C was very active for the debenzoylation of benzyl methyl ether, and benzyl methyl ether was quickly and quantitatively reduced to toluene (entry 1). By contrast, using the multiphase conditions, with A336 and a basic aqueous medium, the reaction was practically inhibited (entry 2); while it was a little faster by removing A336 (entry 3). The trend was the same using Pt/C, although the reaction was slower in all cases; *i.e.* the reaction in ethanol

## Green Context

Multiphase reaction systems have proven to be useful in a number of important synthetic transformations and those involving hydrogen have been shown to be effective under mild conditions. Here the multiphase hydrogenolysis of benzyl methyl ether with different catalytic systems is studied. Particularly significant is the observation that the relatively inexpensive Raney-Ni system is effective for debenzoylation under such conditions while simpler systems require Pd/C as catalyst. The methodology enables difficult transformations to be carried out under mild conditions, with a less expensive catalytic system and allowing easy catalyst recovery and reuse.

JHC

proceeded (entry 4), with the multiphase system it did not (entry 5), and with the multiphase system and no A336 it proceeded only very slowly (entry 6).

Ra-Ni behaved in a manner opposite to Pd/C. It reacted sluggishly in ethanol as solvent (entry 7) where, after almost 4 h, conversion was only 37%. In the multiphase system, without A336 the reaction appeared still inhibited (entry 9). By contrast, with A336, Ra-Ni promoted quick hydrogenolysis of benzyl methyl ether (entry 8), yielding complete conversion after 2.5 h, far better than Pd/C and Pt/C under the same multiphase conditions.

To explain this behavior, a surfactant type effect of A336, able to increase catalyst availability, was ruled out, since preceding studies had indicated that phase transfer agents, such as A336, do not act like surfactants. This was also verified by replacing A336 with sodium dodecyl sulfate (SDS), and observing that the reaction was once again slow (entry 10). These observations are in line with a preceding hypothesis on the mode of action of A336, where it coated the catalyst particles, causing a change of the catalytic environment in a way that promoted the activity and the chemoselectivity of the reactions.<sup>1,9,19</sup>

To explore whether chemo- and/or regio-selective deprotection of the benzyl group was possible with the Raney-Ni/A336

system, a series of available benzyl ethers were subjected to the conditions of entry 8 of Table 1. The results are reported in Table 2. The double bond of allyl benzyl ether was rapidly hydrogenated to benzyl propyl ether (entry 1), as could be expected due to its reactivity, followed by debenzylation, to yield propanol. Nopol benzyl ether instead, with a more hindered double bond respect to the preceding case, underwent faster debenzylation initially (entry 2), followed by double bond hydrogenation, to yield a 1:2 mixture of nopol and dihydronopol after 5 h. Tri-*O*-benzylglucal was totally debenzylated after 4 h (entry 3), as indicated by the production of three equivalents of toluene. No regioselectivity was observed in this case, and the product could not be identified.

Benzyl phenyl ether was very rapidly debenzylated to phenol (entry 4). Instead, *O*-benzyloxy-3-phenylpropanol first underwent slow carbonyl reduction, followed by even slower debenzylation (entry 5). The chemoselectivity was therefore totally towards carbonyl reduction.

However, BOC-*O*-benzylserine (BOC = benzyloxycarbonyl) could be chemoselectively deprotected to yield BOC-serine after 2.5 h (entry 6), showing that the BOC protecting group is stable under the reported multiphase conditions.

Previous studies had indicated that Pd/C is a more active reduction catalyst than Raney-Ni under multiphase conditions for the hydrodechlorination of chlorobenzenes,<sup>5</sup> while Raney-Ni is more active, provided A336 is present, in the hydrodechlorination of bromobenzenes.<sup>5</sup> The observed activity of the Raney-Ni/A336 multiphase system for the hydrogenolysis of benzyl ethers, and the opposite behavior of Pd/C, is another case of changes in the chemoselectivity produced by modifications of a component of the catalytic multiphase system (in this case the catalyst).

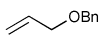
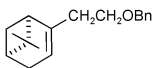
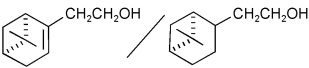
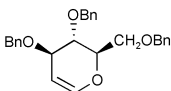
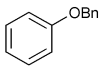
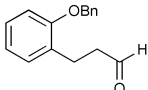
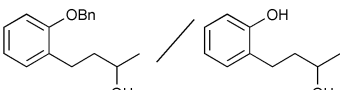
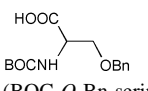
This study evinces that Raney-Ni is active in the hydrogenolysis of benzyl ethers under multiphase conditions, albeit not as active as Pd/C in ethanol. In particular, benzyl hydrogenolysis is possible in the presence of the BOC group, which is instead stable under the investigated conditions. Further studies will be aimed to determine whether the system could prove advantageous for the deprotection of other benzyl protected hydroxyl functions, where chemoselectivity is an

**Table 1** Hydrogenolysis of benzyl methyl ether

| Entry | Catalyst | Solvent system | PT agent | Time/min | Conv. (%)       |
|-------|----------|----------------|----------|----------|-----------------|
| 1     | Pd/C     | Ethanol        | None     | 30       | 100             |
| 2     |          | Multiphase     | A336     | 310      | 3               |
| 3     |          | Multiphase     | None     | 330      | 85              |
| 4     | Pt/C     | Ethanol        | None     | 240      | 33 <sup>a</sup> |
| 5     |          | Multiphase     | A336     | 360      | 0               |
| 6     |          | Multiphase     | None     | 300      | 5 <sup>a</sup>  |
| 7     | Ra-Ni    | Ethanol        | None     | 230      | 37              |
| 8     |          | Multiphase     | A336     | 150      | 100             |
| 9     |          | Multiphase     | None     | 420      | 85              |
| 10    |          | Multiphase     | SDS      | 435      | 98              |

<sup>a</sup> Toluene was further reduced to methylcyclohexane.

**Table 2** Hydrogenolysis of benzyl ethers with Ra-Ni and A336<sup>a</sup>

| Entry          | Substrate  | Time/min  | Product/s  | Yield (%)  |
|----------------|--|-----------|--|------------|
| 1 <sup>a</sup> |                                 | 30<br>180 | <i>n</i> -PrOBn<br><i>n</i> -PrOH  | 100<br>100 |
| 2              | <br>(Nopol- <i>O</i> -Bn-ether) | 320       |  | 20/40      |
| 3              | <br>(Tri- <i>O</i> -Bn-glucal)  | 240       | <i>b</i>   | 100        |
| 4              |                                 | 30        | Phenol   | 100        |
| 5 <sup>c</sup> |                                 | 240       |  | 90/10      |
| 6              | <br>(BOC- <i>O</i> -Bn-serine)  | 150       | BOC-serine   | 100        |

<sup>a</sup> Conditions: 0.25 mmol A336, 250 mg Raney-Ni Actimet M<sup>®</sup>; 10 mL isoctane; 5.5 mL 2% aq. KOH; 0.7 mmol of substrate. Stirred at 1000 rpm and bubbled with H<sub>2</sub>, at 50 °C. <sup>b</sup> The product was not identified, however three equivalents of toluene were produced indicating that debenzylation took place.

<sup>c</sup> Reaction run in the absence of KOH (to avoid aldol condensation).

issue, e.g. in the presence of other reduction sensitive functional and/or of other protecting groups.

## Experimental

All reactions were run in a 25 mL reactor thermostated at 50 °C, loaded with (in this order): 2.32 mL of a 5% isooctane solution (vv) of Aliquat 336 (0.25 mmol), the catalyst (250 mg wet Raney-Ni Actimet M<sup>®</sup> from Engelhardt, or 46 mg Pd/C 5%, or 84 mg Pt/C 5%); 7.7 mL isooctane; 5.5 mL 2% aqueous KOH; 50 mg (0.41 mmol) of benzyl methyl ether. The mixture was stirred at 1000 rpm and bubbled with hydrogen ( $\approx 5 \text{ mL min}^{-1}$ ). Samples were withdrawn at intervals, and were monitored for toluene concentration by GC using the internal standard (decane) technique. For the compounds of Table 2, structures were confirmed by GC-MS analyses by comparison with authentic samples.

## Acknowledgments

Engelhart is acknowledged for the generous gift of Raney-Ni catalyst. The work was partially funded by the Italian Interuniversity Consortium "Chemistry for the Environment" (INCA), Ca' Foscari University, INTAS grant no. 2000-00710, NATO grant no. EST.CLG.977159, and M.I.U.R (Piano "Ambiente Terrestre: Chimica per l'Ambiente", Legge 488/92).

## References

- 1 P. Tundo and A. Perosa, *React. Funct. Polym.*, in press.
- 2 C. A. Marques, M. Selva and P. Tundo, *J. Chem. Soc. Perkin Trans. I*, 1993, 529–533.
- 3 C. A. Marques, M. Selva and P. Tundo, *J. Org. Chem.*, 1993, **58**, 5256–5260.
- 4 C. A. Marques, M. Selva and P. Tundo, *J. Org. Chem.*, 1994, **59**, 3830–3837.
- 5 C. A. Marques, O. Rogozhnikova, M. Selva and P. Tundo, *J. Mol. Catal. A*, 1995, **96**, 301–309.
- 6 A. Perosa, M. Selva, P. Tundo and S. S. Zinovyev, *Appl. Catal. B: Environ.*, 2001, **32**, L1–L7.
- 7 C. A. Marques, M. Selva and P. Tundo, *J. Org. Chem.*, 1995, **60**, 2430–2435.
- 8 M. Selva, P. Tundo and A. Perosa, *J. Org. Chem.*, 1998, **63**, 3266–3271.
- 9 A. Perosa, M. Selva and P. Tundo, *J. Org. Chem.*, 1999, **64**, 3934–3939.
- 10 P. Tundo, S. Zinovyev and A. Perosa, *J. Catal.*, 2000, **196**, 330–338.
- 11 S. Zinovyev, A. Perosa, S. Yufit and P. Tundo, *J. Catal.*, 2002, in press.
- 12 F. Joó, *Acc. Chem. Res.*, 2002, **35**, 738–745.
- 13 T. W. Green and P. G. M. Wuts., *Protective Groups in Organic Chemistry*, 2nd edn., J. Wiley & Sons Inc., New York, 1991, p. 49.
- 14 C. H. Hartung and C. Simonoff, *Org. React.*, 1953, **7**, 263–326.
- 15 C. H. Heathcock and R. Ratcliffe, *J. Am. Chem. Soc.*, 1971, **93**, 1746–1757.
- 16 J. S. Bindra and A. Grodski, *J. Org. Chem.*, 1978, **43**, 3240–3241.
- 17 D. Cain and T. L. Smith., *J. Am. Chem. Soc.*, 1980, **102**, 7568–7570.
- 18 Y. Oikawa, T. Tanaka, K. Horita and O. Yonemitsu, *Tetrahedron Lett.*, 1984, **25**, 5397–5400.
- 19 A. Perosa, P. Tundo and M. Selva, *J. Mol. Catal. A*, 2002, **180**, 169–175.



# An efficient and ecofriendly oxidation of alkenes using iron nitrate and molecular oxygen

Unnikrishnan R. Pillai, Endalkachew Sahle-Demessie,\* Vasudevan V. Namboodiri and Rajender S. Varma

National Risk Management Research Laboratory, Sustainable Technology Division, MS 443  
U.S Environmental Protection Agency, 26 West M. L. King Drive, Cincinnati, OH 45268,  
USA. E-mail: Sahle-Demessie.Endalkachew@epa.gov; Fax: +1 513-569-7677

Received 3rd May 2002

First published as an Advance Article on the web 11th September 2002

An environmentally friendly solventless oxidation of alkenes is accomplished efficiently using relatively benign iron nitrate as catalyst in the presence of molecular oxygen under pressurized conditions.

## Introduction

The catalytic oxidation of hydrocarbons using environmentally benign and economical molecular oxygen is an important goal both in fine and bulk chemical industry and hence is a highly challenging area.<sup>1–4</sup> The oxidation of alkenes to a variety of useful products is one of the most important objectives in view of the commercial value as well the synthetic utility of the ensuing oxidation products. Consequently, there are several groups working towards this goal using a variety of catalyst systems such as polyoxometallates,<sup>5</sup> iron porphyrins,<sup>6</sup> iron phthalocyanines,<sup>7</sup> iron diphenyl phosphines,<sup>8,9</sup> Ru, Mo, Ti metal complex catalysts<sup>10</sup> and also other supported metal oxide catalysts.<sup>11–13</sup> Heterogeneous catalysts generally lack good activity and selectivity whereas homogeneous catalyst systems suffer from the drawbacks of complex preparative methods, difficulty in catalyst separation from the product mixture and very often, the presence of halide ions, which are not environmentally friendly. Catalyst deactivation is also frequently observed.<sup>7</sup> Oxidation in liquid phase usually involves the use of flammable organic solvents, which are a burden on the environment and also pose an explosion hazard.<sup>8</sup>

It has been known that activated oxygen interacts with organic substrates *via* H-atom and O-atom transfer.<sup>14,15</sup> In Fenton chemistry, hydrocarbons are converted to ketones and alcohols in the presence of Fe(II) combined with a donor molecule such as HOOH or reagents like PhNHNHPh, ascorbic acid or PhCH<sub>2</sub>SH.<sup>15–17</sup> On the other hand, anhydrous covalent metal nitrates are known to be strong oxidants wherein the species responsible for the oxidation of organic compounds is the NO<sub>3</sub> radical produced by the dissociation of metal–nitrate bidentate bonds.<sup>18</sup> For an anhydrous metal nitrate to be sufficiently reactive, the metal should preferably have a lower oxidation state available. The nitrate ion *per se* is inert, however, with compounds like ether or aniline, the oxidizing properties of the nitrate group are so strong that the mixture will either explode or burst into flames. Ionic nitrates, however, are not reactive.

Most of the metal nitrates exist as ionic crystals and hence remain unreactive. So is the case with iron nitrate, an abundantly available and relatively less toxic metal nitrate. However, Laszlo *et al.* found that ionic metal nitrates could be made anhydrous with a bidentate nitrate group on iron by solvating with acetone *via* simple evaporation of an acetone solution of the metal nitrate.<sup>19</sup> The resulting solvate, however, is found to be highly unstable and subsequently stabilized by depositing onto mineral solid supports like acidic montmor-

illonite K-10 clay, popularly known as clayfen.<sup>19</sup> Subsequently, other supported metal nitrate salts became available and found widespread use in diverse organic transformations.<sup>20–27</sup> It is postulated that oxidation by the supported nitrates operates by a mechanism involving acidic sites on the support and exploits the high surface area to disperse the reagents effectively. However, these supported reagents also decompose on storage and more than stoichiometric quantities are often required for their effectiveness. Taking cue from our earlier studies,<sup>23–27</sup> we envisaged that the organic substrate itself may be able to solvate iron nitrate to effect similar oxidative transformations. If successful, this approach may lead to the use of this relatively innocuous salt in many industrial oxidation reactions, thereby minimizing the use of toxic and expensive oxidants. Consequently, we explored and succeeded in utilizing iron nitrate to catalyze the oxidation of styrene more efficiently than clayfen.<sup>28</sup> We report here an efficient solventless oxidation of various alkenes using a catalytic amount of iron nitrate and molecular oxygen under different oxidizing conditions.

## Results and discussion

The effect of iron nitrate catalyzed alkene oxidation in the presence of O<sub>2</sub> is initially optimized using cyclooctene as substrate. The results obtained under varying reaction conditions are summarized in Table 1. Apparently, cyclooctene can be oxidized efficiently and in an environmentally benign manner using iron nitrate and molecular oxygen in the absence of any organic solvent. The liquid phase reaction under atmospheric conditions at 80 °C affords around 37% conversion (entry 1) whereas ~53% cyclooctene is converted under pressurized conditions (entry 4) suggesting that a manifold

### Green Context

**The oxidation of alkenes can provide an important route to several important types of products including epoxides. While there are numerous reported methods for achieving this, the most desirable is the combination of oxygen as the consumable oxidant and an inexpensive, environmentally benign catalyst. Here this is accomplished through the use of iron nitrate. The reaction system is solvent free, operates under mild conditions and gives good conversions for a variety of substrates.** JHC



**Table 1** Cyclooctene oxidation using  $\text{Fe}(\text{NO}_3)_3 \cdot 9\text{H}_2\text{O}$  and  $\text{O}_2^a$ 


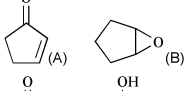
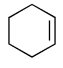
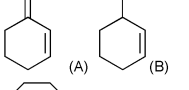
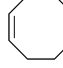

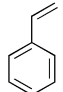
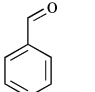
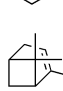
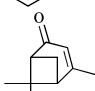
| Entry          | Substrate:<br>catalyst<br>mol ratio | Tempera-<br>ture/°C | $\text{O}_2$ pres-<br>sure/bar | $\text{N}_2$ pres-<br>sure/bar | Conver-<br>sion (%) | Selectivity<br>(%) |
|----------------|-------------------------------------|---------------------|--------------------------------|--------------------------------|---------------------|--------------------|
| 1              | 50                                  | 80                  | Balloon                        | —                              | 37                  | >95                |
| 2 <sup>b</sup> | 50                                  | 80                  | Balloon                        | —                              | 24                  | <5                 |
| 3              | 50                                  | 60                  | 3.4                            | 10.3                           | 20                  | >95                |
| 4              | 50                                  | 80                  | 3.4                            | 10.3                           | 53                  | >95                |
| 5              | 50                                  | 100                 | 3.4                            | 10.3                           | 44                  | >95                |
| 6              | 200                                 | 80                  | 3.4                            | 10.3                           | 35                  | >95                |
| 7              | 100                                 | 80                  | 3.4                            | 10.3                           | 51                  | >95                |
| 8              | 33                                  | 80                  | 3.4                            | 10.3                           | 40                  | >95                |
| 9              | 50                                  | 80                  | 1.4                            | 12.4                           | 36                  | >95                |
| 10             | 50                                  | 80                  | 6.9                            | 6.9                            | 44                  | >95                |
| 11             | 50                                  | 80                  | 3.4                            | 24.1                           | 42                  | >95                |
| 12             | 50                                  | 80                  | 3.4                            | 37.9                           | 32                  | >95                |
| 13             | 50                                  | 80                  | 0.0                            | 10.3                           | 02                  | >95                |
| 14             | 00                                  | 80                  | 3.4                            | 10.3                           | 02                  | >95                |

<sup>a</sup> Cyclooctene (100 mmol), 400 rpm, 6 h. <sup>b</sup>  $\text{FeCl}_3 \cdot 2\text{H}_2\text{O}$ , mainly alkylation products and no oxidation products were detected.

enhancement of the activity of iron nitrate is attainable by conducting the reaction under oxygen pressure in the presence of  $\text{N}_2$ . The only product formed is cyclooctene oxide under both atmospheric and pressurized conditions. Increasing the substrate:catalyst mol ratio above 50 decreases the conversion (entry 6 and 7), indicating that this is the optimum substrate:catalyst ratio achievable under the conditions studied. The optimum condition for the reaction appears to be a temperature of 80 °C under 3.4 bar  $\text{O}_2$  and 10.3 bar  $\text{N}_2$  pressure and a substrate to catalyst mol ratio of 50 (Table 1). The lower conversion obtained at higher temperature and pressure may be due to the effect of partial pressure variations, which influence the reaction kinetics. There was minimal substrate conversion in the absence of oxygen (entry 13) or the iron nitrate catalyst (entry 14). When iron chloride was used instead of iron nitrate, only alkylation products were formed and no oxidation products were detected (entry 2). This suggests that the reaction is essentially catalyzed by the nitrate and oxygen.

This environmentally benign protocol is extended to other cyclic and benzylic alkenes as illustrated in Table 2 and Table 3 which present the results of oxidation studies under atmospheric and pressurized conditions respectively. The liquid phase atmospheric pressure alkene oxidation protocol, in general, is

**Table 2** Liquid phase alkene oxidation at atmospheric pressure using  $\text{Fe}(\text{NO}_3)_3 \cdot 9\text{H}_2\text{O}$  and  $\text{O}_2^a$ 


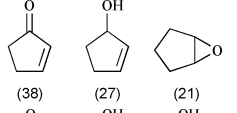
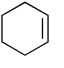
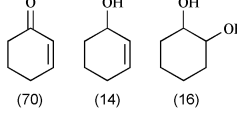
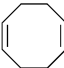
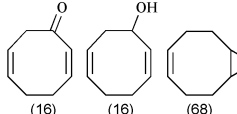
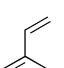
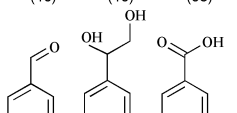
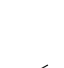
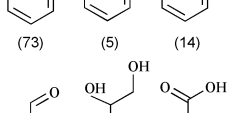
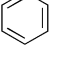
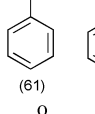
| Entry | Alkene  | Conversion (%) | Products  | Selectivity (%) |
|-------|---|----------------|---|-----------------|
| 1     |  | 4              |  | A = 78, B = 22  |
| 2     |  | 20             |  | A = 55, B = 45  |
| 3     |  | 8              |  | >95             |
| 4     |  | 12             |  | >95             |
| 5     |  | 26             |  | >95             |

<sup>a</sup> Substrate (100 mmol),  $\text{Fe}(\text{NO}_3)_3 \cdot 9\text{H}_2\text{O}$  (2 mmol), 80 °C, 6 h,  $\text{O}_2$  (3.4 bar),  $\text{N}_2$  (10.3 bar).

not very encouraging and may only be useful for selected substrates such as cyclohexene (entry 2, Table 2) and cyclooctene (entry 1, Table 1). On the other hand, the pressurized oxidation protocol appears to be promising and is applicable to a variety of cyclic and benzylic olefins (Table 1, entry 4,5 and Table 3), which show fairly good conversion to the oxidized products. The product distribution for alkene oxidation using iron nitrate and oxygen, however, varies. For example, cyclopentene forms cyclopent-2-en-1-one, cyclopent-2-en-1-ol and cyclopentene oxide in significant proportions (entry 1, Table 3) whereas cyclohexene forms cyclohex-2-en-1-one as the major product (entry 2) with relatively small quantities of cyclohex-2-en-1-ol and cyclohexane-1,2-diol (*cis/trans*). Cyclooctene, on the other hand, forms mainly the epoxide product (entry 4, Table 1). cycloocta-1,5-diene (another 8-member C-ring molecule) also forms the epoxide product selectively (entry 3, Table 3). The formation of the epoxide and other oxygenated products depends upon several factors including the ring strain and stability of the epoxide under the reaction conditions. The reaction temperature also affects the product distribution for styrene oxidation wherein a significant amount of benzoic acid is formed at 80 °C (entry 5, Table 3) when compared to that obtained at 60 °C (entry 4, Table 3). Benzaldehyde, however, is the main oxidation product at both the temperatures.

The oxidation mechanism in the presence of iron nitrate is believed to proceed by the formation of an olefin–nitrate complex followed by the insertion of an oxygen atom of the coordinated nitrate into the substrate, resulting in the oxidized product.<sup>29</sup> This is immediately followed by the recombination of the iron–nitrosyl intermediate with dioxygen. In addition to this,  $\text{Fe}^{3+}$  ions in the presence of oxygen atmosphere may also undergo reduction to the lower valent state ( $\text{Fe}^{2+}$ ), further enhancing the oxidizing capacity of the metal nitrate salt.

**Table 3** Alkene oxidation using  $\text{Fe}(\text{NO}_3)_3 \cdot 9\text{H}_2\text{O}$  and  $\text{O}_2$  under pressurized conditions<sup>a</sup>

| Entry          | Alkene  | Temperature/°C | Conversion (%) | Products (Selectivity, %)   |
|----------------|---|----------------|----------------|---|
| 1 <sup>b</sup> |  | 45             | 17             |  |
| 2              |  | 80             | 62             |  |
| 3              |  | 80             | 18             |  |
| 4 <sup>c</sup> |  | 60             | 83             |  |
| 5              |  | 80             | 90             |  |
| 6              |  | 80             | 44             |  |

<sup>a</sup> Substrate (100 mmol),  $\text{Fe}(\text{NO}_3)_3 \cdot 9\text{H}_2\text{O}$  (20 mmol), 6 h,  $\text{O}_2$  (3.4 bar),  $\text{N}_2$  (10.3 bar), 400 rpm. <sup>b</sup> Cyclopentadiene = 14%. <sup>c</sup> styrene oxide = 8%

Sawyer and co-workers have also reported that labile Fe(II) and Fe(III) complexes like  $[\text{Fe}^{\text{II}}(\text{bpy})_2]^{2+}$ ,  $[\text{Fe}^{\text{II}}(\text{OPPh}_3)_4]^{2+}$ ,  $[\text{Fe}^{\text{III}}(\text{bpy})_2]_{\text{acq}}^{3+}$ ,  $[\text{Fe}^{\text{III}}(\text{H}_2\text{O})_6]_{\text{acq}}^{3+}$  could activate molecular  $\text{O}_2$  to effect similar oxidations in the absence of any base.<sup>30,31</sup> The free radical role of Fe(II) and Fe(III) catalysts is to facilitate homolytic bond cleavage and bond formation *via* metal–oxygen radical–radical coupling which facilitates OH–H and R–O radical–radical coupling.<sup>31</sup>

Further, it is believed in the aforementioned investigations that only the anhydrous metal nitrate may display activity due to the covalent character of the metal–oxygen bond. Similar reactions on supported reagents are carried out in the presence of organic solvents like hexane or pentane where the simple metal nitrate would not have been active. However, this study shows that the hydrated metal nitrates can also be active for the oxidation reactions, especially under pressurized conditions. The results presented here could elicit newfound interest in this old-fashioned ionic salt for use in a variety of industrially important oxidative transformations.

## Conclusions

In summary, the present study shows that some industrially significant alkene oxidation reactions can be accomplished using the relatively benign iron nitrate as catalyst in the presence of an eco-friendly oxidant, molecular oxygen, thereby meeting the dual challenge of cost effectiveness and the benign nature of the process. Usually, alkene oxidation is carried out over complex and expensive metal oxide or homogeneous metal complex catalysts using stoichiometric amounts of oxidants and in the presence of organic solvent media. However, the present process neither involves the use of any complex catalyst nor the use of hazardous organic solvents thereby rendering the method simple, relatively benign and economical.

## Experimental

Iron nitrate and the various alkenes studied in this investigation were all obtained from Aldrich Chemicals. Alkene oxidation was carried out in the liquid phase in a round-bottomed flask at atmospheric pressure and also under pressurized conditions in a stainless steel high-pressure reactor (Pressure Products Industries Inc., PA, USA). In a typical reaction procedure, the alkene (100 mmol) was mixed with the appropriate amount of iron nitrate nonahydrate ( $\text{Fe}(\text{NO}_3)_3 \cdot 9\text{H}_2\text{O}$ ) in a 100 mL round-bottomed flask fixed with a reflux condenser and a thermometer. The mixture was heated to 50–80 °C and stirred for 6 h in the presence of oxygen (balloon). For the pressurized reaction, the substrate (100 mmol) was mixed with iron nitrate nonahydrate (2 mmol) in a 500 mL stainless steel autoclave and pressurized with the required amount of oxygen ( $\text{O}_2$ ) and nitrogen ( $\text{N}_2$ ) and heated at the desired temperature under stirring for 6 h. At the end of the reaction, the mixture was cooled to room temperature, extracted into diethyl ether, filtered through a 2 cm silica column and analyzed by a Hewlett-Packard 6890 gas chromatograph using a HP-5 5% phenyl methyl siloxane capillary column (30 m  $\times$  320  $\mu\text{m}$   $\times$  0.25  $\mu\text{m}$ ) and a quadrupole mass filter equipped HP 5973 mass selective detector under a temperature programmed heating from 40–200 °C at 10 °C  $\text{min}^{-1}$ . Quantification of the oxygenated products was obtained from the ratio of the peak areas corresponding to the reactant and products. The quantification values obtained by

this procedure were found to be in close agreement with those obtained using a multi-point calibration curve for the reactant–product mixture of some representative samples and hence reported as such.

## Acknowledgements

U. R. P. and V. V. N. are postgraduate research participants at the National Risk Management Research Laboratory administered by the Oak Ridge Institute for Science and Education through an interagency agreement between the US Department of Energy and the US Environmental Protection Agency.

## References

- 1 R. A. Sheldon and J. K. Kochi, *Metal Catalyzed Oxidation of Organic Compounds*, Academic Press, New York, 1981.
- 2 I. Ibushi and A. Yazaki, *J. Am. Chem. Soc.*, 1981, **103**, 7371.
- 3 A. Krotz and J. P. Kingsley, *Chemtech*, 1996, 39.
- 4 K. A. Jorgensen, *Chem. Rev.*, 1989, **89**, 431.
- 5 A. Molinari, R. Amadelli, U. Carassiti and A. Maldotti, *Eur. J. Inorg. Chem.*, 2000, 91.
- 6 S. Campestrini and U. Tonellato, *J. Mol. Catal. A: Chem.*, 2001, **171**, 37.
- 7 E. M. Gaigneau, J. Naud, J.-L. Knoden, R. Maggi, P. Ruiz and B. Delmon, *Bulg. Chem. Commun.*, 1998, **30**, 69.
- 8 J. P. Damiano, V. Muneyjabo and M. Postel, *Polyhedron*, 1995, **14**, 1229.
- 9 W. Nam, H. J. Lee, S.-Y. Oh, C. Kim and H. G. Jang, *J. Inorg. Biochem.*, 2000, **80**, 219.
- 10 G. Olason and D. C. Sherrington, *React. Funct. Polym.*, 1999, **42**, 163.
- 11 M. G. Clerici, G. Bellusi and U. Romano, *J. Catal.*, 1991, **129**, 159.
- 12 C. Palazzi, L. Oliva, Michela Signoreto and G. Strukul, *J. Catal.*, 2000, **194**, 286.
- 13 J. M. Fraile, J. I. Garcia, J. A. Mayoral and E. Vispe, *J. Catal.*, 2000, **189**, 40.
- 14 X. Liu, A. Qiu and D. T. Sawyer, *J. Am. Chem. Soc.*, 1993, **115**, 3239.
- 15 J. P. Hage and D. T. Sawyer, *J. Am. Chem. Soc.*, 1995, **117**, 5617.
- 16 A. Sobkowiak, A. Qiu, X. Liu, A. Llobet and D. T. Sawyer, *J. Am. Chem. Soc.*, 1993, **115**, 609.
- 17 D. T. Sawyer, *Coord. Chem. Rev.*, 1997, **165**, 297.
- 18 C. C. Addison, N. Logan, S. C. Wallwork and C. D. Garner, *Q. Rev. Chem. Soc.*, 1971, **25**, 289.
- 19 A. Cornelis and P. Laszlo, *Synthesis*, 1985, 909.
- 20 M. Balogh, P. Penmetreau, I. Hermezc and A. Gerstman, *J. Org. Chem.*, 1990, **55**, 6198.
- 21 T. Cseri, S. Bekassy and F. Figueras, *Bull. Soc. Chim. Fr.*, 1996, **133**, 547.
- 22 M. M. Heravi, D. Ajami, K. Aghapoor and M. Ghassemzadeh, *Chem. Commun.*, 1999, 833.
- 23 R. S. Varma and R. Dahiya, *Tetrahedron Lett.*, 1997, **38**, 2043.
- 24 R. S. Varma and R. K. Saini, *Tetrahedron Lett.*, 1997, **38**, 2623.
- 25 R. S. Varma and R. Dahiya, *Tetrahedron Lett.*, 1998, **39**, 1307.
- 26 R. S. Varma, K. P. Naicker and P. J. Liesen, *Tetrahedron Lett.*, 1998, **39**, 3977.
- 27 R. S. Varma and R. Dhaiya, *Synth. Commun.*, 1998, **28**, 4087.
- 28 R. S. Varma and V. V. Namboodiri, *IUPAC Chemrawn XIV Conference on Green Chemistry*, Bolder, Colorado, June 9–13, 2001.
- 29 H. L. K. Wah, M. Postel and F. Tomi, *Inorg. Chem.*, 1989, **28**, 233; H. L. K. Wah, M. Postel, F. Tomi, L. Mordenti, D. Ballivet-Tkatchenko, F. Dahan and F. Urso, *New J. Chem.*, 1991, **15**, 629.
- 30 J. P. Hage, J. A. Powell and D. T. Sawyer, *J. Am. Chem. Soc.*, 1995, **117**, 12897.
- 31 A. Sobkowiak, D. Narog and D. T. Sawyer, *J. Mol. Catal. A: Chem.*, 2000, **159**, 247.



# Organic synthesis in solid media. Solvent-free Horner–Wadsworth–Emmons reaction in silica gel

Yong Zhi Jin, Noriyuki Yasuda and Junji Inanaga\*

Institute for Fundamental Research of Organic Chemistry (IFOC), Kyushu University, Hakozaki, Higashi-ku, Fukuoka 812-8581, Japan. E-mail: inanaga@ms.ifoc.kyushu-u.ac.jp

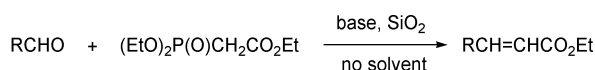
Received 29th May 2002

First published as an Advance Article on the web 24th September 2002

Silica gel was found to be an excellent medium for the aldehyde-selective Horner–Wadsworth–Emmons reaction, which proceeds at room temperature in a short period of time under solvent-free conditions. The silica gel used for the reaction can be recovered and reused many times without losing its activity.

## Introduction

The Horner–Wadsworth–Emmons reaction<sup>1</sup> has been widely used in organic synthesis as a modification of the Wittig reaction to convert carbon–oxygen double bonds of aldehydes and ketones into carbon–carbon double bonds.<sup>2</sup> Recently, we found that silica gel could easily promote the allylation reaction of aldehydes with a stoichiometric amount of tetraallyltin under solvent-free conditions, in which the silica gel acts not only as the reaction medium but also as an activator.<sup>3</sup> Although silica gel has long been known as a mild solid acid reagent or catalyst as well as an effective adsorbent for the chromatographic separation of organic compounds, few examples have been reported for silica gel-mediated organic transformations that do not require any organic solvents.<sup>4</sup> From an environmental point of view, we investigated the solvent-free Horner–Wadsworth–Emmons reaction in silica gel (Scheme 1).<sup>5</sup>



Scheme 1

## Results and discussion

In the first place, the reaction of benzaldehyde with triethyl phosphonoacetate (TEPA) was carried out in dried silica gel<sup>6</sup> using various organic or inorganic bases. As shown in Table 1, 1,8-diazabicyclo[5.4.0]undec-7-en (DBU) was found to be the most effective<sup>2b</sup> thus affording ethyl cinnamate in almost quantitative yield with a high *E*-selectivity (run 4).

Next, the temperature-dependence of the reaction was examined (Table 2). Curiously, although the reaction proceeded

Table 1 Effect of a base on the olefination of benzaldehyde in silica gel<sup>a</sup>

| Run | Base                             | Yield <sup>b</sup> (%) | <i>E</i> : <i>Z</i> : <i>Z</i> <sup>c</sup> |
|-----|----------------------------------|------------------------|---|
| 1   | Et <sub>3</sub> N                | 48                     | 97:3  |
| 2   | DABCO                            | 38                     | 98:2  |
| 3   | ( <i>i</i> -Pr) <sub>2</sub> NEt | 23                     | 96:4  |
| 4   | DBU                              | 99                     | 97:3  |
| 5   | K <sub>2</sub> CO <sub>3</sub>   | 8                      | 98:2  |
| 6   | KOH                              | 20                     | 98:2  |

<sup>a</sup> Reactions were carried out at 90 °C for 4 h using Davisil<sup>TM</sup>-646. <sup>b</sup> GC yield. <sup>c</sup> Determined by <sup>1</sup>H NMR and GC.

at room temperature to give 76% yield of the product after 1 h, it required 37 h to reach a 94% yield (run 1).

Since the result seemed to be ascribable to the locally condensed DBU at the beginning of the reaction, silica gel-dispersed DBU was employed in place of the neat DBU. As expected, the yield was much improved thus affording a 94% GC yield for a 1 h reaction at room temperature.

As shown in Table 3, a variety of aldehydes could conveniently be converted into the corresponding  $\alpha,\beta$ -unsaturated esters at room temperature within 1 h and in good to excellent yields. Ketones hardly reacted under these conditions *e.g.*, a completely benzaldehyde-selective olefination took place in the presence of acetophenone. The protocol was also effective for the formation of  $\alpha$ -fluoro- $\alpha,\beta$ -unsaturated esters (runs 12, 14 and 16).

Finally, the recovery-reuse experiment of the silica gel used in the Horner–Wadsworth–Emmons reaction was examined. After the reaction, the silica gel was washed with diethyl ether or a mixture of ethyl acetate–hexane (1:20) solution to remove the olefination product and then dried by a heat gun under vacuum. In Table 4 are shown the results of the reaction of benzaldehyde with TEPA which was performed at room

Table 2 Effect of the reaction time and temperature on the yield<sup>a</sup>

| Run | Temp./°C | Time/h | Yield <sup>b</sup> (%) | <i>E</i> : <i>Z</i> <sup>c</sup> |
|-----|----------|--------|------------------------|----------------------------------|
| 1   | rt       | 1 (37) | 76 (94)                | 98:2                             |
| 2   | 50       | 1 (5)  | 87 (96)                | 97:3                             |
| 3   | 80       | 1      | 96                     | 97:3                             |

<sup>a</sup> Reactions were performed using DBU as a base. <sup>b</sup> GC yield. <sup>c</sup> The ratio was determined by GC.

## Green Context

Solvent-free organic synthesis is one of the most valuable of the clean technologies available to the green chemist. Here we see the successful application of this to the synthetically useful Horner–Wadsworth–Emmons reaction: a commonly used method for the conversion of carbonyl groups to C=C bonds. The reactions are carried out using silica as the solid reaction medium. Reactions proceed quickly at room temperature and the products are easily separated with the by-products remaining on the silica gel. Furthermore, the silica gel can be quantitatively recovered and reused many times.

JHC



240 (M + 2, 17), 225 (13), 221 (21), 196 (17), 170 (18), 168 (18), 166 (12), 150 (100), 146 (13), 142 (29), 130 (15), 124 (11), 122 (11), 110 (16), 91 (20), 77 (23), 69 (11), 65 (12).

### Ethyl perillylideneacetate (run 15)

An oil (70%, *E/Z* = 99/1). <sup>1</sup>H NMR (CDCl<sub>3</sub>) δ 7.30 (d, 1H, *J* = 15.6 Hz), 6.18 (d, 1H, *J* = 3.4 Hz), 5.77 (d, 1H, *J* = 15.6 Hz), 4.74 (dd, 2H, *J* = 11.7, 1.5 Hz), 4.21 (dd, 2H, *J* = 14.2, 7.3 Hz), 2.22–2.37 (m, 2H), 2.10–2.20 (m, 3H), 1.90–1.95 (m, 1H), 1.75 (s, 3H), 1.43–1.54 (m, 1H), 1.30 (t, 3H, *J* = 7.3 Hz). CI-MS (2-methylpropane) *m/z* (rel. intensity) (*E*-isomer) 222 (M + 2, 58), 193 (30), 177 (34), 166 (14), 149 (27), 132 (35), 106 (40), 92 (49), 80 (100), 75 (77), 69 (65). (*Z*-isomer) 222 (M + 2, 42), 193 (34), 179 (34), 165 (13), 153 (42), 132 (64), 106 (41), 92 (54), 80 (100), 75 (82), 68 (49).

### Ethyl fluoroperillylideneacetate (run 16)

An oil (65%, *E/Z* = 46/54). (*E*-isomer) <sup>1</sup>H NMR (CDCl<sub>3</sub>) δ 6.33 (d, 1H, *J* = 23.9 Hz), 5.93 (s, 1H), 4.73 (d, 2H, *J* = 8.8 Hz), 4.28 (dd, 2H, *J* = 14.2, 7.3 Hz), 2.29–2.35 (m, 2H), 2.20–2.25 (m, 2H), 1.84–2.18 (m, 2H), 1.74 (s, 3H), 1.43–1.53 (m, 1H), 1.34 (t, 3H, *J* = 7.3 Hz). (*Z*-isomer) <sup>1</sup>H NMR (CDCl<sub>3</sub>) δ 6.47 (d, 1H, *J* = 37.1 Hz), 6.13 (s, 1H), 4.73 (d, 2H, *J* = 13.7 Hz), 4.28 (dd, 2H, *J* = 14.2, 6.8 Hz), 2.43–2.59 (m, 2H), 2.14–2.33 (m, 2H), 1.87–2.10 (m, 2H), 1.75 (s, 3H), 1.44–1.54 (m, 1H), 1.34 (t, 3H, *J* = 6.8 Hz). CI-MS (2-methylpropane) *m/z* (rel. intensity) (*E*-isomer) 241 (M + 3, 7), 240 (M + 2, 47), 225 (5), 212 (15), 211 (72), 199 (24), 198 (38), 196 (16), 183 (84), 182 (23), 168 (26), 166 (22), 150 (24), 146 (24), 138 (19), 124 (22), 123 (26), 110 (26), 106 (30), 104 (23), 98 (24), 97 (100), 96 (24), 94 (26), 91 (35), 81 (24), 80 (21), 79 (49), 78 (39), 77 (66), 68 (97), 65 (22). (*Z*-isomer) 241 (M + 3, 8.8), 240 (M + 2, 52), 225 (8), 212 (20), 211 (100), 197 (23), 183 (57), 182 (41), 168 (50), 166 (29), 150 (78), 146 (37), 143 (48), 138 (21), 130

(17), 124 (27), 123 (66), 118 (23), 116 (21), 110 (32), 106 (38), 104 (31), 97 (91), 96 (29), 95 (20), 94 (34), 93 (30), 91 (47), 83 (21), 81 (28), 80 (22), 79 (60), 78 (50), 77 (81), 69 (20), 67 (80), 65 (35).

### Acknowledgments

This work was supported by a Grant-in-Aid for Exploratory Research from the Ministry of Education, Culture, Sports, Science and Technology, Japan, and also by the Kyushu University P&P Programs 'Green Chemistry' (to J. I.).

### References

- 1 W. S. Wadsworth, Jr., in *Organic Reactions*, ed. W. G. Dauben, John Wiley & Sons, 1977, vol. 25, ch. 2.
- 2 (a) W. C. Still and C. Gennari, *Tetrahedron Lett.*, 1983, **24**, 4405; (b) M. A. Blanchette, W. Choy, J. T. Davis, A. P. Essensfeld, S. Masamune, W. R. Roush and T. Skai, *Tetrahedron Lett.*, 1984, **25**, 2183; (c) H. Rehwinkel, J. Skupsch and H. Vorbruggen, *Tetrahedron Lett.*, 1988, **29**, 1775; (d) H. J. Gais, G. Schiedl, W. A. Ball, J. Bund, G. Hellmann and I. Erdelmeier, *Tetrahedron Lett.*, 1988, **29**, 1773.
- 3 Y. Z. Jin and J. Inanaga, presented at the 9th Tohwa University International Symposium, Book of Abstracts, p. 33, 1999. The manuscript is in preparation.
- 4 (a) P. Diddams and M. Butters, in *Solid Supports and Catalysts in Organic Synthesis*, ed. K. Smith, Ellis Horwood and PTR Prentice Hall, New York and London, 1992, ch. 1, 3 and 5; (b) R. S. Varma, *Green Chem.*, 1999, **1**, 43.
- 5 For other Wittig-type reactions under no-solvent conditions, see: (a) F. Toda and H. Akai, *J. Org. Chem.*, 1990, **55**, 3446; (b) C. D. Xe, G. Y. Chen, C. Fu and X. A. Huang, *Synth. Commun.*, 1995, **25**, 2229; (c) A. Spinella, T. Fortunati and A. Soriente, *Synlett*, 1997, 93.
- 6 Notable differences due to mesh size, pore size or commercial sources of the silica gel were not observed in the present reaction.



# Catalysis in inverted supercritical CO<sub>2</sub>/aqueous biphasic media

Mary McCarthy,<sup>ab</sup> Heike Stemmer<sup>b</sup> and Walter Leitner<sup>\*ab</sup>

<sup>a</sup> Institut für Technische Chemie und Makromolekulare Chemie, RWTH Aachen, Worringerweg 1 D-52074, Germany. E-mail: leitner@itmc.rwth-aachen.de

<sup>b</sup> Max-Planck-Institut für Kohlenforschung, Kaiser-Wilhelm-Platz 1, D-45470 Mülheim/Ruhr, Germany

Received 22nd May 2002

First published as an Advance Article on the web 15th August 2002

A new inverted biphasic catalysis system using supercritical CO<sub>2</sub> as the stationary catalyst phase and water as the continuous phase is described for Rh-catalysed hydroformylation of polar substrates. Product separation and catalyst recycling is possible without depressurising the autoclave. Turnover numbers of up to 3560 were obtained in three consecutive runs and Rh leaching into the aqueous phase was below 0.3 ppm. The absence of organic solvents allows convenient product isolation from the aqueous layer without the need for waste water treatment.

## Introduction

Product separation and catalyst recycling are among the main challenges in the development of sustainable homogeneous catalytic processes. Biphasic catalysis, where the soluble catalyst is immobilised in one liquid phase and the substrates and products are in another liquid phase, has been established as an approach to facilitate this separation and recycling.<sup>1</sup> The Ruhrchemie/Rhône Poulenc (RCH/RP) oxo process is based on such an aqueous/organic biphasic system where a water-soluble rhodium catalyst is employed for the large scale industrial hydroformylation of propylene. The olefin and aldehyde reside in the liquid organic layer<sup>2,3</sup> and the gaseous reactants CO and H<sub>2</sub> constitute a third phase in this system which implies that this system is actually triphasic (g/l/l) in nature.

Compressed (liquid or supercritical) carbon dioxide is an environmentally benign alternative to hazardous organic solvents.<sup>4,5</sup> Furthermore, the use of compressed or supercritical CO<sub>2</sub> (scCO<sub>2</sub>) as solvent reduces gas–liquid mass transfer limitations, as gaseous reactants are highly soluble in CO<sub>2</sub>. This has led to extensive studies using CO<sub>2</sub> as solvent for homogeneously catalysed reactions that involve gaseous reagents such as CO. Examples include the carbonylation of methanol,<sup>6</sup> hydroformylation,<sup>7,8</sup> hydroaminomethylation<sup>9</sup> and the Pauson–Khand reaction.<sup>10</sup> Recently several aqueous biphasic catalytic systems using CO<sub>2</sub> instead of an organic solvent have been developed with the catalyst immobilised in the water layer.<sup>11,12</sup> These systems are truly biphasic (sc/l) in nature and have been mainly applied to hydrogenation reactions.

The developmental emphasis of biphasic catalysis has so far been mainly based on catalysis employing non-polar substrates as they separate readily from the aqueous catalyst phase. However, many fine chemicals and biologically active compounds are polar in nature and cannot be separated easily from an aqueous catalyst solution. Consequently, there remains a need for systems that allow for effective isolation of polar products in biphasic catalysis. One possible approach is inverted aqueous biphasic catalysis where the catalyst is immobilised in the organic phase and the polar substrates and products reside in the aqueous phase.<sup>13,14</sup> Selective hydroformylation using a toluene/water biphasic system with a hydrophobic catalyst immobilised in the organic phase to generate a water soluble product was recently reported.<sup>13</sup> However, the use of classical organic solvents as the catalyst

phase causes significant cross-contamination into the aqueous product phase and the resulting waste water stream.

We report here an inverted biphasic catalyst system using environmentally benign CO<sub>2</sub> as the stationary catalyst phase and water as a continuous phase. This approach allows easy separation of the products from the catalyst and convenient disposal of the water layer. The general principles are exemplified for rhodium catalysed hydroformylation of water soluble acid **1**.<sup>15</sup>

## Results and discussion

A preliminary screening was carried out to identify a suitable catalyst system for rhodium catalysed hydroformylation of polar substrate **1** in CO<sub>2</sub>/water, Scheme 1. Three catalyst systems were investigated, namely unmodified rhodium carbonyls, phosphine modified rhodium and phosphine modified rhodium in the presence of a buffer. A schematic representation of the experimental set up is outlined in Fig. 1. Snapshots of the biphasic system at various process stages are shown in Fig. 2.

Hydroformylation of **1** in CO<sub>2</sub>/water occurred cleanly and no hydrogenation side products were detectable within the limits of the NMR analysis. Hydroformylation using the phosphine modified catalyst afforded two isomers of product aldehyde **2a** and **2b** in a ratio of 1 : 1. The isomers exhibit *exo*-configuration according to NMR analysis,<sup>16</sup> but differ in the position of the formyl group relative to the ester function. The corresponding signals of the two chemically inequivalent protons of the

## Green Context

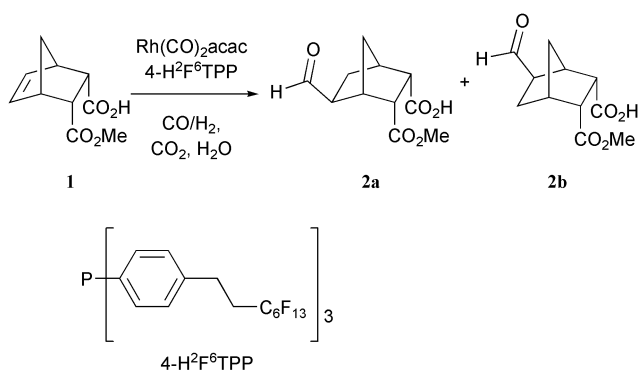
While homogeneous catalysts offer many advantages, including high activity, they generally present problems at the separation stage of a process, both in terms of product purification and catalyst recovery. Biphasic systems present one way to deal with these problems and this article is a nice illustration of the approach. Here the catalyst is maintained in a supercritical CO<sub>2</sub> layer while the organic substrate and product stay in a separate water layer. In this way efficient rhodium-catalysed hydroformylations of polar substrates are achieved.

JHC

aldehyde groups differ only slightly with chemical shifts at 9.70 and 9.71 ppm. Similarly, the  $^{13}\text{C}$  resonances of the aldehyde carbonyl group show a small, but significant difference (202.78 and 202.73 ppm, respectively). Differences of less than 0.25 ppm were also observed for most other carbon centers of the two regioisomers of *exo*-**2** and a full assignment was therefore not attempted. A largely identical chemo-, stereo-, and regio-selectivity was observed upon hydroformylation of **1** under comparable conditions in pure toluene or toluene/water mixtures, indicating that the presence of  $\text{CO}_2$  does not interfere with the catalyst-controlled selectivity in this system.

### Unmodified catalyst

Highly  $\text{CO}_2$  soluble rhodium carbonyls were formed *in situ* from  $[\text{Rh}(\text{CO})_2(\text{acac})]$  or the hexafluoro-analogue,  $[\text{Rh}(\text{CO})_2(\text{hfacac})]$ , by its addition to the autoclave followed by successive pressurisation with  $\text{CO}/\text{H}_2$  and  $\text{CO}_2$ . The autoclave was then heated to  $60^\circ\text{C}$  and a solution of alkene **1** in  $\text{H}_2\text{O}$  was added using a HPLC pump (see Fig. 2(a)). Stirring at 2000 rpm afforded a white emulsion (Fig. 2(b)) that separated rapidly when stirring was stopped (Fig. 2(c)). The reaction was typically run for 20 h after which the lower water layer was removed using a needle valve at the bottom of the reactor. The water layer contained a mixture of **1** and **2** in practically



Scheme 1

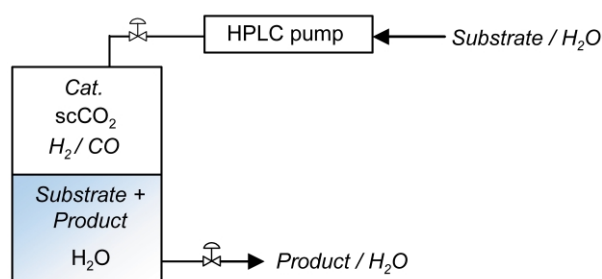


Fig. 1 Schematic representation of the reaction set-up for recycling.

quantitative mass balance and their ratio was determined by  $^1\text{H}$  NMR spectroscopy.

The hydroformylation of **1** using unmodified rhodium catalysts gave very low conversions to **2** of between 4 and 14% (Table 1: runs 1a, 2a). Furthermore, a large amount of metallic rhodium was observed on the reactor walls on opening the autoclave.<sup>17</sup> Recycling experiments showed similar or slightly lower conversions in the second cycle. Rhodium contamination of 68 ppm was determined in the aqueous layer indicating a large amount of leaching had taken place (Table 1: run 2a).

### Modified rhodium catalysts

The modified catalysts were formed by mixing the rhodium precursor  $[\text{Rh}(\text{CO})_2(\text{acac})]$  and the  $\text{CO}_2$ -philic phosphine ligand 4- $\text{H}_2\text{F}_6\text{TPP}$ <sup>18</sup> (Scheme 1). Complete conversion to aldehyde was obtained in 20 h using a rhodium : phosphine : substrate ratio of 1 : 10 : 500 (Table 2: run 1a) corresponding to a turnover number of 500. When the catalyst loading was reduced to a rhodium concentration of  $0.05\text{ mmol L}^{-1}$ , 86% conversion was obtained giving a turnover number of 1720 (Table 2: run 2a). On opening the autoclave small amounts of rhodium black was observed but to a much lesser extent than in the unmodified system.<sup>17</sup>

### Modified rhodium with added buffer

The third set of reaction conditions investigated involved the addition of a buffer to the modified rhodium catalyst system. Rhodium catalysed hydroformylation is generally believed to operate best at neutral to slightly basic conditions. The pH of unbuffered water at elevated pressures of  $\text{CO}_2$  however is in the range of 2.85–2.95.<sup>19</sup> The buffer MOPS ( $\gamma$ -morpholinopropane sulfonic acid) has been successfully introduced to keep the aqueous solution at about 50 bar  $\text{CO}_2$  at pH 5.5.<sup>20</sup> Therefore we

Table 1 Hydroformylation of **1** in  $\text{scCO}_2/\text{H}_2\text{O}$  using unmodified rhodium catalyst

| Run <sup>a</sup> | Rh : 1  | [Rh] (mmol $\text{L}^{-1}$ ) in $\text{CO}_2$ | Conv. <sup>b</sup> (%) | TON  | Rh leaching <sup>c</sup> /ppm |
|------------------|---------|---|------------------------|------|-------------------------------|
| 1a <sup>d</sup>  | 1 : 500 | 0.2   | 4.5                    | 22.5 | n.d.                          |
| 1b               | 1 : 500 | 0.2   | 4.6                    | 23   | n.d.                          |
| 2a <sup>e</sup>  | 1 : 500 | 0.2   | 14                     | 70   | 68.3                          |
| 2b               | 1 : 500 | 0.2   | 6.4                    | 32   | n.d.                          |

<sup>a</sup> Reaction conditions: 8 mmol alkene **1**, 20 bar  $\text{CO}/\text{H}_2$ , 50 g  $\text{CO}_2$ , 20 mL  $\text{H}_2\text{O}$ ,  $60^\circ\text{C}$ , 2000 rpm, 20 h, 100 mL total reaction volume. <sup>b</sup> % Conversion determined by  $^1\text{H}$  NMR spectroscopy. <sup>c</sup> % Rhodium leaching determined by atomic absorption spectroscopy. <sup>d</sup> 0.016 mmol  $[\text{Rh}(\text{CO})_2(\text{acac})]$ . <sup>e</sup> 0.016 mmol  $[\text{Rh}(\text{CO})_2(\text{hfacac})]$ .

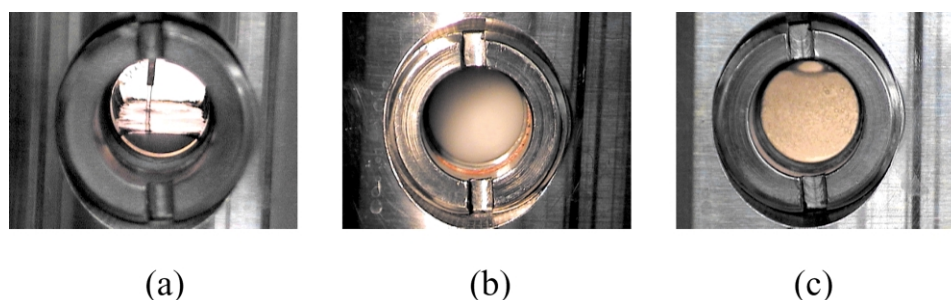
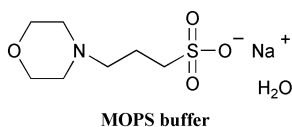


Fig. 2 Snapshots of the biphasic system at various stages of the process: (a) filling with  $\text{H}_2\text{O}$ , (b) emulsion during the reaction, (c) separation of layers after the reaction.



carried out the hydroformylation reaction as described in the previous section but in the presence of 1.078 M MOPS. The substrate: buffer ratio was 2 : 5.4 and the buffer was added to the aqueous substrate solution before addition to the autoclave (Table 3: run 1a).

The conversions to aldehyde **2** in the presence of MOPS buffer were unexpectedly low. The  $^1\text{H}$  NMR spectrum of the reaction mixture revealed that hydrolysis of the ester in **1** had taken place to give symmetrical alkene **3**, Scheme 2. The symmetrical alkene **3** and its sodium salt are considerably more soluble in water and less soluble in  $\text{CO}_2$  than substrate **1** and this may at least partly explain the lower conversions observed. In accord with this consideration, a somewhat higher conversion of 30% was obtained when a 0.13 M MOPS solution was employed (substrate: buffer = 2:0.65) (Table 3: run 2). On opening the autoclave no metallic rhodium was visible which can be attributed to the higher pH in the autoclave during the reaction time.<sup>17</sup>

**Table 2** Hydroformylation of **1** in  $\text{scCO}_2/\text{H}_2\text{O}$  using 4- $\text{H}^2\text{F}^6\text{TPP}$  (L) modified rhodium catalyst.

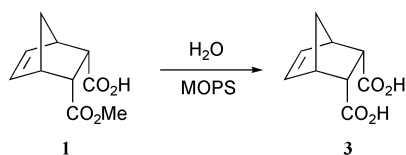
| Run <sup>a</sup> | Rh:L:1    | [Rh] (mmol L <sup>-1</sup> ) in $\text{CO}_2$ | Conv. <sup>b</sup> (%) | TON  | Rh leaching <sup>c</sup> /ppm |
|------------------|-----------|---|------------------------|------|-------------------------------|
| 1a <sup>d</sup>  | 1:10:500  | 0.2   | 100                    | 500  | 0.26                          |
| 1b               | 1:10:500  | 0.2   | 100                    | 500  | 0.16                          |
| 1c               | 1:10:500  | 0.2   | 100                    | 500  | 0.07                          |
| 2a <sup>e</sup>  | 1:10:2000 | 0.05  | 86                     | 1720 | 0.05                          |
| 2b               | 1:10:2000 | 0.05  | 60                     | 1200 | 0.05                          |
| 2c               | 1:10:2000 | 0.05  | 32                     | 640  | 0.08                          |

<sup>a</sup> Reaction conditions: 8 mmol substrate **1**, 20 bar  $\text{CO}/\text{H}_2$ , 50 g  $\text{CO}_2$ , 20 mL  $\text{H}_2\text{O}$ , 60 °C, 2000 rpm, 20 h, 100 mL total reaction volume. <sup>b</sup> % Conversion determined by  $^1\text{H}$  NMR spectroscopy. <sup>c</sup> % Rhodium leaching determined by atomic absorption spectroscopy. <sup>d</sup> 0.016 mmol  $[\text{Rh}(\text{CO})_2(\text{acac})]$ , 0.16 mmol 4- $\text{H}^2\text{F}^6\text{TPP}$ . <sup>e</sup> 0.004 mmol  $[\text{Rh}(\text{CO})_2(\text{acac})]$ , 0.04 mmol 4- $\text{H}^2\text{F}^6\text{TPP}$ .

**Table 3** Hydroformylation of **1** in  $\text{scCO}_2/\text{H}_2\text{O}$  using 4- $\text{H}^2\text{F}^6\text{TPP}$  modified rhodium catalyst and MOPS buffer

| Run <sup>a</sup> | MOPS Buffer/<br>M | Rh:L:1    | [Rh] (mmol L <sup>-1</sup> ) in $\text{CO}_2$ | Conv. <sup>b</sup> (%) | TON |
|------------------|-------------------|-----------|---|------------------------|-----|
| 1a <sup>c</sup>  | 1                 | 1:10:2000 | 0.2   | 13                     | 260 |
| 1b <sup>c</sup>  | 1                 | 1:10:2000 | 0.2   | 8                      | 160 |
| 1c <sup>c</sup>  | 1                 | 1:10:2000 | 0.2   | 1                      | 20  |
| 2 <sup>d</sup>   | 0.1               | 1:10:2000 | 0.2   | 30                     | 600 |

<sup>a</sup> Reaction conditions: 0.01 mmol  $[\text{Rh}(\text{CO})_2(\text{acac})]$ , 0.1 mmol 4- $\text{H}^2\text{F}^6\text{TPP}$ , 20 mmol substrate **1**, 16 bar  $\text{CO}/\text{H}_2$ , 31.5 g  $\text{CO}_2$ , 50 mL  $\text{H}_2\text{O}$ , 60 °C, 2000 rpm, 20 h, 100 mL total reaction volume. <sup>b</sup> % Conversion determined by  $^1\text{H}$  NMR spectroscopy. <sup>c</sup> 54 mmol MOPS (1.078 M). <sup>d</sup> 6.47 mmol MOPS (0.13 M).



Scheme 2

## Recycling experiments

The 4- $\text{H}^2\text{F}^6\text{TPP}/[\text{Rh}(\text{CO})_2(\text{acac})]$  (P:Rh = 10:1) catalyst system was chosen for more detailed batch-wise recycling studies to demonstrate the principle of catalyst immobilisation in the inverted  $\text{H}_2\text{O}/\text{scCO}_2$  system. The aqueous phase was removed after phase separation through a needle valve at the bottom of the reactor. A new batch of substrate was then introduced as aqueous solution using a HPLC pump. It is important to note that no expansion/recompression of the  $\text{CO}_2$  phase is required in this operation. The gas recycling is usually the most energy demanding and costly step of  $\text{CO}_2$ -based separation schemes. A total of three cycles were performed using a rhodium:substrate ratio of 1:500 (Table 2: runs 1a–c) and in each cycle complete conversion was obtained. The amount of rhodium that leached into the aqueous phase was less than 0.26 ppm in each case showing that the fluorinated ligand successfully immobilised the catalyst in the aqueous layer. Recovery of the product from the autoclave was high in all cases; about 90–95% was retrieved. When the reaction was performed using a lower catalyst loading with a Rh concentration of 0.05 mmol L<sup>-1</sup> and a rhodium:substrate ratio of 1:2000 the first cycle gave 86% conversion to aldehyde after 20 h with a turnover number of 1720 (Table 2: run 2a). A significant reduction in conversion was observed in recycling experiments where the conversion dropped to 60% in the second cycle and then to 32% in the third cycle (Table 2: runs 2b, c). This reduction in conversion is most likely due to deactivation of the catalyst as leaching was again below 0.1 ppm.

## Conclusions

We have shown that inverted supercritical  $\text{CO}_2$ /aqueous biphasic media provide a promising approach to catalytic synthesis of highly polar products. This new system allows for effective catalyst immobilisation while simultaneously alleviating the problems associated with waste treatment of the aqueous layer. For hydroformylation, a  $\text{CO}_2$ -philic phosphine ligand was effective to successfully immobilise the rhodium catalyst in the  $\text{CO}_2$  layer as is shown by the very low level of rhodium found in the aqueous phase. Total turnover numbers of up to 3560 were achieved using low rhodium concentrations but the catalyst stability is yet to be optimised under these conditions.

The catalyst was recycled three times with stable conversion at higher rhodium concentrations (0.2 mmol L<sup>-1</sup>). The development of such sustainable systems using  $\text{CO}_2$  and water has great potential. This technology can be economically transferred to a continuous process because the  $\text{CO}_2$  is the stationary phase and this implies that repeated gas compression/decompression cycles are not required. The scope of this system is currently under investigation and will form the subject of future publications.

## Experimental

### General

Reactions involving air-sensitive materials were performed under argon using Schlenk techniques. The water was distilled and deoxygenated before use. The gases  $\text{CO}/\text{H}_2$  (1:1), argon (99.995%) and  $\text{CO}_2$  (99.9995%) were purchased from Messer Griesheim. **1** was synthesised from *cis*-5-norbornene-*endo*-2,3-dicarboxylic acid anhydride<sup>21</sup> and 4- $\text{H}^2\text{F}^6\text{TPP}$  was synthesised according to literature procedures.<sup>18</sup> *cis*-5-Norbornene-*endo*-2,3-dicarboxylic acid anhydride was used as supplied by



Aldrich. NMR spectra were recorded on a Bruker AMX 300 or AV 400 spectrometer. Chemical shifts are given in ppm relative to TMS ( $^1\text{H}$ ,  $^{13}\text{C}$ ). Rhodium content was determined by atomic absorption spectroscopy (AAS) in the analytical laboratories of Celanese GmbH, Werk Ruhrchemie.

**CAUTION:** working with highly compressed gases must be carried out only using suitable equipment and with appropriate safety precautions.

### General procedure for autoclave experiments

*Note:* for catalyst, reagent and solvent amounts see Tables 1–3. Ligand 4- $\text{H}^2\text{F}^6\text{TTP}$  and  $[\text{Rh}(\text{CO})_2(\text{acac})]$  were added to a Schlenk flask and dissolved in toluene (3 mL). This solution was filled in to a 100 mL autoclave and the toluene was removed *in vacuo*. Alternatively the ligand and rhodium precursor were placed in the autoclave as solids. No significant difference was observed for these procedures. The reactor was pressurised with  $\text{CO}/\text{H}_2$  (16–20 bar) and then filled with  $\text{CO}_2$  (31.5–50 g) by means of a compressor. The substrate solution in water (0.4 M) was added to the autoclave using a HPLC pump keeping the tubing heated at all times to prevent the substrate from precipitating. The reaction mixture was heated to 60 °C and stirred at 2000 rpm for 20 h. The heating and stirring were then stopped and the lower water solution was removed from the autoclave using a capillary needle valve and collected in a Schlenk. A 2 mL sample was worked up by removing the water *in vacuo*. The conversion was determined by  $^1\text{H}$  NMR spectroscopy. The recovery of the substrate/product mixture from the autoclave ranged from 90 to 95%. Recycling experiments were carried out by adding a new batch of **1** in  $\text{H}_2\text{O}$  to the autoclave using the HPLC pump. Experiments using MOPS buffer were carried out using the same procedure except that the buffer was added to the aqueous substrate solution. NMR data of **2a/2b**:  $^1\text{H}$  NMR ( $\delta$ ,  $\text{CDCl}_3$ , 400 MHz) 9.71/9.70 (1H, s, H-10), 3.67/3.66 (3H, s,  $\text{CH}_3\text{O}$ ), 3.26–3.15 (2H, m, H-2, H-4), 3.08–3.01 (1H, m, H-4), 2.9 (1H, br s, H-5), 2.7 (1H, br d, H-6), 1.9–1.74 (2H, m,  $\text{CH}_2$ , H-3), 1.41–1.31 (2H, m,  $\text{CH}_2$ , H-7).  $^{13}\text{C}$  NMR ( $\delta$ ,  $\text{CDCl}_3$ , 100.6 MHz) 202.78/202.73 (CHO), 177.83/177.63 (COOH), 172.57/172.39 (COOCH<sub>3</sub>), 51.72/51.56 (COOCH<sub>3</sub>), 48.29/48.27 (C-2), 46.53/46.30 (C-1), 46.47 (C-4), 40.78/40.64 (C-6), 40.43 (C-5), 37.54/37.54 (C-7), 25.28/25.18 (C-3).

### Acknowledgements

The Deutsche Forschungsgemeinschaft (Gerhard-Hess-Award to W. L.) and the bmb+f (ConNeCat lighthouse project ‘Tuneable Systems for Organometallic Multiphase Catalysis’) supported this work. We thank Celanese GmbH, Werk Ruhrchemie, for atomic absorption spectroscopy measurements. The technical assistance of Axel Brinkmann is gratefully acknowledged.

### References

- Catal. Today*, 1998, **42**, issue 4.
- B. Cornils and J. Falbe, *Proc. 4th Int. Symp. Homogeneous Catalysis*, Leningrad, Sept. 1984, p. 487; G. Kessen, B. Cornils, J. Hibbel, H. Bach and W. Gick, *Eur. Pat.*, EP 0 216 151, 1986 (Hoechst AG).
- Aqueous-Phase Organometallic Catalysis*, ed. B. Cornils and W. A. Herrmann, Wiley-VCH, Weinheim, 1998.
- Chemical Synthesis Using Supercritical Fluids*, ed. P.G. Jessop and W. Leitner, Wiley-VCH, Weinheim, New York, 1999.
- P. G. Jessop, T. Ikariya and R. Noyori, *Chem. Rev.*, 1999, **99**, 475; W. Leitner, *Acc. Chem. Res.*, 2002, in press.
- R. J. Sowden, M. F. Sellin, N. DeBlasio and D. J. Cole-Hamilton, *Chem. Commun.*, 2000, 2511.
- D. Koch and W. Leitner, *J. Am. Chem. Soc.*, 1998, **120**, 13398; G. Franciò, K. Wittmann and W. Leitner, *J. Organomet. Chem.*, 2001, **621**, 130.
- J. W. Rathke, R. J. Klingler and T. R. Krause, *Organometallics*, 1991, **10**, 1350; Y. Guo and A. Akgerman, *J. Supercrit. Fluids*, 1999, **15**, 63; D. R. Palo and C. Erkey, *Organometallics*, 2000, **19**, 81; M. F. Sellin and D. J. Cole-Hamilton, *J. Chem. Soc., Dalton Trans.*, 2000, 1681; P. G. Jessop, D. C. Wynne, S. DeHaai and D. Nakawatase, *Chem. Commun.*, 2000, 693; N. J. Meehan, A. J. Sandee, J. N. H. Reek, P. C. J. Kamer, P. W. N. M. van Leeuwen and M. Poliakoff, *Chem. Commun.*, 2000, 1497; A. M. B. Osuna, W. Chen, E. G. Hope, R. D. W. Kemmitt, D. R. Paige, A. M. Stuart, J. Xiao and L. Xu, *J. Chem. Soc., Dalton Trans.*, 2000, 4052; D. Bonafoux, Z. Hua, B. Wang and I. Ojima, *J. Fluorine Chem.*, 2001, **112**, 101.
- K. Wittmann, W. Wisniewski, R. Mynott, W. Leitner, C. L. Kranemann, T. Rische, P. Eilbracht, S. Kluwer, J. M. Ernstring and C. L. Elsevier, *Chem. Eur. J.*, 2001, **7**, 4584.
- N. Jeong, S. H. Hwang, Y. W. Lee and J. S. Lim, *J. Am. Chem. Soc.*, 1997, **119**, 10549.
- B. M. Bhanage, Y. Ikushima, M. Shirai and M. Arai, *Chem. Commun.*, 1999, 1277; G. B. Jacobson, C. T. Lee Jr., K. P. Johnson and W. Tumas, *J. Am. Chem. Soc.*, 1999, **121**, 11902; B. M. Bhanage, Y. Ikushima, M. Shirai and M. Arai, *Tetrahedron Lett.*, 1999, **40**, 6427.
- R. J. Bonilla, B. R. James and P. G. Jessop, *Chem. Commun.*, 2000, 941.
- G. Verspui, G. Elbertse, F. A. Sheldon, M. A. P. J. Hacking and R. A. Sheldon, *Chem. Commun.*, 2000, 1363; G. Verspui, G. Elbertse, G. Papadogianakis and R. A. Sheldon, *J. Organomet. Chem.*, 2001, **621**, 337.
- R. M. Deshpande, S. S. Divekar, B. M. Bhanage and R. V. Chaudhuri, *J. Mol. Catal.*, 1992, **75**, L19.
- A  $\text{CO}_2$ -soluble palladium catalyst was used in a  $\text{scCO}_2$ /water system for the synthesis of aqueous  $\text{H}_2\text{O}_2$  from  $\text{H}_2$  and  $\text{O}_2$ , but no water-soluble substrate was involved in this case: D. Hăncu and E. J. Beckman, *Green Chem.*, 2001, **3**, 80.
- C. Botteghi, S. Paganelli, A. Perosa, R. Lazzaroni and G. Uccello-Barretta, *J. Organomet. Chem.*, 1993, **447**, 153.
- The Rh deposit formed in the absence of buffer is able to serve as a reservoir for highly active Rh carbonyls under certain hydroformylation conditions. For example, 1-hexene was hydroformylated in  $\text{scCO}_2$  under single phase conditions in such a contaminated autoclave. However, no hydroformylation of **1** took place in  $\text{H}_2\text{O}/\text{CO}_2$  under identical conditions. The Rh deposit could be removed by thorough washing of the reactor with HCl. All reactors were checked for hydroformylation activity routinely prior to use.
- S. Kainz, D. Koch, W. Baumann and W. Leitner, *Angew. Chem., Int. Ed. Engl.*, 1997, **36**, 1628; S. Kainz, Z. Luo, D. P. Curran and W. Leitner, *Synthesis*, 1998, 1425.
- K. L. Toews, R. M. Shroll, C. M. Wai and N. G. Smart, *Anal. Chem.*, 1995, **67**, 4040.
- See the electronic supplementary information of ref. 12.
- H. M. Walton, *J. Org. Chem.*, 1957, **22**, 308.



# New role of carbon dioxide in Lewis assisted Brønsted acid accelerated diiodination of alkynes in water

Jin-Heng Li,\* Ye-Xiang Xie and Du-Lin Yin

Institute of Fine Catalysis and Synthesis, College of Chemistry and Chemical Engineering, Hunan Normal University, Yuelushan, Changsha 410081, China

Received 5th July 2002

First published as an Advance Article on the web 13th September 2002

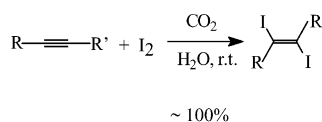
CO<sub>2</sub> is reported here as a Lewis assisted Brønsted acid accelerator to promote diiodination of alkynes. In the presence of CO<sub>2</sub>, quantitative yields of *trans*-1,2-diiodoalkenes were obtained by diiodination of both electron-rich and electron-deficient alkynes with I<sub>2</sub> in H<sub>2</sub>O.

The application of carbon dioxide in organic synthesis is one of the challenges in organic chemistry. Most of the studies on carbon dioxide generally concern the applications of carbon dioxide as a raw material<sup>1</sup> and a reaction medium.<sup>2</sup> Thus, development of some new routes to apply carbon dioxide in organic chemistry still seems highly interesting.

1,2-Diiodoalkenes are useful intermediates in organic synthesis.<sup>3</sup> Earlier studies have shown that they were prepared stereospecifically, with only *trans*-adducts being obtained, by direct addition of iodine to alkynes.<sup>4</sup> However, the reactions proceeded very slowly with low conversion. Thus, alumina<sup>5</sup> or CuI,<sup>6</sup> a solid inorganic Lewis acid, was added to improve efficiency of the reaction. Although the addition of solid inorganic Lewis acids can improve the reaction, their residues not only make the separation more difficult but also pollute the environment. On the other hand, harmful solvents such as CH<sub>3</sub>CN, CH<sub>2</sub>Cl<sub>2</sub>, methanol, and petroleum ether were used in all cases. Thus, a search for a green and general route to diiodination of alkynes is still of current considerable interest to synthetic organic chemists. Herein we report the first use of carbon dioxide as a Lewis assisted Brønsted acid accelerator for diiodination of alkynes with I<sub>2</sub> in water (Scheme 1).

We found that diiodination of alkynes was performed smoothly with I<sub>2</sub> using CO<sub>2</sub> (a gaseous Lewis acid) as a Lewis assisted Brønsted acid accelerator and H<sub>2</sub>O as the reaction medium.† Results of the diiodination of alkynes were summarized in Table 1. As shown in Table 1, the results indicated that the presence of CO<sub>2</sub> was critical: in its absence, the diiodination of phenylacetylene was slow. Only 21% of phenylacetylene was converted and 19% of *trans*-1,2-diiodophenylethylenes (*E*-isomer) was obtained in 8 h at room temperature (entry 1 in Table 1). Remarkably, phenylacetylene was converted completely in 3 h and 100% of the desired diiodide was obtained under 1.0 MPa pressure of CO<sub>2</sub>. The *trans* structure of 1,2-diiodoalkenes were assigned on the basis of the chemical shift of the olefinic proton in their <sup>1</sup>H NMR spectra, which match the reported data in the references 4 and 6.

The diiodination of other alkynes including both electron-rich and electron-deficient alkynes was carried out smoothly and afforded the corresponding *trans*-1,2-diiodoalkenes in



Scheme 1

Table 1 CO<sub>2</sub> promote diiodination of alkynes in water<sup>a</sup>

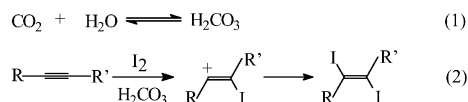
| Entry          | Alkyne   | Reaction time/h | Isolated yield (%) |
|----------------|--|-----------------|--------------------|
| 1 <sup>b</sup> | PhC≡CH   | 8               | 19                 |
| 2              | PhC≡CH   | 3               | Quantitative       |
| 3              | C <sub>8</sub> H <sub>17</sub> C≡CH                            | 4               | Quantitative       |
| 4              | C <sub>3</sub> H <sub>7</sub> C≡CC <sub>3</sub> H <sub>7</sub> | 4               | Quantitative       |
| 5              | CH <sub>3</sub> C≡CCOOMe                                       | 6               | Quantitative       |
| 6              | HC≡CCOOEt  | 6               | Quantitative       |

<sup>a</sup> Reaction conditions: alkyne (1 mmol), I<sub>2</sub> (1.0 mmol), and CO<sub>2</sub> (1.0 MPa) in H<sub>2</sub>O (5 mL) at room temperature. <sup>b</sup> In the absence of CO<sub>2</sub>, the conversion of phenylacetylene was 21% which was detected by GC analysis.

about quantitative yields, although the latter required a prolonged time (entries 3–6).

It should be noted that the diiodination products were readily isolated. After the release of CO<sub>2</sub>, either the solvent (water) is evaporated or the reaction mixture is extracted with diethyl ether followed by evaporation of diethyl ether to afford the pure products.

A radical mechanism and an ionic mechanism have been proposed in the literature<sup>4–6</sup> for the reaction of alkynes with iodine. Comparing with the earlier reports and basing upon our results, we presume that the CO<sub>2</sub>-promoted reaction under our conditions might occur by an ionic mechanism as outlined in Scheme 2. It is well known that carbon dioxide in water generates carbonic acid (H<sub>2</sub>CO<sub>3</sub>) readily, so the first step may be the reaction of CO<sub>2</sub> with H<sub>2</sub>O to afford H<sub>2</sub>CO<sub>3</sub> followed by H<sub>2</sub>CO<sub>3</sub>, a Brønsted acid, to accelerate the diiodination. In



Scheme 2

## Green Context

One of the most renewable reaction media must be a mixture of CO<sub>2</sub> and water. Here this medium is used to bring about the diiodination of alkynes, something which normally requires an acid catalyst and an organic solvent. Here, both of these are done away with, with dissolved CO<sub>2</sub> providing sufficient acidity to drive the reaction DJM

summary, although further investigation is needed to precisely settle the mechanism, we have provided a green and general method for the synthesis of *trans*-1,2-diiodoalkenes *via* CO<sub>2</sub>-promoted the diiodination of alkynes with I<sub>2</sub> in H<sub>2</sub>O. Further efforts related to the role of carbon dioxide and synthetic applications of the reaction are underway in our laboratory.

## Acknowledgement

We thank Hunan Normal University for financial support.

## Notes and references

† General procedure for the diiodination of alkynes: a mixture of alkyne (1 mmol), I<sub>2</sub> (1.0 mmol), CO<sub>2</sub> (1.0 MPa) and H<sub>2</sub>O (5 mL) was stirred for 3–6 h at room temperature in a HF-25 autoclave. After release of CO<sub>2</sub>, the mixture was extracted with ethyl ether, followed by evaporation of diethyl ether to afford the pure product.

- 1 T. Matsuda, Y. Ohashi, T. Harada, R. Yanagihara, T. Nagasawa and K. Nakamura, *Chem. Commun.*, 2001, 2194 and references therein; M. Abia, J. C. Choi and T. Sakakura, *Chem. Commun.*, 2001, 2238 and references therein.
- 2 For representative reviews, see: P. G. Jessop and W. Leitner, eds. *Chemical Synthesis using Supercritical Fluids*, Wiley-VCH, Weinheim, 1999; P. G. Jessop, T. Ikariya and R. Noyori, *Chem. Rev.*, 1999, **99**, 475; J. Li, L. Jia and H. Jiang, *Chinese J. Org. Chem.*, 2000, **20** (3), 293; R. S. Oakes, A. A. Clifford and C. M. Rayner, *J. Chem. Soc., Perkin Trans. 1*, 2001, 917.
- 3 J. Barluenga, J. M. Montserrat and J. Flórez, *J. Org. Chem.*, 1993, **58**, 5976; M. E. Wright and C. K. Lowe-Ma, *Organometallics*, 1990, **9**, 347; N. Hénaff and A. Whiting, *J. Chem. Soc., Perkin Trans. 1*, 2000, 395 and references therein.
- 4 R. A. Hollins and M. P. A. Campos, *J. Org. Chem.*, 1979, **44**, 3931; V. L. Heasley, D. F. Shellhamer, L. E. Heasley and D. B. Yaeger, *J. Org. Chem.*, 1980, **45**, 4649.
- 5 S. Larson, T. Luidhardt, G. W. Kabalka and R. M. Pagni, *Tetrahedron Lett.*, 1988, **29**, 35; G. Hondrogiannis, L. C. Lee, G. W. Kabalka and R. M. Pagni, *Tetrahedron Lett.*, 1989, **30**, 2069; R. M. Pagni, G. W. Kabalka, R. Boothe, K. Gaetano, L. J. Stewart, R. Conaway, C. Dial, D. Gray, S. Larson and T. Luidhard, *J. Org. Chem.*, 1988, **53**, 4477.
- 6 J. Duan, W. R. Dolbier, Jr. and Q.-Y. Chen, *J. Org. Chem.*, 1998, **63**, 9486.



# Hydroformylation of 1-hexene in supercritical carbon dioxide using a heterogeneous rhodium catalyst. 3. Evaluation of solvent effects

Orin Hemminger,<sup>a</sup> Anne Marteel,<sup>b</sup> Mark R. Mason,<sup>b</sup> Julian A. Davies,<sup>b</sup> Andrew R. Tadd<sup>a</sup> and Martin A. Abraham<sup>\*a</sup>

<sup>a</sup> Department of Chemical Engineering, University of Toledo, Toledo, OH 43606, USA

<sup>b</sup> Department of Chemistry, University of Toledo, Toledo, OH 43606, USA

Received 17th May 2002

First published as an Advance Article on the web 21st August 2002

The heterogeneously catalyzed hydroformylation of 1-hexene in supercritical carbon dioxide is demonstrated as an alternative to homogeneous catalysis through the use of a rhodium–phosphine catalyst tethered to a silica support. Reaction over the heterogeneous catalyst in supercritical CO<sub>2</sub> is compared with the use of this catalyst in liquid-phase toluene, and toluene expanded with CO<sub>2</sub>. Likewise, the performance of the tethered catalyst is compared with a homogeneous rhodium–phosphine catalyst, and shown to be equally effective under identical reaction conditions. Comparable reaction rates were obtained using the heterogeneous rhodium catalyst in supercritical CO<sub>2</sub> and CO<sub>2</sub>-expanded toluene, both of which were superior to the reaction rate with the heterogeneous catalyst in liquid-phase toluene. Initial aldehyde selectivity obtained with the heterogeneous species was also comparable to that obtained with the homogeneous catalyst, but decreased over the course of the reaction. These results demonstrate the value of using phase behavior, and the importance of understanding this behavior in the development and analysis of greener solvent/catalyst systems.

## Introduction

Also referred to as the ‘oxo reaction,’ hydroformylation adds one equivalent each of carbon monoxide and hydrogen to an alkene, producing an aldehyde, in the presence of a catalyst. The hydroformylation of ethene produces propanal exclusively, but for C<sub>3</sub> and higher alkenes mixtures of linear and branched aldehydes are observed. Processes were originally developed using cobalt catalysts. All current commercial processes are based on homogeneous catalysts, mostly using rhodium, which has supplanted cobalt due to its higher activity. These processes also use phosphine ligands to increase the regioselectivity to the linear aldehyde.

Hydroformylation was first carried out using cobalt catalysts at high temperatures and high syngas pressures.<sup>1,2</sup> Since that time, there has been a significant amount of research devoted to the development of hydroformylation catalysts. This research has included novel ligands and their synthesis, evaluation of process parameters and their effects on activity and selectivity, and the development of heterogeneous catalyst systems.

All homogeneously catalyzed systems require catalyst separation and recovery steps. For low molecular weight substrates, the Ruhrchemie/Rhone–Polenc (RCH–RP) process is used. The RCH–RP process uses a water-soluble catalyst, and the recovery step is simple and effective.<sup>1,2</sup> For substrates of C<sub>6</sub> and greater, RCH–RP does not give sufficient activities to be commercially feasible. The processes applied for these substrates have complex rhodium recovery operations;<sup>2</sup> half of the unit operations deal with separating the catalyst from the crude product stream. The phase separation is simple and similar to the RCH–RP process, but the water added to produce the phase split must be pulled out of the catalyst stream before it is returned to the reactor.

The development of a successful heterogeneous catalyst would allow a much simpler commercial process to be implemented; it would eliminate the need for catalyst recovery and allow the use of a fixed bed type reactor. Attempts have

been made to produce a selective heterogeneous catalyst by anchoring a homogeneous catalyst, or its analogue, to a solid support. For example, catalysts that have been prepared include HRh(CO)(PPh<sub>3</sub>)<sub>3</sub> absorbed by incipient wetness on carbon nanotubes,<sup>3</sup> rhodium supported on polysiloxane polymers with grafted alkylphosphine chains,<sup>4</sup> rhodium supported on Ti-hexagonal mesoporous silica (Ti-HMS),<sup>5</sup> and rhodium supported on activated carbon.<sup>6</sup> In general, high selectivities could only be achieved at low conversions, and hydrogenation and loss of rhodium from the supports to the reaction mixtures have been recurring problems.

The switch from a homogeneous catalyst to a heterogeneous one would be expected to give rise to lower rates of reaction. The parallel introduction of scCO<sub>2</sub> as a reaction solvent, however, would bring the substrate and the gaseous reactants into one phase. Additionally, scCO<sub>2</sub> has high diffusivities and low surface tension, both of which would facilitate mass

## Green Context

**Hydroformylation is an extremely important industrial chemical process based entirely on the use of homogeneous transition metal catalysts. All homogeneous catalysed systems require catalyst separation and recovery steps although this has been simplified in some cases through the use of water-soluble catalysts. A heterogeneous catalytic process would offer substantial advantages including simplified processes and the possibility for fixed-bed reactors. This is one of a series of papers dedicated to achieving that goal. Here it is shown that an immobilised rhodium–phosphine catalyst is equally effective when compared to homogeneous catalysts. Solvent effects in the heterogeneous system are studied and supercritical CO<sub>2</sub> is shown to be effective thus adding to the green chemistry credentials of the work.**

JHC

transport. These factors would be expected to offset the lowering of rates due to the use of a heterogeneous system. This was first demonstrated several years ago<sup>7</sup> for the hydroformylation of propene in scCO<sub>2</sub> using a cobalt catalyst. Careful design of the catalyst to capitalize on the unique solvent properties of scCO<sub>2</sub> may afford other advantages, including enhanced activity, selectivity, and stability.

The use of scCO<sub>2</sub> as a replacement for organic solvents falls in line with the pollution prevention paradigm. Carbon dioxide has been identified as a greenhouse gas, but its use as a solvent, as opposed to its production (*e.g.* by automobiles or in power generation), is considered to be environmentally benign. Carbon dioxide is nontoxic, does not form air-polluting daughter products and, additionally, is cheap and plentiful. As compared to water, which is all of the above as well, its critical properties are milder, making it simpler, safer, and less expensive to use as the centerpiece of a commercial process.

Maximum environmental benefit is achieved when scCO<sub>2</sub> is used both as a reaction solvent and to optimize the product separation train and the catalyst recovery system. Because of its tunable solvent properties, some product/reactant separations should be achievable by manipulating pressure. Recently, Poliakoff and co-workers<sup>8</sup> reported a 90% recovery of substrate (1-octene) from reaction products (nonanals) by use of a two-stage depressurization. In a commercial process, the product stream could be expanded after the reactor, separating the solvent from the reaction products, and a high-pressure solvent/reactant stream could be recycled at lower compressor costs.

An interesting opportunity is further presented when CO<sub>2</sub> is dissolved into a liquid solvent to provide favorable reaction conditions while simultaneously decreasing the amount of organic solvent used in the process. For example, Chouchi *et al.*<sup>9</sup> determined that the hydrogenation of pinene over palladium on carbon was slower in the two-phase region than in a single supercritical phase, because phase partitioning of the reactant decreased its concentration in the liquid phase that contained the catalyst. In addition, the transport resistances are reduced and the solubilities of the gaseous reactants are enhanced in the expanded liquid, increasing the rate of reaction over that which can be obtained in the pure liquid.<sup>10,11</sup>

Over the last several years, we have been working to demonstrate the feasibility of using a heterogeneous catalyst in combination with scCO<sub>2</sub> to promote the hydroformylation reaction. Dharmidhikari and Abraham<sup>12</sup> first reported the use of rhodium supported on activated carbon for propene hydroformylation in scCO<sub>2</sub>, but had limited success because of strong adsorption of the product aldehyde onto the carbon support. Improvement was obtained by adsorbing rhodium on low-surface-area silica, however, these catalysts exhibited significant rhodium leaching.<sup>13</sup> Tadd *et al.*<sup>14</sup> demonstrated the feasibility of the process using a rhodium catalyst chemically bound to a phosphinated silica, demonstrated the effect of pressure on the rate of the reaction and product selectivity, and showed that the tethered catalyst is stable at reaction conditions. Within the current paper, we compare the performance of our tethered catalyst with that of its homogeneous analog, and evaluate their performances in liquid, supercritical, and expanded-liquid solvents.

## Experimental

Catalysts were evaluated in the reaction of 1-hexene with carbon monoxide and hydrogen in scCO<sub>2</sub> using a 300 mL batch reactor system manufactured by Autoclave Engineers, shown in Fig. 1. The reactor was equipped with a Type K thermocouple and a pressure transducer (Sensotech) and heated by use of a clamp-on ceramic heating jacket supplied by Industrial Heater Corporation. A nylon mesh material with an opening of 5 μm

(Spectrum Labs) was used to make envelopes in which the catalyst was placed. The catalyst envelopes were clamped between two heavy gauge screens, which were mounted on discs fixed to the reactor stirrer shaft. Further details of the reactor system are provided in ref. 14.

Carbon monoxide and hydrogen were measured by determining the mass difference within a filling cylinder. A high-pressure liquid pump (LDC Analytical) forced the desired amount of liquid CO<sub>2</sub> into the reactor, which was then brought to 75 °C and a stable pressure approximately 35 bar below the desired reaction pressure. 1-Hexene was then injected into the reactor using additional CO<sub>2</sub>, and the pressure was adjusted to the chosen operating pressure. *n*-Heptane was used as the internal GC standard and was added by syringe through an open fitting prior to final sealing of the reactor. Samples were taken during the reactor runs by use of a tubing sample loop. Quantitative analysis was performed using a gas chromatograph (HP-5890), equipped with a 30 m Alltech EC-1 capillary column and an FID detector, using He as the carrier gas. Further experimental details are contained in ref. 14.

All experiments were performed at a total pressure of 184 atm and a temperature of 75 °C. For experiments with toluene as the solvent or co-solvent, pressure was achieved by either compressing helium into the reactor to the desired pressure (toluene/He) or by adding an overpressure of CO<sub>2</sub> (toluene/CO<sub>2</sub>). Because of the solubility of CO<sub>2</sub> in toluene, the latter case produced an expanded liquid solvent.

Catalysts were prepared in our laboratory using procedures described in more detail elsewhere.<sup>14</sup> Tetraethoxysilane (Aldrich Chemical) and Ph<sub>2</sub>PCH<sub>2</sub>CH<sub>2</sub>Si(OEt)<sub>3</sub> (United Chemical Technology) were added to a 95:5 ethanol–water mixture under an atmosphere of nitrogen. The pH was adjusted to 5.5 using acetic acid and, after stirring for 2 d, the solution was heated under vacuum and the resulting phosphinated support dried under nitrogen overnight at room temperature. Rhodium incorporation was achieved by mixing Rh<sub>2</sub>Cl<sub>2</sub>(COD)<sub>2</sub> (COD = 1,5-cyclooctadiene) (0.38 g, 1.55 mmol)<sup>15</sup> with the phosphinated support (4.00 g, 4.65 mmol P) in an ethanol/water mixture under nitrogen.

Catalysts were characterized using solid state <sup>31</sup>P NMR spectroscopy with cross polarization and magic angle spinning. The NMR results indicated that the support as synthesized had phosphine sites available for rhodium coordination. After reaction between Rh<sub>2</sub>Cl<sub>2</sub>(COD)<sub>2</sub> and the support, the <sup>31</sup>P NMR spectrum showed the reduction of the free phosphine peak, accompanied by the appearance of new signals indicating formation of the Rh–P linkage. Elemental analyses were performed by Schwarzkopf Microanalytical Laboratories, Woodside, NY, which revealed a catalyst that contained 2.85 wt% P and 3.7 wt% Rh, giving a molar Rh:P ratio of 1:2.6.

Homogeneous catalysts were prepared *in-situ* from 0.022 g of Rh(acac)<sub>3</sub> and 0.036 g of ethyldiphenylphosphine, providing a

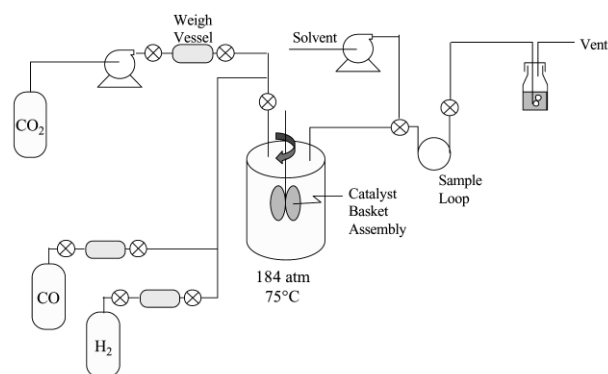


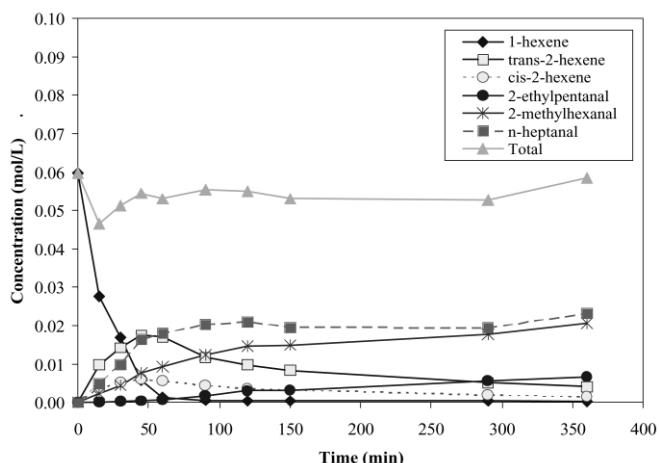
Fig. 1 Schematic diagram of experimental apparatus.

Rh:P ratio of 1:3.0. The precursors were dissolved in 5 mL of toluene and added to the reactor following the method used for addition of the internal standard. The reactor was held at reaction temperature and pressure for 1 h prior to introduction of the substrate to allow formation of the catalyst from the precursor compounds.

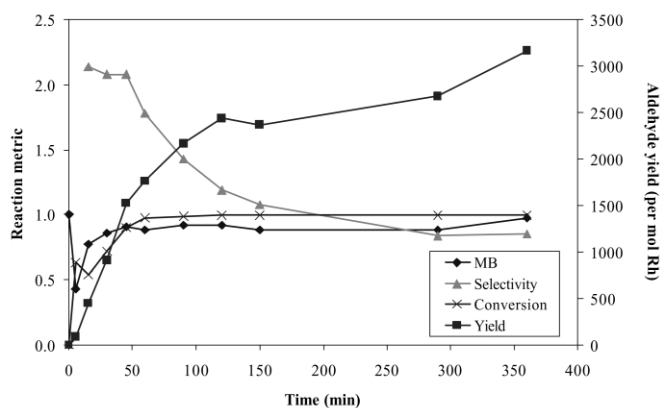
## Results and discussion

All reactions were carried out in a batch reactor, so all data is unsteady state in nature. Fig. 2 shows the concentrations of various species for a typical reaction, performed at 184 atm and 75 °C, and initial concentration of  $[\text{CO}] = 1.22 \text{ M}$ ,  $[\text{H}_2] = 1.16 \text{ M}$  and  $[\text{1-hexene}] = 0.06 \text{ M}$ . The 1-hexene is rapidly depleted, reaching negligible concentration after only about 75 min. *Cis*- and *trans*-2-hexene are produced rapidly, but then are depleted at longer reaction times, with the *trans*-2-hexene produced in greater yield. The normal and branched aldehyde products, *n*-heptanal and 2-methylhexanal, are also produced in significant yield, and 2-ethylpentanal, a hydroformylation product from 2-hexene, is produced in minor quantities at longer reaction times. The total concentration represents the total concentration of organic species in the reactor at any time, and remains near the initial concentration of 1-hexene for the entire duration of the run.

Important performance metrics are conversion, yield, and regioselectivity, each of which changed with time, as shown in Fig. 3 for the same conditions as reported in Fig. 2. A mole balance was also calculated for the hydrocarbon components.



**Fig. 2** Concentration profile for hydroformylation of 1-hexene at 75 °C and 184 atm,  $[\text{1-hexene}]_0 = 0.06 \text{ M}$ ,  $[\text{CO}]_0 = 1.22 \text{ M}$ ,  $[\text{H}_2]_0 = 1.16 \text{ M}$ .



**Fig. 3** Temporal variation of relevant reaction metrics (conversion, aldehyde yield, material balance, and selectivity) for the data shown in Fig. 2.

The conversion of 1-hexene is the amount of 1-hexene that has been consumed by the reaction. It is calculated as:

$$X_{\text{1-hexene}} = \frac{[\text{1-Hexene}]_0 - [\text{1-Hexene}]}{[\text{1-Hexene}]_0} \quad (1)$$

Approximately complete conversion was obtained after about 75 min of reaction time.

The yield is defined as the total aldehyde yield per mol of rhodium,

$$Y = \frac{[\text{Heptanal}] + [\text{2-Methylhexanal}] + [\text{2-Ethylpentanal}]}{[\text{1-Hexene}]_0} \text{ mol Rhodium} \quad (2)$$

Aldehyde yield increased to approximately 2500 mol aldehyde per initial mol of 1-hexene per mol of rhodium in 150 min, and then increased more slowly for the remaining 250 min of reaction. This is consistent with previously reported reaction pathways,<sup>2,14</sup> which indicated rapid hydroformylation of the terminal olefin to produce normal and branched aldehydes, followed by slower hydroformylation of the internal olefin to produce branched aldehydes only.

The regioselectivity is a measure of the quantity of the linear aldehyde product relative to the quantity of branched aldehyde products formed during the reaction. The regioselectivity is defined as:

$$S = \frac{[\text{Heptanal}]}{[\text{2-Methylhexanal}] + [\text{2-Ethylpentanal}]} \quad (3)$$

As shown in Fig. 3, the selectivity was initially above 2, which is in the range expected for rhodium-catalyzed hydroformylation using comparable catalysts.<sup>2</sup> Note that after 75 min the selectivity decreased due to hydroformylation of the internal alkene, which cannot yield the desired heptanal.

In order to ensure that the measured concentrations of different species in the reactor were accurate, a mole balance was calculated. Hydrogen and carbon monoxide concentrations were not measured during the reaction, so they could not be included in any balances. Because both the hydroformylation reaction and the isomerization reaction produce only one mol of product for one mol of reactant (excluding  $\text{H}_2$  and  $\text{CO}$ ), the quantity of 1-hexene and products at any point can be compared to the initial amount of 1-hexene added to the reactor. So, the mole balance was calculated as:

$$\text{MB} = \frac{[\text{1-Hexene}] + [\text{2-Hexenes}] + [\text{Aldehydes}]}{[\text{1-Hexene}]_0} \quad (4)$$

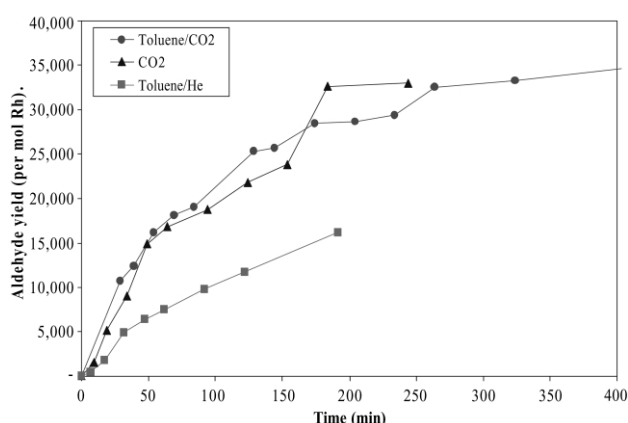
The mole balance remains near 1 over the course of the reaction, indicating that we have observed all of the significant products within the reaction sequence. The small deficit in mole balance observed at 10 min was seen consistently in all experiments and is attributed to heat transfer and phase behavior creating a brief non-uniformity in the system and so are not included in our analysis of the results. 1-Heptanol was observed in some experiments, but in very low concentrations. In experiments where 1-heptanol was observed, it was not included when calculating reaction yield.

### Solvent effects on reaction rate

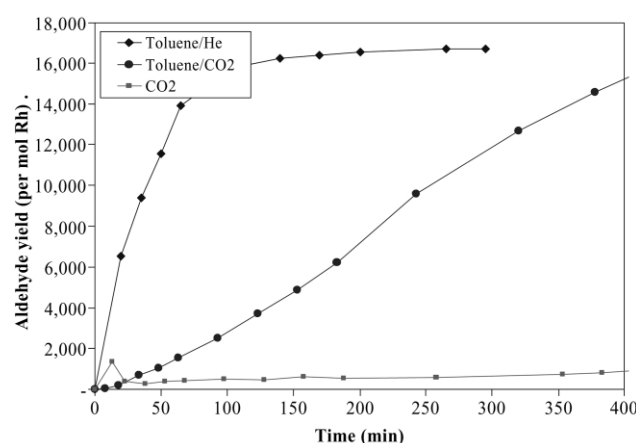
The performance of the heterogeneous catalyst in various solvent media is compared in Fig. 4, in terms of the yield of aldehyde produced. The case of heterogeneous catalysis in supercritical  $\text{CO}_2$  has been reported in previous work.<sup>14</sup> The aldehyde yield increased monotonically with reaction time, achieving a value of greater than 30000 mol aldehyde per initial mol of 1-hexene per mol of rhodium. This corresponds to consumption of approximately 90% of the available 1-hexene

for reaction. When the heterogeneous catalyst was used in liquid toluene (toluene/He), the aldehyde yield at comparable reaction conditions was approximately one-half that obtained in the supercritical case. The lower rate of aldehyde formation can be attributed to the greater mass transfer resistances existing in the liquid phase relative to the supercritical solvent. Interestingly, in the expanded liquid solvent (toluene/CO<sub>2</sub>), the aldehyde yield closely paralleled that obtained in the supercritical phase, although the 1-hexene conversion was actually faster in this case (substantial isomerization was observed). Thus, we conclude that the high solubility of CO and H<sub>2</sub> and high diffusivity of the reactants in the expanded liquid enhances the reaction rate compared to the liquid and provides an observed rate that may exceed that observed in the supercritical solvent, as well.

The hydroformylation results obtained using a catalyst produced *in situ* from Rh(acac)<sub>3</sub> and ethyldiphenylphosphine (Rh:P = 1:3) are compared over the same series of solvents in Fig. 5, as was previously reported for the corresponding heterogeneous catalyst in Fig. 4. For the case of the liquid-phase reaction carried out in toluene, the aldehyde yield increased to a value of approximately 16000 mol aldehyde per initial mol of 1-hexene per mol of rhodium. However, in the case of the reaction performed in supercritical CO<sub>2</sub>, very low yield of aldehyde was observed because the Rh(acac)<sub>3</sub>/PPh<sub>2</sub>Et catalyst has low solubility in the supercritical fluid.<sup>16</sup> The yield obtained in our experiments is substantially greater than that observed by previous researchers who have noted product formation using insoluble 'homogeneous' catalysts modified with oxygenated species.<sup>17</sup> For the expanded liquid solvent, the aldehyde yield



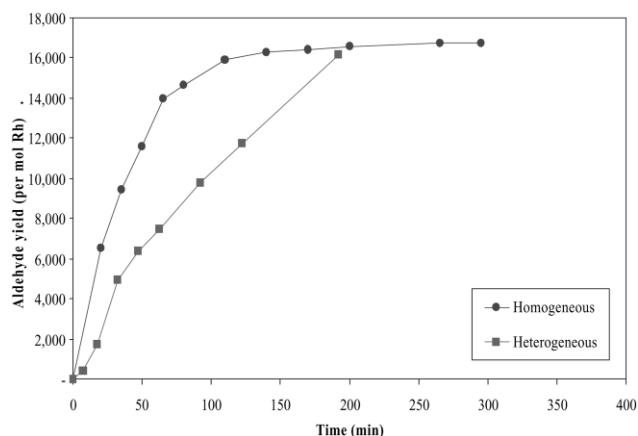
**Fig. 4** Comparison of the total aldehyde yield (per mol of rhodium on the catalyst) for the supported rhodium catalyst in liquid toluene, supercritical CO<sub>2</sub>, and CO<sub>2</sub>-expanded toluene.



**Fig. 5** Comparison of the total aldehyde yield (per mol of rhodium in solution) for Rh(acac)<sub>3</sub> and ethyldiphenylphosphine (PPh<sub>2</sub>Et) in liquid toluene, supercritical CO<sub>2</sub>, and CO<sub>2</sub>-expanded toluene.

increased slowly but, after sufficient reaction time, the yield became comparable to the yield that was obtained for the liquid solvent. This result may be explained by the solubility behavior of the species in this two-phase mixture; 1-hexene distributes between the CO<sub>2</sub>-rich phase and the toluene-rich phase, whereas the rhodium remains exclusively within the toluene phase. Because the concentration of 1-hexene in the presence of the catalyst is thus reduced, the rate of reaction is decreased, as was observed previously for the hydrogenation of pinene.<sup>9</sup> A crystalline material was found on the interior surfaces of the reactor following depressurization, but the material was not analyzed.

A direct comparison of the results obtained from the homogeneous catalyst with those obtained from the tethered catalyst is shown in Fig. 6, for the liquid solvent in both cases. While the ultimate aldehyde yields of approximately 16000 mol of aldehyde per initial mol of 1-hexene per mol of rhodium were comparable in these cases, the rate of aldehyde formation was slower in the heterogeneous system. Although this result can be attributed to mass transfer limitations present in the heterogeneous system, the heterogeneous catalyst was a low surface area material with limited internal pore volume and would not be expected to be significantly impacted by mass transfer. However, the calculation of yield assumed that all rhodium bound to the catalyst was available for reaction. In the heterogeneous case, this may not have been true, and the available rhodium may only have been some fraction of the rhodium loaded onto the catalyst.

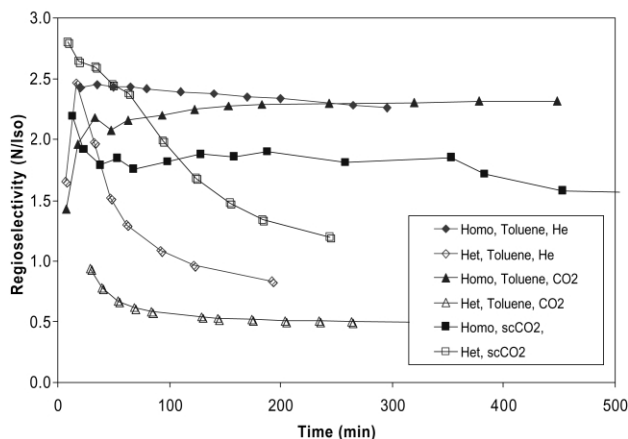


**Fig. 6** Comparison of the total aldehyde yield (per mol of rhodium) for homogeneous and heterogeneous catalysts in liquid toluene.

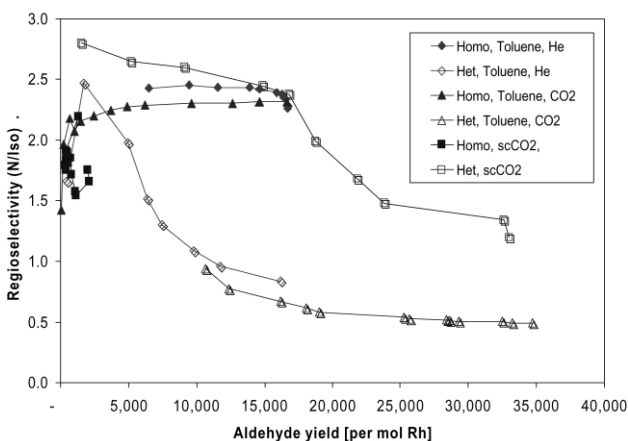
### Aldehyde selectivity

In addition to the aldehyde yield, the selectivity to the linear aldehyde is a critical performance metric. The results are compared in Fig. 7, in which reaction time is the independent variable and in Fig. 8, in which the selectivities (*S*) are compared as a function of aldehyde yield.

Looking first at the initial selectivity, Fig. 7 reveals that *S* was initially greater than 2 in most cases, with the heterogeneous catalyst in the expanded liquid being the notable exception. However, as shown in Fig. 8, when compared on the basis of equivalent conversion to aldehyde, the reaction in the expanded liquid solvent had a selectivity that was nearly identical to that of the liquid solvent. The isomerization reaction occurred very rapidly in the expanded liquid solvent, with nearly complete 1-hexene conversion obtained within the first 30 min. Since the hydroformylation of the internal alkene was slower than that of the terminal alkene and cannot yield the normal aldehyde, the selectivity was less than 1 for all points at which data is recorded. This may have been simply an artifact of the inability



**Fig. 7** Temporal variation of the aldehyde selectivity for homogeneous and heterogeneous catalysts in various solvent media.



**Fig. 8** Comparison of the aldehyde selectivity as a function of total aldehyde yield.

to collect data at shorter reaction times, since the selectivity was comparable to that in the liquid solvent at a constant aldehyde yield (Fig. 8).

For all of the reactions performed with the heterogeneous catalyst, the selectivity decreased with both reaction time and aldehyde yield. We have previously proposed that this is a consequence of the formation of the internal alkene through the isomerization reaction, which is more slowly hydroformylated to produce the two branched aldehydes. However, if this were the case, then the reaction with the homogeneous catalyst system should also show a decrease in selectivity with increasing aldehyde yield, indicating that some alternative mechanism may be at work for the tethered catalyst that does not exist in the homogeneous case. Previous researchers<sup>2,7</sup> have suggested that excess CO may adsorb favorably onto the heterogeneous rhodium catalyst, leading to a decrease in catalyst activity over extended reaction times. In a steady-state process, an equilibrium CO concentration would be obtained, and the catalyst would appear stable (following an initial transient), but in the batch reactor, the catalyst activity would continuously decrease with reaction time. By analogy, our tethered catalyst may also interact with CO, leading to a continuously decreasing selectivity arising from changes in the active state of the catalytic species over the course of the reaction.

The selectivity obtained using the heterogeneous catalyst in supercritical CO<sub>2</sub> was initially higher than 2.5 and greater than that obtained using the homogeneous catalyst under any conditions or using the heterogeneous catalyst in the presence of toluene. While the selectivity decreased with increasing aldehyde yield for the heterogeneous catalyst, an increase in

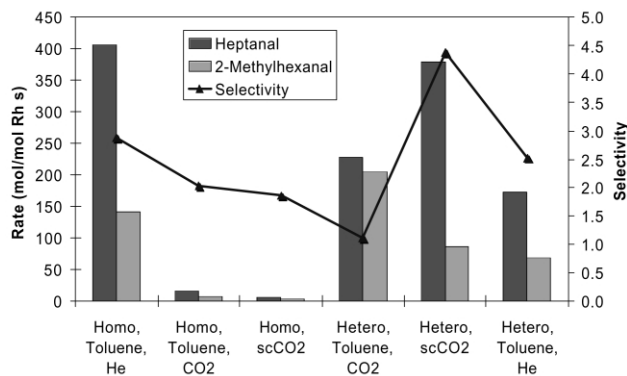
selectivity was observed for the homogeneous catalyst. Thus, the selectivities of the heterogeneous and homogeneous catalysts were similar: between 15000 and 20000 mol aldehyde per initial mol of 1-hexene per mol of rhodium. Although a selectivity of 2.5 is not sufficient for commercial operation, there is no ligand modification in the current system to promote greater selectivity. These results therefore strongly suggest the potential to achieve high selectivity using a heterogeneous rhodium catalyst when the phosphine ligands are adjusted according to the techniques known to promote selectivity for homogeneous systems.

## Summary

To compare the activities of the homogeneous and heterogeneous catalysts, initial rates of hydroformylation were determined by fitting a third-order polynomial to the aldehyde concentration as a function of reaction, differentiating, and determining the intercept of the resulting equation. Using this technique, described in more detail previously,<sup>14</sup> we were able to estimate an intrinsic selectivity, calculated as the initial rate of heptanal formation divided by the initial rate of 2-methylhexanal formation. The results are reported in Fig. 9, which compares the performance (reaction rate and aldehyde selectivity) of both catalysts in three solvent systems simultaneously.

The heterogeneous catalyst showed similar overall rates of reaction (rate of formation of heptanal plus 2-methylhexanal) in the presence and absence of CO<sub>2</sub>, with a somewhat lower rate in liquid-phase toluene. However, the selectivity was substantially different, and was far superior (approaching 4.5) in supercritical CO<sub>2</sub>. The overall rate of aldehyde formation was the greatest for the homogeneous catalyst in liquid-phase toluene; the rates of formation of both heptanal and 2-methylhexanal were greater than those obtained with the heterogeneous system in supercritical CO<sub>2</sub>, so the selectivity was slightly lower in this case. Using the metric of fastest rate of heptanal formation and highest selectivity, it is clear that our heterogeneous catalyst performed better in supercritical CO<sub>2</sub> than did its homogeneous analog in liquid toluene, demonstrating the validity of our proposal to develop a heterogeneous hydroformylation catalyst for reaction in supercritical CO<sub>2</sub>.

In addition, the performance of the homogeneous catalyst in supercritical CO<sub>2</sub> was very poor, since the catalyst would not dissolve in the supercritical phase that contains all of the reactants. Likewise, the homogeneous catalyst performed worse in an expanded liquid solvent than in the pure liquid, because the 1-hexene partitioned among the phases whereas the catalyst remained in the toluene phase. As a result, the concentration of reactant was decreased in the presence of the catalyst, lowering the rate of reaction. Interestingly, there was no decrease in



**Fig. 9** Summary comparison of the rate of heptanal and 2-methylhexanal formation as calculated from the initial rate of a third-order polynomial fit to the concentration vs. time data.



activity with the heterogeneous catalyst in the expanded liquid solvent. The reasons for this are obscure, but the heterogeneous catalyst was suspended in the reactor on the stirrer shaft and may have been equally well in contact with both the CO<sub>2</sub>- and toluene-rich phases.

## Acknowledgement

This research was supported by a grant from the US Environmental Protection Agency's Science to Achieve Results (STAR) program. Although the research described in the article has been funded wholly or in part by the U.S. Environmental Protection Agency's STAR program through grant number R 828206, it has not been subjected to any EPA review and therefore does not necessarily reflect the views of the Agency, and no official endorsement should be inferred.

## References

- 1 B. Cornils and W. A. Herrmann, *Applied Homogeneous Catalysis with Organometallic Compounds*, VCH, New York, 1996.
- 2 P. W. N. M. van Leeuwen and C. Claver, *Rhodium Catalyzed Hydroformylation*, Kluwer Academic Publishers, Dordrecht, 2000.
- 3 Y. Zhang, H. Zhang, G. Lin, P. Chen, Y. Yuan and K. R. Tsai, *Appl. Catal. A: Gen.*, 1999, **187**, 213.
- 4 E. Lindner, F. Auer, A. Baumann, P. Wegner, H. A. Mayer, H. Bertagnolli, U. Reinohl, T. S. Ertel and A. Weber, *J. Mol. Catal. A: Chem.*, 2000, **157**, 97.
- 5 A. N. Ajjou and H. Alper, *Mol. Online*, 1998, **2**, 53.
- 6 T. A. Kainulainen, M. K. Niemela and A. O. I. Krause, *J. Mol. Catal. A: Chem.*, 1997, **122**, 39.
- 7 Y. Guo and A. Akgerman, *Ind. Eng. Chem. Res.*, 1997, **36**, 4581.
- 8 N. J. Meehan, A. J. Sandee, J. N. H. Reek, P. C. J. Kamer, P. W. N. M. van Leeuwen and M. Poliakoff, *Chem. Commun.*, 2000, 1497.
- 9 D. Chouchi, D. Gourgouillon, M. Courel, J. Vital and M. N. da Ponte, *Ind. Eng. Chem Res.*, 2001, **40**, 2551.
- 10 A. Bertucco, P. Canu, L. Devetta and A. G. Zwahlen, *Ind. Eng. Chem. Res.*, 1997, **36**, 2626.
- 11 L. Devetta, A. Giovanzana, P. Canu, A. Bertucco and B. J. Minder, *Catal. Today*, 1999, **48**, 337.
- 12 S. Dharmidhikari and M. A. Abraham, *J. Supercrit. Fluids*, 2000, **18**, 1.
- 13 G. Snyder, A. Tadd and M. A. Abraham, *Ind. Eng. Chem. Res.*, 2001, **40**, 5317.
- 14 A. R. Tadd, A. Marteel, M. R. Mason, J. A. Davies and M. A. Abraham, *J. Supercrit. Fluids*, 2002, in press.
- 15 G. Giordano and R. H. Crabtree, *Inorg. Synth.*, 1990, **28**, 88.
- 16 P. G. Jessop, T. Ikariya and R. Noyori, *Chem Rev.*, 1999, **99**, 475–493.
- 17 M. F. Sellin and D. J. Cole-Hamilton, *J. Chem. Soc., Dalton Trans.*, 2000, 1681–1683.



# Vapour phase ammoxidation of toluene over vanadium oxide supported on Nb<sub>2</sub>O<sub>5</sub>-TiO<sub>2</sub>

Chinthala Praveen Kumar, Kondakindi Rajender Reddy, Vattikonda Venkat Rao and Komandur V.R. Chary\*

Catalysis Division, Indian Institute of Chemical Technology, Hyderabad- 500 007, India.  
E-mail: kvrchary@iict.ap.nic.in

Received 8th July 2002

First published as an Advance Article on the web 23rd September 2002

Vanadium oxide catalysts with V<sub>2</sub>O<sub>5</sub> loadings ranging 1 to 9% (w/w) supported on 1:1 wt% Nb<sub>2</sub>O<sub>5</sub>-TiO<sub>2</sub> mixed oxide have been prepared by the wet impregnation method. The calcined samples were characterized by X-ray diffraction (XRD), pulse oxygen chemisorption and temperature programmed desorption (TPD) of NH<sub>3</sub>. Dispersion of vanadia was determined by oxygen chemisorption at 643 K in a dynamic method. At low V<sub>2</sub>O<sub>5</sub> loadings, vanadia is found to be present in a highly dispersed state. X-Ray diffraction results also suggest that vanadium oxide exists in a highly dispersed state at lower loadings and in a crystalline V<sub>2</sub>O<sub>5</sub> phase at higher vanadia loadings (5 wt% and above). The dispersion of vanadia was found to decrease with V<sub>2</sub>O<sub>5</sub> loading due to the formation of V<sub>2</sub>O<sub>5</sub> crystallites. The catalytic properties were evaluated for the vapor phase ammoxidation of toluene to benzonitrile and correlated with characterization results.

## Introduction

Supported vanadia catalysts have found a wide variety of commercial applications. For example selective oxidation of o-xylene to phthalic anhydride,<sup>1,2</sup> ammoxidation of alkyl aromatics<sup>3,4</sup> and selective catalytic reduction of NO<sub>x</sub> with NH<sub>3</sub>.<sup>5</sup> In addition to these oxidation reactions, supported vanadia catalysts have also been investigated for the oxidative dehydrogenation of alkanes to olefins,<sup>6</sup> oxidation of butane to maleic anhydride<sup>7</sup> and selective oxidation of methanol to formaldehyde<sup>8</sup> or methyl formate.<sup>9</sup> Generally, bulk V<sub>2</sub>O<sub>5</sub> cannot be used as a catalyst because of its poor thermal stability and mechanical strength. Therefore, vanadia is normally supported on different carriers depending on the nature of reaction to be catalyzed. Titania, in the form of anatase, is considered to be the most successful support for the selective oxidation reactions<sup>1,2</sup> as well as for NO reduction with NH<sub>3</sub>.<sup>1,3,5</sup> Similarly, niobia supported vanadia reported to be very active for oxidation/ammoxidation reactions.<sup>10,11</sup> The beneficial functions of each individual support can be explored fully by using them in combination, which constitute yet another important class of solid supports whose characteristics are not yet studied.

The most commonly used supports are Al<sub>2</sub>O<sub>3</sub>, TiO<sub>2</sub>, ZrO<sub>2</sub> and SiO<sub>2</sub>. In the last decade niobium based materials have attracted considerable interest in various reactions. Niobia can be used as support, promoter and as a unique solid acid. Smits *et al.*<sup>12</sup> emphasized the advantages of niobia as a catalyst support for vanadia. These include: (i) niobium is in the same group of the periodic table as vanadium or molybdenum and is expected to have similar properties. (ii) niobium is much more difficult to reduce than vanadium or molybdenum (easy reduction often causes low selectivity in selective oxidation reaction). (iii) The addition of niobium oxide to a mixture of molybdenum and vanadium oxides improves the activity and selectivity for oxidation, ammoxidation and oxidative dehydrogenation reactions.<sup>12,13</sup> A fundamental problem in catalytic oxidation is the estimation of the number of active sites on the surface of oxide catalysts. Simple methods to titrate surface metal centers in oxides would greatly assist in understanding the effect of structure in oxidation reactions. The efficiency of supported vanadium oxide catalysts mainly depends on the

dispersion of active phase, which in turn can be greatly influenced by the nature of supported oxide and the method of preparation of the catalysts. In this paper we report the activity of V<sub>2</sub>O<sub>5</sub>/Nb<sub>2</sub>O<sub>5</sub>-TiO<sub>2</sub> catalysts for the vapour phase ammoxidation of toluene to produce benzonitrile. Benzonitrile is used as a precursor for resins and coatings. It is also used as an additive in fuels and fibers. The V<sub>2</sub>O<sub>5</sub>/Nb<sub>2</sub>O<sub>5</sub>-TiO<sub>2</sub> catalysts are found to be highly active and selective in the ammoxidation of toluene. Stobbelaar<sup>14</sup> reported the ammoxidation of toluene over various supported metal oxide catalysts and concluded that V/NaY and Mn/NaY catalysts show relatively high benzonitrile yield under optimum conditions.

## Results and discussion

Powder X-ray diffraction patterns of various V<sub>2</sub>O<sub>5</sub>/Nb<sub>2</sub>O<sub>5</sub>-TiO<sub>2</sub> (1:1 wt%) catalysts are shown in Fig. 1. In all the samples XRD reflections due to low temperature niobia (shown with closed triangles in Fig. 1) are observed at  $d = 3.95, 3.14, 2.45, 1.97$  and  $1.66 \text{ \AA}$  (corresponding  $2\theta$  values are  $22.5, 28.4, 36.6, 46$  and  $55.3^\circ$ , respectively), in addition to anatase titania reflections (shown with open circles in Fig. 1) at  $d = 3.52, 1.89, 2.37$  and  $1.48 \text{ \AA}$  (corresponding  $2\theta$  values are  $25.3, 48.1, 37.8$  and  $62.7^\circ$  respectively). However, XRD reflections corresponding to V<sub>2</sub>O<sub>5</sub> (shown with closed circles in Fig. 1) at  $2\theta = 20.26^\circ$  can also be seen from 5 wt% sample, and its intensity is found to increase with increase of vanadia loading. The absence of

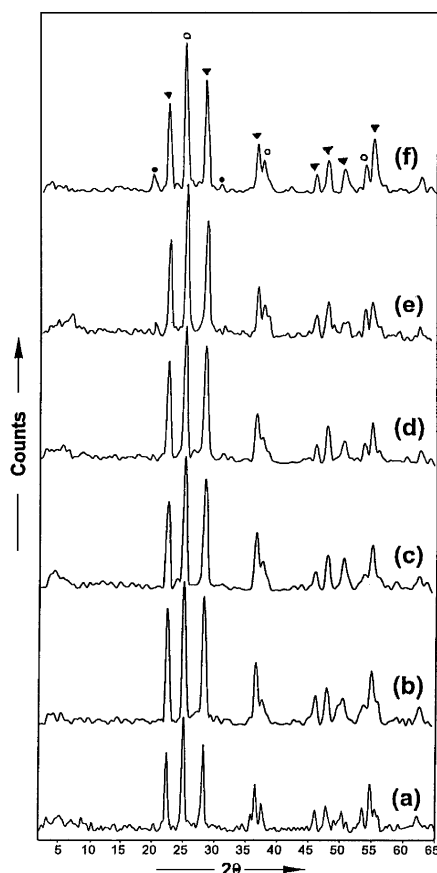
## Green Context

The conversion of toluene to benzonitrile *via* ammoxidation is a convenient and direct functionalisation of hydrocarbon feedstock. Recently, Nb<sub>2</sub>O<sub>5</sub>-TiO<sub>2</sub> mixed oxide supported vanadium oxide catalyst has been shown to be highly active and selective in toluene ammoxidation, partly due to the limited redox chemistry of the support. This paper indicates careful analysis of the surface species, which can lead to improvement in catalytic efficiency, leading to a cleaner process.

DJM

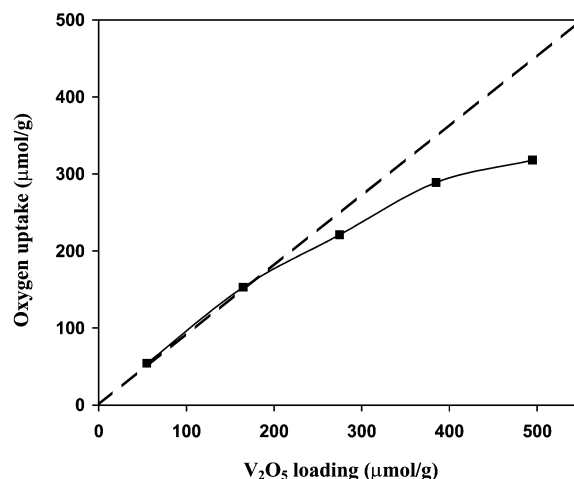
XRD reflections due to vanadia at lower composition indicates that vanadium oxide is present in a highly dispersed amorphous state on the Nb<sub>2</sub>O<sub>5</sub>-TiO<sub>2</sub> support. However, at lower loadings of vanadia (< 5 wt%), the possibility cannot be ruled out for the presence of vanadia crystallites having size less than 4 nm, which is beyond the detection capacity of the powder X-ray diffraction technique. Ko and Weissman<sup>15</sup> reported that samples calcined at low calcination temperature (< 773 K) are X-ray amorphous. Samples calcined between 773–873 K show the TT-phase of Nb<sub>2</sub>O<sub>5</sub>, and samples calcined between 873–973 K favor the formation of the T-phase of Nb<sub>2</sub>O<sub>5</sub>. At 1073 K the M-phase forms and at 1273 K and above the H-phase of Nb<sub>2</sub>O<sub>5</sub> is observed. In the present study, we observed the TT phase of Nb<sub>2</sub>O<sub>5</sub> in samples calcined at 773 K. The present XRD results are in well agreement with our earlier studies on V<sub>2</sub>O<sub>5</sub>/Nb<sub>2</sub>O<sub>5</sub><sup>10</sup> and V<sub>2</sub>O<sub>5</sub>/TiO<sub>2</sub><sup>16</sup> catalysts, wherein crystalline V<sub>2</sub>O<sub>5</sub> appeared above monolayer coverage.

Fig. 2 shows the oxygen uptake at 640 K of various V<sub>2</sub>O<sub>5</sub>/Nb<sub>2</sub>O<sub>5</sub>-TiO<sub>2</sub> catalysts plotted as a function of V<sub>2</sub>O<sub>5</sub> loading on



**Fig. 1** X-Ray diffraction (XRD) patterns of V<sub>2</sub>O<sub>5</sub>/Nb<sub>2</sub>O<sub>5</sub>-TiO<sub>2</sub> catalysts: (a) Nb<sub>2</sub>O<sub>5</sub>-TiO<sub>2</sub> (1:1) (b) 1% V<sub>2</sub>O<sub>5</sub>/Nb<sub>2</sub>O<sub>5</sub>-TiO<sub>2</sub>, (c) 3% V<sub>2</sub>O<sub>5</sub>/Nb<sub>2</sub>O<sub>5</sub>-TiO<sub>2</sub>, (d) 5% V<sub>2</sub>O<sub>5</sub>/Nb<sub>2</sub>O<sub>5</sub>-TiO<sub>2</sub>, (e) 7% V<sub>2</sub>O<sub>5</sub>/Nb<sub>2</sub>O<sub>5</sub>-TiO<sub>2</sub>, (f) 9% V<sub>2</sub>O<sub>5</sub>/Nb<sub>2</sub>O<sub>5</sub>-TiO<sub>2</sub>. (●) Reflections due to V<sub>2</sub>O<sub>5</sub>; (○) reflections due to anatase phase of TiO<sub>2</sub>; (▼) Reflections due to Nb<sub>2</sub>O<sub>5</sub>.

niobia-titania mixed oxide. The oxygen uptake values, BET specific surface areas and dispersion values are presented in Table 1. The oxygen uptake values are doubled to get atomic oxygen values, which are given, in Fig. 2. The oxygen chemisorption capacities are found to increase with vanadia loading up to 5 wt% of V<sub>2</sub>O<sub>5</sub> and level off at higher vanadia loadings. The leveling off of oxygen uptake values at this composition of vanadia was attributed to the formation of a V-oxide monolayer on niobia-titania. This loading corresponds closely to the theoretical monolayer capacity of vanadium oxide. From the unit cell dimensions of V<sub>2</sub>O<sub>5</sub> an average value for a loading corresponding to a monolayer can be calculated as 1.2 mg of V<sub>2</sub>O<sub>5</sub> per m<sup>2</sup> of the support.<sup>17</sup> The theoretical monolayer of V<sub>2</sub>O<sub>5</sub> on the support was calculated from the BET specific surface area of the support using the method reported by Roozeboom *et al.*<sup>17</sup> Thus Bond and Tahir<sup>18</sup> reported that weight concentration of V<sub>2</sub>O<sub>5</sub> necessary to form a monolayer was 0.09 per m<sup>2</sup>. Accordingly in the present work the support Nb<sub>2</sub>O<sub>5</sub>-TiO<sub>2</sub> mixed oxide having a specific surface area of 55 m<sup>2</sup> g<sup>-1</sup> requires 4.95 wt% of V<sub>2</sub>O<sub>5</sub>. Similarly XRD results also show the presence of V<sub>2</sub>O<sub>5</sub> crystallites from 5 wt%. The leveling off of oxygen uptake at higher loadings might be due to the presence of a crystalline vanadia phase and this phase upon reduction with hydrogen does not appreciably reduce and subsequently oxygen chemisorption amounts are lowered. Pure niobia-titania support was also reduced under identical conditions, and its oxygen uptake was corrected for the supported catalysts. The dispersion of vanadia can be defined as the fraction of total O atoms (determined from oxygen chemisorption uptake) to total V atoms in the sample. At lower vanadia loadings the dispersion was found to be closer to the dashed line, which corresponds to 100% dispersion and the dispersion was found to deviate from this dashed line with further increase



**Fig. 2** Oxygen uptake plotted as a function of V<sub>2</sub>O<sub>5</sub> loading on Nb<sub>2</sub>O<sub>5</sub>-TiO<sub>2</sub> support; T<sub>ads</sub> = T<sub>red</sub> = 643 K.

**Table 1** Results of oxygen chemisorption and temperature-programmed desorption of NH<sub>3</sub> of various V<sub>2</sub>O<sub>5</sub>/Nb<sub>2</sub>O<sub>5</sub>-TiO<sub>2</sub> catalysts

| V <sub>2</sub> O <sub>5</sub> loading on Nb <sub>2</sub> O <sub>5</sub> -TiO <sub>2</sub> (wt%) | Surface area/ m <sup>2</sup> g <sup>-1</sup> | O <sub>2</sub> uptake <sup>a</sup> /μmol g <sup>-1</sup> | Oxygen atom site density (10 <sup>18</sup> /m <sup>2</sup> ) | Dispersion <sup>b</sup> O/V T <sub>1</sub> /K | NH <sub>3</sub> uptake/ μmol g <sup>-1</sup> | T <sub>2</sub> /K | NH <sub>3</sub> uptake/ μmol g <sup>-1</sup> | Total acidity/ μmol g <sup>-1</sup> |
|---|--|--|--|---|--|-------------------|--|-------------------------------------|
| 1   | 41.5   | 54   | 1.57   | 0.98  | 513  | 573               | 72   | 147                                 |
| 3   | 39.2   | 153  | 4.7  | 0.93  | 495  | 585               | 87   | 190                                 |
| 5   | 37.6   | 221  | 7.1  | 0.80  | 476  | 593               | 102  | 236                                 |
| 7   | 33.0   | 289  | 10.5   | 0.75  | 482  | 602               | 127  | 262                                 |
| 9   | 36.8   | 318  | 10.4   | 0.64  | 475  | 611               | 136  | 273                                 |

<sup>a</sup> T (reduction) = T (adsorption) = 643 K. <sup>b</sup> Dispersion = fraction of vanadium atoms at the surface assuming O<sub>ads</sub>/V<sub>surf</sub> = 1.

of vanadia loading. These findings are in consistent with the oxygen chemisorption results of our earlier study<sup>19</sup> also with Went *et al.*<sup>20</sup> on vanadia supported titania in which they also employed a pulse technique for measuring oxygen chemisorption. The dispersion values of  $V_2O_5/Nb_2O_5-TiO_2$  catalysts are higher than  $V_2O_5/Nb_2O_5$  catalysts.<sup>10</sup> Went *et al.*<sup>20</sup> reported from laser Raman spectroscopy studies on  $V_2O_5/TiO_2$  catalysts the presence of three types of vanadia species, namely, monomeric vanadyls, one and two dimensional vanadia chains, and crystallites of vanadia.

The acidity values of  $V_2O_5/Nb_2O_5-TiO_2$  catalysts determined by  $NH_3$ -TPD method are given in Table 1. Both Tanabe<sup>21</sup> and Kung<sup>22</sup> have proposed the models to predict the formation of acid sites when two oxides are combined to form a mixed oxide. Dumesic and coworkers<sup>23,24</sup> have discussed the generation of acid sites when one oxide is deposited onto another to form a surface phase oxide. Thus it is interesting to study the acidity of the vanadia supported on niobia-titania binary oxide catalysts. Okazaki and Okuyama<sup>25</sup> showed that  $Nb_2O_5-TiO_2$  binary oxides prepared by coprecipitation method are found to be acidic and active in the reduction of NO with  $NH_3$ . In the present study, the acidity measurements have been carried out by  $NH_3$ -TPD. The ammonia uptake by various catalysts and the temperature positions are given in Table 1. From the TPD profiles it is observed that the acid sites are distributed in two regions *i.e.* 475–515 and 570–615 K. Desorption in the temperature region 475–515 K is due to weak acidic sites and that in the temperature region 570–615 K is due to moderate acidic sites. It is found that both types of acidic sites increase with increase of vanadia loading up to 5 wt% and no appreciable change is observed above this loading, and both the conversion and selectivity in the ammoxidation of toluene are also found to increase up to this loading and remained constant at higher vanadia loadings in similar lines to acidity measurements. This indicates that both (weak and moderate) the acidic sites are responsible for activity during the ammoxidation of toluene. The acidity of the catalysts is mainly due to the vanadia phase since ammonia uptake increases with increase in vanadia loading.

The results of ammoxidation of toluene on various  $V_2O_5/Nb_2O_5-TiO_2$  catalysts at 643 K are shown in Fig. 3. Table 2 shows the catalytic activity results of various binary oxide supported vanadia catalysts for comparison in our present study during the ammoxidation of toluene. Both the conversion and selectivity are found to increase with increase in  $V_2O_5$  loading up to 5 wt%  $V_2O_5$  and beyond this loading the activity/selectivity do not change much due to the formation of  $V_2O_5$

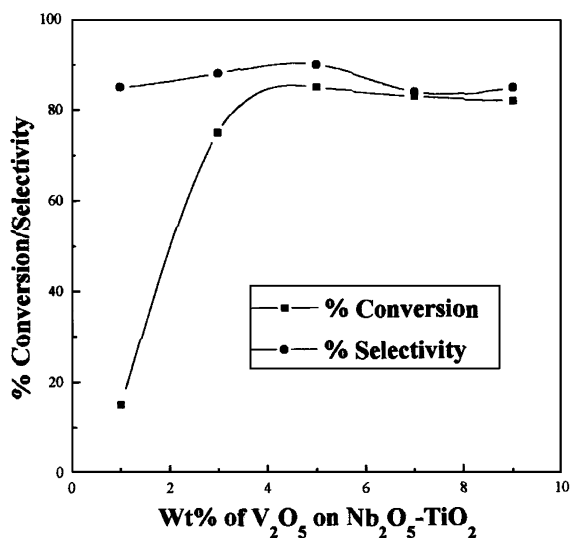


Fig. 3 Ammoxidation of toluene over various  $V_2O_5/Nb_2O_5-TiO_2$  catalysts (reaction temperature 643 K).

Table 2 Activity of various binary oxides supported vanadium oxide catalysts in the ammoxidation of toluene to benzonitrile.

| Catalyst                  | Conversion (%) | Selectivity (%) |
|---------------------------|----------------|-----------------|
| 5% $V_2O_5/TiO_2-Nb_2O_5$ | 85             | 90              |
| 5% $V_2O_5/TiO_2-SiO_2$   | 77             | 67              |
| 5% $V_2O_5/TiO_2-ZrO_2$   | 75             | 72              |

crystallites on the surface of  $Nb_2O_5-TiO_2$  support. The catalytic activity results presented in this paper are high when compared to  $V_2O_5/TiO_2$  catalysts.<sup>26</sup> Both the conversion and selectivity in the ammoxidation of toluene were found to be more in the case of  $V_2O_5/Nb_2O_5-TiO_2$  catalysts compared to  $V_2O_5/ZrO_2-TiO_2$  and  $V_2O_5/SiO_2-TiO_2$  catalysts and these results are shown in Table 2.

Oxygen is chemisorbed at low temperatures selectively on coordinatively unsaturated sites (CUS), generated upon reduction, having a particular coordination environment. These sites are located on a highly dispersed vanadia phase, which is formed only at low vanadia loadings and remain as a 'patchy monolayer' on the support surface. At higher vanadia loadings, a second phase is formed, in addition to the already existing monolayer, and this post monolayer phase does not appreciably chemisorb oxygen (Fig. 2). In the perspective of the above background, the correlation shown here indicates that the catalytic functionality of the dispersed vanadia phase supported on  $Nb_2O_5-TiO_2$ , which is responsible for the ammoxidation of toluene to benzonitrile, is located on a patchy-monolayer phase and this functionality can be titrated by the oxygen chemisorption method reported in this work.

## Experimental

The niobia-titania (1:1 wt%) mixed oxide support was prepared by coprecipitation of niobium(v) oxide hydrate and titanium isopropoxide. The details of the preparation method are given elsewhere.<sup>25</sup> A typical method involves coprecipitation of niobium(v) oxide hydrate (HY-340 AD/1599, CBMM, Brazil), titanium isopropoxide (Lancaster) and neutralization with 28% aqueous ammonia at pH 8, followed by washing and drying. The support was calcined at 773 K for 6 h. The  $Nb_2O_5-TiO_2$  supported vanadia catalysts with various  $V_2O_5$  loadings ranging from 1 to 9 wt% were prepared by the standard impregnation using oxalic acid solution containing ammonium metavanadate as the vanadium precursor. The impregnated samples were dried at 393 K for 12 h and calcined in muffle furnace at 773 K for 6 h.

X-Ray diffractograms were recorded on Siemens D-5000 diffractometer using graphite filtered  $Cu-K\alpha$  radiation.

Oxygen chemisorption was measured by the dynamic method on an AutoChem 2910 (Micromeritics, USA) instrument. Prior to adsorption measurements, *ca.* 0.5 g of the samples were reduced in a flow of hydrogen ( $50\text{ ml min}^{-1}$ ) at 643 K for 2 h and flushed in pure He flow (purity 99.995%) for 1 h at the same temperature. Oxygen uptakes were determined by injecting pulses of oxygen from a calibrated on-line sampling valve onto a He stream passing over reduced samples at 643 K. Adsorption was deemed to be complete after at least three successive peaks showed the same area.

Temperature-programmed desorption (TPD) of  $NH_3$  experiments were also conducted on the same AutoChem 2910 instrument, which is used for oxygen chemisorption measurements and more details regarding TPD are found elsewhere.<sup>19</sup> In a typical method the sample was pretreated at 473 K for 1 h and saturated at 353 K for 1 h with a 10%  $NH_3$ -He mixture and subsequently flushed at 378 K for 3 h to remove physisorbed ammonia. Desorbed ammonia amount are calculated using GRAMS/32 software.

The ammoxidation of toluene to benzonitrile reaction was carried out in a fixed-bed down-flow, cylindrical Pyrex reactor with 20 mm internal diameter. About 0.5 g of the catalyst with a 18–25 mesh size diluted with an equal amount of quartz grains of the same dimensions was charged into the reactor and were supported on a glass wool bed. Prior to introducing the reactant toluene with a syringe pump (B-Braun perfusor, Germany) the catalyst was oxidized at 673 K for 2 h in air flow ( $40 \text{ ml min}^{-1}$ ) and then the reactor was fed with toluene, ammonia and air in the mole ratio of 1:13:26. There is a preheated zone filled-up with quartz glass particles heated up to 423 K for adequate vaporization of liquid feed. The reaction products were analyzed using a HP 6890 gas chromatograph. The only by-products formed are carbon oxides during the reaction and were determined by HP-5973 GC-MS using a Porapak Q column. The mass balance was found to be >95%.

## Conclusions

$\text{Nb}_2\text{O}_5\text{-TiO}_2$  binary oxide is an interesting support to investigate the dispersion of vanadium oxide and catalytic properties. The oxygen chemisorption results suggested that vanadium oxide is highly dispersed on  $\text{Nb}_2\text{O}_5\text{-TiO}_2$  support at lower vanadia loadings (<5 wt%) and the dispersion decreases at higher vanadia loadings due to the formation of  $\text{V}_2\text{O}_5$  crystallites. XRD results further support these above findings.  $\text{NH}_3\text{-TPD}$  results and pulse oxygen chemisorption results are directly related to the catalytic properties during ammoxidation of toluene to benzonitrile.

## Acknowledgements

CBMM Brazil is greatly acknowledged for providing a gift sample of niobium oxide hydrate. C. H. P. K. and K. R. R. thank the Council of Scientific and Industrial Research (CSIR) for Senior Research Fellowships (SRF).

## References

- 1 M. S. Wainwright and N. R. Foster, *Catal. Rev.-Sci. Eng.*, 1979, **19**, 211.
- 2 V. Nikolov, D. Klissurski and A. Anastasov, *Catal. Rev.-Sci. Eng.*, 1991, **33**, 1.
- 3 F. Cavalli, F. Cavani, I. Manenti and F. Trifiro, *Catal. Today.*, 1987, **1**, 245.
- 4 M. Sanati and A. Anderson, *J. Mol. Catal.*, 1990, **59**, 233.
- 5 H. Bosch and F. Janssen, *Catal. Today*, 1998, **2**, 369.
- 6 E. A. Mamedov and V. Cortes Corberan, *Appl. Catal. A*, 1995, **127**, 1.
- 7 W. Hardling, K. E. Birkeland and H. H. Kung, *Catal. Lett.*, 1994, **28**, 1.
- 8 G. Dev and I. E. Wachs, *J. Catal.*, 1994, **146**, 323.
- 9 P. Forzatti, E. Tronconi, G. Busca and P. Tittarelli, *Catal. Today.*, 1987, **1**, 209.
- 10 K. V. R Chary, G. Kishan and T. Bhaskar, *JCS Chem. Commun.*, 1999, 1399.
- 11 Jane Huhtanen, S. Lars and T. Andersson, *Appl. Catal. A: General*, 1993, **98**, 159.
- 12 R. H. H. Smits, K. Seshan, J. R. H. Ross, L. C. A. Van den Oetelaar, J. H. J. M. Helwegen, M. R. Anantharaman and H. H. Brongersma, *J. Catal.*, 1995, **157**, 584.
- 13 T. C. Watling, G. Deo, K. Seshan, I. E. Wachs and J. A. Lercher, *Catal. Today*, 1996, **28**, 139.
- 14 P. J. Stobbelaar, Ph.D. Thesis, University of Eindhoven, 2000.
- 15 E. I. Ko and J. G. Weissman, *Catal. Today*, 1990, **8**, 27.
- 16 K. V. R. Chary, G. Kishan, T. Bhaskar and Ch. Sivaraj, *J. Phys. Chem.*, 1998, **102**, 6792.
- 17 F. Roozeboom, T. Fransen, P. Mars and P. Gellings, *Z. Anorg. Allg. Chem.*, 1979, **25**, 449.
- 18 G. C. Bond and S. F. Tahir, *Appl. Catal.*, 1991, **71**, 1.
- 19 K. V. R. Chary, G. Kishan, K. Srilakshmi and K. Ramesh, *Langmuir*, 2000, **16**, 7692.
- 20 G. T. Went, L. J. Leu and A. T. Bell, *J. Catal.*, 1992, **134**, 4.
- 21 K. Tanabe, in *Catalysis Science and Technology*, ed. J. R. Anderson and M. Boudart, Springer-Verlag, Berlin, 1981, vol. **2**, p. 231.
- 22 H. H. Kung, *J. Solid State Chem.*, 1984, **52**, 191.
- 23 G. Connel and J. A. Dumesic, *J. Catal.*, 1987, **105**, 285.
- 24 T. Kataoka and J. A. Dumesic, *J. Catal.*, 1988, **112**, 66.
- 25 S. Okazaki and T. Okuyama, *Bull. Chem. Soc. Jpn.*, 1983, **56**, 2159.
- 26 P. Cavalli, F. Cavani, I. Manenti and F. Trifiro, *Ind. Eng. Chem. Res.*, 1987, **26**, 639.



# The role of hydrogen bonding in controlling the selectivity of Diels–Alder reactions in room-temperature ionic liquids

Ajay Aggarwal, N. Llewellyn Lancaster, Alick R. Sethi and Tom Welton

Department of Chemistry, Imperial College, London, UK SW7 2AY.

E-mail: t.welton@ic.ac.uk

Received 3rd July 2002

First published as an Advance Article on the web 8th August 2002

The reaction of cyclopentadiene with methyl acrylate has been investigated in a range of ionic liquids. The origin of the *endo*-selectivity for the reactions and associated rate enhancements has been attributed to a hydrogen bond formed between the cation of the ionic liquid and the methyl acrylate.

## Introduction

Room-temperature ionic liquids are liquids that are constituted entirely of ions and provide a solvent environment that is quite unlike any other available at room temperature. They have recently excited much interest in both synthetic and catalytic chemistry.<sup>1</sup> However, little is known about how the use of an ionic liquid solvent can affect the reactions of solute species. With their unique character, the ionic liquids may induce solvent effects on a wide range of processes. Hence, the investigation of the effect of the solute microenvironment on reactivity in these solvents forms a central theme in our research. In this paper, we report how a specific solvent–solute interaction in room-temperature ionic liquids can lead to changes in both the rate and product selectivity of the Diels–Alder reaction.

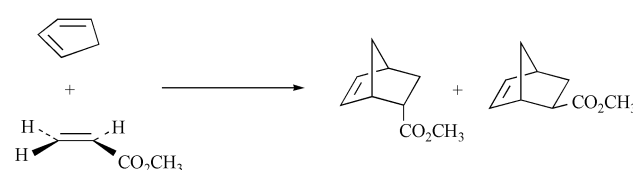
The Diels–Alder reaction remains one of the most useful carbon–carbon bond-forming reactions in organic chemistry. It is an addition reaction and so potentially highly ‘atom efficient’, but the reaction is often not selective, giving a mixture of isomers. Therefore, there is an interest in finding methodologies by which Diels–Alder reactions may be performed to give one product. Further, as an addition process with a negative entropy of reaction, attempts to accelerate Diels–Alder reactions by heating meet the obstacle of reducing the equilibrium constant for the reaction. Hence there is also an interest in methodologies that increase the rates of these reactions.

Many Diels–Alder reactions show strong solvent dependence and they are useful to study quantitative effects of the reaction environment on the reaction outcome. It has been proposed that improved reaction rates and selectivity arise from a number of factors, such as the polarity of the solvent,<sup>2</sup> or its solvophobicity.<sup>3</sup> The addition of a Lewis acid is also known to have a dramatic effect on these reactions.<sup>4</sup>

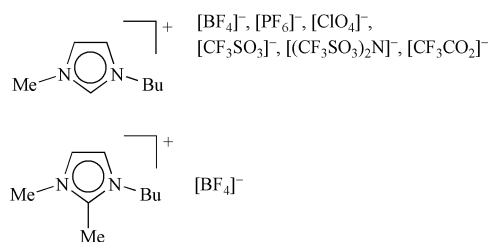
The first study of the Diels–Alder reaction in an ionic liquid was performed by Jaeger, using ethylammonium nitrate.<sup>5</sup> More recently a number of Diels–Alder reactions in imidazolium ionic liquids have been reported.<sup>6–9</sup> Lee has also used the Lewis acidity of chloroaluminate ionic liquids to greatly accelerate Diels–Alder reactions.<sup>10</sup> Ionic liquids that contain ZnCl<sub>2</sub> and SnCl<sub>2</sub> have been used similarly.<sup>11</sup> Here we are using the reaction of cyclopentadiene with methyl acrylate, which leads to a mixture of *exo* and *endo* products, as a probe of the solvent behaviour.

## Results and discussion

In this work we report a study of the reaction of cyclopentadiene (**1**) with methyl acrylate (**2**) (Scheme 1).<sup>12</sup> The reaction was performed in a range of ionic liquids, described in Fig. 1. Most of these ionic liquids are based on 1-butyl-3-methylimidazolium cations {[bmim]<sup>+</sup>}, although one example where the 2-position on the ring was methylated was when {[bm<sub>2</sub>im]<sup>+</sup>} was used.



**Scheme 1** The reaction of methyl acrylate with cyclopentadiene to give a mixture of *endo*- and *exo*-bicyclo-[2.2.1]-hept-5-ene-2-carboxylic acid methyl ester.



**Fig. 1** The ionic liquids used in this study.

## Green Context

Ionic liquids continue to attract considerable interest in the chemistry research community as non-volatile solvents for organic reactions. Some reactions have been observed to give unusual kinetics or selectivities when carried out in ionic liquids and this includes a high *endo*-selectivity in the Diels–Alder reaction of cyclopentadiene and methyl acrylate. Here the origin of that selectivity is shown to be due to hydrogen bonding between the cation of the ionic liquid and the dienophile. The ability to use such specific interactions to control organic reactions could well prove to be of widespread importance.

## Kinetic study

In a preliminary kinetic study, the reaction in the ionic liquids [bmim][BF<sub>4</sub>], [bmim][OTf] and [bmim][N(Tf)<sub>2</sub>] has been investigated. An excess of cyclopentadiene was used, allowing the yield of products to be plotted as a function of time using a *pseudo*-first order kinetic model. This is an example of an 'A to B' reaction. The formation of the products was modelled by the expression below [eqn. (1)], using the *SCIENTIST*<sup>13</sup> package, where *B* is the sum of isomers formed and *B*<sub>inf</sub> is the estimated final amount of products formed.

$$B = B_{\text{inf}} (1 - \exp^{-kt}) \quad (1)$$

The values of the *pseudo*-first order rate constants, *k*<sub>obs</sub>, thus determined are shown (Table 1). The value of *k*<sub>obs</sub> for the reaction in ethylammonium nitrate<sup>5</sup> is included. Simple comparison with the results reported here is not possible because of the different conditions used for the studies. However, it can be seen that the values are of the same order of magnitude.

**Table 1** Rates and selectivities of reaction of cyclopentadiene with methyl acrylate in different ionic liquids

| Solvent   | 10 <sup>5</sup> <i>k</i> <sub>obs</sub> /s <sup>-1</sup> | <i>endo:exo</i> | <i>E</i> <sub>T</sub> <sup>N</sup> | Viscosity <sup>14</sup> |
|---|--|-----------------|------------------------------------|-------------------------|
| [bmim][BF <sub>4</sub> ]                            | 13.0   | 4.6             | 0.670                              | 233 (303 K)             |
| [bmim][OTf]   | 12.4   | 4.5             | 0.656                              | 90 (293 K)              |
| [bmim][N(Tf) <sub>2</sub> ]                         | 11.0   | 4.3             | 0.644                              | 52 (293 K)              |
| [EtNH <sub>3</sub> ][NO <sub>3</sub> ] <sup>5</sup> | 3.4  | 6.7             | 0.954 <sup>15</sup>                |                         |

The fastest rate of reaction was observed in the most viscous ionic liquid, and the rate of reaction fell as the viscosity of the ionic liquid was reduced. Therefore, the rate of reaction is not limited by the migration of the reagents through the ionic liquid. It can be seen that the increase in the rate of the reaction is concurrent with an increased *endo*-selectivity. Hence in this study, we report the effects of the ionic liquids on the *endo*-selectivity of the reaction as a preliminary, crude guide to the velocity of the reaction. We are continuing this investigation and will report the results of a full kinetic investigation including measurements of Arrhenius activation energies in the future.

## Endo/exo selectivity

The first study of selectivity of the Diels–Alder reaction was made in two tetrafluoroborate ionic liquids, the results of which are shown (Table 2). There was little change in the yield of the

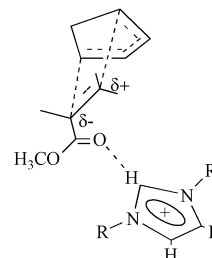
**Table 2** The reaction of cyclopentadiene with methyl acrylate in a variety of ionic liquids and some molecular solvents<sup>a</sup>

| Ionic liquid   | $\delta_{\text{H}}(H^2)/$<br>ppm | <i>E</i> <sub>T</sub> <sup>N</sup> | Yield<br>(%)     | <i>endo:</i><br><i>exo</i> |
|--|----------------------------------|------------------------------------|------------------|----------------------------|
| [bmim][BF <sub>4</sub> ]   | 8.83                             | 0.670                              | 85               | 4.6                        |
| [bm <sub>2</sub> mim][BF <sub>4</sub> ]  | N/A                              | 0.576                              | 84               | 3.3                        |
| [bmim][ClO <sub>4</sub> ]  | 8.89                             | 0.680                              | 74               | 4.8                        |
| [bmim][PF <sub>6</sub> ]   | 8.68                             | 0.669                              | 93               | 4.8                        |
| [bmim][OTf]  | 9.00                             | 0.656                              | 87               | 4.5                        |
| [bmim][N(Tf) <sub>2</sub> ]  | 8.70                             | 0.645                              | 90               | 4.3                        |
| [bmim][CF <sub>3</sub> CO <sub>2</sub> ]   | 9.80                             | 0.620                              | 89               | 4.0                        |
| [bmim][BF <sub>4</sub> ] + [bmim]Cl (2 M)  | —                                | N/A                                | 49               | 3.7                        |
| [HO(CH <sub>2</sub> ) <sub>2</sub> mim][N(Tf) <sub>2</sub> ] <sup>9</sup>                | —                                | 0.929                              | 6.1              |                            |
| [CH <sub>3</sub> O(CH <sub>2</sub> ) <sub>2</sub> mim][N(Tf) <sub>2</sub> ] <sup>9</sup> | —                                | 0.722                              | 5.7              |                            |
| [EtNH <sub>3</sub> ][NO <sub>3</sub> ]   | N/A                              | 0.954 <sup>15</sup>                | 6.7 <sup>5</sup> |                            |
| Methanol   | N/A                              | 0.762 <sup>20</sup>                | 6.7 <sup>2</sup> |                            |
| Ethanol  | N/A                              | 0.654 <sup>20</sup>                | 5.2 <sup>2</sup> |                            |
| Acetone  | N/A                              | 0.355 <sup>20</sup>                | 4.2 <sup>2</sup> |                            |
| Diethyl ether  | N/A                              | 0.117 <sup>20</sup>                | 2.9 <sup>2</sup> |                            |

<sup>a</sup> Work in imidazolium ionic liquids: [cyclopentadiene]<sub>0</sub> = 1.27 M, [methylacrylate]<sub>0</sub> = 1.11 M, 72 hours at 25 °C.

reaction using these ionic liquids. There was, however, a definite effect on the selectivity of the reaction when changing the ionic liquid from [bmim][BF<sub>4</sub>] (*endo:exo* = 4.6) to [bm<sub>2</sub>mim][BF<sub>4</sub>] (*endo:exo* = 3.3). The principal difference between [bmim]<sup>+</sup> and [bm<sub>2</sub>mim]<sup>+</sup> is that the ability of the latter to hydrogen bond through the proton on the C<sup>2</sup> position of the imidazolium ring has been blocked, although weaker hydrogen bonds can still be formed with the protons at the C<sup>4</sup> and C<sup>5</sup> positions.<sup>16</sup> The selectivity of the reaction is even greater in [HO(CH<sub>2</sub>)<sub>2</sub>mim][N(Tf)<sub>2</sub>] (*endo:exo* = 6.7),<sup>9</sup> which is an O–H hydrogen bond donor, and [EtNH<sub>3</sub>][NO<sub>3</sub>] (*endo:exo* = 6.7),<sup>5</sup> which is an N–H hydrogen bond donor. These results show that the ability of the cation to act as a hydrogen bond donor is important in determining the role that the ionic liquid has in controlling the *endo* selectivity of the reaction. This effect has been noted in molecular solvents.<sup>17</sup>

It is well known that Lewis acid catalysts can have a dramatic effect on both the rates and selectivities of Diels–Alder reactions.<sup>4</sup> This occurs by the Lewis acid coordinating to the carbonyl oxygen of the methyl acrylate. The formation of a hydrogen bond from the cation of the ionic liquid to the dienophile (Fig. 2) is a Lewis acid–base interaction.<sup>18</sup> In work where the Diels–Alder reaction was studied in dichloromethane, imidazolium salts were added and proposed to act as Lewis acid catalysts.<sup>19</sup>



**Fig. 2** The hydrogen bond (Lewis acid) interaction of an imidazolium cation with the carbonyl oxygen of methyl acrylate in the activated complex of the Diels–Alder reaction.

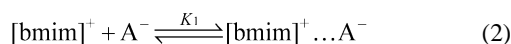
Having varied the cation while keeping the anion constant, a series of [bmim]<sup>+</sup> ionic liquids were used to study the effect of changing the anion on the Diels–Alder reaction (Table 2). The yields were generally high and changed little, with the exception of [bmim][ClO<sub>4</sub>]. The lower yield in this ionic liquid was probably the result of a poor extraction of the products from the ionic liquid. The selectivity of the reaction for the *endo* isomer is clearly affected by the anion used. The lowest selectivity was observed in [bmim][CF<sub>3</sub>CO<sub>2</sub>] (*endo:exo* = 4.0) whilst the highest was observed in [bmim][PF<sub>6</sub>] (*endo:exo* = 4.8). Since the ionic liquids all contained the same cation ([bmim]<sup>+</sup>), this change in selectivity cannot be attributed to a change in the hydrogen bond donor ability of the cation. So why is any effect seen?

Preliminary studies into the solvent properties of these ionic liquids according to Reichardt's dye<sup>20</sup> measurements (*E*<sub>T</sub><sup>N</sup> value, Table 2) have been made.<sup>21,22</sup> It can be seen that there is a clear relationship between the *E*<sub>T</sub><sup>N</sup> value of the ionic liquid and the *endo:exo* ratio observed when the Diels–Alder reaction is performed within it (Table 2). This relationship was also noted in a recent paper showing the effect of changing the cation of the ionic liquid on its polarity, as determined by its *E*<sub>T</sub><sup>N</sup> value, and the *endo:exo* ratio of the reaction of cyclopentadiene and methyl acrylate.<sup>9</sup> It is known that when a solvent is capable of acting as a hydrogen bond donor, this property dominates its *E*<sub>T</sub><sup>N</sup> value,<sup>23</sup> giving a measurement of the liquid's ability to hydrogen bond to a *solute*.

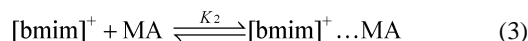
We have demonstrated elsewhere that the ability of the ionic liquid to hydrogen bond to a probe solute arises from the hydrogen bond donor ability of the cation, moderated by the hydrogen bond acceptor ability of the anion.<sup>22</sup> It is interesting to

note that  $[\text{CH}_3\text{O}(\text{CH}_2)_2\text{mim}][\text{N}(\text{Tf})_2]$  contains a basic site on its side chain that can act as a potential hydrogen bond acceptor, yet by both the *endo:exo* selectivity and the  $E_{\text{T}}^{\text{N}}$  measurements it is a strongly hydrogen bond donating solvent. This shows that the electron-withdrawing effect of the substituent far outweighs its own basicity.

The *endo:exo* ratio and associated acceleration of the Diels–Alder addition of cyclopentadiene and methyl acrylate in ionic liquids is controlled by the ability of the liquid to hydrogen-bond to the methyl acrylate as determined by two competing equilibria. The cation can hydrogen bond to the anion (A) of the ionic liquid [eqn. (2)].



or to the methyl acrylate (MA, eqn. (3)).



It can be clearly seen that the concentration of the hydrogen bonded cation–methylacrylate adduct is inversely proportional to the equilibrium constant for the formation of the cation–anion hydrogen bonded adduct ( $K_1$ ).

In order to test our theory we added  $[\text{bmim}]\text{Cl}$  to  $[\text{bmim}][\text{BF}_4]$  and repeated the reaction. The chloride anion is a better hydrogen bond acceptor than tetrafluoroborate. Therefore one would anticipate that addition of  $[\text{bmim}]\text{Cl}$  to  $[\text{bmim}][\text{BF}_4]$  would lead to formation of an ionic liquid that was less able to coordinate to the methyl acrylate, thus reducing the *endo:exo* ratio [eqns. (2) and (3)]. The salt  $[\text{bmim}]\text{Cl}$  was chosen so that only one cation would be present in the system. Addition of  $[\text{bmim}]\text{Cl}$  caused a reduction in the yield to 49%, with the remaining being unreacted starting material, suggesting a reduction in the rate of the reaction. This was matched by a reduction in the *endo* selectivity (*endo:exo* ratio = 3.7), showing that the addition of a more basic anion to the  $[\text{bmim}][\text{BF}_4]$  does indeed lead to a reduction in the selectivity of the reaction.

It is possible that other effects may also influence the rates and selectivities of Diels–Alder reactions in ionic liquids. The  $E_{\text{T}}^{\text{N}}$  scale, while dominated by hydrogen bonding effects, also reports the influence of general dipolarity. Solvophobicity may also be important. Unfortunately, no measurements of solvophobicity (*e.g.* Abraham's solvophobicity parameter  $S_{\text{p}}$ ) have been made in ionic liquids. However, Table 2 also reports the  $^1\text{H}$  NMR chemical shift of the proton at the 2-position of the imidazolium ring of the neat  $[\text{bmim}]^+$  salts  $\{\delta_{\text{H}}(H^2)\}$ . This reports the strength of the cation–anion hydrogen bond.<sup>16,24</sup> It would be expected that, if the solvophobicity of the ionic liquids is driven by hydrogen bonding and increasing solvophobicity was driving the change in the *endo*-selectivity of the reaction, the selectivity should increase with increasing  $\delta_{\text{H}}(H^2)$ . In fact, the reverse is seen. It is not possible to say more than this until a more sophisticated analysis, based on a wider range of solvent parameters, is possible.

## Conclusions

In the reaction of cyclopentadiene with methyl acrylate, room-temperature ionic liquids can give substantial increases in *endo*-selectivity and associated rate enhancements, when compared to non-polar solvents. They offer the potential to be useful solvents for Diels–Alder cycloadditions, and related reactions, particularly for moisture and oxygen sensitive reagents, or those that are sensitive to strong Lewis acids. The greatest selectivities will be observed in ionic liquids with the strongest hydrogen-bond donor cation coupled with the weakest hydrogen-bond accepting anion.

We can predict that this behaviour will be general and, in similar reactions where a reactive centre is activated by a neighbouring electron-withdrawing carbonyl group (*e.g.*, Michael additions), ionic liquids that are hydrogen bond donors will further enhance reactivity. We are continuing to investigate this proposition.

## Experimental

$^1\text{H}$  NMR spectra were recorded on a JEOL JNM-EX270 Fourier-transform spectrometer on neat samples of the ionic liquids, to avoid the complications of interactions with an additional solvent. Deuterium locks were achieved using an internal capillary containing  $d_6$  DMSO. GC measurements were performed using an Agilent 4890D GC spectrometer. The column fitted was a Hewlett Packard HP-5 (Crosslinked 5% PH ME Siloxane) column, of length 15 m, diameter 0.53 mm, and with a 1.5  $\mu\text{m}$  film thickness. The conditions used for all runs were as follows: flow rate: 100  $\text{mL min}^{-1}$  of argon; inlet temperature: 200  $^{\circ}\text{C}$ ; detector temperature: 250  $^{\circ}\text{C}$ ; Total run time: 14 min; oven conditions: maintained at 50  $^{\circ}\text{C}$  for 6 min, then ramped at +15  $^{\circ}\text{C min}^{-1}$  for 4 min, then maintained at 110  $^{\circ}\text{C}$  for 1 min.

All manipulations were carried out using standard vacuum and Schlenk techniques under an atmosphere of dry nitrogen, or in a dry-box under an atmosphere of dry nitrogen. Methyl acrylate was dried by distillation from  $\text{CaCl}_2$ . Dicyclopentadiene was cracked by distillation from  $\text{Mg}(\text{ClO}_4)_2$  through a column packed with glass beads.

The synthesis and characterisation of the ionic liquids used in this work has been published elsewhere.<sup>25</sup> The ionic liquids were thoroughly dried by heating to 60  $^{\circ}\text{C}$  for 72 h immediately prior to use. Chloride content of the ionic liquids was determined by a  $\text{AgNO}_3$  test.

## Diels–Alder reactions

In a typical procedure to measure the *endo:exo* ratio, methyl acrylate (3.0  $\text{cm}^3$ , 0.03 mol) and freshly cracked cyclopentadiene (3.0  $\text{cm}^3$ , 0.04 mol) were added to 10  $\text{cm}^3$   $[\text{emim}][\text{BF}_4]$  giving a single solution, which was stirred for 72 h at 25  $^{\circ}\text{C}$ . The product mixture was extracted from the ionic liquid with diethyl ether (3  $\times$  20  $\text{cm}^3$ ). The diethyl ether was removed by rotary evaporation, and the product ratio determined by gas chromatography. GC analysis: *exo*-product appears at 12.7 min; *endo*-product appears at 13.0 min.

For kinetic experiments, into a round bottom flask under a nitrogen atmosphere was added ionic liquid (10  $\text{cm}^3$ ), chlorobenzene (internal GC standard) and cyclopentadiene (4  $\text{cm}^3$ , 50 mmol). This biphasic mixture was maintained at 25  $^{\circ}\text{C}$  with stirring. The reaction was started by adding methyl acrylate (0.8  $\text{cm}^3$ , 9 mmol) at a known time. The system remained biphasic. Periodically the upper (organic) phase was sampled by withdrawal of 2  $\mu\text{L}$  by syringe into ether (1  $\text{cm}^3$ ) and analysed by GC.

## References

- (a) T. Welton, *Chem. Rev.*, 1999, **99**, 2071; (b) K. R. Seddon and J. D. Holbrey, *Clean Products and Processes*, 1999, **1**, 223; (c) P. Wasserschied and W. Keim, *Angew. Chem., Int. Ed. Engl.*, 2000, **39**, 3772.
- J. A. Berson, Z. Hamlet and W. A. Mueller, *J. Am. Chem. Soc.*, 1962, **84**, 297.
- R. Breslow, *Acc. Chem. Res.*, 1991, **24**, 159.
- U. Pindur, G. Lutz and C. Otto, *Chem. Rev.*, 1993, **93**, 741.



- 5 D. A. Jaeger and C. E. Tucker, *Tetrahedron Lett.*, 1989, **30**, 1785.
- 6 A. R. Sethi, T. Welton and J. Wolff, *Tetrahedron Lett.*, 1999, **40**, 793.
- 7 M. J. Earle, P. B. McCormac and K. R. Seddon, *Green Chem.*, 1999, **1**, 23.
- 8 P. Ludley and N. Karodia, *Tetrahedron Lett.*, 2001, **42**, 2011.
- 9 S. V. Dzyuba and R. A. Bartsch, *Tetrahedron Lett.*, 2002, **43**, 4657.
- 10 C. W. Lee, *Tetrahedron Lett.*, 1999, **40**, 2461.
- 11 A. P. Abbott, G. Capper, D. L. Davies, R. K. Rasheed and V. Tambyrajah, *Green Chem.*, 2002, **4**, 24.
- 12 N. L. Lancaster, A. R. Sethi and T. Welton, in "*Ionic Liquids industrial applications for Green Chemistry*", ACS Symposium Series No. 818, in press.
- 13 SCIENTIST, Micromath Scientific Software, [www.micromath.com](http://www.micromath.com).
- 14 R. Hagiwara and Y. Ito, *J. Fluorine Chem.*, 2000, **105**, 221.
- 15 S. K. Poole, P. H. Shetty and C. F. Poole, *Anal. Chim. Acta*, 1989, **218**, 241.
- 16 (a) A. G. Avent, P. A. Chaloner, M. P. Day, K. R. Seddon and T. Welton, *J. Chem. Soc., Dalton Trans.*, 1994, 3405; (b) A. K. Abdul-Sada, S. Al-Juaid, A. M. Greenway, P. B. Hitchcock, M. J. Howells, K. R. Seddon and T. Welton, *Struct. Chem.*, 1990, **1**, 391.
- 17 C. Catiuela, J. I. García, J. Mayoral and L. Salvatella, *J. Chem. Soc., Perkin Trans. 2*, 1994, 847.
- 18 P. R. Schreiner and A. Wittkopp, *Org. Lett.*, 2002, **4**, 217.
- 19 J. Howarth, K. Hanlon, D. Fayne and P. McCormac, *Tetrahedron Lett.*, 1997, **38**, 3097.
- 20 C. Reichardt, *Chem. Rev.*, 1994, **94**, 2319.
- 21 M. J. Muldoon, C. M. Gordon and I. R. Dunkin, *J. Chem. Soc., Perkin Trans. 2*, 2001, 433.
- 22 L. Crowhurst, J. M. Perez-Arlandis, P. A. Salter and T. Welton, *Anal. Chem.*, submitted for publication.
- 23 R. W. Taft and M. J. Kamlet, *J. Am. Chem. Soc.*, 1976, **98**, 2886.
- 24 A. D. Headley and N. M. Jackson, *J. Phys. Org. Chem.*, 2002, **15**, 52.
- 25 L. Cammarata, S. G. Kazarian, P. A. Salter and T. Welton, *Phys. Chem. Chem. Phys.*, 2001, **3**, 5192.